THERMOPLASTIC ELASTOMER MICROFLUIDIC DEVICES FOR BIOLOGY AND CHEMISTRY

Alexander H. MCMILLAN

Supervisors:
Prof. Maarten B. J. Roeffaers, KU Leuven
Dr. Sasha Cai Lesher-Pérez, Elvesys

Members of the Examination Committee:
Prof. Jozef A. Deckers, KU Leuven, Chair
Prof. Johan Hofkens, KU Leuven
Prof. Rob Ameloot, KU Leuven
Prof. Jeroen Lammertyn, KU Leuven
Prof. Davide Bonifazi, University of Vienna
Dr. Julia Sepulveda Diaz, Elvesys

Dissertation presented in partial fulfilment of the requirements for the degree of Doctor of Bioscience Engineering (PhD)

February 2021

Here I sit, painstakingly searching for the right words where there are none to be found, asking, "How did I find myself here?" Arriving at the end of anything always has us thinking of its beginning, with far too much clarity and reflection – if not some melancholy – than can be good for us. It seems absurd to sum up what has defined these past few years of life into a humble word document, and more absurd yet to collect the sentiments to describe it in a short preface – but I'll stop myself there, for perhaps I am investing undue meaning in what is becoming the most challenging part of this dissertation. But then again, how could I not? In any case, I will get on with thanking everyone – as one should – for there are many thanks to be given.

First off, I would like to warmly thank my supervisor, Professor Maarten Roeffaers. While I was only occasionally in Leuven during my PhD, I was welcomed into his group and he was always prepared to give me invaluable feedback and advice. I must also thank Professor Johan Hofkens and Professor Rob Ameloot, as my assessors, for their critical questions and comments that helped define the narrative of this dissertation.

Next, I would like to thank my co-supervisor, Sasha Cai Lesher-Pérez. I can wholeheartedly say that I could not have completed this PhD without him. His mindset, knowledge, and creativity never ceased to astound me. He provided crucial scientific guidance and inspiration, while leaving room for me to grow as an independent researcher. I believe that any future PhD student would be lucky to have him as a PI. I thank him in particular for his continued support this past year – not even a 9-hour time difference could get in the way of long (but never too long) discussions.

I thank my friend Walter Minnella for helping me get this whole thing started and for looking out for me back in the day. His advice and understanding, based on his own experience doing a PhD at Elvesys, was irreplaceable. Grazie, zio.

To my two thésards-in-arms, Emma and Alessandra, I am grateful for the work done and time spent together during this ridiculous adventure. How boring things would have been without them.

I thank Julia Sepulveda Diaz, Guilhem Velvé Casquillas, and the rest of the Elvesys crew for their constant support and the many good times had. Julia's

support in these final stages were essential to the completion of this PhD, and for that I am grateful.

I also thank the European Union for its financial support of the Horizon 2020 Marie Skłodowska-Curie project, PhotoTrain, and all of the students and PIs involved. It was great pleasure to work with them.

Finally, I would like to extend my deepest thanks and gratitude to my family, friends, and especially Eva. This certainly would not have been possible without their love and support.

And how to finish? The words continue to escape me, so it is best to leave it at that.

Until next time.

Alex

Paris, November 2020

Since its emergence, microfluidics has proven to be a powerful tool in chemistry and the life sciences. Microfluidic devices, consisting of networks of micron-scale flow channels, leverage high surface-area-to-volume ratios and precision fluid control to provide advantages over conventional methods in chemistry and biology. In chemistry, reactions with greater speed, selectivity, and safety can be achieved thanks to fast mixing and efficient heat transfer. In biology, greater control over mechanical and biochemical microenvironments allow cell culture studies with greater relevance to living organisms.

The progression of microfluidics over the past three decades, however, has not lived up to the high expectations that were held at its beginnings. While numerous factors can be identified as bottlenecks in the continued development of microfluidics, one critical element is the need for new microfluidic materials. Microfluidic devices, or "chips," can be fabricated from a variety of different materials, such as silicon, glass, and polymers, with each one possessing its intrinsic advantages and drawbacks, as discussed in **Chapter 1**. A material must possess suitable material properties for the microfluidic application at hand, but one must also evaluate its fabrication and cost as factors key to its accessibility and transferability across manufacturing scales. The most common microfluidic material, an elastomer called polydimethylsiloxane (PDMS), possesses numerous drawbacks in its material properties that make it unideal for many biology applications and unusable for many chemistry applications. Moreover, the techniques used for its fabrication are low-throughput, limiting the possibility of large-scale implementation (i.e., a transfer from academic research to industry). A group of materials called soft thermoplastic elastomers (sTPE) have been recently developed for microfluidics, with preliminary reports in literature demonstrating their favorable material properties and transferable fabrication methodologies. This PhD, conducted between academia and industry, focuses on two distinct sTPE materials, Flexdym™ and Fluoroflex, and their use for cell culture and flow chemistry applications, respectively. It aims to evaluate the properties of these novel sTPE materials and capitalize on them by providing sTPE device demonstrations that give scope for broader and more widespread microfluidic applications in these fields.

Chapter 2 describes the development of a composite microfluidic platform for membrane-based cell culture, consisting of two micropatterned Flexdym™ layers separated by a commercially available porous polycarbonate membrane. Membrane-based cell culture can be used to simulate tissue-tissue interface, valuable for drug development and disease modeling, and provides the basis for cutting-edge organ-on-chip technology. The thermoplastic platform leverages the rapid hot embossing and self-sealing property of Flexdym™, as well as the simplicity of the off-the-shelf polycarbonate membrane, to improve upon the fabrication time and complexity of similar microfluidic geometries made in PDMS. The pressure capacity of the bond formed between Flexdym™ and polycarbonate was characterized and found to be sufficient for cell culture applications (> 500 mbar). To validate the device's utility for membrane-based cell culture, cell culture trials were performed, showing cell adhesion and proliferation inside the device.

Chapter 3 reports the extensive material characterization of Fluoroflex and the development of a modular microfluidic platform using the material. Fluoroflex was found to exhibit good chemical resistance in comparison to PDMS and other polymers, allowing its use with common organic solvents, such as toluene, dichloromethane, and hexane. Key optical, mechanical, and surface properties of Fluoroflex were also characterized, and showed the material's appropriateness for use as a microfluidic device. A 30 s hot embossing protocol was developed, allowing for the rapid micropatterning of Fluoroflex. Like Flexdym™, Fluoroflex possesses an intrinsic adhesive property, allowing spontaneous bonding with itself to occur after the formation of conformal contact. This self-sealing was evaluated through burst testing and found to withstand a pressure of 1.4 bar after only five minutes of conformal contact between two Fluoroflex surfaces. This fast, reversible bonding was used to create a modular microfluidic platform, with which microfluidic droplet generation (water in toluene) of variable size was demonstrated.

Chapter 4 expands on the microfluidic applications of Fluoroflex by presenting the preliminary work toward a microfluidic packed bed photoreactor consisting of a Fluoroflex microchannel and PDMS microbeads. PDMS microbeads were synthesized and subsequently injected into a Fluoroflex microchannel and trapped by a micropillar array. An on-chip functionalization protocol was used to create an aminosilane surface layer on the microbeads, to which fluorescein was then coupled. Separately, a derivative of perixanthenoxanthene (PXX), a photoactive molecule, was coupled to PDMS microbeads (off-chip) in a similar manner, and subsequently shown to retain its photocatalytic properties

through a debromination reaction. These results provide a proof-of-concept and clear next steps toward the implementation of microbead-supported heterogeneous photocatalysis in a Fluoroflex device.

Finally, **Chapter 5** consists of a market evaluation of flow chemistry microreactors, aimed at providing industrial context to the Fluoroflex characterization and microfluidic development work. A competitive landscape analysis summarizes commercially available microreactors. Interviews of flow chemistry researchers were conducted to understand the needs of microreactor end-users and any technological difficulties they face. Lastly, a market size assessment is conducted, in which publication metrics are used to estimate the size, value, and growth trends of the flow chemistry research market for a Fluoroflex microreactor offering.

Microfluïdica hebben vele mogelijkheden binnen de scheikunde en de biowetenschappen. Microfluïdische toestellen, die bestaan uit een netwerk van micron-schaal stroomkanalen, hebben een hoge oppervlakte-tot-volume ratio en geven de gebruiker controle over de vloeistofstromen. De voordelen ten opzichte van conventionele methoden zijn snel mengen en een efficiënte warmtegeleiding die kunnen benut worden om scheikundige reacties veiliger en met hogere snelheid en selectiviteit uit te voeren. Verder geven ze ook een grotere controle over mechanische en biomechanische micro-omgevingen.

De progressie binnen de microfluïdica de laatste drie decennia heeft echter niet aan de grote verwachtingen kunnen voldoen. Hiervoor kunnen talrijke factoren worden ingeroepen maar een belangrijke uitdaging lijkt weg gelegd voor de ontwikkeling van nieuwe microfluïdische materialen. Voor het fabriceren van microfluïdische chips is er nu keuze uit een aantal materialen, zoals silicium, glas en polymeren, met elk intrinsieke voor- en nadelen. Dit wordt besproken in **Hoofdstuk 1**. Naast de materiaaleigenschappen speelt in de selectie ook de materiaal- en productiekost een sleutelfactor. Momenteel is polydimethylsiloxaan (PDMS) het meest gebruikte materiaal voor de ontwikkeling van microfluïdische chips, maar de chip-productie hiervan heeft een beperkte doorvoer, wat grootschalige productie limiteert (d.w.z. een transfer van academisch onderzoek naar industrie). Zachte thermoplastische elastomeren (sTPE), recent ontwikkeld voor microfluïdica, bezitten gunstige materiaaleigenschappen en zijn in productie makkelijker opschaalbaar. Dit doctoraat, uitgevoerd tussen universiteit en industrie, richt zich op twee verschillende sTPE materialen, Flexdym™ en Fluoroflex, en hun respectievelijk gebruik in biowetenschappen en scheikundige toepassingen. Het werk richt zich op het evalueren van de eigenschappen van deze nieuwe sTPE materialen en het kapitaliseren ervan voor microfluïdische toepassingen.

Hoofdstuk 2 beschrijft de ontwikkeling van een microfluïdisch platform voor celcultuur dat bestaat uit twee microgepatterneerde Flexdym™ lagen gescheiden door een poreus polycarbonaatmembraan. Membraangebaseerde celcultuur kan gebruikt worden om de weefsel-weefsel interfase te simuleren, wat waardevol is voor geneesmiddelontwikkeling en ziektemodelering, en het geeft de basis voor baanbrekende orgaan-op-een-chip-technologie. Het thermoplastisch platform gebruikt de snelle patternering op hoge temperatuur en zelfhelende eigenschappen van Flexdym™, in combinatie met de simpliciteit

van het commercieel beschikbare polycarbonaatmembraan om de productietijd en complexiteit van gelijkaardige microfluïdische geometrieën uit PDMS te verbeteren. De druk capaciteit van de gevormde binding tussen Flexdym™ en polycarbonaat werd gekarakteriseerd en bleek voldoende voor celcultuur toepassingen (> 500 mbar). Om het nut van het apparaat voor membraan gebaseerde celculturen te valideren, werden celcultuur testen uitgevoerd. Deze testen toonden celadhesie en -proliferatie in de chip aan.

In **Hoofdstuk 3** wordt Fluoroflex in detail gekarakteriseerd en de ontwikkeling van een modulaire microfluïdische platform met dit materiaal uitgewerkt. Fluoroflex heeft een goede chemische compatibiliteit in vergelijking met PDMS en andere polymeren, en maakt het gebruik van veelgebruikte organische solventen, zoals tolueen, dichloromethaan en hexaan, mogelijk. Belangrijke optische, mechanische en oppervlakte eigenschappen van Fluoroflex werden gekarakteriseerd en toonden de geschiktheid van het materiaal voor gebruik in een microfluïdische toepassingen. Een procedure van dertig seconden onder hoge temperatuur werd ontwikkeld om Fluoroflex te micropatterneren. Net als Flexdym™ bezit Fluoroflex een intrinsieke adhesie eigenschap wat spontane binding met zichzelf toelaat na de vorming van contact. Deze zelfafdichting werd geëvalueerd door barsttesten en hieruit bleek dat drukken tot 1.4 bar worden weerstaan na slechts vijf minuten conformcontact tussen de twee Fluoroflexoppervlakken. Deze snelle, reversibele binding werd gebruikt om een modulaire microfluïdische platform te ontwerpen. Hiermee werd microfluïdische druppel generatie (water in tolueen) van verschillende groottes gedemonstreerd.

Hoofdstuk 4 breidt de microfluïdische toepassingen van Fluoroflex uit naar een microfluïdisch gepakt-bed-fotoreactor bestaande uit een Fluoroflexmicrokanaal en PDMS microkorrels. PDMS microkorrels werden gesynthetiseerd en geïnjecteerd in het Fluoroflexmicrokanaal waarin ze gevangen werden door een micropillaarstructuur. Na een chemische functionalizering met aminosilaan in de chip werd fluoresceïne gekoppeld aan het oppervlak van de microkorrels. Daarnaast werd in de chips de fotokatalytische debrominatie reactie succesvol uitgevoerd met een fotoactief molecule, perixanthenoxantheen, gekoppeld aan de PDMS microkorrels ('off-chip'). Deze proof-of-concept resultaten geven duidelijk de mogelijkheden aan voor implementatie van microkorrel-ondersteunde heterogene fotokatalyse in een microfluïdische chip gemaakt uit Fluoroflex.

Als laatste beschrijft **Hoofdstuk 5** de marktstudie van microreactoren voor scheikundige toepassingen met als doel het voorzien van een industriële context voor de verdere ontwikkeling van Fluoroflex. Een competitieve landschapsanalyse vat de commercieel beschikbare microreactoren samen. Interviews van onderzoekers die specifiek werken met 'flow chemistry' werden uitgevoerd om de noden van de eindgebruikers en de technologische beperkingen te begrijpen. Ten slotte werd de marktgrootte ingeschat. Hiervoor werden de publicatiestatistieken gebruikt om de grootte, waarde en groeitrends van de 'flow chemistry' onderzoeksmarkt voor Fluoroflexmicroreactoren in te schatten.

2D	two-dimensional
3D	three-dimensional
ACN	acetonitrile
AFM	atomic force microscopy
ANOVA	analysis of variance
APTES	(3-aminopropyl)triethoxysilane
BCP	block copolymer
COC	cyclic olefin copolymer
COP	cyclic olefin polymer
DI	deionized
DIPEA	diisopropylethylenediamine
DMEM	Dulbecco's Modified Eagle Medium
DRIE	deep reactive ion etching
E	ethylene
EB	ethylene-butylene
ECM	extracellular matrix
FD	Flexdym™
FEP	fluorinated ethylene propylene
FFKM	perfluoroelastomer
FTIR	Fourier transform infrared
HDF	human dermal fibroblast
HFP	hexafluoropropylene
HPLC	high-performance liquid chromatography
HSP	Hansen Solubility Parameter
HTGS	high-throughput gas separation
ID	inner diameter
LED	light-emitting diode
MEMS	microelectromechanical systems
NMR	nuclear magnetic resonance
NOA	Nordland optical adhesive

OD	outer diameter
OOC	organ-on-chip
OSTE	off-stoichiometric thiol–ene
OSTE+	off-stoichiometric thiol–ene–epoxy
PC	polycarbonate
PDMS	polydimethylsiloxane
PEEK	polyether ether ketone
PFA	perfluoroalkoxy
PFPE	perfluoropolyether
PMMA	polymethylmethacrylate
PS	polystyrene
PTFE	polytetrafluoroethylene
PXX	perixanthenoxanthene
RT	room temperature
SAM	serviceable available market
SOM	serviceable obtainable market
SS	stainless steel
sTPE	soft thermoplastic elastomer
TAM	total addressable market
TEOS	tetraethoxysilane
TFE	tetrafluoroethylene
THF	tetrahydrofuran
TPE	thermoplastic elastomer
UV-Vis	ultraviolet-visible
YoY	year-on-year
μPADs	microfluidic paper-based analytical devices
μPS	micropatterned stickers

Table of Contents

CHAPTER 1

Introduction

Abstract

This chapter provides a brief introduction to microfluidics, its applications in biology and chemistry research, and the need for new microfluidic materials. The advantages and drawbacks of the most common materials used to make microfluidic devices are summarized and soft thermoplastic elastomers are introduced. The chapter concludes by presenting the aims and scope of this dissertation and by briefly outlining the four experimental chapters that follow.

CHAPTER 1 - INTRODUCTION

1.1 INTRODUCTION TO MICROFLUIDICS

The recent decades have seen the emergence of microfluidics as a technological toolset for precision control and monitoring of fluids at the micro-scale. Having origins in microelectronics, molecular biology, and molecular analysis,[1] microfluidics centers around a microfluidic device (or "chip"), made from polymers, glass, silicon, and other materials, containing microchannels (**Figure 1.1**). Minute volumes of fluid can be manipulated inside the channels using external flow controllers (i.e., syringe pumps and pressure controllers) or integrated micro-pumps. Microfluidic device channel geometries range from tens to hundreds of micrometers and entail the use small fluid volumes. This results in high surface-area-to-volume ratios and predictable laminar flow regimes inside the channels, characterized by a low Reynolds Number, indicating the dominance of viscous forces over inertial forces in the fluid flow (**Figure 1.2**).[2] Leveraging these fundamental fluid mechanical characteristics by controlling channel geometries and fluid flow rates, microfluidics gain notable advantages over fluid handling at larger scales. In addition to the use of smaller amounts of reagent, rapid heat and mass transfer allows thermal homogeneity across the working fluid as well as highly controllable diffusive mixing and fluid separation. Moreover, microfluidic devices can be interfaced with external characterization equipment, allowing for *in situ* analyses and online monitoring of process conditions with high precision and sensitivity.
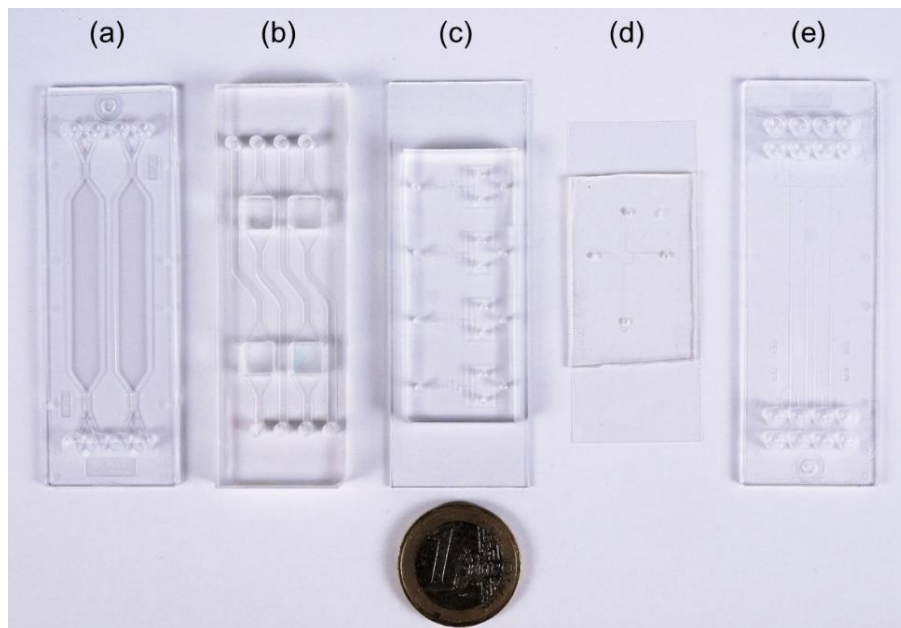
Figure 1.1. Microfluidic devices ("chips"). An assortment of microfluidic chips made from (a) polystyrene, (b) polymethylmethacrylate, (c) polydimethylsiloxane/glass, (d) soft thermoplastic elastomer, and (e) cyclic olefin polymer.

Devices can thus be designed in a highly modular nature with discrete subunits in mind to perform a series of specific functions, such as reagent addition, mixing, chemical reactions, product separation, and detection.[3] The idea of a "lab-on-a-chip" or a "micro total analysis system" describes the possibility of integrating and parallelizing entire laboratory processes onto a single microfluidic device.[4,5] These advantages have made microfluidic techniques an attractive tool for a wide range of biology and chemistry-based applications, including organic synthesis,[6] protein crystallization,[7] high-throughput screening for drug discovery,[8] single-cell analysis,[9] point-of-care diagnostics,[10] and multiphase flow systems.[11] Since its beginnings, microfluidics has increasingly demonstrated its potential to change the way that many of these biological and chemical processes are performed.
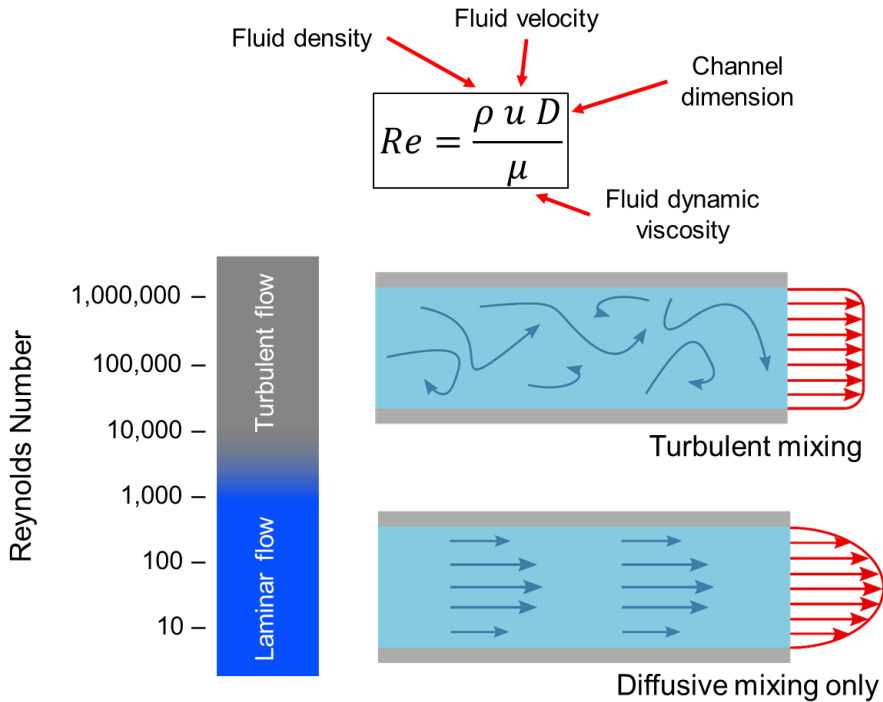
Figure 1.2. Fluid flow regimes. Fluid flow can be characterized by the non-dimensional Reynolds number, Re, describing the ratio of inertial forces to viscous forces in a fluid flow. At high Reynolds numbers (i.e., high fluid density, fluid velocity, and/or flow channel dimensions), turbulent flow occurs. This chaotic and unpredictable flow regime is characterized by unstable eddies, vortices, and advective mixing. At low Reynolds numbers, laminar flow occurs and can be characterized by smooth, parallel flow patterns dominated by relatively slow diffusive mixing. By using micro-scale flow channels, microfluidic devices take advantage of the stable and highly controllable laminar flow regime for precision fluid manipulation.

1.2   MICROFLUIDIC MATERIALS

The design and fabrication of a microfluidic device is a crucial aspect of the implementation of microfluidic techniques. Various material properties, such as optical, mechanical, gas permeability, and surface wetting properties, play a role in determining what a microfluidic device can be used for and with what efficacy. The secondary consideration of the fabrication techniques required to process a given material is important in defining the engineering practicalities

involved in creating a device and has significant implications in the feasibility and transferability of the processes throughout diverse settings, such as in small-scale lab production, or large-scale industrial production. The choice of material thus becomes a critical first step in the realization and ultimate function of a microfluidic system.

1.2.1 Glass and Silicon

Early microfluidics was based on the microfabrication techniques developed for microelectronics and microelectromechanical systems (MEMS), namely fabricating devices on silicon wafers using photolithography and subsequent wet etching, or micromachining.[12] These techniques were adapted to glass[13] and quartz[14] substrates for more favorable optical properties and suitable conductivity for electro-osmotic flow. Microfluidic devices of these materials offer excellent chemical resistance, can withstand high temperature and pressure, allow the facile integration of electrodes, and, in the case of glass and quartz, possess superlative optical properties. However, these materials suffer from notable disadvantages:

(i)   Cost: while the physical size of microfluidic devices is inherently small, only so much miniaturization can take place before fluid manipulation performance or integration with analytical equipment begins to suffer. Consequently, the cost of the microfluidic material plays a non-negligible role; raw silicon and glass materials represent a many-fold increase in cost when compared to polymers, such as polymethylmethacrylate (PMMA).[15] The involvement of dangerous chemicals for wet etching (most commonly hydrofluoric acid or potassium hydroxide) incur additional costs for protective facilities, waste management, and the reagents themselves.

(ii)   Multi-step process: the multi-step serial nature of standard glass wet etching (cleaning of the substrate, coating of the photoresist, photolithography, development of the photoresist, wet etching)[16] results in a large time investment to fabricate individual devices. Furthermore, the requirement for sophisticated equipment and expertise (consequently further increasing the cost), as well as the need for the aforementioned hazardous chemicals, can make these procedures relatively prohibitive. Downstream bonding of

micropatterned glass to create sealed microfluidic devices and interfacing with microfluidic setups requires further time, equipment, or material-intensive processing steps. These processes can, for example, require high temperatures and pressures,[17,18] adhesives,[19] anodic bonding,[20] or chemical washing.[21,22] Alternative fabrication techniques, such as glass micromachining[23] and more recently developed techniques of laser-based modification of glass substrates[24–26] also share many of these disadvantages regarding numerous, process-intensive steps. Another practical concern that arises with such multi-step, technically complex processes is that the techniques involved are often inaccessible and unfamiliar to many of the end-users of microfluidic technology, be it biologists or chemists, reducing or even eliminating rapid transitions between idea and prototype.

(iii)   Etching: the isotropic nature of standard wet etching produces shallow, rounded channels, limiting what channel geometries can be achieved and making precise control of final shape difficult. Anisotropic, dry etching, such as deep reactive ion etching (DRIE), can overcome this limitation and produce high aspect ratio channels and pillars with high precision,[27] but requires high amounts of energy and brings with it increased processing times and costs. The fabrication time and cost of etching processes largely inhibit glass and silicon microfluidics from being used in applications where large numbers of disposable devices are a necessity.

As a result, while some microfluidic applications may warrant the high cost of materials, equipment, and expertise involved in the manufacturing of glass and silicon devices, there has been a trend toward materials offering more facile and inexpensive methods of fabrication.[28]

1.2.2   **PDMS**

Following the initial steps in microfluidics made largely with silicon and glass as microfluidic device substrates, there was a push toward polymeric materials, which require faster, less specialized fabrication techniques, to encourage wider adoption of microfluidics. Since its introduction as a microfluidic material in 1998 by George Whitesides' group at Harvard University,[29] polydimethylsiloxane (PDMS) has revolutionized the field, and much of the

formative research and progress in microfluidics was performed with this material.

PDMS is a siloxane-based (silicone) two-part polymer, produced by mixing a liquid base and a crosslinking agent, that has properties very different from those of silicon.[30] It is optically transparent to ~300nm, non-toxic to cells once cured,[31] compatible with proteins,[32] and relatively permeable to non-polar gases, such as O_2, N_2, and CO_2.[33] Its gas permeability can be an important factor for life sciences applications involving mammalian cell cultures, which require oxygen to survive. It has hydrophobic surface properties that can be readily modified to a hydrophilic, high surface energy state using oxygen plasma treatment,[34] allowing biological separation applications leveraging electro-osmotic flow, as well as facilitating surface treatments through the attachment and patterning of various molecules to the activated surface.[35]

Microfluidic devices in PDMS are fabricated using a technique called soft lithography, referring to the casting of the flexible elastomer onto a master mold (**Figure 1.3**).[36] This technique of replica molding consists of pouring the liquid PDMS base and crosslinker mixture onto a mold. Molds having complex features can be fabricated by a variety of methods, most commonly using the micromachining and photolithographic techniques discussed above, and subsequently used to transfer their three-dimensional (3D) geometries to the PDMS substrate atop it once fully cured. The soft, elastomeric properties of PDMS are vital in facilitating its subsequent separation from the molds, which are typically made from rigid and/or brittle materials. This technique can be used to quickly and inexpensively produce PDMS substrates patterned with single or multidimensional layers[37] with sub-micron resolution.
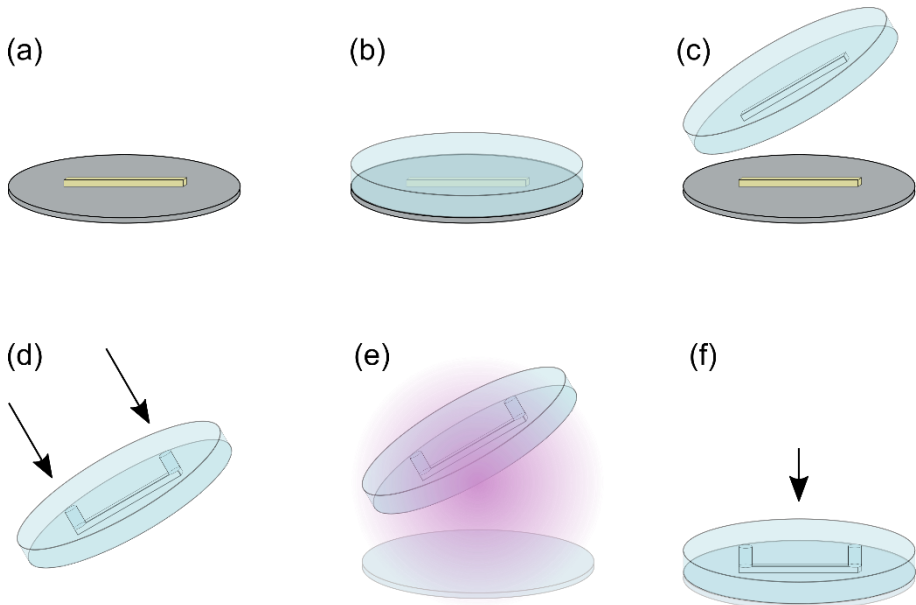
Figure 1.3. PDMS soft lithography. The most common method of fabricating PDMS microfluidic devices is with a technique called soft lithography. (a) A positive relief master microfluidic mold contains the shapes of a microchannel(s). (b) After the mixing of a PDMS polymer base and crosslinker and degasing, the mixture is poured atop the mold and cured for approximately 1–48 hours, depending on the baking parameters used. (c) After curing, the solid PDMS can be removed from the master mold; it now possesses the negative relief of the channel structures. (d) Access ports can be punched or drilled for later interfacing with microfluidic tubing. (e) Oxgyen plasma is used to activate the surface of the PDMS, which, when put in contact with glass (f), forms covalent bonds with the glass surface. The process is usually finished with a final baking step for robust sealing. A second PDMS surface can be used instead of glass for a full-PDMS device.

For photolithographic mold fabrication, Whitesides proposed the use of film transparency sheets as photomasks printed with commercially available high-resolution printers for inexpensive and rapid prototyping of microfluidic designs with features down to ~20 μm, generally sufficient for most microfluidic applications.[38] These masks are commonly used to create molds using liquid photoresists, such as SU-8 and AZ®, or dry film photoresists, such as Riston® and Ordyl®, for even faster processing on silicon or glass substrates.[39]

Microfluidic devices can be assembled into microfluidic devices both through irreversible and reversible bonding techniques. After plasma activation, the

oxidized surface of PDMS can form an irreversible bond with another PDMS or glass surface when dehydration reactions take place between hydroxyl groups on the two surfaces, forming Si-O-Si bonds to create a sealed device.[40] Alternatively, leveraging the elastomeric properties of PDMS, lower pressure sealing can be achieved with simple conformal contact with PDMS, glass, or other materials.[41] Similarly taking advantage of the high compliance of PDMS, on-chip pneumatic micro valves utilize a deformable PDMS membrane that can be integrated into a device for *in situ* flow management and micro pumping.[42] Moreover, from a purely practical, user-friendliness standpoint, elastomeric PDMS does not break as readily as brittle glassy materials and also allows for the facile introduction of tubing and other connections with its external microfluidic setup.

PDMS combined with soft lithography represented a significant advancement in microfluidics in terms of accessibility, ease of use, and rapid prototyping, and stimulated the rapid growth of microfluidics as a field of research and enabling tool,[43] particularly in biological settings. Early uses of PDMS microfluidics were focused on proofs-of-concept, demonstrating the technical capabilities of the platform,[44–46] but it has since been used in studies addressing our fundamental understanding throughout a range of biological questions.[47–49] It has also been used in some chemical synthesis applications, taking advantage of multi-step reaction integration and leveraging the precise fluid control achievable at the micro-scale.[50–52]

While PDMS triggered momentous growth in microfluidics research, the material is not without its drawbacks, both regarding its material properties and its fabrication process; depending on the intended application, some inherent material properties can be seen as both benefits and disadvantages:

(i)   Solvent incompatibility: PDMS exhibits an incompatibility with a wide range of organic solvents, whereby the material will swell, altering channel geometries or altogether unsealing the device, or will completely dissolve when exposed to organic solvents, acids, and bases.[53] This severely limits the use of PDMS for applications in chemical synthesis and has resulted in a relatively small adoption of microfluidics for chemistry applications as compared to for those in biology. While solutions involving the coating of PDMS microchannels with solvent-resistant materials exist,[54,55] these often entail additional, and non-facile steps that make their wide-scale use unrealistic, especially if a solvent-resistant material can be used from the start.

(ii)   Absorption/leaching: PDMS's permeability also makes it susceptible to absorption of hydrophobic compounds into the bulk of the material,[56] whereby the advantages gained by working at the micro-scale versus conventional macro-scale methods may be offset by the depletion of a compound key to the study at hand. This becomes problematic in cell culture applications involving soluble factors, such as hormones, cytokines, growth factors, and dyes,[57] cell signaling,[58] and drug compounds,[59] making PDMS largely unsuitable for high-throughput drug screening and drug discovery studies. Additionally, cured PDMS contains residual uncrosslinked oligomers; leaching of the oligomers from the bulk of the material into the fluid can contaminate the working solution and adversely affect cell cultures.[58]

(iii)   Temperature/pressure resistance: similarly posing an issue for some chemistry applications, PDMS is unable to handle the high temperature and high pressure flow, beginning to degrade at ~250 °C[60] and generally de-bonding below 5 bar pressure.[61] This inhibits PDMS to be used for reactions at extreme conditions that can be performed in glass and silicon devices.

(iv)   Gas permeability: while the high permeability of PDMS to O_2 and CO_2 can provide important benefits for maintaining healthy gas exchange in cell cultures, especially during long term experiments, in the case of very thin microfluidic devices this has been shown to produce a hyperoxic environment that can have adverse effects on cells.[62] Conversely, PDMS's permeability to water vapor can cause the non-negligible loss of the inherently low-volume working fluid in microfluidic devices, leading to significant shifts in volumes and critical chemical concentrations and gradients.[63,64] Evaporation of fluids from microchannels can also result in the propagation of bubbles, which can change flow characteristics, block channels, and damage cells.

(v)   Hydrophobic recovery: as previously discussed, plasma treatment of PDMS renders the normally hydrophobic surface hydrophilic, allowing bonding with other materials, surface functionalization, and reliable fluid filling of microchannels, all important considerations when culturing cells inside a device. Closely related to the aforementioned leaching of uncrosslinked oligomers from the bulk of PDMS, the mobile polymer chains diffuse from the bulk to the surface of the

material, minimizing surface energy in replacing hydroxyl groups at the activated, hydrophilized surface in a process known as hydrophobic recovery.[65] This poses problems in the practical considerations of using PDMS. Devices requiring hydrophilic behavior and surface treatments must be prepared within hours of their experimental use. The poor shelf-life of PDMS devices in this respect complicates the transferability from fabricators to end-users and impedes the larger-scale fabrication of PDMS-based devices for later use.

(vi)   Transferability of fabrication: following from the concerns of larger-scale fabrication immediately above, the nature of PDMS's discrete fabrication steps does not lend itself well to industrial-scale mass production. The numerous mixing and degassing steps of the liquid polymer, thermal curing, and subsequent plasma bonding can be achieved relatively simply and inexpensively at a laboratory scale when compared to glass and silicon microfluidics.[66] However, the lengthy process is rather low-throughput and not easily transferred to large numbers of devices, limiting its feasibility for a transition from the research settings, where microfluidics was born and continues to mainly exist, to greater industrial acceptance. Additionally, the cost of raw PDMS polymer, when considered at larger scales, presents another roadblock in its transferability.

PDMS undoubtedly shaped the early development of microfluidics and continues to play a large role in the ongoing research in the field. However, its inherent drawbacks have highlighted important questions about the utility of the material in key biological and chemical applications as well as its transferability from laboratory to industrial scales. These problems have thus limited it from replacing traditional materials in conventional biology and chemistry research, namely polystyrene (PS) and glass, respectively.

1.2.3   Hard Thermoplastics

There has been an increasing interest in thermoplastic materials, which have the potential to address many of PDMS's drawbacks and already possess a wealth of processing knowledge from the well-established thermoplastic manufacturing processes found in industry. Thermoplastics are a set of

uncrosslinked polymers (as opposed to thermosets) characterized by their glass transition temperatures (T_g), around which they soften. Between this temperature and their degradation temperature, they can be rapidly processed by thermoforming replication methods, such as injection molding, hot embossing, and casting. As no curing at elevated temperatures occurs, thermoplastics can be repeatedly molded with limited degradation and at a low material cost.[67] Progress has been made in alternative methods of processing thermoplastics for microfluidics, such as 3D printing[68] and micro milling,[69] but these serial methods fall short in their speed of fabrication and often lack resolution compared to the microfabrication techniques discussed above.

Common thermoplastics that have been adapted for microfabrication include PMMA, PS, polycarbonate (PC), cyclic olefin polymers and copolymers (COP and COC), perfluoroalkoxy (Teflon PFA), and fluorinated ethylene propylene (Teflon FEP).[70–76] While the material properties of each thermoplastic vary, in general, they offer good optical properties, low gas permeability, relatively stable surface properties, biocompatibility, and, in the case of the fluorinated thermoplastics, high chemical compatibility. A more detailed discussion on individual thermoplastics is outside the scope of this chapter, but more detail can be found in the comprehensive review by Becker and Gärtner.[77]

While the intrinsic material aspects can unquestionably offer improvements on PDMS in certain applications (these will be discussed further in the following sections), perhaps the greatest value that a shift toward thermoplastics for microfluidics can provide is one of manufacturability. Thermoplastics offer streamlined and inexpensive fabrication processes with which mass production of microfluidic devices can easily be envisioned. This is a proposition that is particularly interesting in the push for microfluidics to become a tool that can replace and improve upon tried-and-true conventional academic and industrial methods, in which case highly standardized, reproducible and disposable devices are necessities.[78,79]

The inevitable drawbacks of this family of hard thermoplastics that have kept them from overtaking PDMS in popularity are principally related to their fabrication implications:

(i)   Molding: to process rigid thermoplastics with the necessary high resolution and reproducibility of microfluidic features, the two most popular methods are injection molding and hot embossing. While hot embossing is the more accessible, less expensive option of the two,

generation of a master mold for both injection molding and hot embossing usually entails precision CNC milling or laser ablation, time-intensive processes with high price tags[80] that can result in high surface roughness, which must often be corrected with further polishing for reliable bonding and imaging. The master molds can be dependably reused for large-volume device production, but the development requires in-depth decisions of device design and processing conditions before the master mold production, thus it is not appropriate nor feasible for prototyping at low-volume production, as is normally the case in research settings. High-strength epoxy molds fabricated from familiar soft lithography methods have been developed[74,81] and ameliorate these concerns of cost, making them less prohibitive to lab settings. Epoxy molds, however, are less robust than their metal counterparts and do not allow for features of high density or high aspect ratio due to de-molding complications.[43] These are consequences of working with rigid materials and the high temperatures and pressures required to process them. These technical considerations in achieving high-quality molding can necessitate non-trivial expertise in molding technologies and polymer science.[82]

(ii) Bonding: assembling a sealed microfluidic device from molded thermoplastic substrates poses another challenge. The most common methods of achieving this are solvent assisted and thermal bonding.[78] Solvent bonding, for thermoplastics such as PMMA and PC, is performed by applying an organic solvent, such as dimethyl sulfoxide, acetone, or methanol, to the surface of the polymer, which becomes partially solubilized to allow for subsequent bonding with another component.[73,83] This creates strong bonds but can also result in substantial deformation of microfluidic features and alter final channel dimensions. Moreover, traces of solvents may remain, and even at picomolar concentrations can have detrimental effects on cells that are subsequently cultured in the devices.[84] Thermal bonding is performed by heating the two substrates to near their glass transition temperature before pressing them into contact. The diffusion and reorganization of polymer chains at the interface of the two substrates produce strong bonding once cooling has occurred.[85] Due to the rigidity of the thermoplastics (having Young's Moduli in the range of GPa[82]) complete conformal contact is difficult to achieve, especially across larger dimensioned devices, meaning that effective thermal bonding requires careful balancing of applied pressure so as to provide sufficient

pressure to promote thermal diffusion while not too much to cause microstructure deformation. Other thermoplastic bonding methods exist, but require additional, often specialized processing steps.[78]

(iii)   Interfacing: Unlike elastomeric PDMS, which allows facile interfacing of external fluidic equipment (i.e., tubings, pipettes, and needles), hot-embossed hard thermoplastics will most often require subsequent drilling of access ports to make world-to-chip connections.[86,87] This becomes impractical when making devices where tens or hundreds of ports are required, such as with tubeless microfluidic devices,[88] and is compounded by the inability to integrate flexible membrane-based pneumatic valves on-chip for channel multiplexing.[42] Laser ablation can be used to increase processing speed but with the consequences of reduced precision and polymer melt-back, complicating subsequent assembly procedures.[89] Soft materials permit more facile coring for port access and PDMS has even been shown to integrate the access port fabrication into the soft lithography casting process.[90] Access ports can similarly be integrated into injection molding masters, but again, the costs of initial setup are impractical in most lab settings.

There is much potential for the production of microfluidics with the favorable material properties of hard thermoplastics at scales fit for industrial adoption, especially factoring in the existing processing expertise in the field. However, the accessibility and transferability of such techniques at smaller scales, where microfluidics continues to reside, remains problematic, encouraging the persistence of simple and accessible PDMS in this domain despite its flaws.

1.2.4   Soft Thermoplastic Elastomers

The more recent development of a class of materials called thermoplastic elastomers (TPE), or soft thermoplastic elastomers (sTPE)[91,92] has introduced a novel combination of material properties that leverages the processing ease of thermoplastics with the soft, rubber-like handling of elastomers. sTPEs have been made in several commercially-available formulations at a low cost that are generally extruded into polymer sheets that can be stored for later use with long shelf-life and having favorable material properties of optical clarity and biocompatibility.[82] Regarding their microfabrication potential, sTPEs are compatible with thermoforming techniques such as injection molding and hot

embossing, but, due to their low stiffness, are feasible for production at laboratory scale in addition to industrial scale and can leverage soft lithography-based molds and expertise in place of the more robust processing requirements of hard thermoplastics.[93–95]

One such commercially available sTPE, Flexdym™, has been demonstrated to have particularly favorable material characteristics for microfluidics[96–99]:

(i)   Self-sealing: Like other sTPEs with which most of the development of sTPE microfluidics has been done, Flexdym™ is a styrenic block copolymer (BCP), indicating a chemical structure of repeating blocks of styrene and ethylene-butylene (EB) components. Thermodynamic instability of PS with neighboring EB groups induces a nano-scale bi-phasic morphology that provides the foundation of the unique material properties of these sTPEs, whereby the PS domain provides structural integrity to the polymer matrix whereas the EB domain provides characteristics of an elastomer.[82] Furthermore, the presence of two polymer blocks entails two distinct glass transition temperatures; the positive T_g (~100 °C) of the hard PS blocks give the melt-processing capabilities characteristic of traditional thermoplastics, whereas the negative T_g (~-70 °C) of the EB blocks allows amorphous mobility of polymers chains for room temperature and reversible bonding without the need for adhesives, solvents, or high temperatures that could deform microfluidic structures and add additional processing steps. Thanks to the flexibility of the material, bonding can be achieved with simple conformal contact and enhanced by varying bonding time and temperature [97].

(ii)   Low absorption: compared to PDMS, Flexdym™ showed considerably lower absorption of small hydrophobic molecules (e.g., drug and dye compounds).[97] Flexdym™ differs from earlier commercially available sTPEs that have been used for microfluidics, such as Versaflex™ CL30, MD6945, and G1657,[100] which contain high amounts of additives, such as plasticizers and processing agents, that can affect their bonding and microfabrication properties.

(iii)   Transferrable fabrication: as mentioned above, the fabrication implications due to the unique combination of thermoplastic and elastomeric properties of Flexdym™ and other sTPEs are perhaps the most significant innovations for their use in microfluidics. Where

PDMS device production is infeasible at large scales and rigid thermoplastic device production remains complicated at small scales, sTPEs can be micropatterned using similarly low-cost molds as those used in PDMS soft lithography, with comparatively low molding temperatures and pressures to rigid thermoplastic molding. The rapid (30 s) hot embossing of pre-extruded Flexdym™ sheets,[97] followed by self-sealing after conformal contact can be easily achieved with little expertise and low-cost equipment for small quantities of devices and additionally gives scope for high throughput roll-to-roll processing for industrial-scale production of microfluidics.

sTPE materials effectively bridge the gap that has existed in the microfluidic world between PDMS and hard thermoplastics, merging the high-throughput fabrication potential, low-cost, and satisfactory material properties of thermoplastics with the simple and accessible procedures that are demanded at the lab-scale for rapid prototyping and early-stage development of effective microfluidic platforms.

1.2.5   **Alternative and Emerging Materials**

Soft thermoplastic elastomers are not the only materials that offer novel or alternative solutions to mainstream materials (i.e., glass, PDMS, and hard thermoplastics) for microfluidic device fabrication. For example, since the introduction of the paper-based analytical device (μPADS) concept in 2007,[101,102] paper-based microfluidics has made innovative progress. It has shown notable efficacy in the field of point-of-care diagnostics, where the simplicity, low cost, easy manufacturability, and disposability of cellulosic paper make it an ideal material.[103] However, paper-based devices, typically relying on capillary-driven flow during material wetting, do not facilitate the implementation of continuous flow systems, thus remain limited to the specific, single-use applications in which they excel.

As an alternative to PDMS for microfluidics, DeSimone et al. presented photocurable perfluoropolyethers (PFPEs), a group of thermoset elastomers they dubbed "Liquid Teflon" for its resistance to organic solvents.[104] It has since been used in several microfluidics demonstrations,[105–109] and more recently been synthesized in a fully-recyclable version that can be degraded back to its raw material, analogous to the processability of thermoplastics.[110] Fabrication of PFPE devices involves an initial, partial UV cure of two polymer

pieces before placing them in contact and fully curing to achieve microchannel sealing.[104] These works emphasized the value of a solvent resistant, soft polymeric material in which deformable on-chip valves, pumps, and mixers can be integrated, something that is not feasible when limited to using silicon and glass for their solvent resistance. Despite this, PFPEs have not garnered widespread attention in microfluidics, and commercially available formulations, like Fluorolink® MD700 and SIFEL®, find greater use in coating and electronic cladding applications.

Another group of polymers for microfluidics that has emerged for both chemistry and the life sciences is thiol-ene based thermoset resins.[111] This was first introduced by using Nordland Optical Adhesive (NOA), an established multi-purpose UV-curable adhesive resin, to create micropatterned "microfluidic stickers" (µPS).[112,113] These biocompatible and optically transparent devices share key rapid prototyping aspects of PDMS while overcoming some of its drawbacks, notably through greater solvent resistance and increased pressure capacity. While NOA devices have proven excellent for rapid prototyping of solvent-resistant devices, they run into similar issues of low-throughput device fabrication as PDMS. Due to the material rigidity upon curing, NOA necessitates soft master molds, most often made of PDMS, to facilitate de-molding, intrinsically linking its fabrication workflow to that of PDMS.

Perhaps the most recently promising of this group of materials are off-stoichiometry thiol-ene (OSTE) and off-stoichiometry thiol-ene-epoxy (OSTE+) polymers, commercialized under the name Ostemer®, that have been developed specifically for microfluidics applications.[111] Similar to NOA, OSTE materials possess good biocompatibility, solvent resistance, and optical properties. In contrast to NOA, however, OSTE materials remain elastomeric after an initial UV-curing micropatterning step,[114] enabling facile de-molding from standard (rigid) soft lithography master molds. A subsequent heat cure step allows dry bonding to a variety of substrates[115] and, notably, renders the material mechanically stiff (~1 GPa) to allow for increased pressure capacity. The OSTE material formulation can be tuned such that the final cured material retains elastomeric properties to enable the integration of both stiff and flexible components in the same microfluidic device. Additionally, OSTE fabrication has been shown to be compatible with reaction injection molding,[116] giving scope for the fabrication quantity scale-up of these thiol-ene devices. While the material cost is greater than that of thermoplastics, and approximately two

times the cost of PDMS, OSTE materials offer an advantageous set a of material properties and fabrication practicalities that is growing in popularity.[117–123]

From a microfabrication standpoint, OSTE materials have significant commonalities with sTPEs in that they both allow for rapid prototyping, yet maintain scope for scalable fabrication of polymer microfluidic devices. Their differences lie primarily in their respective fabrication mechanisms – the former being a thermoset, and the latter being a thermoplastic. sTPE thermoforming and self-bonding offers a more streamlined, and likely less expensive, fabrication workflow with fewer steps than OSTE microfabrication (consisting of mixing the two-component polymer, de-bubbling the mixture, casting over a mold, and a two-part curing process). However, OSTE material properties and its versatility in being either elastomeric or rigid can provide high value for certain applications. Indeed, each microfluidic application comes with its specific requirements of a material, and both of these materials have the potential to not only become significant additions to the microfluidics designer's toolset, but also support the expansion of the field as a whole. **Table 1.1** presents a comparative generalized summary of microfluidic materials and their key material and microfabrication properties.

Finding the perfect material that combines optimal material properties for the application at hand with rapid, low-cost, accessible, and transferrable fabrication methods, is a challenging, if not impossible task. A balance must be struck amongst these material characteristics to encourage the continued development of microfluidics in key application areas, two of which, cell biology and chemical synthesis, will be discussed further below. While the various applications of microfluidics have been previously alluded to, the following sections elaborate on the utility of microfluidics in both cell biology and chemical synthesis, areas long-identified as would-be beneficiaries of a microfluidic revolution. They additionally evaluate the bottlenecks in these fields related to conventional materials that have hindered their progress.

Table 1.1. Comparative table of microfluidic material properties, summarizing advantages and drawbacks of available materials for given applications.

	PDMS	Glass/ Silicon	Hard TP	sTPE	Thermoset (OSTE)
Optical properties	Good	Excellent	Good	Good	Good
Biocompatible	Yes	Yes	Yes	Yes	Yes
Drug absorption	High	Low	Low	Low	Low
Solvent resistance	Poor	Excellent	Moderate/ Good	Moderate/ Good	Moderate/ Good
Ease of microchannel formation	Easy, slow. Casting of liquid pre-polymer, thermal cure. Soft material de-molding	Difficult, slow. Chemical or high-energy dry etching	Moderate, fast. High temperature / pressure, robust molds required	Easy, fast. Melt-processing, soft material de-molding	Easy, fast. Casting of liquid pre-polymer, UV cure. Soft material de-molding
Resolution	<50 nm	10 nm	<50 nm	<50 nm	<50 nm
Complex/multi-layer channels	Easy	Difficult	Moderate/ Difficult	Easy	Easy
Ease of bonding	Moderate. Plasma bonding or weak conformal contact bonding	Difficult. Thermal, chemical, or anodic bonding	Moderate. Thermal or solvent assisted bonding	Easy. Self-bonding upon conformal contact w/ and w/o heat treatment	Easy. Heat cured dry bonding
High throughput	Not suited. Multi-step procedure not easily transferred. Plasma bonding	Suited. Medium to large scale wet etching	Well suited. Injection molding, reel-to-reel processing. Low cost per device	Well suited. Injection molding, reel-to-reel processing	Suited. Reaction injection molding.
Accessibility	High. Low equipment cost, low technical threshold	Low. High-cost, hazardous chemicals involved	Moderate. Possible, but expensive at small scales.	High. Low equipment cost, low technical threshold	High. Low equipment cost, low technical threshold
Cost	Low/ Moderate	High	Low/ Moderate	Low	Low/ Moderate

1.3   MICROFLUIDICS FOR CELL CULTURE

1.3.1   **In vitro Cell Culture**

Since its advent more than one century ago,[124] *in vitro* cell culture techniques have allowed the study of human cells outside of the body, traditionally in two-dimensional (2D) models based in plates or flasks, whereby cells are taken from the body, seeded onto a protein-coated plastic substrate, and incubated at body temperature and elevated humidity. Key aspects of cell behavior, such as growth, differentiation, migration, and death in response to biological, chemical, physical, and material cues can subsequently be studied in an attempt to better understand how the human body functions and to develop therapeutics and biomaterials.[125] *In vitro* cell culture provides a necessary alternative to non-analogous animal models and inherently restrictive human clinical studies; it has undeniably been the basis of advancement in modern biology.

That being said, the reductionist, static approach of conventional *in vitro* cell biology lacks the intrinsic complexity of cell differentiation, tissue function, and drug response that exist in *in vivo* systems,[126] failing to recreate the intricate and dynamic mechanical and biochemical microenvironments (e.g., extracellular matrix, pH, temperature, chemical and gas gradients, and shear stress) in the human body (**Figure 1.4**).[127] These cues are vital in the development and behavior of cells that determine their phenotype and ultimate function, and their exclusion can result in poorly informed translations to *in vivo* biology.[128] These imperfections can further be evidenced in the insufficient predicting power of drug safety and efficacy in existing pharmaceutical research models, where poor translation between preclinical methods and clinical trials results in increasing attrition rates in drug development,[129] resulting in increasingly inefficient and costly processes.
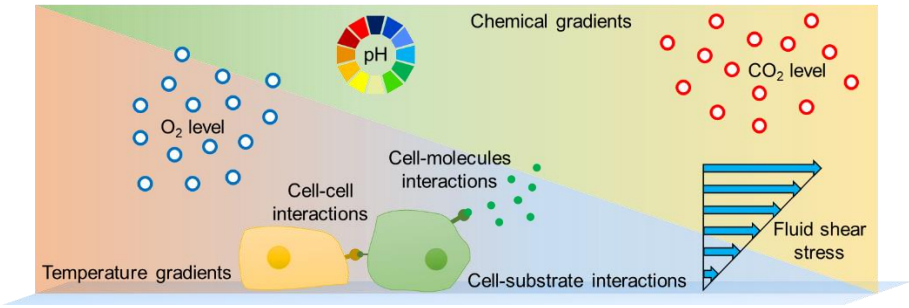
Figure 1.4. Illustration of the cell microenvironment. Factors such as temperature, chemical gradients, pH, gas concentrations, fluid shear stress, cell-cell interactions, cell-molecule interactions, and cell-substrate interactions all play a role in determining cell development and behavior. In comparison to conventional *in vitro* cell culture platforms, microfluidics can enable greater control of the cell microenvironment and facilitate cell co-culture models. Figure adapted from reference.[127]

1.3.2 The Microfluidic Advantage in Cell Culture

The incorporation of microfluidic techniques in *in vitro* cell culture research offers researchers the possibility to address some of the deficiencies that have limited our more complete understanding of human biology. The use of microfluidics can entail the following advantages when applied to cell culture:

(i)   Control of microenvironment: leveraging precision fluid control and micro-scale geometries, microfluidics allows the fabrication of more *in vivo*-like 2D and 3D extracellular matrix (ECM) structures and increases the user's control over the mechanical and biochemical environments experienced by cells. This can be done through the dosing or constant perfusion of nutrients, gases, and other soluble factors and the imposition of mechanical stresses (e.g., fluid shear, compressive and tensile stresses) with highly localized spatiotemporal precision and physiological relevance.[130] The flexibility and customizability of microfluidic devices further enhance the range of conditions that can be simulated, and consequently, the amount of relevant information that can be obtained.

(ii)   Complex cell behavior: working on the scale of microfluidic channels inherently implies handling cells in much smaller

quantities, reducing heterogeneity in cell cultures[131] and allowing the more focused study of complex cells behavior that is not feasible on larger scales, such as the relationship between collective cell migration and single-cell movements.[132] Indeed, microfluidics allows the concentrated probing of single cells through techniques of cell confinement[133] and "label-free" cell sorting,[9] often taking advantage of droplet-based techniques.

(iii)   High throughput analysis: parallelization and the incorporation of *in situ* monitoring and analysis has allowed continuous high throughput assays,[134] and direct on-chip analysis of living cells in less invasive manners.[135] Optical analysis, electrode arrays,[136] biosensors,[137] and antibody capture structures[138] can all be directly integrated into a device and multiply the amount of information obtained from a single experiment as well as the speed at which it is gathered. The versatility of microfluidic platforms also allows them to be coupled with analytical chemistry systems for highly accurate and reproducible characterization.[139]

(iv)   Reagent consumption: replacing macroscopic cell culture with miniaturized devices allows the use of far smaller quantities of both biological reagents and cells themselves. In addition to a transition toward more sustainable practices and savings on costly materials, such as cells, culture media, and drug compounds, this is particularly interesting in applications involving cells with limited availability, such as human primary cells (i.e., those taken directly from patients as opposed to from immortalized cell lines).[140] The parallelization and automation in microsystems can be used to streamline processes and further reduce material consumption and operating costs.

(v)   Cell co-culture: *in vivo*, the aforementioned biochemical and mechanical cues that govern cell differentiation and function are closely related to the presence of cells of different types in close proximity to one another (e.g., tissue-tissue interfaces).[141] Co-cultures in macro-scale models lack sufficient complexity and often rely on planar substrates.[142,143] 3D co-culture models exist,[144,145] but are limited by their cellular resolution and screening possibilities. Microfluidics provides a platform more suited to establishing and controlling co-cultures. Its precision,

high-throughput nature allows combinatorial approaches for rapid screening of co-cultured cells with variable soluble factors[146] down to single-cell resolution.[147]

These micro-scale approaches to cell culture, which can more closely mimic *in vivo* cellular microenvironments and provide the ability for complex and high-throughput operations with low material input, have provided promising new insights toward better understanding human biology and may allow us to address questions otherwise impossible with conventional methods.

1.3.3 Microfluidic Cell Culture Development and Bottlenecks

Building on the demonstrations of improved cell culture methods using microfluidics, the notion of the "organ-on-chip" (OOC) emerged, representing the cutting-edge of microfluidic cell culture. OOCs are specialized *in vitro* models typically defined by their attempt to simulate three crucial aspects of human organ functional units: intricate mechanical and biochemical environments, 3D microarchitecture with spatially defined multiple cell types, and functional tissue-tissue interfaces.[148] These platforms permit the investigation of complex human physiology and the organ-level response to diseases, drugs, and biomaterials. They provide the potential to complement (and perhaps one day replace) conventional *in vitro* cell culture models as well as the imprecise and ethically questionable animal models that currently dominate biological research.[149]

While far from technologically mature, OOC platforms have been developed to recapitulate a wide range of human organs and tissues, including the liver,[150] lung,[151] kidney,[152] heart,[153] intestine,[154] bone marrow,[155] nerve,[156] blood vessels,[157] and blood-brain barrier.[158] Their enhanced complexity, based on microfluidic cell culture techniques, has been shown to increase cell differentiation and drug transport, resulting in toxicity responses more similar to those *in vivo* when compared to findings from conventional cell culture models.[159] The use of OOC devices with induced pluripotent stem cells is particularly interesting, as it gives scope for patient-derived systems of microfluidic devices toward a patient-specific "human-on-chip" network of interconnected organ-level functions, which has the potential to be the future of personalized medicine.

Current microfluidic cell culture and OOC devices are most commonly constructed in PDMS, owing to its ever-prevailing position as the established standard material in microfluidics for biology for the reasons discussed above, if not primarily for the lack of a preferable alternative. Taking into account the aforementioned drawbacks of PDMS, these problems limit the advancement and utility of these platforms and serve to highlight the necessity of new material solutions in microfluidics. Most notably, the absorption of hydrophobic molecules, unfavorable hydrophobic recovery behavior, and non-transferable, low-throughput fabrication procedure of PDMS represent significant bottlenecks. These have mitigated the efforts to push microfluidic cell culture technology from its research-based roots toward its potential as a mainstream toolset for pharmaceutical and biomaterial screening to offer an alternative to current industrial methods.

1.3.4   Soft Thermoplastic Elastomer for Cell Biology

Flexdym™ has been demonstrated to be advantageous in the context of microfluidic cell culture. Specifically, at the cutting-edge of microfluidics in biological and drug development research, the sTPE addresses some of the key material limitations associated with microfluidic cell culture progress. It has the potential to play a pivotal role in the advancement and wider acceptance of microfluidic platforms as scientifically robust and industrially viable solutions to the growing need for improved biomimetic models and therapeutic screening technologies.

In addition to the primarily fabrication-focused advantages of sTPE materials discussed above, Flexdym™ also exhibits an enhanced hydrophilization behavior that is highly pertinent to its use for microfluidic cell culture. Like PDMS, Flexdym™ naturally exhibits hydrophobic surface behavior, which for cell culturing often requires surface hydrophilization before use. In contrast to the rapid hydrophobic recovery of PDMS, the sTPE shows highly stable plasma-activated hydrophilization for days.[97] Flexdym™ possesses EB blocks that are mobile at room temperature (above their negative T_g), similar to the mobile oligomeric PDMS chains that ultimately induce PDMS's characteristic return to a hydrophobic surface state. However, the EB blocks are covalently bonded to the PS blocks, which remain immobile (below their positive T_g) and serve to maintain the plasma-modified surface properties. Thus, in contrast with PDMS devices, Flexdym™ devices for cell culture may be stored without losing its

surface hydrophilicity. This could free the device end-user from this final device preparation step, whereby a chip manufacturer could instead handle the hydrophilization process and the devices would remain operational with some shelf-life. The hydrophilization and low absorption characteristics of Flexdym™ place it more in line with the behavior of pure PS,[97,160,161] the most ubiquitous and well-understood material for cell culture applications.

1.4 MICROFLUIDICS FOR FLOW CHEMISTRY

1.4.1 Microreactors for Chemical Synthesis in Flow

While the early development of microfluidics held high hope for uses in synthetic chemistry (indeed, many of the initial advances in microfluidics were focused on chemical analysis[162] and synthesis[163–166]), the emphasis soon shifted toward its utility for cell biology.[167] That being said, the same fluid physical properties of large surface-area-to-volume ratios for rapid heat and mass transfer and highly controllable laminar flow that have proven to be advantageous for biologists have long been attractive to chemists.[168] When compared to conventional batch methods of chemical synthesis, the key benefits that microfluidic systems can deliver are summarized below:

(i)   Speed and selectivity: while it can be challenging to directly compare the speed of reactions conducted in batch with those in microfluidic devices (batch reactions are often engineered to ensure completion by running longer than might be required, whereas microfluidic reactions allow closer monitoring for termination[169]), space-time yields of microfluidic reactors are consistently reported to be higher than their batch counterparts.[170] This enhanced reaction speed is particularly interesting in studies aiming to optimize reactions, or otherwise rapidly acquire large amounts of chemical information in a short time using high-throughput screening methods and precise control over reaction conditions.[171] This will certainly be the case for reactions that are limited by mass transfer, where the micro-scale dimensions of microfluidic reactors will increase diffusion-based reaction rates.[172] Additionally, in reactions that can produce more than one product, which are highly dependent on local kinetic and thermodynamic conditions, the increased control over

heat and mass transport in microchannels gives greater control over individual product selection, providing for more efficient syntheses that reduce reagent consumption and can simplify downstream processes.[173]

(ii)   Multistep, multiphase synthesis: taking advantage of unprecedented fluid manipulation and integration of discrete and parallel operations on a single device, microreactors can enable the facile and continuous implementation of multistep reactions. Where the step-wise manner in which batch reactors must perform these reactions can be time and space-consuming and inefficient, microfluidic flow chemistry has shown great potential to simplify these processes with proper device design and manipulation.[174–176] Again, taking advantage of large surface-area-to-volume ratios, microfluidics has the potential to produce highly effective interactions between different phases in multiphase synthesis. The increased control over fluid interfaces and mixing of flows has shown increased reaction rate and selectivity in reactions involving gas-liquid[177] and gas-liquid-solid[178] interactions involving heterogeneous catalysis.[179] The walls of microchannels themselves can be used as solid supports of catalyst coatings for direct integration.[180]

(iii)   Safe, small footprint reactions: flow chemistry with microfluidics entails miniaturized devices that intrinsically have small footprints. While this comes as no surprise, when compared on a per-kilogram of product basis, microreactors will most often demand less space.[181] This space-saving is compounded by the fact that more effective heat transfer in microchannels reduces the need for the additional, and large, heat exchangers required for bulk reactions. Closely related to this, the rapid heat transfer and small instantaneous reaction volumes involved in microreactors allow the safer processing of highly exothermic reactions[182] and handling of highly toxic, reactive, or otherwise dangerous reagents and their intermediates.[50] Moreover, the small characteristic dimensions of microfluidic channels facilitate more homogeneous light irradiation during photoreactions (**Figure 1.5**).[183]
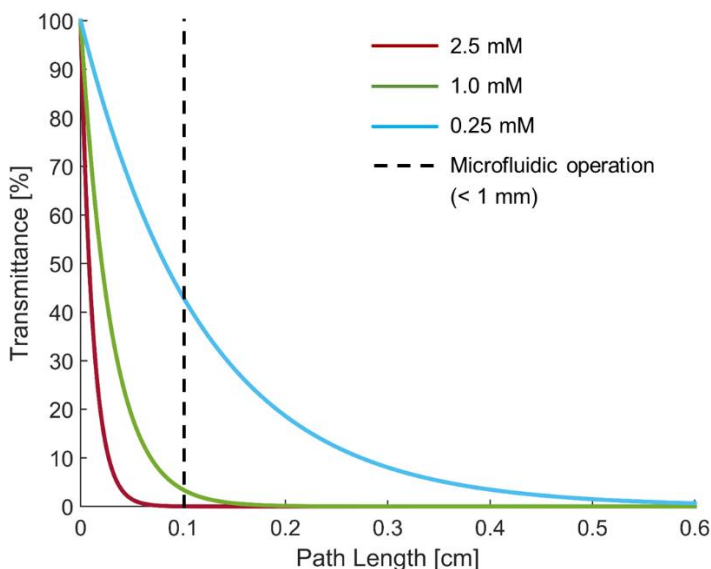
Figure 1.5. The attenuation of light (*A*) traveling through a substance is described by the Beer-Lambert Law, $A = \varepsilon c l$, where ε is the molar attenuation coefficient of a given molecule, c is the concentration of the molecule, and l is the path length of the light. Using a common photocatalyst, tris(bipyridine)-ruthenium(II) chloride (ε=14600 M^{-1} cm^{-1} in methanol), as an example, the transmittance of light (%T=100%×10$^{(-\varepsilon c l)}$) is plotted against the light path length in solutions at varying photocatalyst concentrations. It can be seen that at a standard photocatalyst concentration (2.5 mM), less that 0.1% of incident light is transmitted beyond 0.1 cm into the solution. The dashed line represents the upper threshold of what is considered as microfluidic dimensions (< 1 mm). This underscores the advantages of using micro-scale reaction vessels (i.e., microfluidic channels) in a photochemistry context. Figure adapted from reference.[184]

(iv)   Green chemistry: taking into account the above features of microfluidics as applied to chemical synthesis, a microfluidics-encouraged shift toward greener, more sustainable chemistry practices should not be neglected.[185] Improved selectivity allows for more efficient use of reagents and simpler clean-up procedures, and when the characteristic rapid heat transfer and short residence times are factored in, significant savings on energy input can be made.

(v)   Scale-out: in the pursuit of achieving industrial-scale chemical synthesis with improved methods, the miniature scale of microfluidics is an obvious limitation; batch reactors can quite

simply produce more product (albeit less efficiently) due to their size. As opposed to scaling up the reactions and losing the advantages gained at the micro-scale, microreactors can be scaled out (i.e., multiplied in number). While at large scales, this parallelization would require sophisticated flow systems,[186] scaling out more easily facilitates the transition between lab-based development and industrial implementation, as the individual microreactors, and thus the reactions within them, in a scaled-out scheme would be unchanged from those optimized on an individual basis. This would avoid the supplementary optimization required when transferring production scales in bulk scenarios.[187]

When the versatility of microfluidic systems and their potential for analytical integration from an engineering perspective is factored in, it is clear that there are strong motivations toward performing chemistry in this format. The question then becomes, "why isn't microfluidics being used more for chemical synthesis?" To answer this question, a few key bottlenecks must be recognized, not least of which is the choice of material for microreactors.[169]

As discussed in Section 1.2, there are significant shortcomings in the mainstream microfluidic materials available today. PDMS and many common thermoplastics are not compatible with most organic solvents, swelling, or dissolving with exposure. This severely limits these materials' use for most chemical synthesis applications, without mentioning the fabrication limitations. As a result, most flow chemistry microreactors are made in solvent resistance materials, such as glass, silicon, stainless steel, and ceramics.[184] These materials have been proven worthy of a wide variety of flow chemistry work, but become more complicated when the fabrication considerations are taken into account. While metals and ceramics have not been discussed, they are similar to glass and silicon in that their fabrication techniques are rather intensive, high-cost, low-throughput, and specialized compared to those of polymeric materials, rendering them largely inaccessible to many. This highlights the need for alternative materials that can both encourage wider adoption of microfluidic flow chemistry practices as well as provide the long term scope for the transfer of flow chemistry progress from the research lab to industry, such that the advantages of microfluidics in this field can be fully realized.

1.4.2 Soft Thermoplastic Fluoroelastomer for Flow Chemistry

The sTPE class of materials provides an attractive prospect for bringing rapid fabrication and process transferability to microfluidics for chemistry. Flexdym™ and other styrenic block copolymers, however, like the polystyrene from which they are derived, do not address the need for resistance to organic solvents. Fluoropolymers, on the other hand, demonstrate high chemical inertness and resistance to organic solvents,[188,189] and present potential for utilization in microfluidic fabrication. Indeed, groups have developed fluoropolymer-based microfluidic devices. Fluoropolymer coatings of PDMS devices provide resistance to solvents and absorption of small molecules,[190,191] but still rely on the entire fabrication process of PDMS soft lithography, with the added steps of coating microchannels post-fabrication, thus have not gained wide attention. Devices made completely of fluoropolymer (including the aforementioned PFPE material) have been microfabricated with hot embossing,[75,192] 3D printing,[109] photocurable molding,[104] xurography (precision cutting),[193] and micromachining.[194] While these methods resulted in polymeric solvent resistant microfluidic devices with more facile fabrication than that of glass microfluidics, they have not been widely adopted. This is likely due to the persistence of fabrication complexities, such as additional bonding steps of rigid polymers, limited resolution, and the use of polymer precursors that limit the utility, practicality, throughput, and transferability of these techniques.

A new thermoplastic fluoroelastomer derived from an extruded fluorocarbon blend of has been developed by the creators of Flexdym™ with chemistry microfluidic applications in mind. While little material characterization has been done, the material, called "Fluoroflex," behaves similarly to its styrene-based sister-polymer in that it is a flexible material that can be rapidly hot embossed for patterning of microchannels and subsequently self-sealed with simple conformal contact, without the need for adhesive additives or additional processing steps. Moreover, given its fluoropolymer origins, it is expected to exhibit enhanced resistance to organic solvents when compared to PDMS and other non-fluorinated thermoplastics. These material characteristics suggest its potential to address the need for alternative materials in microfluidics for chemical synthesis from two perspectives: the appropriate material properties to be effectively applied to chemical synthesis and the fabrication processes that are favorable for lab-scale research as well as the large-scale production that would be necessary for the widespread adoption of flow chemistry techniques that has long been posited but never realized.

1.5   AIMS AND SCOPE OF DISSERTATION

There is currently a lack of material options for microfluidic device fabrication that allow rapid prototyping in scientific research and development contexts but also have the potential to easily be transitioned to larger-scale industrial development at low cost.

The material properties of sTPEs have shown the potential to serve as effective substrates for microfluidic devices that allow a wide range of applications. Importantly, their thermoplastic fabrication methods that bridge the gap between small-scale and large-scale production can allow the wider dissemination of microfluidic techniques. This capability to straightforwardly use a single material for innovative research and technological validation as well as for subsequent high-throughput commercial implementation introduces the, until now, unrealized prospect of microfluidic translation and could have a large impact on not only the development of microfluidic technologies but the diverse fields in which their benefits can be utilized.

However, while promising, limited reports of using sTPEs for microfluidics exist, representing a gap in the knowledge needed to inform their utility and better understand their potential as microfluidic devices.

The aim of this PhD dissertation is to further establish the sTPEs introduced above – Flexdym™ and Fluoroflex – as alternative, lower-cost, and higher-adoption materials that allow for effective and scalable implementation of microfluidic systems for cell culture and flow chemistry.

In the case of Flexdym™, which targets microfluidic cell culture, the objective is to leverage its unique microfabrication properties, building on previously established material and biological validation, to enable expanded microfluidic cell culture applications with the material. For Fluoroflex, which targets microfluidic flow chemistry, the objective is to build the foundational material characterization data and proof-of-concept demonstrations necessary to enable the informed fabrication and use of Fluoroflex as a flow chemistry microreactor. While the two materials target different end-uses, both sets of experimental work share a focus of developing facile and robust fabrication methodologies toward fully exploiting the ostensible advantages of sTPE materials that have

been previously presented but supported by only limited practical demonstration.

This work is approached from two perspectives:

1. Characterizing material and associated microfluidic platform properties in order to inform their capacity for given application areas while keeping transferable and high-throughput fabrication considerations in mind.

2. Capitalizing on novel sTPE material properties with demonstrations of sTPE devices that may be applied to microfluidic cell culture and flow chemistry to provide scope for wider use and subsequent advancement in these fields.

Chapter 2 describes the development of a membrane-based cell culture platform based on Flexdym™ and commercially available polycarbonate membranes. This fully thermoplastic system enables streamlined fabrication of the "barrier model" microfluidic geometry, commonly used for OOC devices. The spontaneous adhesion that occurs between the sTPE and polycarbonate membranes is evaluated through delamination testing, and composite devices are subsequently evaluated with cell culture trials.

Chapter 3 presents the material characterization and device microfabrication of Fluoroflex. Among the range of microfluidics-pertinent material properties characterized is Fluoroflex's chemical resistance, critical for informing its use for microfluidic flow chemistry. A system of modular microfluidics is demonstrated, taking advantage of Fluoroflex's rapid and reversible self-sealing.

Chapter 4 further explores Fluoroflex's utility for flow chemistry applications through preliminary work toward a microfluidic packed bed photoreactor. PDMS microbeads are synthesized and used as polymer supports for photoactive molecules inside of a Fluoroflex microchannel with an on-chip functionalization procedure. Functionalized microbeads are also investigated for their effectiveness for photocatalytic reactions.

Finally, Chapter 5 presents a flow chemistry microreactor market study that provides industrial context to the material characterization and microfluidic demonstration of Fluoroflex in Chapters 3 and 4. It consists of a microreactor competitive technology analysis, flow chemistry researcher interviews, and a

market size estimation based on publication metrics, with the aim of evaluating the market potential of a Fluoroflex microreactor product.

1.6 REFERENCES

[1]   G. M. Whitesides, *Nature* **2006**, *442*, 368.

[2]   D. J. Beebe, G. A. Mensing, G. M. Walker, *Annu. Rev. Biomed. Eng.* **2002**, *4*, 261.

[3]   K. C. Bhargava, B. Thompson, N. Malmstadt, *Proc. Natl. Acad. Sci. U. S. A.* **2014**, *111*, 15013.

[4]   D. Figeys, D. Pinto, *Anal. Chem.* **2000**, *72*, 330.

[5]   N. Graber, H. Lüdi, H. M. Widmer, *Sensors Actuators B Chem.* **1990**, *1*, 239.

[6]   T. Razzaq, C. O. Kappe, *Chem. - An Asian J.* **2010**, *5*, 1274.

[7]   C. L. Hansen, E. Skordalakes, J. M. Berger, S. R. Quake, *Proc. Natl. Acad. Sci.* **2002**, *99*, 16531.

[8]   P. S. Dittrich, A. Manz, *Nat. Rev. Drug Discov.* **2006**, *5*, 210.

[9]   A. Reece, B. Xia, Z. Jiang, B. Noren, R. McBride, J. Oakey, *Curr. Opin. Biotechnol.* **2016**, *40*, 90.

[10]   C. M. Pandey, S. Augustine, S. Kumar, S. Kumar, S. Nara, S. Srivastava, B. D. Malhotra, *Biotechnol. J.* **2018**, *13*, 1700047.

[11]   S. Mashaghi, A. Abbaspourrad, D. A. Weitz, A. M. van Oijen, *TrAC - Trends Anal. Chem.* **2016**, *82*, 118.

[12]   A. Manz, J. C. Fettinger, E. Verpoorte, H. Lüdi, H. M. Widmer, D. J. Harrison, *TrAC - Trends Anal. Chem.* **1991**, *10*, 144.

[13]   C. S. Effenhauser, A. Manz, H. M. Widmer, *Anal. Chem.* **1993**, *65*, 2637.

[14]   S. C. Jacobson, A. W. Moore, J. M. Ramsey, *Anal. Chem.* **1995**, *67*, 2059.

[15]   H. Becker, C. Gärtner, *Electrophoresis* **2000**, *21*, 12.

[16]   S. C. Jacobson, R. Hergenroder, L. B. Koutny, J. M. Ramsey, *Anal. Chem.* **1994**, *66*, 1114.

[17]   D. J. Harrison, A. Manz, Z. Fan, H. Luedi, H. M. Widmer, *Anal. Chem.* **1992**, *64*, 1926.

[18]   A. Sayah, D. Solignac, T. Cueni, M. A. . Gijs, *Sensors Actuators A Phys.* **2000**, *84*, 103.

[19]   H. . Wang, R. . Foote, S. . Jacobson, J. . Schneibel, J. . Ramsey, *Sensors Actuators B Chem.* **1997**, *45*, 199.

[20]   J. Liu, J. Shang, J. Tang, Q.-A. Huang, *J. Microelectromechanical Syst.* **2011**, *20*, 909.

[21]   Z. J. Jia, Q. Fang, Z. L. Fang, *Anal. Chem.* **2004**, *76*, 5597.

[22]   P. B. Allen, D. T. Chiu, *Anal. Chem.* **2008**, *80*, 7153.

[23]   D. J. Harrison, K. Fluri, K. Seiler, Z. Fan, C. S. Effenhauser, A. Manz, *Science (80-.).* **1993**, *261*, 895.

[24]   C. Hnatovsky, R. S. Taylor, E. Simova, P. P. Rajeev, D. M. Rayner, V. R. Bhardwaj, P. B. Corkum, *Appl. Phys. A Mater. Sci. Process.* **2006**, *84*, 47.

[25]   N. Burshtein, S. T. Chan, K. Toda-Peters, A. Q. Shen, S. J. Haward, *Curr. Opin. Colloid Interface Sci.* **2019**, *43*, 1.

[26]   T.-L. Chang, Z.-C. Chen, Y.-W. Lee, Y.-H. Li, C.-P. Wang, *Microelectron. Eng.* **2016**, *158*, 95.

[27]   S.-J. Paik, S. Byun, J.-M. Lim, Y. Park, A. Lee, S. Chung, J. Chang, K. Chun, D. "Dan" Cho, *Sensors Actuators A Phys.* **2004**, *114*, 276.

[28]   C. Iliescu, H. Taylor, M. Avram, J. Miao, S. Franssila, *Biomicrofluidics* **2012**, *6*, 1.

[29]   D. C. Duffy, J. C. McDonald, O. J. A. Schueller, G. M. Whitesides, *Anal. Chem.* **1998**, *70*, 4974.

[30]   J. M. K. Ng, I. Gitlin, A. D. Stroock, G. M. Whitesides, *Electrophoresis* **2002**, *23*, 3461.

[31]   R. Kane, S. Takayama, E. Ostuni, D. Ingber, G. Whitesides, *Biomaterials* **1999**, *20*, 2363.

[32]   E. Delamarche, A. Bernard, H. Schmid, B. Michel, H. Biebuyck, *Science (80-.).* **1997**, *276*, 779.

[33]   T. C. Merkel, V. I. Bondar, K. Nagai, B. D. Freeman, I. Pinnau, *J. Polym. Sci. Part B Polym. Phys.* **2000**, *38*, 415.

[34]   M. K. Chaudhury, G. M. Whitesides, *Langmuir* **1991**, *7*, 1013.

[35]   J. Zhou, A. V. Ellis, N. H. Voelcker, *Electrophoresis* **2010**, *31*, 2.

[36]   G. M. Whitesides, E. Ostuni, X. Jiang, D. E. Ingber, *Annu. Rev. Biomed. Eng.* **2001**, *3*, 335.

[37]   J. R. Anderson, D. T. Chiu, R. J. Jackman, O. Cherniavskaya, J. C. McDonald, H. Wu, S. H. Whitesides, G. M. Whitesides, *Anal. Chem.* **2000**, *72*, 3158.

[38]   D. Qin, Y. Xia, A. Black, G. Whitesides, *J. Vac. Sci. Technol. B Microelectron. Nanom. Struct.* **1998**, *16*, 98.

[39]   K. Stephan, P. Pittet, L. Renaud, P. Kleimann, P. Morin, N. Ouaini, R. Ferrigno, *J. Micromechanics Microengineering* **2007**, *17*, N69.

[40]   M. K. CHAUDHURY, G. M. WHITESIDES, *Science (80-.).* **1992**, *255*, 1230.

[41]   J. C. McDonald, D. C. Duffy, J. R. Anderson, D. T. Chiu, H. Wu, O. J. Schueller, G. M. Whitesides, *Electrophoresis* **2000**, *21*, 27.

[42]   M. A. Unger, H. Chou, T. Thorsen, A. Scherer, S. Quake, *Science (80-.).* **2000**, *288*, 113.

[43]   E. Berthier, E. W. K. Young, D. Beebe, *Lab Chip* **2012**, *12*, 1224.

[44]   S. Takayama, E. Ostuni, P. LeDuc, K. Naruse, D. E. Ingber, G. M. Whitesides, *Nature* **2001**, *411*, 1016.

[45]   P. J. Hung, P. J. Lee, P. Sabounchi, N. Aghdam, R. Lin, L. P. Lee, *Lab Chip* **2005**, *5*, 44.

[46]   H. Yu, C. M. Alexander, D. J. Beebe, *Lab Chip* **2007**, *7*, 726.

[47]   J. W. Song, L. L. Munn, *Proc. Natl. Acad. Sci.* **2011**, *108*, 15342.

[48]   P. J. Cavnar, E. Berthier, D. J. Beebe, A. Huttenlocher, *J. Cell Biol.* **2011**, *193*, 465.

[49]   R. Sudo, S. Chung, I. K. Zervantonakis, V. Vickerman, Y. Toshimitsu, L. G. Griffith, R. D. Kamm, *FASEB J.* **2009**, *23*, 2155.

[50]   C. C. Lee, G. Sui, A. Elizarov, C. J. Shu, Y. S. Shin, A. N. Dooley, J. Huang, A. Daridon, P. Wyatt, D. Stout, H. C. Kolb, O. N. Witte, N. Satyamurthy, J. R. Heath, M. E. Phelps, S. R. Quake, H. R. Tseng, *Science (80-.).* **2005**, *310*, 1793.

[51]   Y. Yu, W. Wei, Y. Wang, C. Xu, Y. Guo, J. Qin, *Adv. Mater.* **2016**, *28*, 6649.

[52]   J. Sun, L. Zhang, J. Wang, Q. Feng, D. Liu, Q. Yin, D. Xu, Y. Wei, B. Ding, X. Shi, X. Jiang, *Adv. Mater.* **2015**, *27*, 1402.

[53]   J. N. Lee, C. Park, G. M. Whitesides, *Anal. Chem.* **2003**, *75*, 6544.

[54]   B. Y. Kim, L. Y. Hong, Y. M. Chung, D. P. Kim, C. S. Lee, *Adv. Funct. Mater.* **2009**, *19*, 3796.

[55]   A. R. Abate, D. Lee, T. Do, C. Holtze, D. A. Weitz, *Lab Chip* **2008**, *8*, 516.

[56]   M. W. Toepke, D. J. Beebe, *Lab Chip* **2006**, *6*, 1484.

[57]   G. T. Roman, T. Hlaus, K. J. Bass, T. G. Seelhammer, C. T. Culbertson, *Anal. Chem.* **2005**, *77*, 1414.

[58]   K. J. Regehr, M. Domenech, J. T. Koepsel, K. C. Carver, S. J. Ellison-Zelski, W. L. Murphy, L. A. Schuler, E. T. Alarid, D. J. Beebe, *Lab Chip* **2009**, *9*, 2132.

[59]   X. Su, E. W. K. Young, H. A. S. Underkofler, T. J. Kamp, C. T. January, D. J. Beebe, *J. Biomol. Screen.* **2011**, *16*, 101.

[60]   T. S. Radhakrishnan, *J. Appl. Polym. Sci.* **2006**, *99*, 2679.

[61]   M. A. Eddings, M. A. Johnson, B. K. Gale, *J. Micromechanics Microengineering* **2008**, *18*, 067001.

[62]   J. S. Gewandter, R. J. Staversky, M. A. O'Reilly, *Free Radic. Biol. Med.* **2009**, *47*, 1742.

[63]   E. Berthier, J. Warrick, H. Yu, D. J. Beebe, *Lab Chip* **2008**, *8*, 852.

[64]   N. Scott Lynn, C. S. Henry, D. S. Dandy, *Lab Chip* **2009**, *9*, 1780.

[65]   D. T. Eddington, J. P. Puccinelli, D. J. Beebe, *Sensors Actuators, B Chem.* **2006**, *114*, 170.

[66]   R. Mukhopadhyay, *Anal. Chem.* **2007**, *79*, 3248.

[67]   T. D. Boone, Z. H. Fan, H. H. Hooper, A. J. Ricco, H. Tan, S. J. Williams, *Anal. Chem.* **2002**, *74*, 78 A.

[68]   S. Waheed, J. M. Cabot, N. P. Macdonald, T. Lewis, R. M. Guijt, B. Paull, M. C. Breadmore, *Lab Chip* **2016**, *16*, 1993.

[69]   D. J. Guckenberger, T. E. de Groot, A. M. D. Wan, D. J. Beebe, E. W. K. Young, *Lab Chip* **2015**, *15*, 2364.

[70]   S. A. Soper, S. M. Ford, S. Qi, R. L. McCarley, K. Kelly, M. C. Murphy, *Anal. Chem.* **2000**, *72*, 642 A.

[71]   L. Brown, T. Koerner, J. H. Horton, R. D. Oleschuk, *Lab Chip* **2006**, *6*, 66.

[72]   C. W. Tsao, L. Hromada, J. Liu, P. Kumar, D. L. DeVoe, *Lab Chip* **2007**, *7*, 499.

[73]   D. Ogończyk, J. Węgrzyn, P. Jankowski, B. Dąbrowski, P. Garstecki, *Lab Chip* **2010**, *10*, 1324.

[74]   E. W. K. Young, E. Berthier, D. J. Guckenberger, E. Sackmann, C. Lamers, I. Meyvantsson, A. Huttenlocher, D. J. Beebe, *Anal. Chem.* **2011**, *83*, 1408.

[75]   K. Ren, W. Dai, J. Zhou, J. Su, H. Wu, *Proc. Natl. Acad. Sci. U. S. A.* **2011**, *108*, 8162.

[76]   W. H. Grover, M. G. von Muhlen, S. R. Manalis, *Lab Chip* **2008**, *8*, 913.

[77]   H. Becker, C. Gärtner, *Anal. Bioanal. Chem.* **2008**, *390*, 89.

[78]   C. W. Tsao, D. L. DeVoe, *Microfluid. Nanofluidics* **2009**, *6*, 1.

[79]   J. S. Kuo, D. T. Chiu, *Lab Chip* **2011**, *11*, 2656.

[80]   M. L. Hupert, W. J. Guy, S. D. Llopis, H. Shadpour, S. Rani, D. E. Nikitopoulos, S. A. Soper, *Microfluid. Nanofluidics* **2006**, *3*, 1.

[81]   G. Mehta, J. Lee, W. Cha, Y.-C. Tung, J. J. Linderman, S. Takayama, *Anal. Chem.* **2009**, *81*, 3714.

[82]   E. Roy, A. Pallandre, B. Zribi, M.-C. Horny, F. D. Delapierre, A. Cattoni, J. Gamby, A.-M. Haghiri-Gosnet, in *Adv. Microfluid. - New Appl. Biol. Energy, Mater. Sci.* (Ed.: X.-Y. Yu), InTechOpen, London, UK, **2016**.

[83]   P. Zhou, L. Young, Z. Chen, *Biomed. Microdevices* **2010**, *12*, 821.

[84]   M. Ghisari, E. C. Bonefeld-Jorgensen, *Toxicol. Lett.* **2009**, *189*, 67.

[85]   B.-Y. Pemg, C.-W. Wu, Y.-K. Shen, Y. Lin, *Polym. Adv. Technol.* **2010**, *21*, 457.

[86]   S. K. Njoroge, M. A. Witek, M. L. Hupert, S. A. Soper, *Electrophoresis* **2010**, *31*, 981.

[87]   P.-C. Chen, C.-W. Pan, W.-C. Lee, K.-M. Li, *Int. J. Adv. Manuf. Technol.* **2014**, *71*, 1623.

[88]   I. Meyvantsson, J. W. Warrick, S. Hayes, A. Skoien, D. J. Beebe, *Lab Chip* **2008**, *8*, 717.

[89]   Š. Selimović, F. Piraino, H. Bae, M. Rasponi, A. Redaelli, A. Khademhosseini, *Lab Chip* **2011**, *11*, 2325.

[90]   B. H. Jo, L. M. Van Lerberghe, K. M. Motsegood, D. J. Beebe, *J. Microelectromechanical Syst.* **2000**, *9*, 76.

[91]   A. P. Sudarsan, J. Wang, V. M. Ugaz, *Anal. Chem.* **2005**, *77*, 5167.

[92]   E. Roy, M. Geissler, J. C. Galas, T. Veres, *Microfluid. Nanofluidics* **2011**, *11*, 235.

[93]   M. D. Borysiak, K. S. Bielawski, N. J. Sniadecki, C. F. Jenkel, B. D. Vogt, J. D. Posner, *Lab Chip* **2013**, *13*, 2773.

[94]   D. Brassard, L. Clime, K. Li, M. Geissler, C. Miville-Godin, E. Roy, T. Veres, *Lab Chip* **2011**, *11*, 4099.

[95]   A. Wasay, D. Sameoto, *Lab Chip* **2015**, *15*, 2749.

[96]   E. Roy, G. Stewart, M. Mounier, L. Malic, R. Peytavi, L. Clime, M. Madou, M. Bossinot, M. G. Bergeron, T. Veres, *Lab Chip* **2015**, *15*, 406.

[97]   J. Lachaux, C. Alcaine, B. Gómez-Escoda, C. M. Perrault, D. O. Duplan, P.-Y. J. Wu, I. Ochoa, L. Fernandez, O. Mercier, D. Coudreuse, E. Roy, *Lab Chip* **2017**, *17*, 2581.

[98]   M. D. Guillemette, E. Roy, F. A. Auger, T. Veres, *Acta Biomater.* **2011**, *7*, 2492.

[99]   D. J. Case, Y. Liu, I. Z. Kiss, J. R. Angilella, A. E. Motter, *Nature* **2019**, *574*, 647.

[100]   E. Roy, J. C. Galas, T. Veres, *Lab Chip* **2011**, *11*, 3193.

[101]   A. W. Martinez, S. T. Phillips, M. J. Butte, G. M. Whitesides, Angew. Chemie Int. Ed. 2007, 46, 1318.

[102]   A. W. Martinez, S. T. Phillips, G. M. Whitesides, Proc. Natl. Acad. Sci. U. S. A. 2008, 105, 19606.

[103]   C. Carrell, A. Kava, M. Nguyen, R. Menger, Z. Munshi, Z. Call, M. Nussbaum, C. Henry, Microelectron. Eng. 2019, 206, 45.

[104]   J. P. Rolland, R. M. Van Dam, D. A. Schorzman, S. R. Quake, J. M. DeSimone, J. Am. Chem. Soc. 2004, 126, 2322.

[105]   N. S. G. K. Devaraju, M. A. Unger, Lab Chip 2011, 11, 1962.

[106]   A. Vitale, M. Quaglio, S. L. Marasso, A. Chiodoni, M. Cocuzza, R. Bongiovanni, Langmuir 2013, 29, 15711.

[107]   K. W. Bong, J. Lee, P. S. Doyle, Lab Chip 2014, 14, 4680.

[108]   Y. Huang, P. Castrataro, C. C. Lee, S. R. Quake, Lab Chip 2007, 7, 24.

[109]   F. Kotz, P. Risch, D. Helmer, B. Rapp, Micromachines 2018, 9, 115.

[110]   S. Liao, Y. He, Y. Chu, H. Liao, Y. Wang, J. Mater. Chem. A 2019, 7, 16249.

[111]   D. Sticker, R. Geczy, U. O. Häfeli, J. P. Kutter, ACS Appl. Mater. Interfaces 2020, 12, 10080.

[112]   D. Bartolo, G. Degré, P. Nghe, V. Studer, Lab Chip 2008, 8, 274.

[113]   L. H. Hung, R. Lin, A. P. Lee, Lab Chip 2008, 8, 983.

[114]   C. F. Carlborg, T. Haraldsson, K. Öberg, M. Malkoch, W. Van Der Wijngaart, Lab Chip 2011, 11, 3136.

[115]   F. Saharil, C. F. Carlborg, T. Haraldsson, W. Van Der Wijngaart, Lab Chip 2012, 12, 3032.

[116]   N. Sandström, R. Z. Shafagh, A. Vastesson, C. F. Carlborg, W. van der Wijngaart, T. Haraldsson, J. Micromechanics Microengineering 2015, 25, 075002.

[117]   D. Sticker, M. Rothbauer, S. Lechner, M. T. Hehenberger, P. Ertl, Lab Chip 2015, 15, 4542.

[118]   A. Martin, S. Teychené, S. Camy, J. Aubin, Microfluid. Nanofluidics 2016, 20, 4.

[119]   L. El Fissi, R. Fernández, P. García, M. Calero, J. V. García, Y. Jiménez, A. Arnau, L. A. Francis, Sensors Actuators A Phys. 2019, 285, 511.

[120]   T. Lange, S. Charton, T. Bizien, F. Testard, F. Malloggi, Lab Chip 2020, 20, 2990.

[121]   S. R. A. Kratz, B. Bachmann, S. Spitz, G. Höll, C. Eilenberger, H. Goeritz, P. Ertl, M. Rothbauer, Sci. Rep. 2020, 10, 1400.

[122]   Y.-J. Fan, H.-Y. Hsieh, S.-F. Tsai, C.-H. Wu, C.-M. Lee, Y.-T. Liu, C.-H. Lu, S.-W. Chang, B.-C. Chen, Lab Chip 2021, DOI 10.1039/D0LC01009J.

[123]   R. Krenger, M. Cornaglia, T. Lehnert, M. A. M. Gijs, Lab Chip 2020, 20, 126.

[124]   R. G. Harrison, J. Exp. Zool. 1910, 9, 787.

[125]   K. Duval, H. Grover, L. H. Han, Y. Mou, A. F. Pegoraro, J. Fredberg, Z. Chen, Physiology 2017, 32, 266.

[126]   R. Greek, A. Menache, Int. J. Med. Sci. 2013, 10, 206.

[127]   M. L. Coluccio, G. Perozziello, N. Malara, E. Parrotta, P. Zhang, F. Gentile, T. Limongi, P. M. Raj, G. Cuda, P. Candeloro, E. Di Fabrizio, Microelectron. Eng. 2019, 208, 14.

[128]   T. Mammoto, A. Mammoto, D. E. Ingber, Annu. Rev. Cell Dev. Biol. 2013, 29, 27.

[129]   J. Bowes, A. J. Brown, J. Hamon, W. Jarolimek, A. Sridhar, G. Waldron, S. Whitebread, Nat. Rev. Drug Discov. 2012, 11, 909.

[130]   J. El-Ali, P. K. Sorger, K. F. Jensen, Nature 2006, 442, 403.

[131]   S. Halldorsson, E. Lucumi, R. Gómez-Sjöberg, R. M. T. Fleming, Biosens. Bioelectron. 2015, 63, 218.

[132]   S. Vedel, S. Tay, D. M. Johnston, H. Bruus, S. R. Quake, Proc. Natl. Acad. Sci. 2013, 110, 129.

[133]   J. Q. Boedicker, L. Li, T. R. Kline, R. F. Ismagilov, Lab Chip 2008, 8, 1265.

[134]   P. J. Hung, P. J. Lee, P. Sabounchi, R. Lin, L. P. Lee, Biotechnol. Bioeng. 2005, 89, 1.

[135]   Q. Liu, C. Wu, H. Cai, N. Hu, J. Zhou, P. Wang, Chem. Rev. 2014, 114, 6423.

[136]   G. W. Gross, A. Harsch, B. K. Rhoades, W. Göpel, Biosens. Bioelectron. 1997, 12, 373.

[137] M. B. Gu, R. J. Mitchell, B. C. Kim, **2004**, pp. 269–305.

[138] K. Sato, M. Yamanaka, H. Takahashi, M. Tokeshi, H. Kimura, T. Kitamori, *Electrophoresis* **2002**, *23*, 734.

[139] C. A. Croushore, S. Supharoek, C. Y. Lee, J. Jakmunee, J. V. Sweedler, *Anal. Chem.* **2012**, *84*, 9446.

[140] E. Berthier, J. Surfus, J. Verbsky, A. Huttenlocher, D. Beebe, *Integr. Biol.* **2010**, *2*, 630.

[141] J. Voog, D. L. Jones, *Cell Stem Cell* **2010**, *6*, 103.

[142] J. A. Spector, J. A. Greenwald, S. M. Warren, P. J. Bouletreau, F. E. Crisera, B. J. Mehrara, M. T. Longaker, *Plast. Reconstr. Surg.* **2002**, *109*, 631.

[143] E.-J. Lee, E. W. L. Chan, M. N. Yousaf, *ChemBioChem* **2009**, *10*, 1648.

[144] A. P. McGuigan, M. V. Sefton, *J. Tissue Eng. Regen. Med.* **2007**, *1*, 136.

[145] A. Y. Hsiao, Y. Torisawa, Y.-C. Tung, S. Sud, R. S. Taichman, K. J. Pienta, S. Takayama, *Biomaterials* **2009**, *30*, 3020.

[146] E. Tumarkin, L. Tzadu, E. Csaszar, M. Seo, H. Zhang, A. Lee, R. Peerani, K. Purpura, P. W. Zandstra, E. Kumacheva, *Integr. Biol.* **2011**, *3*, 653.

[147] S. Hong, Q. Pan, L. P. Lee, *Integr. Biol.* **2012**, *4*, 374.

[148] E. W. Esch, A. Bahinski, D. Huh, *Nat. Rev. Drug Discov.* **2015**, *14*, 248.

[149] D. Huh, G. A. Hamilton, D. E. Ingber, *Trends Cell Biol* **2011**, *21*, 745.

[150] E. Novik, T. J. Maguire, P. Chao, K. C. Cheng, M. L. Yarmush, *Biochem. Pharmacol.* **2010**, *79*, 1036.

[151] D. Huh, B. D. Matthews, A. Mammoto, M. Montoya-Zavala, H. Y. Hsin, D. E. Ingber, *Science (80-.).* **2010**, *328*, 1662.

[152] K.-J. Jang, A. P. Mehr, G. A. Hamilton, L. A. McPartlin, S. Chung, K.-Y. Suh, D. E. Ingber, *Integr. Biol.* **2013**, *5*, 1119.

[153] A. Grosberg, P. W. Alford, M. L. McCain, K. K. Parker, *Lab Chip* **2011**, *11*, 4165.

[154] H. J. Kim, D. E. Ingber, *Integr. Biol.* **2013**, *5*, 1130.

[155] Y. Torisawa, C. S. Spina, T. Mammoto, A. Mammoto, J. C. Weaver, T. Tat, J. J. Collins, D. E. Ingber, *Nat. Methods* **2014**, *11*, 663.

[156] M. Shi, D. Majumdar, Y. Gao, B. M. Brewer, C. R. Goodwin, J. A. McLean, D. Li, D. J. Webb, *Lab Chip* **2013**, *13*, 3008.

[157] A. D. van der Meer, V. V. Orlova, P. ten Dijke, A. van den Berg, C. L. Mummery, *Lab Chip* **2013**, *13*, 3562.

[158] R. Booth, H. Kim, *Lab Chip* **2012**, *12*, 1784.

[159] S. N. Bhatia, D. E. Ingber, *Nat. Biotechnol.* **2014**, *32*, 760.

[160] Y. Wang, J. Balowski, C. Phillips, R. Phillips, C. E. Sims, N. L. Allbritton, *Lab Chip* **2011**, *11*, 3089.

[161] V. Jokinen, P. Suvanto, S. Franssila, *Biomicrofluidics* **2012**, *6*, 1.

[162] A. Manz, N. Graber, H. M. Widmer, *Sensors Actuators B Chem.* **1990**, *1*, 244.

[163] R. Srinivasan, S. L. Firebaugh, I.-M. Hsing, J. Ryley, M. P. Harold, K. F. Jensen, M. A. Schmidt, in *Proc. Int. Solid State Sensors Actuators Conf. (Transducers '97)*, IEEE, **n.d.**, pp. 163–166.

[164] W. Ehrfeld, K. Golbig, V. Hessel, H. Löwe, T. Richter, *Ind. Eng. Chem. Res.* **1999**, *38*, 1075.

[165] M. C. Mitchell, V. Spikmans, A. Manz, A. J. de Mello, *J. Chem. Soc. Perkin Trans. 1* **2001**, 514.

[166] E. Garcia-Egido, S. Y. F. Wong, B. H. Warrington, *Lab Chip* **2002**, *2*, 31.

[167] D. T. Chiu, A. J. deMello, D. Di Carlo, P. S. Doyle, C. Hansen, R. M. Maceiczyk, R. C. R. Wootton, *Chem* **2017**, *2*, 201.

[168] T. Schwalbe, V. Autze, G. Wille, *Chim. Int. J. Chem.* **2002**, *56*, 636.

[169] K. S. Elvira, X. C. i Solvas, R. C. R. Wootton, A. J. DeMello, *Nat. Chem.* **2013**, *5*, 905.

[170] T. Illg, V. Hessel, P. Löb, J. C. Schouten, *ChemSusChem* **2011**, *4*, 392.

[171]   K. Koch, B. J. A. van Weerdenburg, J. M. M. Verkade, P. J. Nieuwland, F. P. J. T. Rutjes, J. C. M. van Hest, *Org. Process Res. Dev.* **2009**, *13*, 1003.

[172]   R. L. Hartman, J. P. McMullen, K. F. Jensen, *Angew. Chemie - Int. Ed.* **2011**, *50*, 7502.

[173]   T. Asai, A. Takata, Y. Ushiogi, Y. Iinuma, A. Nagaki, J. Yoshida, *Chem. Lett.* **2011**, *40*, 393.

[174]   C.-C. Lee, *Science (80-.).* **2005**, *310*, 1793.

[175]   D. R. Snead, T. F. Jamison, *Angew. Chemie Int. Ed.* **2015**, *54*, 983.

[176]   L. Zhang, Q. Feng, J. Wang, J. Sun, X. Shi, X. Jiang, *Angew. Chemie Int. Ed.* **2015**, *54*, 3952.

[177]   P. W. Miller, N. J. Long, A. J. de Mello, R. Vilar, H. Audrain, D. Bender, J. Passchier, A. Gee, *Angew. Chemie Int. Ed.* **2007**, *46*, 2875.

[178]   J. Kobayashi, Y. Mori, K. Okamoto, R. Akiyama, M. Ueno, T. Kitamori, S. Kobayashi, *Science (80-.).* **2004**, *304*, 1305.

[179]   A. Tanimu, S. Jaenicke, K. Alhooshani, *Chem. Eng. J.* **2017**, *327*, 792.

[180]   V. Meille, *Appl. Catal. A Gen.* **2006**, *315*, 1.

[181]   L. Saias, J. Autebert, L. Malaquin, J.-L. Viovy, *Lab Chip* **2011**, *11*, 822.

[182]   J. Pelleter, F. Renaud, *Org. Process Res. Dev.* **2009**, *13*, 698.

[183]   M. Oelgemöller, O. Shvydkiv, Molecules 2011, 16, 7522.

[184]   M. B. Plutschack, B. Pieber, K. Gilmore, P. H. Seeberger, Chem. Rev. 2017, 117, 11796.

[185]   L. Vaccaro, D. Lanari, A. Marrocchi, G. Strappaveccia, Green Chem. 2014, 16, 3680.

[186]   C. Amador, A. Gavriilidis, P. Angeli, Chem. Eng. J. 2004, 101, 379.

[187]   N. Kockmann, M. Gottsponer, B. Zimmermann, D. M. Roberge, Chem. - A Eur. J. 2008, 14, 7470.

[188]   V. Arcella, A. Ghielmi, G. Tommasi, Ann. N. Y. Acad. Sci. 2003, 984, 226.

[189]   W. R. Dolbier, J. Fluor. Chem. 2005, 126, 157.

[190]   C. T. Riche, C. Zhang, M. Gupta, N. Malmstadt, Lab Chip 2014, 14, 1834.

[191]   T. Yang, J. Choo, S. Stavrakis, A. de Mello, Chem. – A Eur. J. 2018, 24, 12078.

[192]   S. Begolo, G. Colas, J. L. Viovy, L. Malaquin, Lab Chip 2011, 11, 508.

[193]   T. Hizawa, A. Takano, P. Parthiban, P. S. Doyle, E. Iwase, M. Hashimoto, Biomicrofluidics 2018, 12, 064105.

[194]   O. Cybulski, S. Jakiela, P. Garstecki, Lab Chip 2016, 16, 2198.

CHAPTER 2

Rapid Fabrication of Membrane-Integrated Thermoplastic Elastomer Microfluidic Devices for Cell Culture

Alexander H. McMillan, Emma K. Thomée, Alessandra Dellaquila, Hussam Nassman, Tatiana Segura, and Sasha Cai Lesher-Pérez

Abstract

Leveraging the advantageous material properties of recently developed soft thermoplastic elastomer materials, this work presents the facile and rapid fabrication of composite membrane-integrated microfluidic devices consisting of Flexdym™ polymer and commercially available porous polycarbonate membranes. The three-layer devices can be fabricated in under 2.5 hours, consisting of a two-minute hot embossing cycle, conformal contact between device layers, and a low-temperature baking step. The strength of the Flexdym™-polycarbonate seal was characterized using a specialized microfluidic delamination device and an automated pressure controller configuration, offering a standardized and high-throughput method of microfluidic burst testing. Given a minimum bonding distance of 200 μm, the materials showed bonding that reliably withstood pressures of 500 mbar and above, which is sufficient for most microfluidic cell culture applications. Bonding was also stable when subjected to long term pressurization (10 hours) and repeated use (10,000 pressure cycles). Cell culture trials confirmed good cell adhesion and sustained culture of human dermal fibroblasts on a polycarbonate membrane inside the device channels over the course of one week. In comparison to existing porous membrane-based microfluidic platforms of this configuration, most often made of PDMS, these devices offer a streamlined fabrication methodology with materials having favorable properties for cell culture applications and the potential for implementation in barrier model organ-on-chips.

CHAPTER 2 – RAPID FABRICATION OF MEMBRANE-INTEGRATED THERMOPLASTIC ELASTOMER MICROFLUIDIC DEVICES FOR CELL CULTURE

2.1 INTRODUCTION

The choice of the materials used to create a microfluidic device is critical to its ultimate function. A given material should be evaluated from two perspectives: its material properties and its fabrication processes. The latter becomes particularly influential when complex device geometries are desired. An increasingly relevant example of this is porous membrane-integrated microfluidic devices for cell culture, whose non-trivial construction has been the attention of much research. The use of thin, porous membranes as a cell culture substrate has shown great value for studying cell-cell signalling, cell filtration, and cell migration, in both static[1–5] and more recapitulative dynamic microfluidic models[6–8]. At the forefront of membrane-based cell culture is "organ-on-chip" (OOC) technology, which often consists of two adjacent compartments separated by a porous membrane. By culturing cells on both sides of the thin porous membrane, tissue-tissue-like interfaces can be generated that simulate critical physiological barriers, such as that of the blood-brain barrier,[9] liver,[10] and the epithelial-endothelial membranes in the lung,[11] kidney,[12] and gut,[13] among other human organs and tissues.[14–16]

While a variety of materials have been used, many of the cutting edge microfluidic membrane-based cell culture platforms have been based around polydimethylsiloxane (PDMS) devices.[17] PDMS, the most ubiquitous microfluidic material for biology, has undoubtedly shaped the advancement of microfluidics since George Whitesides' group introduced its soft lithography microfabrication techniques in 1998.[18] Its acceptance as a standard material for microfluidics can be attributed to its favorable material properties of high optical clarity, biocompatibility, and easy handling due to its elasticity and low stiffness (tensile modulus of ~1–3 MPa[19–21]). Furthermore, PDMS microfabrication could be achieved at relatively low cost and little required expertise as compared to other materials at that time.

PDMS suffers, however, from a number of drawbacks in its use as a microfluidic device substrate, the most prevalent of which are small molecule absorption, hydrophobic recovery, and transferability of fabrication. (i) Absorption of small hydrophobic molecules into the bulk of the material[22] is problematic in applications that involve soluble factors, namely drug, cell signalling, and dye compounds,[23–25] where essential concentrations can be altered and experimental outcomes changed. This severely limits the utility of PDMS for drug screening, a key area of therapeutic research and development that membrane-based cell culture platforms can address. (ii) Fast hydrophobic recovery after surface hydrophilization due to mobile polymer chains[26] limits the shelf-life of PDMS devices post-fabrication, imposing a burden on the end-user to handle the hydrophilization, whereby devices must be experimentally used within hours of their preparation for effective surface treatments and channel filling. (iii) Finally, the poor transferability of fabrication from small to large-scale limits PDMS from greater industrial implementation. While PDMS allows relatively facile fabrication of microfluidic devices when compared to glass or silicon-based microdevices,[27] its multi-step process involving liquid polymer mixing and degassing, curing, plasma bonding (or other less-traditional bonding techniques), and the aforementioned hydrophilization, does not lend itself well to being transferred to larger, industrial-scales.[28] Microfluidic models developed in labs using PDMS must thus be reimagined with different materials if large-scale implementation is to be feasible, a modification likely to have side-effects on experimental outcomes. This presents complications for encouraging the wider adoption of microfluidics to replace more conventional biological research methods in industry. Additionally, the fabrication of thin, porous PDMS membranes is time-consuming and intricate,[29–34] and further hinders the reproducible high-throughput production of PDMS membrane platforms. As an alternative, the utilization of commercially available track-etched porous polymer membranes that are biocompatible and available in a range of material compositions, thicknesses (down to 7 μm[35]), pore sizes, and porosities circumvents the custom fabrication of membranes for membrane-based cell culture devices.[36]

Track-etched membranes reflect one aspect of a growing interest in thermoplastic microfluidic devices, which can not only address some of the material property concerns around PDMS but also leverage the wealth of industrial processing knowledge that exists for this class of materials for high throughput manufacturing.[37] The fact alone that the vast majority of current cell biology research is conducted on substrates of polystyrene (PS) should not be neglected when considering the forces at play in a shift toward greater

adoption of thermoplastics for microfluidic techniques.[38] Hard thermoplastics, such as PS, polycarbonate (PC), polymethylmethacrylate (PMMA), and cyclic olefin copolymer (COC), are low-cost materials that can be melt-processed with high-throughput techniques, namely injection molding and hot embossing, and have shown much promise and utility as microfluidic substrates.[39–43] These materials, however, largely due to their rigidity (of tensile moduli in the order of ~1–4 GPa[44]), entail difficulties in processing at small scales, including the need for expensive molds and process-intensive bonding and interfacing to fluidic setups that make their use rather prohibitive to those without the sufficient means or fabrication expertise.

The introduction of a class of materials known as soft thermoplastic elastomers (sTPE) for microfluidics has provided for a unique combination of the rapid and high-throughput processing of thermoplastics with the flexible and easy handling of elastomers like PDMS.[45–48] One such commercially-available polymer called Flexdym™ (FD) has been shown to have particularly advantageous material properties for its use as a microfluidic device substrate.[49,50] It is a soft (tensile modulus of ~1 MPa) and flexible styrenic block co-polymer that is biocompatible and optically transparent. It can be rapidly hot embossed with high resolution within minutes using microfluidic molds that are simple and low-cost as compared to the molds needed for molding hard thermoplastics, which tend to be more expensive and require more complex fabrication. Thanks to its hard and soft block co-polymeric structure, FD has adhesive and cohesive bonding properties to allow for facile and spontaneous sealing of microfluidic devices after molding without the need for additional adhesives or plasma surface treatment.[49] Indeed, FD has been described as a "slow" adhesive polymer foil and has been shown to create reversible bonds with itself and other polymer surfaces, which can be strengthened at elevated temperatures.[49,51] The sTPE has additionally demonstrated more stable hydrophilization with plasma treatment and lower absorption of small hydrophobic molecules as compared to PDMS.[49] This material very importantly offers the transferability of fabrication that both PDMS and hard thermoplastics lack; it permits rapid and accessible fabrication in research laboratory settings, while also providing a feasible scope for scaling up to industrial production. This transition can be made without altering the material and, very critically, any influence this may have on the test at hand.

In this work, we present a composite microfluidic device based on the FD polymer and a commercially available porous polycarbonate membrane designed for use as a membrane-integrated cell culture platform. We developed

a rapid and scalable fabrication protocol and characterized the bonding integrity that can be achieved as well as the flow characteristics in devices representing typical microfluidic cell culture geometries for a practical translation of device pressure capabilities. Finally, we confirmed that cell attachment and sustained cell adhesion and culturing was possible inside the devices, giving a proof-of-concept for a facile, robust, and scalable microfluidic platform for membrane-based cell culture.

2.2 MATERIALS AND METHODS

2.2.1 Composite Device Microfabrication

Mold Fabrication

Microfluidic molds were fabricated using Ordyl® SY 300 dry film negative photoresist (55 µm thickness, ElgaEurope s.r.l., Milan, Italy) on 75 x 50 mm borosilicate glass slides (Corning Inc., Corning, NY, USA). After cleaning with acetone and isopropanol and dehydration of the glass slide on a hotplate (Thermo Fisher Scientific, Waltham, MA, US) for 5 minutes at 150 °C, two sheets of photoresist were laminated onto the slide using a thermal laminator (325R6, FalconK, France) at 120 °C and roller speed 4. Using an exposure masking UV LED lamp (UV-KUB 2, Kloé, Montpellier, France) the photoresist was then exposed to UV light (365 nm, 23.3 mW cm^{-2}), for 7 seconds with a film photomask (Selba S.A., Versoix, Switzerland) and subsequently developed with a solvent blend (Ordyl® SY Developer, ElgaEurope s.r.l., Milan, Italy) for approximately 10 minutes to remove unexposed sections of the photoresist. The mold fabrication process was finished with a hard bake of 30 minutes at 120 °C on a hotplate. This mold can be used for both sTPE hot embossing as well as PDMS soft lithography. Molds with thicker features can be achieved by laminating successive layers of the photoresist before the exposure masking step.

Hot Embossing

Extruded sheets of FD polymer (Eden Microfluidics SAS, Paris, France) of 1.3 mm thickness were cut with scissors to approximately the size of the glass slide and cleaned with tape to remove any large dust particles (**Figure 2.1a**). They were then manually placed into contact with the photoresist features on the mold, ensuring good contact and minimal air bubbles between the FD sheet

and the mold. A clean, blank glass slide was then similarly pressed into contact with the other side of the FD sheet and the entire assembly (mold-FD-glass slide) was placed in a vacuum-assisted heat press (Sublym100™, Eden Microfluidics SAS, Paris, France) between two aluminum plates. The assembly was subjected to an isothermal hot embossing cycle of 2 minutes at 150 °C and 0.7 bar applied pressure, corresponding to approximately 6.5 bar of pressure on the stacked assembly. Spacers of 2.3 mm thickness were additionally placed in between the aluminum plates to control for a final FD thickness of 1.1mm (**Figure 2.1b**). The assembly was removed and separated using isopropanol to facilitate separation of the hot embossed FD from the mold and glass slide. Four holes were punched in one sTPE sheet with a steel hole punch at the appropriate port locations, and the resulting micropatterned FD could again be cut with scissors to the desired size before microfluidic device assembly (**Figure 2.1c**).
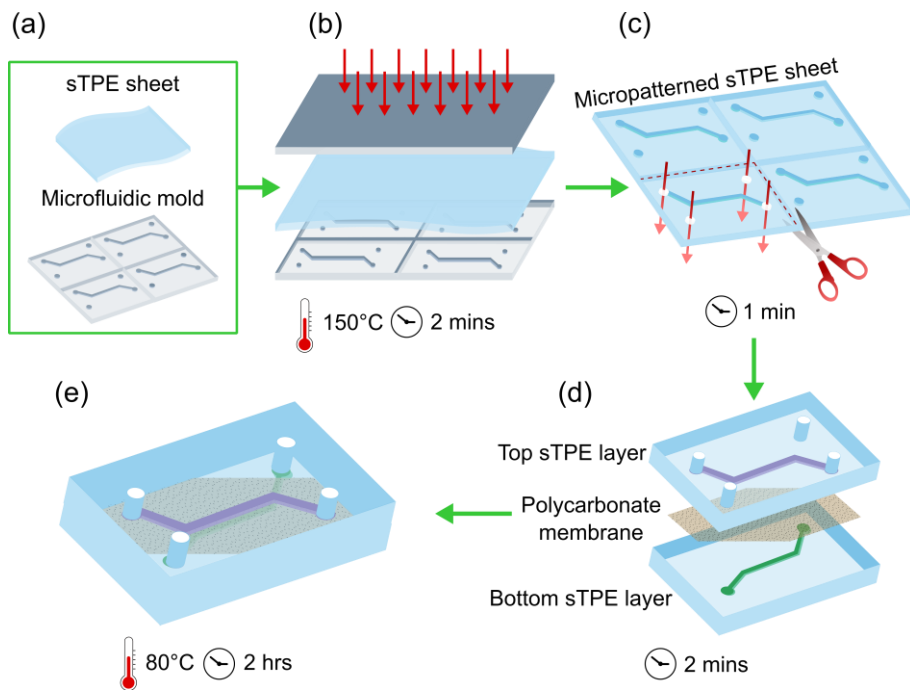
Figure 2.1. Schematics of the composite membrane-integrated cell culture device fabrication workflow starting from (a) a pre-extruded Flexdym™ sTPE sheet and a microfluidic mold. Fabrication consists of (b) a 150 °C hot embossing cycle of the sTPE sheet atop a microfluidic mold, (c) cutting of the micropatterned sTPE to appropriate device size, (d) layering of the micropatterned sTPE layers with an off-the-shelf porous polycarbonate membrane, and (e) baking at 80 °C to achieve device bonding resulting from the mobility of the intrinsically adhesive "soft" block polymer chains. Devices of

this configuration used for cell culture contained channels of cross-section 800 × 110 µm (width × height) and 27 mm length. The duration of each fabrication step is included.

Device Assembly and Bonding

The assembly of a FD-PC composite device was achieved by layering a porous track-etched polycarbonate membrane (2 µm pores, 5.6% porosity, 23 µm thickness, Isopore™, Merck KGaA, Darmstadt, Germany) in conformal contact with the micropatterned side of the FD sheet, applying pressure with tweezers to ensure contact and avoid air bubbles. Light, reversible adhesion occurs immediately between the PC membrane and the sTPE sheet. The PC membrane was manually placed with tweezers on the sTPE layer such that it covered the entirety of the channel and its two access holes (top layer in **Figure 2.1d**) but left the remaining two holes unobstructed for access to the channel on the second sTPE layer (bottom layer in **Figure 2.1d**). The second micropatterned sheet of FD, with no holes punched, was then similarly layered manually with tweezers atop the PC membrane with the aid of a stereoscope to ensure proper channel alignment. The two central channels were in direct superposition and the second channel inlet and outlet aligned with the access holes punched in the first sTPE layer (**Figure 2.1d**). The light adhesion that occurs immediately upon placement of the second sTPE layer can easily be reversed, allowing for any poor alignment to easily be corrected. The device was then inverted such that the sTPE layer with access holes was on top (**Figure 2.1e**). This configuration represents a three-layer, two-channel device, where channel geometries exist on both sides of the membrane. Alternatively, the second FD sheet can be devoid of features in order to create a single-channel device; this variation will be discussed in further detail below in section 2.2.2.

Conical FD connectors (Eden Microfluidics SAS, Paris, France), to interface with microfluidic tubing (not shown in **Figure 2.1**), were fixed atop the device ports by first placing the connector on a silicon wafer on a hotplate at 150 °C for 10 s in order to achieve a smooth, flat surface, then immediately transferring it in contact with the FD substrate at the desired port location. This final assembly step can vary depending on the desired method of device interfacing and connection (such as compression or adhesive-based connectors). The entire FD-PC-FD assembly was then baked in a forced convection oven (DKN612C, Yamoto Scientific Co. Ltd., Tokyo, Japan) at 80 °C for 2 hours to achieve bonding between the three layers (**Figure 2.1e**) without the need for plasma activation or adhesives, thanks to the intrinsic adhesive characteristics of the sTPE (described further in Section 2.3.1). The entire device fabrication

process is summarized in **Figure 2.1**, and **Figure 2.S1** shows more detailed step-by-step images of the fabrication process. The same protocol can be followed, minus the addition of the polycarbonate membrane, to fabricate single or multi-channeled devices made entirely of FD, such as the devices made entirely of FD for delamination testing, as detailed further in Section 2.2.2.

2.2.2 Delamination Testing

Delamination Device

The integrity of bonding between FD and the PC membrane, as well as between FD and FD substrates, was evaluated by using a device with two disconnected channels separated by varying gap distances (**Figure 2.2a–c**). A FD-PC-FD device (containing one micropatterned FD sheet and one featureless FD sheet, separated by a PC membrane) was fabricated with a mold of this channel-gap design. When pressure was applied to the input, no fluid could flow except in cases where delamination across the gap occurred, that is, the PC and FD bonded at the gap separated and allowed for the passage of fluid from the input to the output channel.
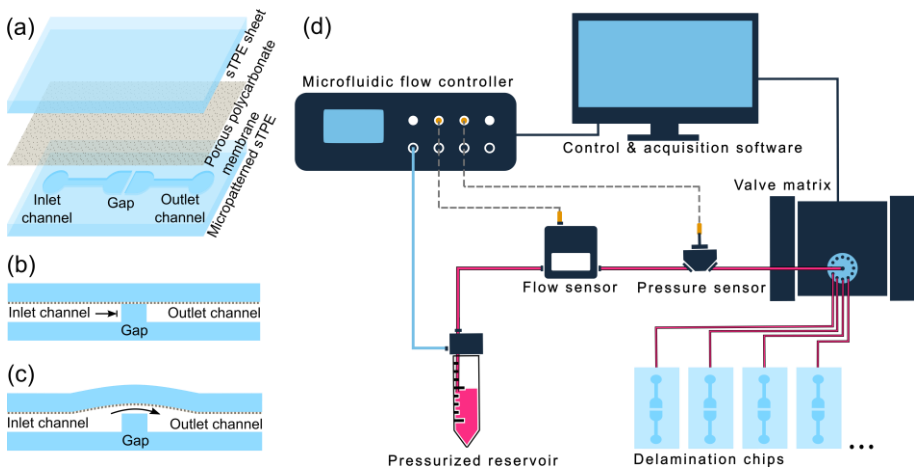
Figure 2.2. (a) Expanded view of the FD-PC-FD microfluidic chip design for delamination tests, consisting of two disconnected channels separated by a gap of varying distances. The inlet channel is increasingly pressurized, with no flow occurring until the delamination of the PC membrane from the FD gap structure occurs, at which point fluid crosses the gap into the outlet channel. (b) And (c) respectively show cross sections of the gap portion of the device before and after delamination. (d) Schematic of the automated delamination testing setup utilizing flow and pressure sensors and a valve

matrix in series with a water-filled reservoir pressurized by a pressure controller. Continuous data logging and sensor feedback allowed the sequential testing of the pressure capacities of up to 10 microfluidic devices with no user monitoring.

Automated Delamination Testing

FD-PC delamination devices were tested with a microfluidic setup (**Figure 2.2d**) consisting of an OB1® MK3+ pressure controller (0–2000 ± 0.1 mbar), thermal flow sensor (MFS3, -80–80 µL min^{-1} ± 5% m.v.) and capillary pressure sensor (MPS3, -1000–2000 ± 6 mbar), where pressure was applied from the pressure controller and transmitted to the device via water in a reservoir and polytetrafluoroethylene (PTFE) microfluidic tubing (all microfluidic equipment from Elveflow®, Elvesys SAS, Paris, France). Delamination devices were connected ensuring that no bubbles were present in the microfluidic system. A stepwise pressure profile between 0 and 2000 mbar gauge pressure, with 50 mbar steps lasting 30 s each, was executed using the Elveflow® Smart Interface software. The pressure controller interface logged the in-line flow and pressure sensor data and was programmed to stop the pressure sequence if a leak was detected. Such a leak was indicated by a sudden increase to a non-zero flow rate and a drop in pressure at the device inlet. A valve multiplexer (MUX Distributor) allowed for the sequential testing of up to ten devices in a single program execution.

This synchronized logging of data from both the sensors as well as the pressure controller itself offered redundancy to reduce erroneous results and allowed for the precise confirmation of the moment and pressure at which delamination between the FD and PC occurred. By using a single software interface for both data logging and equipment control, feedback loops could be straightforwardly implemented to cut a testing cycle short as soon as a delamination event was detected and subsequently switch devices.

Delamination devices with gap distances between 100 and 1000 µm were tested in this manner (n=5 per gap distance) to evaluate the effect of the bonding distance on the resulting FD-PC bond strength. Delamination tests were repeated on a set of devices lacking PC membranes, for comparison of FD-PC bond strength with that of FD-FD self-bonding.

To investigate the stability of device bonding over time in order to simulate long-term cell culture and repetitive use, similar pressure delamination tests were conducted on devices of 400 µm gap distance at different time points after

fabrication (1, 7, and 14 days post fabrication). Devices were aged at either room temperature or in an incubator (Model H2200-H, Benchmark Scientific Inc., Sayreville, NJ, USA) at 37 °C and high humidity to simulate cell culture conditions. Statistical analysis consisted of a one-way analysis of variance (ANOVA) between the six FD-PC delamination groups to evaluate if time and incubation resulted in a statistically significant difference in delamination pressure of FD-PC devices, where variation was considered significant when $p < 0.05$.

Device stability under long term pressure conditions was tested with devices in the same delamination setup both with static and cyclic pressures to evaluate the device robustness and durability. Static tests were conducted by pressurizing the devices to 500 mbar for a period of 10 hours (n=5) and cyclic tests by subjecting devices to 10,000 cycles of 0 to 500 mbar pressure at 0.2 Hz (n=5).

2.2.3 Flow Evaluation

Flow tests were conducted on FD-PC devices consisting of a simple channel of 27 mm length, 55 μm height, and varying width (200, 400, 800 μm) atop a PC membrane and second sheet of un-patterned FD. This design was a single-channel version of the two-channel device represented in **Figure 2.1e**. The microfluidic circuit consisted of (i) approximately 50 cm of 0.8 mm inner-diameter (ID) PTFE tubing; (ii) a flow sensor with a quartz capillary of 430 μm ID and 3 cm in length (MFS, -80–80 μL min^{-1} ± 5% m.v.); (iii) a capillary pressure sensor with an effective ID of 0.8 mm and length of 8 mm (MPS3, -1000–2000 ± 6 mbar); (iv) the microfluidic channel; and (v) a 5 cm section of polyether ether ketone (PEEK) tubing of 120 μm ID. The PEEK tubing was inserted into the microfluidic circuit downstream from the chip for added microfluidic resistance to simulate additional components in the system. Pressure and flow rate data were collected across the microfluidic setup (n=3 devices per channel size) and corresponding fluid shear stresses experienced on the PC membrane surface were calculated in order to provide an evaluation of the fluid mechanical conditions achievable within the pressure range that the composite devices can withstand.

2.2.4   Cell Evaluation

Three-layer devices (see **Figure 2.1e**) were fabricated to have two chambers separated by a PC membrane, with each chamber having cross section 800 × 110 µm (width × height) and 27 mm length. These devices were UV-sterilized prior to any cell culture work. After sterilization, devices were pre-treated with plasma (BD-20AC laboratory corona treater, Electro-Technic Products, Chicago, IL, US) for 10 seconds to increase hydrophilicity of the membranes prior to incubating the devices with 10 µg mL^{-1} fibronectin (MilliporeSigma, Burlington, MA, USA) for 1 hour at 37 °C. After fibronectin incubation, devices were flushed with 1X PBS supplemented with 1% penicillin/streptomycin (Gibco®, Thermo Fisher Scientific). The upper channel was then loaded by pipette with 7 µL of human dermal fibroblasts (HDFs) (ATCC, Manassas, VA, USA) at a concentration of 2x10^5 cells mL^{-1} in Dulbecco's Modified Eagle Medium (DMEM) (high glucose, GlutaMAX™ supplement, Thermo Fisher Scientific, Waltham, MA, USA) supplemented with 10% FBS (Corning Inc., Corning, NY, USA) and 1% penicillin/streptomycin. Cells were initially cultured for 12 hours atop the PC membrane prior to exchanging media by flow to remove non-adhered cells. Calcein AM (Sigma-Aldrich, St. Louis, MO, USA) was applied to cells after 48 hours of culturing in the devices by supplementing Calcein AM at 4 µM in 1X PBS for 20 minutes. Cells were imaged (Zeiss Observer Z1, Carl Zeiss AG, Oberkochen, Germany) after Calcein AM treatment, to verify the presence and distribution of cells in devices. Imaging was similarly repeated at 7 days after seeding.

Cell fixing and staining with Alexa Fluor™ 488 Phalloidin (Thermo Fisher Scientific, Waltham, MA, USA) and DAPI (Sigma-Aldrich, St. Louis, MO, USA) was done after 7 days of culturing cells in the upper channel of the devices. Briefly, cells were washed with PBS, treated with 4% PFA for 15 minutes at room temperature, and then washed three times with PBS. Cells were then permeabilized with 0.3% Triton-X (Sigma-Aldrich, St. Louis, MO, USA) in PBS. Cells were subsequently stained with 488 Phalloidin and DAPI at 0.66 µM and 1 µg mL^{-1}, respectively, in PBS for 30 minutes prior to rinsing with PBS and imaging (Nikon C2 Confocal, Nikon, Tokyo, Japan).

2.3 RESULTS AND DISCUSSION

2.3.1 Composite Device Microfabrication

Through vacuum-assisted isothermal hot embossing, FD sheets were patterned with microfluidic channels in two minutes. It is a molding technique that is highly compatible with the already existing soft lithography expertise that is widespread in microfluidics labs, as there is no need for a specialized master mold; molds that are commonly used for PDMS micropatterning, namely those derived from SU-8, epoxy,[49] and dry film photoresists (such as the Ordyl® mold used in this work) can also be used for sTPE hot embossing.

Hot embossing was followed by punching of ports then layering of subsequent PC and FD device layers in conformal contact. The soft, flexible properties of the sTPE allow for facile punching and readily achievable conformal contact, which can be both reproducibly completed in a matter of minutes (depending on the complexity of multi-layer devices requiring alignment), with little training. The co-polymeric properties of the materials allow for a reversible bond to be formed while avoiding the necessity of adhesives or plasma activation of surfaces that are usually associated with polymeric microfluidic device sealing. This bonding results from macro-molecular motion of the sTPE's ethylene-butylene (EB) soft polymer portion. The EB block possesses a negative glass transition temperature, allowing polymer chain mobility that can be promoted at elevated temperatures to facilitate spontaneous bonding with itself and other materials.[49,52] Full material and microstructure deformation is inhibited, however, by the PS hard block portion of FD, whose glass transition temperature remains above the baking temperature. This streamlines the process and simplifies any bonding optimization that may be required. Finally, the baking at 80 °C for 2 hours is the most time-intensive step in the fabrication process, however, baking time and temperature could be modified depending on the bonding strength required for specific device applications. **Figure 2.S2** shows a completed composite device.

From start to finish, beginning with the molding procedure, the developed fabrication protocol results in devices in under 2.5 hours. This presents a significant improvement on the production time of a comparable three-layer PDMS porous membrane device, and the time savings are multiplied when the prospect of fabricating numerous devices is considered, a ubiquitous necessity for cell biology applications. In addition, a single master mold can be used to fabricate multiple devices in parallel, since it is only needed for the two-minute

hot embossing channel formation step. PDMS, on the other hand, relies on relatively slow curing of its base polymer-crosslinker mixture, demanding that a single mold be in use for the entirety of the most time-intensive phase of fabrication, typically requiring between 1 to 4 hours with baking or 48 hours at room temperature.[21,53]

The Isopore™ membranes used in this study represent a readily available and inexpensive option within this class of track-etched polymeric membranes. Similar PC membranes have been effectively used in microfluidic cell culture studies and indeed for OOC applications.[9,54–58] The membranes are structurally robust, not requiring special handling techniques, and their interaction with FD very crucially retains the spontaneous sealing property that the sTPE has with itself, allowing uncomplicated interfacing of composite layers. Thin porous membranes in literature, central to barrier model platforms, are often made of PDMS, requiring diverse and often complicated processes that are limited in their accessibility, reproducibility, and ability to be high throughput. In combination with extruded FD sheets, which can similarly be stored and employed off-the-shelf, the PC membranes allow for rapid full-device fabrication with minimal time investment and planning that contrasts from PDMS methods. While the ability to elastically stretch the PC membranes was not evaluated, the mechanical properties of PC would suggest difficulty in achieving this at scales relevant to cellular mechanical stimuli. This presents a limitation when mechanical actuation is of greater significance and more elastic materials would be desirable, i.e., modelling the alveolar interface in lung-on-chip systems.[11] Another potential drawback of these track-etched membranes is their micro-scale thickness, which can limit bright field imaging (discussed further in Section 3.4) and cell-cell juxtracrine signalling.[35,59,60] More recent advances in ultra-thin nano-scale membranes have shown improved optical clarity, permeability, and cell contact,[61] but they have yet to be made readily available for widespread implementation.

The fabrication of these composite devices represents a highly accessible, yet transferrable process. It leverages the elastomeric properties of sTPE materials for facile and inexpensive production at small lab-scales that shares equipment and know-how from soft lithography techniques (only requiring the addition of a heat press), while at the same time being higher throughput than PDMS production. Moreover, the thermoplastic nature of FD as well as the simplicity of fabrication steps gives scope for the scaling up of the developed fabrication protocol. Injection molding or roll to roll hot embossing can be envisioned for the fabrication of large quantities of highly reproducible devices after

prototyping and development at small research-scales, but, critically, using the same materials in both settings. This transferability between lab and industrial-scale is in sharp contrast to both PDMS and hard thermoplastic microfluidics (elaborated upon in the Introduction section).

2.3.2   **Material Bonding Characterization**

Automated Delamination Testing

We developed an automated pressure testing setup to characterize the bonding strength between FD and PC membranes in a robust and precise manner. The developed setup allowed the sequential testing of up to ten samples with no user monitoring, regulated by feedback from continuous logging of pressure and flow rate data (**Figure 2.S3**). This allowed a streamlined process of burst testing, reducing clean-up, observation, and the total time of experimentation required. Testing could be parallelized with the employment of multiple pressure and flow sensors for higher-throughput testing, but the setup that was developed needs only two sensors, balancing speed with cost and practicality.

Additionally, by varying the gap distance of the delamination device itself, the bonding characteristics of small features inherent to microfluidics could be investigated. This is significant in understanding the minimum feature sizes attainable with given materials in cases where, for example, thin channel walls or micropillars are desired.

A method of effectively sealing a microfluidic device is an integral part of its design and implementation and remains a continual challenge faced by the microfluidics community in the evaluation of new materials.[62] Leak/burst testing thus becomes imperative in assessing sealing techniques. Accordingly, while no standardized method specific to microfluidic applications exists, a wide variety of bond testing techniques have been used. This includes flow rate-based evaluation in flow-through channels and the pressurization of closed channel structures, both of which often rely on optical detection of leaks.[63–72]

In comparison to the automated system developed here, these existing methods of burst testing remain low-throughput and examine the leaking of devices from a channel structure toward the exterior of the device in its entirety, often representing millimeters or centimeters of bonding distance (that is, the distance of bonded material that must delaminate for a leak/burst to occur).

They do not consider the dynamics of delamination on smaller scales, which alter both small features and overall channel geometries and inevitably occur sooner than the delamination of the device in its entirety. In this work, we thus propose a technique to test bonding that is both more representative in a microfluidic context and higher-throughput than existing methods, two aspects that will be vital in the future development and evaluation of new materials for microfluidic devices.

Flexdym™-Polycarbonate Bonding Strength

Balancing the integrity of a material bond with how easily it can be created is an engineering challenge in microfluidics that is highly dependent on the application at hand; the pressure capacity of devices made for cell culture will not be the same as that of devices made to handle supercritical fluids. We thus carried out delamination testing to evaluate the suitability of the composite FD-PC devices in the context of their utility for cell culture applications. More specifically, by using the above-described gap-channel delamination device, we investigated the minimum bonding distance that could be attained with the fabrication protocol developed in order to achieve sufficient and reliable bonding. This reproducibility in novel device development is something that is not often discussed but is vital in the realization of a robust microfluidic platform and the evaluation of its usability.
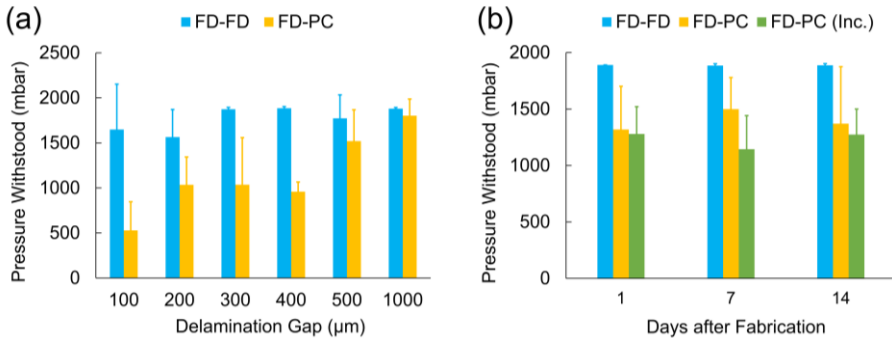
Figure 2.3. (a) FD-PC and FD-FD bonding evaluation through pressure delamination testing of devices with gap distances from 100 to 1000 μm. FD-PC devices show reduced bonding strength compared to FD-FD bonding, but reliably withstand pressures of 500 mbar at gap distances of 200 μm and above. (b) Pressure delamination testing of FD-FD and FD-PC devices (fixed 400 μm gap distance) at 1, 7, and 14 days after fabrication. An additional set of FD-PC devices was aged in high humidity, 37 °C incubation conditions (abbreviated "Inc." in the graph), which revealed no significant impact on the

device sealing due to time post-fabrication or incubation conditions (n=5 devices per dataset; error bars represent one standard deviation).

The pressure capacities of delamination devices (**Figure 2.3a**) investigating the FD-PC bond show an increase from 529 ± 318 mbar with a gap distance of 100 μm to 1802 ± 186 mbar with a gap distance of 1000 μm (noting that a maximum testing pressure of 2000 mbar was used, which, accounting for some pressure drop between the pressure controller and the devices, corresponded to a maximum pressure of ~1880 mbar measured at the devices). This positive trend is characterized by high variability throughout the range of gap distances tested. The FD-FD devices show an overall increase in pressure capacity to ~1500 mbar and above at all gap distances. At gap distances of 300 μm and above the pressure capacity consistently corresponds with the bulk pressure capacity found by Lachaux et al. using a similar bonding protocol.[49] It is critical to note that an increased variability was also apparent at FD-FD gap distances of 100 and 200 μm. This could indicate a limitation of the manual process using tweezers to ensure reliable conformal contact at the gap when small dimensions are concerned. One potential way to minimize this variation would be through the use of microscope-assisted or automated procedures for more precision when creating conformal contact but would require more time invested per device. Minor spontaneous resealing of gap devices was observed after delamination occurred and device pressurization was released, without an additional baking step. Further characterization of FD-PC resealing was outside the scope of this work, as the focus was on microfluidic devices for cell culture, in which single-use devices are common practice. However, this phenomenon could prove to be interesting in other applications, such as normally-closed valves responding to varying pressure profiles, like those seen in microfluidic circuits and logic.[73,74]

The superior pressure capacity of FD-FD devices as compared to FD-PC devices likely indicates a greater material interaction of FD with itself than with PC, as the bonding mechanism of such styrenic block copolymers relies on the mobility of EB polymer chains at the interface of the two like surfaces in contact.[52] It then follows that the PC, which does not contain the same EB blocks, has a weaker interaction with FD. Furthermore, PC has a higher glass transition temperature of ~150 °C that is not reached in the bonding procedure, which could result in reduced interaction due to polymer chain immobility. The reduced bonding strength could additionally underline lesser contact between the FD and PC surface as compared to FD-FD contact, which is facilitated due to the elastomeric properties of both device layers. Any unreliable contact

would be accentuated at smaller scales and is indeed evident in the variability of FD-PC bonding at smaller gap distances, as well as in that of FD-FD.

Nevertheless, at a bonding distance of 1 mm, a distance more representative of the milli-scale dimensions that typically define the material bond that seals a channel from its external environment, FD-PC devices frequently withstood maximum testing pressures. This quality of bonding at larger distances would characterize channels that do not contain thin separating walls or micro-scale structures and is more analogous to results reported using previously reported methods of bulk microfluidic burst testing.[63–68,70–72] Despite reduced bonding performance of FD-PC compared to FD-FD, at gap distances of 200 μm and above, FD-PC devices reliably withstood pressures of 500 mbar and greater, pressures that are generally sufficient for cell culture applications. The suitability of FD-PC device capacities in the context of their use for cell culture is discussed further in Section 3.3.4.

While PDMS membrane-integrated cell culture systems have not expressly characterized the bond strength between the porous membrane and the rest of the device, most platforms of this type utilize oxygen plasma bonding between the PDMS slabs and the PDMS membrane.[11,13,29,30,32] Thus, the closest analog to FD-PC delamination data may be found in burst testing conducted in PDMS-PDMS plasma bonded systems. These PDMS-PDMS, covalent Si-O-Si, bonds are generally stronger than those exhibited by the FD-PC system, most often withstanding pressures between 2 and 3 bar,[72,75] but are highly dependent on oxygen plasma parameters and have been reported ranging from approximately 0.7 to 4 bar.[71] In contrast, PDMS-PDMS sealing based only on conformal contact (without plasma surface activation) has been shown to leak at pressures above ~400 mbar.[75] Additionally, PDMS devices that use thermoplastic membranes, in a similar "sandwiched" configuration, primarily use a PDMS glue/mortar method,[63] or chemical surface modification for covalent bonding.[76] These methods result in crosslinked or covalent bonds more representative of the PDMS to PDMS bonding strength, with maximum burst pressures of 1–1.2 bar for PDMS mortar and 2.27 bar for chemical bonding.

A complementary set of delamination tests were performed using devices of 400 μm gap distance with and without incubation at 37 °C and high humidity (similar to cell incubation conditions) for up to 14 days to investigate any bonding degradation that could occur resulting from the increased temperature and humidity conditions representative of the cell culture applications envisioned (**Figure 2.3b**). Only one gap distance was used for these tests, which

were aimed at evaluating uniquely the effects of time and incubation-like conditions. 400 μm devices were chosen, as they were found to be the largest gap size that consistently delaminated within the test pressure range. After 14 days in incubation conditions, FD-PC devices withstood pressures of 1274 ± 225 mbar, as compared to FD-PC devices tested one day after fabrication, which withstood pressures of 1280 ± 241 mbar and 1319 ± 382 mbar, with and without incubation conditions, respectively. This testing revealed no significant difference in the integrity of the FD-PC bond resulting from time after fabrication or exposure to cell culture conditions bond (ANOVA: $F_{(5, 24)}=0.61$, $p=0.69$), indicating the suitability of such devices for long term cell culture studies.

To further evaluate the quality of bonding of the composite devices in a manner relevant to cell culture applications, we investigated the bonding performance of FD and PC with pressurization over periods longer than the 20-minute pressure cycle discussed thus far. Long-term fluid perfusion across cell cultures for continuous transport of nutrients, waste, and soluble factors has long been cited as one of the numerous advantages of studying cells on microfluidic platforms.[77] Thus, bonding behaviour under the influence of constant pressure for extended time periods, in addition to cyclic pressures, is critical to understanding the effectiveness and longevity of these devices. Devices of 400 μm gap distance showed no delamination resulting from pressurization at 500 mbar for 10 hours, nor at cyclic pressurization (0 to 500 mbar, 0.2 Hz, 10,000 cycles), demonstrating robust and reproducible performance under realistic working conditions.

2.3.3 Flow-Pressure Correlation

The influence of shear stress on cells is a significant factor that must be considered in the attempt to recapitulate *in vivo* conditions inside of a microfluidic device. It has been shown to have a major impact on cell differentiation and ultimate function, such as drug metabolism and cytokine secretion, in various cell types from across the body.[78–80] Thus, the ability to implement and control the appropriate shear stresses on a cell population is a central enabling characteristic of microfluidic technology and a consideration that must be made at the design and fabrication stage of device development. With this in mind, flow tests of FD-PC composite devices were conducted to understand the flow rates and calculate the shear stresses attainable inside of our devices, serving as a contextualization of the device pressure capacity

results obtained through delamination testing. A design consisting of a simple channel of varying widths atop a PC membrane was used as a model to represent geometries and flow characteristics present in typical barrier model cell culture chambers in literature in which there is no flow across the membrane, most notably models developed by Harvard University's Wyss Institute.[11,12,81,82]
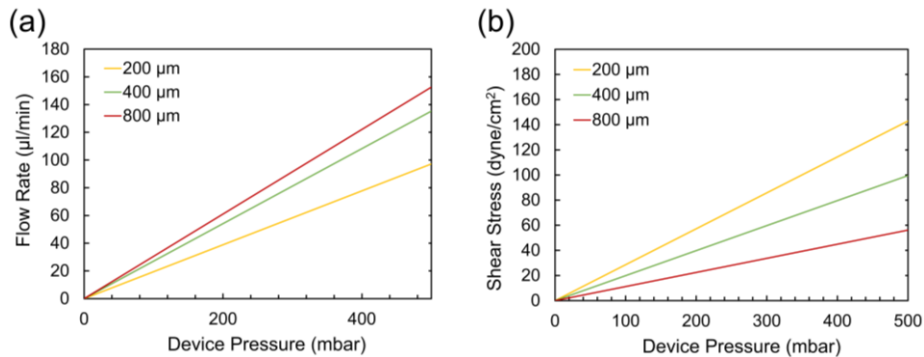
Figure 2.4. (a) Flow-pressure correlation in FD-PC devices from tests measuring the flow rate in a straight microfluidic channel (of width 200, 400, or 800 μm) and the corresponding pressure at the channel inlet. Within 500 mbar of pressure applied at the device, flow rates of up to approximately 150 μL min^{-1} can be reached. (b) Wall shear stresses that can be achieved in each of the example devices, as calculated from the flow rate data in (a), depending on the pressure applied. Shear stresses of up to approximately 140 dyne cm^{-2} can be generated with pressures of 500 mbar and below.

Figure 2.4a shows the linear relationships between the pressure measured at the inlet of the device and the flow rates in the given microfluidic setup, and **Figure 2.4b** shows the corresponding shear stresses imposed on the surface of the membrane, as determined by the following equation describing the wall shear stresses, τ_w, of laminar Newtonian fluids in a closed rectangular geometry:

$$\tau_w = \frac{6\mu Q}{bh^2} \tag{2.1}$$

where μ is the dynamic viscosity of the fluid (water, 8.90×10^{-4} Pa·s at 25 °C), Q is the fluid flow rate, b is the channel width and h is the channel height.[83] This approximation of wall shear stress assumes parabolic Poiseuille flow in the microchannel, useful for estimating wall shear stresses in rectangular channels when flow is along the length of the channel and b > h. Depending on the

channel dimensions used, flow rates of up to ~150 μL min^{-1} and shear stresses of up to ~140 dyne cm^{-2} could be achieved using 500 mbar or less of pressure applied to the composite devices. This gives an ample range of control over fluid conditions inside the device and is sufficient for the shear stresses desired for *in vivo*-like cell culture conditions, which rarely surpass 25 dyne cm^{-2}.[84] The relatively low pressures required for such applications indicate that the FD-PC bonding strength discussed in section 2.3.2, even with the presence of small features, would be sufficient for cell culture applications.

It must be noted that these relationships are dependent on the microfluidic resistance of the entire microfluidic system, which will inevitably vary from experiment to experiment, depending on the type and amount of devices, instruments, and tubing that are being used. The introduction of a section of high-resistance PEEK tubing in the experimental flow setup downstream from the FD-PC devices served to simulate additional resistance that may exist in a setup, and thus provide a conservative estimate of what pressures would be required to achieve a given flow rate. These results provide an aid in translating the pressure-based delamination findings into a more practically useful context (many microfluidic cell culture experiments depend on defining fluid flow rates or shear stresses rather than pressures) in order to assist potential users in understanding the capabilities of these devices.

2.3.4 Cell Culture

sTPE microfluidic devices have been used for cell culture in microfluidics,[47,51] however, there has been limited published data associated with FD and its implementation into cell culture systems. To our knowledge, two different FD formulations have been previously reported in only two instances with cell culture work: (i) a moldable film formulation of FD, similar to the one used in this study, and (ii) a spin-coating formulation, FlexdymSC. The first showed cultured yeast cells[49] while demonstrating reduced absorption of a chemical division inhibitor due to FD's material properties, and FlexdymSC was shown to sustain culture of endothelial progenitor cells over four days.[85] Due to the limited published literature on culturing cells within FD microfluidic devices, we wanted to ensure that cultured cells could be maintained within our composite devices. To this end, we cultured HDFs within our devices for one week.
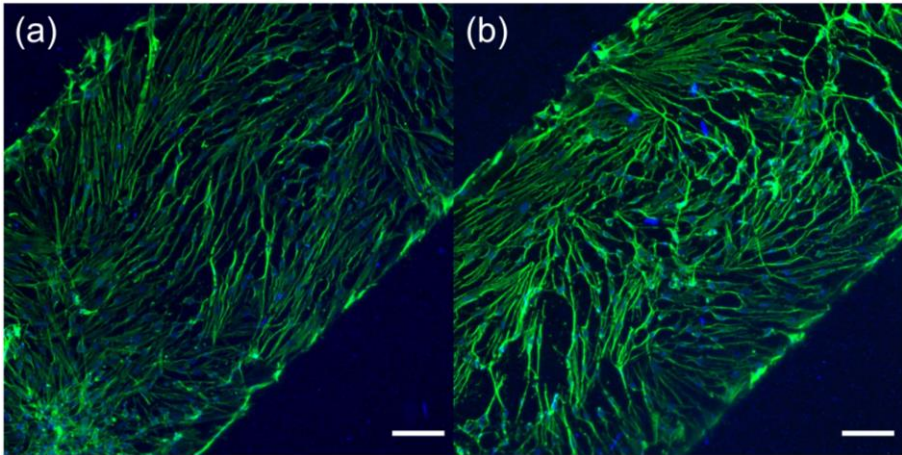
Figure 2.5. (a, b) Representative images of human dermal fibroblasts (HDFs) cultured in FD-PC-FD devices over the course of 7 days. HDFs presented a primarily spindle geometry, commonly seen when HDFs are cultured to high confluency, due to higher density of cells. HDFs were cultured on top of the polycarbonate membrane for 7 days prior to being fixed and stained with 488-Alexa Fluor™ 488 Phalloidin (staining for F-actin, green) and DAPI (nuclear, blue), to demonstrate cell adhesion and maintained presence in static culture within devices over the course of 1 week. Scale bars = 150 μm.

HDFs were cultured in the FD-PC-FD microfluidic devices, with cells being seeded on the top of the polycarbonate membrane in the devices' upper channels. We observed sustained cell adhesion and spread morphologies when cultured for up to one week (**Figure 2.S4**). Additionally, cells were fixed and stained to visualize actin structures in cultured cells (**Figure 2.5**). The thickness of the polycarbonate membranes resulted in some difficulty in observing the cells under bright field illumination but did not pose a problem for fluorescent imaging.

While providing perfusion may be optimal to prime and stimulate more uniform cell alignment, proliferation, and confluency throughout the microfluidic device, we wished to verify principally that the material and device configuration could sustain cells over multiple days. This was particularly of interest as sTPE materials, similar to FD, are known to have one to two orders of magnitude lower oxygen permeability than that of PDMS.[86,87] Static culturing with media exchanges every other day established that cells maintained good adhesion with spread morphologies over a one-week period within these devices without the need for more frequent perfusion. This demonstration, while limited in evaluating biological functions, earmarks the

potential use of this material and device configuration for barrier-like cell culture systems.

2.3.5   **Drawbacks Compared to PDMS**

When compared to three-layer, membrane-integrated PDMS microfluidic devices, our composite sTPE system has a few notable drawbacks. (i) The PC membranes have higher thickness and stiffness in comparison to porous PDMS membranes in the literature.[35,59] The more significant thickness of the thermoplastic membranes and their material properties reduces optical clarity, notably for bright field observation. Additionally, the diffusion and cell-cell contact, from one side of the membrane to the other, are reduced due to the increased distance.[60,61] Furthermore, the non-elastomeric properties of the PC membrane largely prohibit membrane stretching to impose mechanical stresses on cell cultures, similar to those used in certain organ-on-chip devices.[11,82] (ii) Micropatterned sTPE sheets, in this and previous studies, are rather thin substrates, measuring ~1 mm in thickness, which limits the ability to define the final device thickness. This can introduce complications when interfacing microfluidic tubing with the device, requiring an additional connector solution. While numerous connector solutions exist, such as the conical sTPE connectors used in this work, this represents an additional fabrication step to use the sTPE device in a microfluidic setup. PDMS devices, on the other hand, can simply be fabricated with sufficient thickness to interface tubing directly into an access port thanks to its elastomeric properties. (iii) Styrenic block copolymer sTPE materials, like Flexdym™, are known to have significantly lower oxygen permeability than PDMS.[86,87] While this did not pose problems for culturing cells in this work, this will result in a very different passive gas exchange and could potentially present difficulties in certain device geometries or flow regimes, requiring the user to incorporate a more involved gas control protocol to maintain appropriate oxygen levels inside a device.

2.4   CONCLUSIONS

Using the sTPE Flexdym™ and a commercially available porous polycarbonate membrane, we have developed a composite microfluidic platform that can be fabricated in under 2.5 hours with rapid hot embossing and facile self-sealing.

The microfluidic devices consist of a membrane-separated chamber, similar to the geometries of membrane-based cell culture platforms in literature.

The bonding integrity of the devices was evaluated by testing the bond formed between the FD substrate and the PC membrane using an automated pressure delamination system to reproducibly test microfluidic material bonding in a high-throughput manner. FD-PC bond strength reliably withstood pressures of 500 mbar at bonding distances of 200 μm and greater, a pressure capacity that is largely sufficient for the needs of cell culture applications. The suitability of devices for cell culture was further highlighted by confirming no degradation of bonding strength in cell culture-like conditions and long-term pressurization. Finally, cell trials of HDFs showed good cell adhesion, and a maintained culture atop PC membranes inside of composite devices over the course of one week, demonstrating the potential of these devices to be used for more extensive microfluidic cell culture models.

The promise that microfluidic cell culture technology offers in the advancement of *in vitro* platforms for drug testing and disease modeling has been tempered by the drawbacks of PDMS and the subsequent need for novel material solutions.[88] Our work introduces a microfluidic platform combining two materials with proven efficacy for cell culture research with a fabrication methodology that represents a rapid, facile, and transferable solution.

2.5 ACKNOWLEDGEMENTS

2.6 REFERENCES

[1]   S. Boyden, *J. Exp. Med.* **1962**, *115*, 453.

[2]   H. Lin, H. Li, H.-J. Cho, S. Bian, H.-J. Roh, M.-K. Lee, J. S. Kim, S.-J. Chung, C.-K. Shim, D.-D. Kim, *J. Pharm. Sci.* **2007**, *96*, 341.

[3]   S. Qi, Y. Song, Y. Peng, H. Wang, H. Long, X. Yu, Z. Li, L. Fang, A. Wu, W. Luo, Y. Zhen, Y. Zhou, Y. Chen, C. Mai, Z. Liu, W. Fang, *PLoS One* **2012**, *7*, 1.

[4]   R. Harisi, I. Kenessey, J. N. Olah, F. Timar, I. Babo, G. Pogany, S. Paku, A. Jeney, *Anticancer Res.* **2009**, *29*, 2981.

[5]   S. D. Sheridan, S. Gil, M. Wilgo, A. Pitt, *Methods Cell Biol.* **2008**, *86*, 29.

[6]   L.-J. Chen, S. Ito, H. Kai, K. Nagamine, N. Nagai, M. Nishizawa, T. Abe, H. Kaji, *Sci. Rep.* **2017**, *7*, 3538.

[7]   O. Y. F. Henry, R. Villenave, M. J. Cronce, W. D. Leineweber, M. A. Benz, D. E. Ingber, *Lab Chip* **2017**, *17*, 2264.

[8]   J. W. Song, S. P. Cavnar, A. C. Walker, K. E. Luker, M. Gupta, Y.-C. Tung, G. D. Luker, S. Takayama, *PLoS One* **2009**, *4*, e5756.

[9]   A. K. H. Achyuta, A. J. Conway, R. B. Crouse, E. C. Bannister, R. N. Lee, C. P. Katnik, A. A. Behensky, J. Cuevas, S. S. Sundaram, *Lab Chip* **2013**, *13*, 542.

[10]   K. Rennert, S. Steinborn, M. Gröger, B. Ungerböck, A.-M. Jank, J. Ehgartner, S. Nietzsche, J. Dinger, M. Kiehntopf, H. Funke, F. T. Peters, A. Lupp, C. Gärtner, T. Mayr, M. Bauer, O. Huber, A. S. Mosig, *Biomaterials* **2015**, *71*, 119.

[11]   D. Huh, B. D. Matthews, A. Mammoto, M. Montoya-Zavala, H. Y. Hsin, D. E. Ingber, *Science (80-.).* **2010**, *328*, 1662.

[12]   K.-J. Jang, A. P. Mehr, G. A. Hamilton, L. A. McPartlin, S. Chung, K.-Y. Suh, D. E. Ingber, *Integr. Biol.* **2013**, *5*, 1119.

[13]   H. J. Kim, D. E. Ingber, *Integr. Biol.* **2013**, *5*, 1130.

[14]   S. N. Bhatia, D. E. Ingber, *Nat. Biotechnol.* **2014**, *32*, 760.

[15]   E. W. Esch, A. Bahinski, D. Huh, *Nat. Rev. Drug Discov.* **2015**, *14*, 248.

[16]   C. Moraes, G. Mehta, S. C. Lesher-Perez, S. Takayama, *Ann. Biomed. Eng.* **2012**, *40*, 1211.

[17]   K. Ronaldson-Bouchard, G. Vunjak-Novakovic, *Cell Stem Cell* **2018**, *22*, 310.

[18]   D. C. Duffy, J. C. McDonald, O. J. A. Schueller, G. M. Whitesides, *Anal. Chem.* **1998**, *70*, 4974.

[19]   A. Mata, A. J. Fleischman, S. Roy, *Biomed. Microdevices* **2005**, *7*, 281.

[20]   S. Deguchi, J. Hotta, S. Yokoyama, T. S. Matsui, *J. Micromechanics Microengineering* **2015**, *25*, 097002.

[21]   I. D. Johnston, D. K. McCluskey, C. K. L. Tan, M. C. Tracey, *J. Micromechanics Microengineering* **2014**, *24*, 035017.

[22]   M. W. Toepke, D. J. Beebe, *Lab Chip* **2006**, *6*, 1484.

[23]   G. T. Roman, T. Hlaus, K. J. Bass, T. G. Seelhammer, C. T. Culbertson, *Anal. Chem.* **2005**, *77*, 1414.

[24]   X. Su, E. W. K. Young, H. A. S. Underkofler, T. J. Kamp, C. T. January, D. J. Beebe, *J. Biomol. Screen.* **2011**, *16*, 101.

[25]   K. J. Regehr, M. Domenech, J. T. Koepsel, K. C. Carver, S. J. Ellison-Zelski, W. L. Murphy, L. A. Schuler, E. T. Alarid, D. J. Beebe, *Lab Chip* **2009**, *9*, 2132.

[26]   D. T. Eddington, J. P. Puccinelli, D. J. Beebe, *Sensors Actuators, B Chem.* **2006**, *114*, 170.

[27]   R. Mukhopadhyay, *Anal. Chem.* **2007**, *79*, 3248.

[28]   A. K. Capulli, K. Tian, N. Mehandru, A. Bukhta, S. F. Choudhury, M. Suchyta, K. K. Parker, *Lab Chip* **2014**, *14*, 3181.

[29]   W. F. Quirós-Solano, N. Gaio, O. M. J. A. Stassen, Y. B. Arik, C. Silvestri, N. C. A. Van Engeland, A. Van der Meer, R. Passier, C. M. Sahlgren, C. V. C. Bouten, A. van den Berg, R. Dekker, P. M. Sarro, *Sci. Rep.* **2018**, *8*, 1.

[30]   D. Huh, H. J. Kim, J. P. Fraser, D. E. Shea, M. Khan, A. Bahinski, G. A. Hamilton, D. E. Ingber, *Nat. Protoc.* **2013**, *8*, 2135.

[31]   H. Wei, B. Chueh, H. Wu, E. W. Hall, C. Li, R. Schirhagl, J.-M. Lin, R. N. Zare, *Lab Chip* **2011**, *11*, 238.

[32]   X. Fan, C. Jia, J. Yang, G. Li, H. Mao, Q. Jin, J. Zhao, *Biosens. Bioelectron.* **2015**, *71*, 380.

[33]   W. Chen, R. H. W. Lam, J. Fu, *Lab Chip* **2012**, *12*, 391.

[34]   H. Le-The, M. Tibbe, J. Loessberg-Zahl, M. Palma Do Carmo, M. Van Der Helm, J. Bomer, A. Van Den Berg, A. Leferink, L. Segerink, J. Eijkel, *Nanoscale* **2018**, *10*, 7711.

[35]   H. H. Chung, M. Mireles, B. J. Kwarta, T. R. Gaborski, *Lab Chip* **2018**, *18*, 1671.

[36]   P. Apel, *Radiat. Meas.* **2001**, *34*, 559.

[37]   H. Becker, C. Gärtner, *Anal. Bioanal. Chem.* **2008**, *390*, 89.

[38]   E. Berthier, E. W. K. Young, D. Beebe, *Lab Chip* **2012**, *12*, 1224.

[39]   E. W. K. Young, E. Berthier, D. J. Guckenberger, E. Sackmann, C. Lamers, I. Meyvantsson, A. Huttenlocher, D. J. Beebe, *Anal. Chem.* **2011**, *83*, 1408.

[40]   D. Ogończyk, J. Węgrzyn, P. Jankowski, B. Dąbrowski, P. Garstecki, *Lab Chip* **2010**, *10*, 1324.

[41]   C. W. Tsao, L. Hromada, J. Liu, P. Kumar, D. L. DeVoe, *Lab Chip* **2007**, *7*, 499.

[42]   L. Brown, T. Koerner, J. H. Horton, R. D. Oleschuk, *Lab Chip* **2006**, *6*, 66.

[43]   S. A. Soper, S. M. Ford, S. Qi, R. L. McCarley, K. Kelly, M. C. Murphy, *Anal. Chem.* **2000**, *72*, 642 A.

[44]   E. Gencturk, S. Mutlu, K. O. Ulgen, *Biomicrofluidics* **2017**, *11*, 051502.

[45]   A. P. Sudarsan, J. Wang, V. M. Ugaz, *Anal. Chem.* **2005**, *77*, 5167.

[46]   E. Roy, M. Geissler, J. C. Galas, T. Veres, *Microfluid. Nanofluidics* **2011**, *11*, 235.

[47]   M. D. Guillemette, E. Roy, F. A. Auger, T. Veres, *Acta Biomater.* **2011**, *7*, 2492.

[48]   E. Roy, G. Stewart, M. Mounier, L. Malic, R. Peytavi, L. Clime, M. Madou, M. Bossinot, M. G. Bergeron, T. Veres, *Lab Chip* **2015**, *15*, 406.

[49]   J. Lachaux, C. Alcaine, B. Gómez-Escoda, C. M. Perrault, D. O. Duplan, P.-Y. J. Wu, I. Ochoa, L. Fernandez, O. Mercier, D. Coudreuse, E. Roy, *Lab Chip* **2017**, *17*, 2581.

[50]   D. J. Case, Y. Liu, I. Z. Kiss, J. R. Angilella, A. E. Motter, *Nature* **2019**, *574*, 647.

[51]   M. D. Borysiak, K. S. Bielawski, N. J. Sniadecki, C. F. Jenkel, B. D. Vogt, J. D. Posner, *Lab Chip* **2013**, *13*, 2773.

[52]   E. Roy, A. Pallandre, B. Zribi, M.-C. Horny, F. D. Delapierre, A. Cattoni, J. Gamby, A.-M. Haghiri-Gosnet, in *Adv. Microfluid. - New Appl. Biol. Energy, Mater. Sci.* (Ed.: X.-Y. Yu), InTechOpen, London, UK, **2016**.

[53]   J. C. McDonald, G. M. Whitesides, *Acc. Chem. Res.* **2002**, *35*, 491.

[54]   B. E. Dewi, T. Takasaki, I. Kurane, *J. Virol. Methods* **2004**, *121*, 171.

[55]   J. Linnankoski, J. Mäkelä, J. Palmgren, T. Mauriala, C. Vedin, A. Ungell, L. Lazorova, P. Artursson, A. Urtti, M. Yliperttula, *J. Pharm. Sci.* **2010**, *99*, 2166.

[56]   R. Booth, H. Kim, *Lab Chip* **2012**, *12*, 1784.

[57]   D. Gao, H. Liu, J.-M. Lin, Y. Wang, Y. Jiang, *Lab Chip* **2013**, *13*, 978.

[58]   Y. S. Torisawa, B. Mosadegh, G. D. Luker, M. Morell, K. S. O'Shea, S. Takayama, *Integr. Biol.* **2009**, *1*, 649.

[59]   M. Y. Kim, D. J. Li, L. K. Pham, B. G. Wong, E. E. Hui, *J. Memb. Sci.* **2014**, *452*, 460.

[60]   S. H. Ma, L. A. Lepak, R. J. Hussain, W. Shain, M. L. Shuler, *Lab Chip* **2005**, *5*, 74.

[61]   M. Mireles, T. R. Gaborski, *Electrophoresis* **2017**, *38*, 2374.

[62]   Y. Temiz, R. D. Lovchik, G. V. Kaigala, E. Delamarche, *Microelectron. Eng.* **2015**, *132*, 156.

[63]   B. H. Chueh, D. Huh, C. R. Kyrtsos, T. Houssin, N. Futai, S. Takayama, *Anal. Chem.* **2007**, *79*, 3504.

[64]   X. Gong, X. Yi, K. Xiao, S. Li, R. Kodzius, J. Qin, W. Wen, *Lab Chip* **2010**, *10*, 2622.

[65]   L. S. Shiroma, M. H. O. Piazzetta, G. F. Duarte-Junior, W. K. T. Coltro, E. Carrilho, A. L. Gobbi, R. S. Lima, *Sci. Rep.* **2016**, *6*, 26032.

[66]   S. Xie, J. Wu, B. Tang, G. Zhou, M. Jin, L. Shui, *Micromachines* **2017**, *8*, 218.

[67]   J. Wang, S. Wang, P. Zhang, Y. Li, *18th Int. Conf. Electron. Packag. Technol. ICEPT 2017* **2017**, 1051.

[68]   M. Serra, I. Pereiro, A. Yamada, J. L. Viovy, S. Descroix, D. Ferraro, *Lab Chip* **2017**, *17*, 629.

[69]   S. Kim, J. Kim, Y. H. Joung, J. Choi, C. Koo, *Micromachines* **2018**, *9*, 639.

[70]   U. Abidin, N. A. S. M. Daud, V. Le Brun, *AIP Conf. Proc.* **2019**, *2062*, 020064.

[71]   S. Bhattacharya, A. Datta, J. M. Berg, S. Gangopadhyay, *J. Microelectromechanical Syst.* **2005**, *14*, 590.

[72]   M. A. Eddings, M. A. Johnson, B. K. Gale, *J. Micromechanics Microengineering* **2008**, *18*, 067001.

[73]   B. Mosadegh, T. Bersano-Begey, J. Y. Park, M. A. Burns, S. Takayama, *Lab Chip* **2011**, *11*, 2813.

[74]   S.-J. Kim, D. Lai, J. Y. Park, R. Yokokawa, S. Takayama, *Small* **2012**, *8*, 2925.

[75]   J. C. McDonald, D. C. Duffy, J. R. Anderson, D. T. Chiu, H. Wu, O. J. Schueller, G. M. Whitesides, *Electrophoresis* **2000**, *21*, 27.

[76]   K. Aran, L. A. Sasso, N. Kamdar, J. D. Zahn, *Lab Chip* **2010**, *10*, 548.

[77]   J. El-Ali, P. K. Sorger, K. F. Jensen, *Nature* **2006**, *442*, 403.

[78]   J. B. Freund, J. G. Goetz, K. L. Hill, J. Vermot, *Development* **2012**, *139*, 1229.

[79]   H. Rashidi, S. Alhaque, D. Szkolnicka, O. Flint, D. C. Hay, *Arch. Toxicol.* **2016**, *90*, 1757.

[80]   R. S. Reneman, T. Arts, A. P. G. Hoeks, *J. Vasc. Res.* **2006**, *43*, 251.

[81]   D. Huh, H. Fujioka, Y.-C. Tung, N. Futai, R. Paine, J. B. Grotberg, S. Takayama, *Proc. Natl. Acad. Sci.* **2007**, *104*, 18886.

[82]   H. J. Kim, D. Huh, G. Hamilton, D. E. Ingber, *Lab Chip* **2012**, *12*, 2165.

[83]   L. Kim, M. D. Vahey, H. Y. Lee, J. Voldman, *Lab Chip* **2006**, *6*, 394.

[84]   L. Kim, Y. C. Toh, J. Voldman, H. Yu, *Lab Chip* **2007**, *7*, 681.

[85]   J. Lachaux, H. Salmon, F. Loisel, N. Arouche, I. Ochoa, L. L. Fernandez, G. Uzan, O. Mercier, T. Veres, E. Roy, *Adv. Mater. Technol.* **2019**, *4*, 1.

[86]   H. Odani, K. Taira, N. Nemoto, M. Kurata, *Polym. Eng. Sci.* **1977**, *17*, 527.

[87]   A. Senuma, *Macromol. Chem. Phys.* **2000**, *201*, 568.

[88]   A. Cochrane, H. J. Albers, R. Passier, C. L. Mummery, A. van den Berg, V. V. Orlova, A. D. van der Meer, *Adv. Drug Deliv. Rev.* **2019**, *140*, 68.

SUPPORTING INFORMATION TO CHAPTER 2

2.7 SUPPORTING INFORMATION
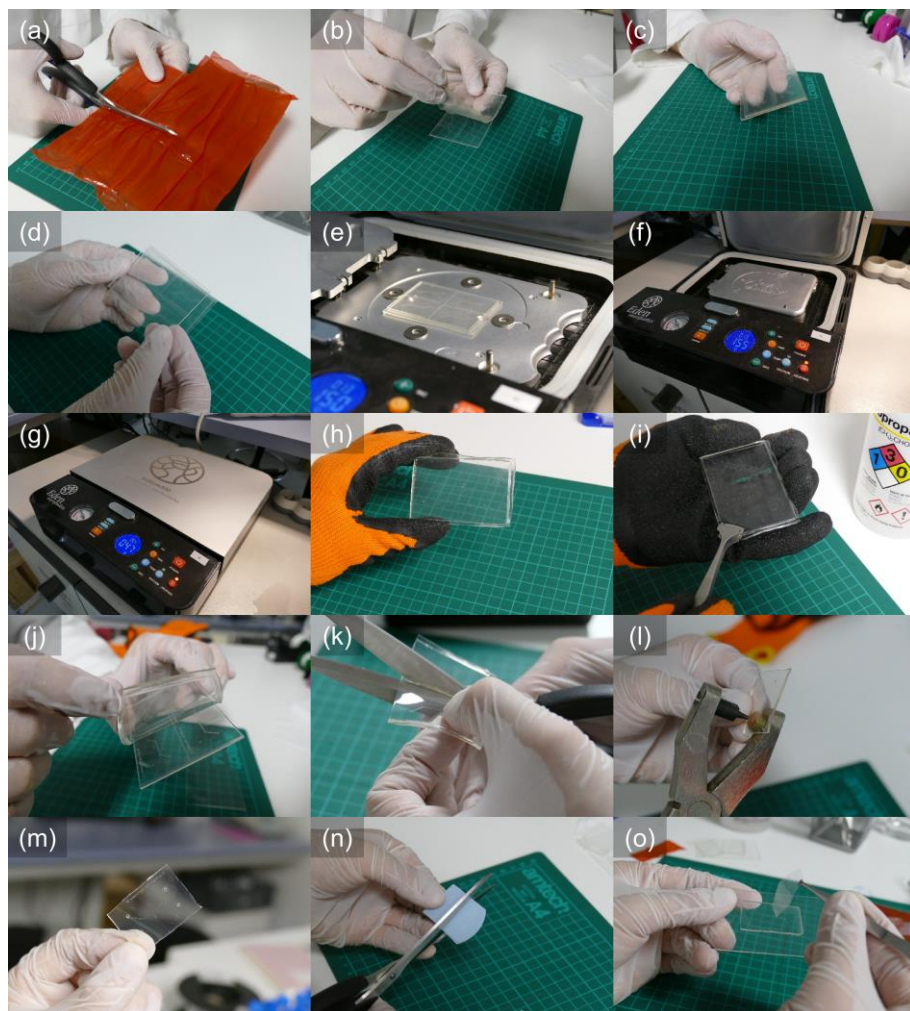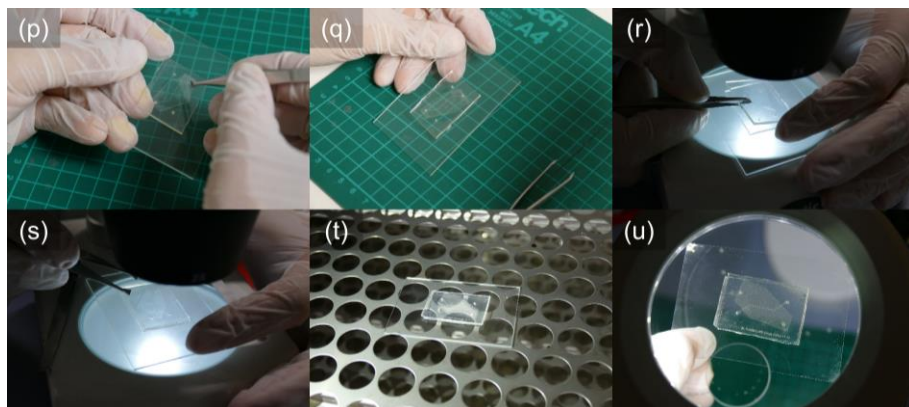
Figure 2.Sl: Step-by-step fabrication procedure of a three layer, membrane-integrated sTPE-PC composite device. (a) Cutting with scissors of raw sTPE extruded sheet to approximately the size of the microfluidic mold (in this case, a glass microscope slide). Photo shows the sTPE sheet covered stored between two red Teflon films (b–c) Laying of the sTPE sheet onto the microfluidic mold, assuring maximum contact and minimal air bubbles between the sTPE and the mold. (d) Laying of a second, plain glass slide into contact with sTPE sheet to act as a stiff, flat back-plate for hot embossing. (e) Placement of the mold-sTPE-glass slide assembly onto the lower metal plate in the vacuum heat press. Image shows four spacers surrounding the assembly for final sTPE thickness control. (f) Placement of the upper metal plate to prepare the assembly for vacuum-assisted hot embossing. (g) Running of the two-minute vacuum assisted hot embossing cycle at 150 °C. (h) Mold-sTPE-glass slide assembly after removal from the vacuum heat press. (i) Removal of the glass slide back-plate from the hot embossed sTPE sheet using tweezers and isopropanol to assist with separation. (j) Removal of the hot embossed sTPE sheet from the mold. (k) Cutting with scissors of the hot embossed sTPE sheet to device-sized pieces. (l–m) Punching of access holes into the upper sTPE layer with a steel hole punch. (n) Cutting with scissors of the PC membrane to a appropriate size for the device. Note that the membrane is shown stored between blue paper films. (o–q) Laying of the PC membrane in conformal contact with the upper sTPE layer. Light adhesion occurs immediately upon conformal contact between the PC membrane and sTPE layer. Note that the PC membrane covers the channel of the upper sTPE layer but leaves the ports accessing the channel to the lower sTPE layer unobstructed. (r–s) Manual alignment with the aid of a stereoscope of the second (lower) sTPE layer such that the central channels are superimposed and the access ports in the upper sTPE layer align with the second sTPE channel. Light adhesion occurs immediately upon contact, but is easily reversible, such that poor alignment can be corrected for. (t) Baking of the membrane-integrated device for 2 hours at 80 °C. (u) Final device after baking, ready for subsequent cell culture use.
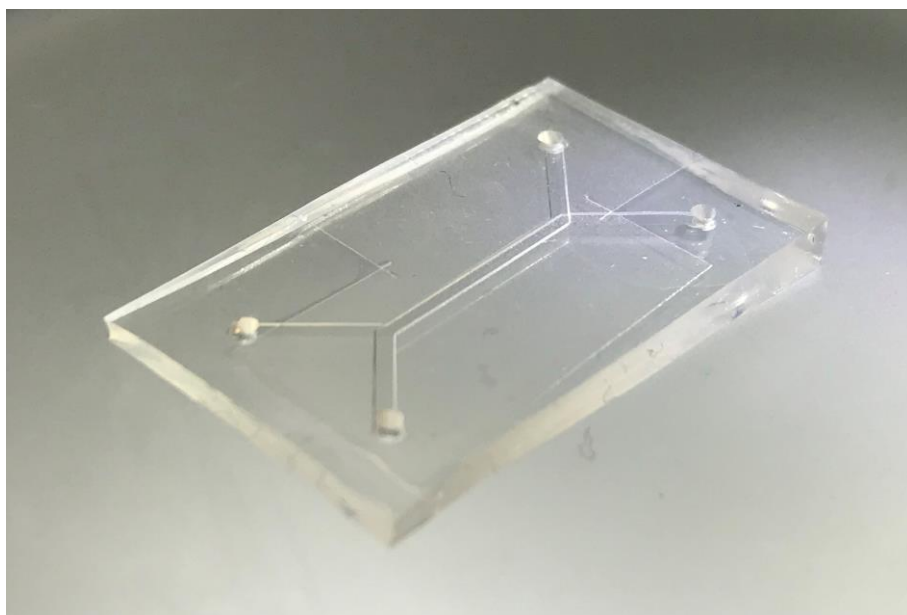
Figure 2.S2: Composite device consisting of two micropatterned layers of Flexdym™ sTPE separated by a porous polycarbonate membrane. The two overlapping channels each measure 800 μm in width and 110 μm in thickness, and the entire device footprint is 25 mm x 35 mm.
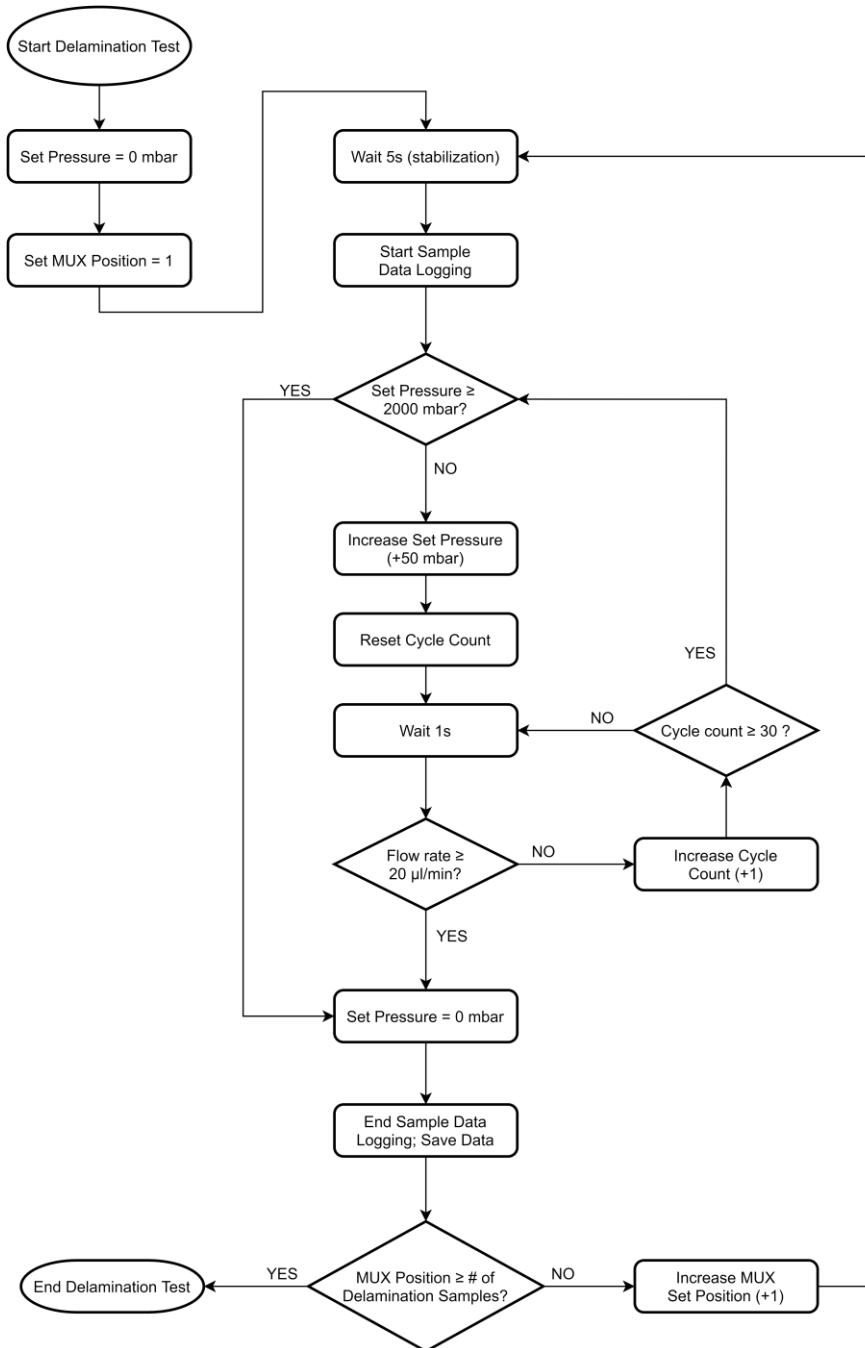
Figure 2.S3: Logic flowchart of the automated delamination testing setup programmed in the Elveflow® Smart Interface software. The sequence uses feedback from a flow sensor in order to detect device delamination (i.e., leak in the system) and stop the pressurization cycle before switching to the subsequent sample.
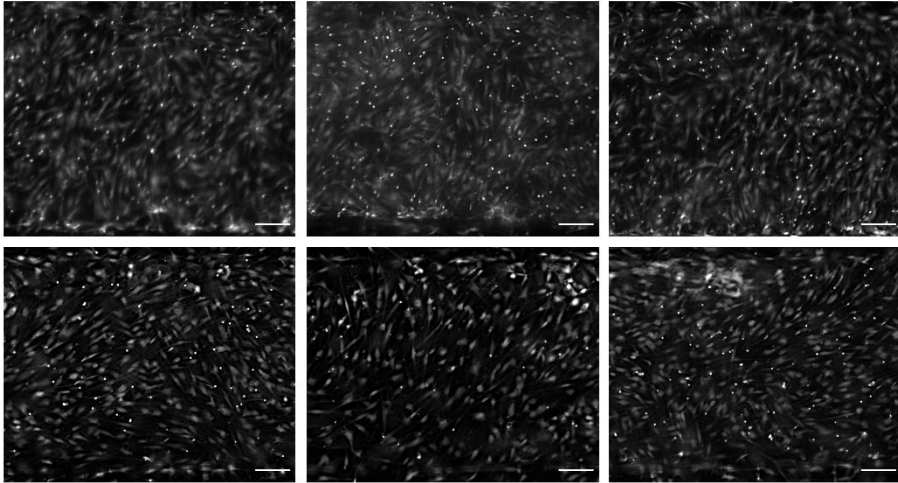
Figure 2.S4: Human dermal fibroblasts cultured in FD-PC-FD devices. HDFs were cultured in the top layer channel, a top of the polycarbonate membrane. Cells were stained with Calcein AM in the device, prior to imaging at day 2 and day 7. Top row are cells imaged at day 2 of culturing; bottom row are cells imaged at day 7 of culturing. Scale bars = 100 μm

CHAPTER 3

Self-sealing Thermoplastic Fluoroelastomer Enables Rapid Fabrication of Modular Microreactors

Alexander H. McMillan, Juan Mora-Macías, Joan Teyssandier, Raymond Thür, Emmanuel Roy, Ignacio Ochoa, Steven De Feyter, Ivo F. J. Vankelecom, Maarten B. J. Roeffaers and Sasha Cai Lesher-Pérez

Abstract

A novel fluorinated soft thermoplastic elastomer (sTPE) for microfluidics is presented. It allows the rapid fabrication of microfluidic devices through a 30 s hot embossing cycle at 220 °C followed by self-sealing through simple conformal contact at room temperature, or with baking. The material shows high chemical resistance, particularly in comparison to polydimethylsiloxane (PDMS), to many common organic solvents and can be rapidly micropatterned with high fidelity using a variety of microfluidic master molds thanks to its low mechanical stiffness. Self-sealing of the material is reversible and withstands pressures of up to 2.8 bar with room temperature sealing and 4 bar with baking at 185 °C for 2 h. The elastomeric, transparent sTPE exhibits material characteristics that make it suited for use as a microreactor, such as low absorption, surface roughness, and oxygen permeability, while also allowing a facile and scalable fabrication process. Modular microfluidic devices, leveraging the fast and reversible room temperature self-sealing, are demonstrated for the generation of water droplets in a toluene continuous phase using T-junctions of variable size. The sTPE offers an alternative to common microfluidic materials, overcoming some of their key drawbacks, and giving scope for low-cost and high-throughput devices for flow chemistry applications.

CHAPTER 3 – SELF-SEALING THERMOPLASTIC FLUOROELASTOMER ENABLES RAPID FABRICATION OF MODULAR MICROREACTORS

3.1 INTRODUCTION

While the evolution of microfluidics has placed an emphasis on its use as a tool for biological research,[1] the initial emergence of microfluidic technology touted its use for chemical analysis and synthesis.[2–6] Indeed, the physical characteristics of fluids at the micro-scale can provide for chemical syntheses with greater speed[7] and selectivity,[8] while also permitting safer[9] and more sustainable reactions[10,11] as compared to batch chemistry methods. The implementation of microfluidic systems in chemical synthesis never proliferated in the same fashion as it did in biological studies.[12] While there are numerous factors as to why, one key bottleneck has been the selection of a material with suitable properties for the demands of flow chemistry that also permits an easily adoptable method of microfluidic device fabrication.

Flow chemists using microfluidic devices have traditionally stuck to what is familiar, most often opting for glass devices, which demonstrate excellent chemical inertness, heat resistance, and optical clarity. The tradeoff for glass devices is their higher material cost and more expensive and intensive fabrication methods as compared to those of polymeric materials.[13] Furthermore, glass microdevice fabrication most often entails the use of dangerous chemicals (such as hydrofluoric acid or potassium hydroxide), whereby stringent, and costly, safety measures must be put in place to ensure proper handling, disposal, and clean-up. The multi-step process of glass wet etching[14] requires sophisticated equipment and expertise, resulting in a large time investment for individual devices. While alternative methods of glass micropatterning exist, such as micromachining,[15] laser-assisted material modification,[16–18] and deep reactive ion etching,[19] they do not significantly improve the ease or speed of device fabrication. The accumulation of cost and fabrication time further increases with subsequent bonding of glass devices, which can be accomplished through adhesives,[20] anodic bonding,[21] high

temperatures and pressures,[22,23] or chemical washing.[24,25] The work-flow of glass microfluidic device processing and development can make it inaccessible to labs in lower-resource settings.

A transition to plastic devices in flow chemistry that addresses the costly and intensive fabrication of glass devices is a complicated endeavor that has not yet been fully realized. Most polymeric materials championed in microfluidics are those used in biological applications. This includes polydimethylsiloxane (PDMS), polystyrene (PS), and polycarbonate (PC), which are incompatible with many organic solvents.[26,27] Organic solvents cause these materials to swell or dissolve entirely, leading to microchannel deformation in minor cases and complete device failure in more serious cases.[26,28]

Fluoropolymers, however, offer higher chemical resistance than that of most other plastics[29,30] and have been used for microfluidic devices through 3D printing,[31] xurography,[32] hot embossing,[33,34] micromachining[35] and photocurable molding,[36] as well as in solvent-resistant coatings for PDMS channels.[37,38] Despite successfully achieving solvent resistant polymeric microfluidic devices, predominantly using polytetrafluoroethylene (PTFE), none of these techniques has been widely adopted for flow chemistry applications. This is likely due to some fabrication complexities that persist in these techniques, such as limited resolution, high initial costs, and low-throughput production that is not easily transferable to large-scale employment. While these techniques are variable in their strengths and drawbacks, they all share a challenge associated with bonding – a common difficulty faced when working with fluoropolymers. The most promising microfabrication methodologies rely on the addition of adhesive layers for sealing[33,39] or thermal bonding,[32,34] which introduces complications of channel collapse or deformation without careful optimization of bonding procedures.

The emergence of soft thermoplastic elastomer (sTPE) materials, such as Flexdym™[40–42] and Versaflex™ CL30,[43] has made steps in bridging the gap between the fabrication accessibility of elastomeric materials (like PDMS) and the high-throughput production potential of thermoplastics.[44] These materials have principally been composed of styrenic co-polymers, which have favorable material properties for biological applications. Moreover, they can be processed to make microfluidic devices through rapid hot embossing and facile self-sealing through conformal contact,[40] thanks in part to their soft, elastomeric properties. This self-sealing is a reversible process that avoids the

additional measures for bonding that are required by other thermoplastics and that have persistently limited the more widespread adoption of thermoplastic devices.[45] These sTPEs can be inexpensively and quickly made into devices in small lab settings, but very critically possess the same scale-up potential as traditional hard plastics through techniques like injection molding and roll-to-roll hot embossing. Consequently, the same material can be implemented across manufacturing scales, in both research-scale development and industrial-scale implementation. This fabrication transferability of sTPEs sharply contrasts with hard thermoplastics, which most often require robust and expensive master molds that must handle high temperatures and pressures and withstand de-molding from rigid substrates.[46,47] The resulting cost and processing expertise becomes largely infeasible for small labs and rapid prototyping, posing a significant bottleneck in microfluidics' transition between research and industry with hard plastics. While these existing sTPE materials have been shown to be effective for biological applications, their material composition suggests chemical resistance similar to that of polystyrene,[48] thus unsuitable for most flow chemistry applications in which organic solvents are used.

In this work, we introduce a Fluoroflex (Eden Tech), a new fluoroelastic terpolymer Poly(TFE-ter-E-ter HFP) material which is melt-processable, transparent, and features enhanced self-sealing properties (where, TFE=tetrafluoroethylene, E=ethylene, HFP=hexafluoropropylene). We evaluate the sTPE's resistance to a variety of common organic solvents by swelling testing, and further characterize the material's optical, mechanical, and surface properties in addition to investigating its absorption of small molecules and oxygen permeability. A microfabrication protocol was developed, allowing the rapid and facile production of microfluidic devices with a hot embossing cycle of less than one minute followed by self-sealing via conformal contact. Finally, a modular Fluoroflex device is used for variable size droplet generation to demonstrate the utility of its fast and reversible self-sealing, highlighting the polymer's potential as a solvent resistant material for flow chemistry microreactors with highly transferable fabrication characteristics.

3.2   MATERIALS AND METHODS

3.2.1   **sTPE Microfabrication**

Hot embossing

Raw Fluoroflex material is processed in an extruded pellet form, requiring a thermoforming procedure to achieve a functional microfluidic device. Two types of microfluidic master mold were used for hot embossing micropatterning of the sTPE: (i) an electroformed nickel-cobalt metallic mold and (ii) dry film photoresist-based molds. The metallic mold (Eden Tech SAS, Paris, France) contained a network of serpentine channels (70 μm × 70 μm). The dry film photoresist molds contained various microchannel designs (to be described further in subsequent sections) and were fabricated using Ordyl® SY 300 dry film negative photoresist (55 μm thickness, ElgaEurope s.r.l., Milan, Italy) laminated on 75 mm × 50 mm borosilicate glass slides (Corning Inc., Corning, USA) as described in Chapter 3.

sTPE hot embossing was performed with a manual heat press (DC8, Geo Knight & Co Inc., Brockton, MA, USA). sTPE pellets were uniformly placed between a microfluidic master mold and a smooth rigid surface (glass slide, silicon wafer, or polished metal plate) opposite the mold to act as a counter-plate for hot embossing. Both the top and bottom heated plates of the press were heated to 220 °C before placing the mold assembly on the lower heated plate. The upper heated plate was brought into contact with the assembly and was left for 15s to heat the assembly under no supplementary pressure. Approximately 5 bar of pressure was applied to the assembly via the lever arm of the upper heated plate for approximately 15s, or until the melted polymer propagated across the desired area of hot embossing. Spacers could be placed between the two heated plates to control for final hot-embossed sTPE sheet thickness.

The pressure was then released and the mold assembly was removed from the heat press and left at room temperature to cool for 1 min before disassembly. Attempted disassembly too soon after hot embossing often resulted in tearing of the resulting sTPE sheet, having insufficiently cooled below hot embossing temperature. Removal of the counter-plate from the hot-embossed sTPE sheet was facilitated with isopropanol. The sTPE sheet itself could subsequently be removed easily from the master mold. This same procedure was repeated with a plain glass slide in place of the master mold in order to obtain un-patterned sTPE sheets for microfluidic device sealing.

Self-sealing & Delamination Testing

Micropatterned sTPE sheets were cut to the desired size with scissors and holes were punched at the desired port locations by a steel hole punch. The sheets were then manually placed in conformal contact with pieces of un-patterned sTPE sheets of similar size, ensuring no air bubbles were present between the sTPE layers. Contact at this stage could easily be reversed and the positioning of the sTPE layers could be adjusted. Assembled devices were baked at 185 °C for 2 h in a forced convection oven (DKN612C, Yamoto Scientific Co. Ltd., Tokyo, Japan) to achieve self-sealing. Self-sealing could alternatively be achieved with simple conformal contact at room temperature, without baking.

The self-sealing bonding strength was evaluated through pressure-regulated burst testing using a microfluidic device design consisting of two disconnected channels separated by a gap of 1 mm. The inlet of the device was interfaced with a microfluidic circuit via PTFE tubing (1/16" OD, 1/32" ID) using a compression-based chip holder (Eden Tech SAS, Paris, France). The inlet channel was increasingly pressurized with water by a pressure controller (OB1® MK3+, 0–8000 ± 0.5 mbar, Elveflow®, Elvesys SAS, Paris, France) in 50 mbar steps of 5 s each until delamination across the sTPE-bonded gap occurred, or until the maximum testing pressure of 4000 mbar was reached. Delamination of the gap bond was accompanied by the flow of water from the previously dead-end inlet channel across the gap and into the device's outlet channel before exiting the device entirely via the second punched hole. Accordingly, an in-line flow sensor (MFS3, -80–80 µL min^{-1} ± 5% m.v.) was used to determine the precise moment at which delamination occurred (indicated by a non-zero flow rate). A more detailed description of the delamination device design and a similar pressure testing setup is described in Chapter 3.

Pressure testing was conducted on devices representing a variety of different sealing conditions following conformal contact in order to test the sealing pressure capacities achievable with and without baking measures. The first step in all sealing conditions was creating conformal contact between the two sTPE layers. Devices were tested in sets of n=5 devices.

Firstly, devices were tested after being baked at 185 °C for 2 h and subsequently left at room temperature for 1 h before delamination testing, i.e., were tested 3 h after the initial conformal contact between the two sTPE layers was made. To investigate the time-dependent self-sealing behavior of Fluoroflex in the absence of baking, delamination devices were tested after room temperature

self-sealing at different time points (5 min, 3 h, 1 day, 4 weeks) after initial conformal contact was made. A second set of devices was tested at 5 min post conformal contact to evaluate the repeatability of the sealing behavior between devices made on different days.

The reversibility of reusability of Fluoroflex sealing was explored through delamination testing of sTPE devices re-bonded after already having been bonded. For example, one set of devices was bonded through baking at 185 °C for 2 h; the devices were then separated manually and replaced in conformal contact and baked again at 185 °C for 2 h before being pressure tested. Another two sets were sealed at room temperature and left for one day before being manually separated and immediately replaced in conformal contact. Delamination testing on the two sets was then conducted 5 min and 3 h, respectively, after this second conformal contact was made. An additional two sets of devices were similarly bonded at room temperature and left for one day at room temperature. They were then manually separated and immediately replaced in conformal contact. This separation and resealing was repeated and additional four times at intervals of five minutes between resealings. After the fifth resealing, one set of devices was left for 5 min at room temperature before being pressure tested, whereas the second set was baked at 185 °C for 2 h then left for 1 h at room temperature before pressure testing.

Finally, to test the reusability of the sTPE material, a set of delamination devices was hot-embossed using pieces of sTPE sheets that had already been hot-embossed and bonded, instead of with raw sTPE pellets, as had been used in the microfabrication of all previous devices.

Profilometry

Optical profilometer measurements (Wyko NT9100, Veeco Instruments Inc., Plainview, NY, USA) were conducted on sTPE sheets patterned with serpentine microchannels using the nickel-cobalt master mold described above to evaluate hot embossing molding resolution and fidelity. Measurements were also taken of the master mold itself for comparison.

3.2.2 Solvent Testing

Patterned sTPE sheets were used to evaluate the effects of organic solvents on the material and microarchitecture. The nickel-cobalt master mold was used to

hot emboss sTPE sheets of approximately 1 mm thickness with channels of 70 μm width and depth, which were then cut with scissors into discrete pieces. Micropatterned sTPE pieces were imaged using a stereoscope (Leica DMS300, Leica Microsystems Inc., Buffalo Grove, IL, USA) and the distances between the microchannels on each piece were measured through image analysis (Fiji[49]). After imaging, the sTPE pieces were placed in containers of 26 common organic solvents (standard laboratory-grade ≥ 95%, Sigma-Aldrich, St, Louis, MO, USA) and water (n=5 pieces per solvent) and left at room temperature for 24 hours under complete immersion. Each piece was subsequently reimaged while remaining immersed in the solvent, and the distances between the microchannels were again measured through image analysis. Polymer swelling was determined by using a standard percent difference evaluation to define a "swelling ratio," $S = D_2/D_1$, where D_1 and D_2 are the measured polymer dimensions before and after solvent swelling, respectively. Additional PDMS samples (SYLGARD™ 184, Dow Inc., Midland, MI, USA) were prepared and tested in the same manner with a few solvents to validate the coherence of swelling data in literature with swelling data obtained through this experimental method.

Fitting of a Hansen Solubility Parameter (HSP) for Fluoroflex followed the standard iterative method developed by Charles Hansen.[50] Solvents were designated as "swelling" ($S > 1.02$) and "non-swelling" solvents based on solvent swelling observations. An initial estimate of the HSP of Fluoroflex with radius, R_O, was made based on the average HSP values of all the swelling solvents. A quality-of-fit was evaluated based on the location of the swelling and non-swelling solvent HSPs in relation to the polymer HSP solubility sphere initial estimate, whereby an error in the fit was denoted by a swelling solvent falling outside of the estimated HSP sphere or a non-swelling solvent falling inside of the sphere. More specifically, the error value is equal to the distance between the erroneous solvent and the edge of the HSP sphere. That is,

$$ERROR\ DISTANCE = R_o - R_a \qquad (3.1)$$

For non-swelling solvents inside the estimated sphere and,

$$ERROR\ DISTANCE = R_a - R_o \qquad (3.2)$$

For swelling solvents outside of the estimated sphere, where R_a denotes the distance between the sphere center, (δ_{D1}, δ_{P1}, δ_{H1}), and a given solvent's HSP, (δ_{D2}, δ_{P2}, δ_{H2}), from literature[50]:

$$R_a = \sqrt{4(\delta_{D2} - \delta_{D1})^2 + (\delta_{P2} - \delta_{P1})^2 + (\delta_{H2} - \delta_{H1})^2}$$ (3.3)

The constant, 4, in the equation was found to be appropriate in representing solubility data as a sphere.[50] The method uses a quality-of-fit function called the "Desirability Function,"[51] where the data fit is calculated as,

$$Data\ Fit = (A_1 * A_2 * \ldots * A_n)^{1/n}$$ (3.4)

When,

$$A_i = e^{-(ERROR\ DISTANCE)}$$ (3.5)

Swelling solvents falling inside of the sphere, as well as non-swelling solvents falling outside of the sphere, contributed to a Data Fit of 1.00 (no error), with fitting iterations aimed at optimizing this case given the experimental swelling data recorded. Subsequent iterations of Fluoroflex's three HSP components and R_O were performed in order to maximize the data fit toward 1.00.

3.2.3   Optical Characterization

All optical characterization was performed on sheets of pristine, un-patterned Fluoroflex hot-embossed between two silicon wafers (University Wafer Inc., South Boston, MA, USA). Sheets of 1.5 mm thickness were cut with scissors to the desired sample size for each of the following optical characterization procedures.

UV-Vis Spectroscopy

To evaluate optical transparency, UV-Vis absorption spectra (200–800 nm) of pristine sTPE samples were measured with a Lambda 950 spectrophotometer (PerkinElmer Inc., Waltham, MA, USA). A second set of UV-Vis measurements were performed on samples that had been exposed to UV light (365nm; 70 mW cm^{-2} for 8 h, or 2016 J cm^{-2}; UV Chamber™, UWAVE, Les Ulis, France). A positive control for swelling was evaluated to determined shifts in spectra post-swelling. Fluoroflex samples were immersed in acetone for 24 hours at room temperature and then allowed to de-swell for 24 hours prior to measurements being taken.

Refractive Index

The refractive index of pristine Fluoroflex samples was measured with an Abbe 5 refractometer (Bellingham + Stanley Ltd., Kent, UK).

Autofluorescence

Autofluorescence measurements (λ_{exc} = 250–600 nm; λ_{em} = (λ_{exc} + 30)–800 nm) were conducted on pristine Fluoroflex samples using an Edinburgh FLS908 spectrometer (Edinburgh Instruments Ltd., Livingston, UK). A MATLAB® script (The MathWorks, Inc., Natick, Massachusetts, USA) was used to plot an autofluorescence excitation/emission heat map across the range of wavelengths tested.

FTIR Spectroscopy

Fourier transform infrared (FTIR) spectroscopy was performed on pristine Fluoroflex samples in the range of 4000–400 cm^{-1} using a Nicolet™ iS™ 5 FTIR spectrometer (Thermo Fisher Scientific, Waltham, MA, USA). The FTIR spectra were compared to those measured of both UV-exposed (1 h, 2 h, 4 h, and 8 h exposure time) and acetone-exposed samples to investigate the effect of UV irradiation and solvent swelling on the material composition.

3.2.4   Mechanical and Surface Characterization

Tensile Testing

Mechanical characterization consisted of uniaxial tensile tests. All tests were performed with an INSTRON 5848 microtester (INSTRON, Norwood, MA, USA). Dog-bone samples of approximately 20 mm length and 2 × 2 mm cross-section were fabricated by pressing sTPE pellets into laser-cut stainless-steel molds using the same hot embossing parameters as described above. A controlled traction displacement of 1 mm min^{-1} was applied (from 0% strain to specimen rupture). In the range of interest (0–20% strain), no reduction in the cross-sectional area of the specimen was assumed to calculate stress and subsequent elastic modulus using Hooke's law. The test was performed in ten different specimens of 19.73 ± 1.65 mm in length (mean ± standard deviation) and 2 × 2 mm cross-section.

Contact Angle

Contact angle measurements were performed using the pendant drop method. Water and diiodomethane droplets were dispensed onto the surface of pristine sTPE sheets hot-embossed between two silicon wafers, as well as onto acetone-exposed sTPE sheets. The droplets were imaged and analyzed using the CAM 200 contact angle goniometer (KSV Instruments, Helsinki, Finland). Determination of the surface energy of Fluoroflex was conducted using Fowke's method.[52]

Atomic Force Microscopy

For a surface roughness evaluation of the sTPE, atomic force microscopy (AFM) measurements were performed. Fluoroflex sheets of 1 mm thickness were hot-embossed between two silicon wafers and topographic images of 6 μm × 6 μm, 4 μm × 4 μm, and 2 μm × 2 μm of the sheets were recorded at three different surface locations per sample in tapping mode with a PicoSPM 5100 scanning probe microscope (Agilent Technologies, Santa Clara, CA, USA). Additional imaging was performed on sTPE sheets after acetone swelling and de-swelling, as well as on the silicon wafers used for hot embossing. Measurements were taken in ambient conditions using silicon cantilevers (AC160TS-R3, Olympus Corporation, Tokyo, Japan) with resonance frequency around 300 kHz and spring constant around 26 N/m, and subsequent roughness analyses were conducted with WSxM 5.0 software[53] to obtain the RMS surface roughness of each image. Surface roughness values are reported as the average RMS values across all the topographic images taken of a given sample type. A one-way analysis of variance (ANOVA) was conducted to evaluate statistically significant variation in surface roughness between pristine and acetone-swelled sTPE sample, where variation was considered significant when $p < 0.05$.

3.2.5 Absorption & Permeability

Rhodamine B Absorption

For an evaluation of small molecule absorption of Fluoroflex, a rhodamine B absorption assay was conducted to compare the Fluoroflex to PDMS. Microfluidic devices consisting of a simple channel of 400 μm width and 55 μm height were fabricated in Fluoroflex using an Ordyl® master mold and the hot embossing and self-sealing procedure described above. The same mold was

used to fabricate PDMS devices. Liquid PDMS base (SYLGARD™ 184, Dow Inc., Midland, MI, USA) was mixed with crosslinker at a ratio of 10:1 (base:crosslinker) then degassed under vacuum for 20 minutes. The mixture was poured atop the master mold and baked at 80 °C for 2 hours (DKN612C forced convection oven, Yamoto Scientific Co. Ltd., Tokyo, Japan). PDMS devices were removed from the mold and cut and 1.5 mm holes were punched with a biopsy punch. Devices were bonded to borosilicate glass microscope slides (76 mm × 26 mm, 1 mm thickness, Thermo Fisher Scientific, Waltham, MA, USA) by making conformal contact with the PDMS surface after plasma treatment with a plasma cleaner (200 mTorr, 30W, 2 minutes PDC-002, Harrick Plasma, Ithaca, NY, USA). Devices were left on a hot plate at 120 °C for 30 min to complete the fabrication process. Rhodamine B dye (100 μM in water, Sigma-Aldrich, St. Louis, MO, USA) was loaded into both a Fluoroflex and PDMS channel and left to incubate in ambient conditions for 24 h. Devices were then imaged with a fluorescent microscope (Zeiss Axio Observer Z1, Carl Zeiss AG, Oberkochen, Germany) and subsequently flushed continuously with DI water for 5 minutes, after which devices were re-imaged.

Oxygen Permeability

The oxygen pure gas permeability of Fluoroflex was measured using a custom-made high-throughput gas separation (HTGS) setup, as previously described.[54–56] The active membrane permeation area was 1.91 cm^2 per coupon. A constant-volume-varying-pressure method was applied to determine the oxygen permeability. Permeate gas is accumulated in a 75 cm^3 measuring cylinder and the change in pressure inside the cylinder is monitored by a pressure sensor (MKS Baratron®, MKS Instruments, Andover, MA, USA) as a function of time (dp/dt). The material's gas permeability is then calculated with the following equation:

$$P_{O2} = 10^{10} \times \frac{V \times V_m \times L}{p_{up} \times A \times R \times T} \times \frac{dp}{dt} \qquad\qquad (3.7)$$

with P_{O2}, the oxygen gas permeability (Barrer), V, the downstream volume (75 cm^3), V_m, the molar volume (22.414 L mol^{-1}), A, the membrane permeation area (1.91 cm^2), L, the membrane thickness (μm), T, the operating temperature (K), p_{up}, the upstream pressure (bar), R, the gas constant (0.082 L atm mol^{-1} K^{-1}), and dp/dt, the pressure increase (Torr s^{-1}). Permeability measurements were conducted at 6 bar feed pressure and 35 °C.

Fluoroflex films of approximately 200 μm thickness were fabricated by hot embossing sTPE pellets between two metal plates for 30 s. PDMS (SYLGARD™ 184, 10:1 base:crosslinker) films of approximately 115 μm thickness were spin-coated using an initial 10 s step at 500 rpm and a subsequent 30 s step at 800 rpm with 300 rpm s^{-1} acceleration (Spin 150 spin coater, SPS-Europe B.V., Putten, The Netherlands) followed by baking for two hours at 80 °C.

3.2.6 **Modular Droplet Generation**

A modular microfluidic device was created using Fluoroflex, consisting of a hot-embossed sTPE base plate, or manifold, containing designated spaces on its surface to host individual sTPE microfluidic modules. Holes punched in the upper layer of the base plate allowed fluid connections between modules and the device inlets and outlets through a simple network of sealed channels. All sTPE parts were hot-embossed using the same parameters as above (220 °C for 30 s) using molds made from Ordyl® dry film photoresist on glass slides. The base plate (approximately 75 mm × 25 mm in size) consisted of one sTPE sheet hot embossed with channels measuring 110 μm × 500 μm (height × width) bonded to a featureless sTPE sheet. PEEK NanoPort assemblies, including perfluoroelastomer (FFKM) gaskets (N-333, Darwin Microfluidics, Paris, France), were fixed to the top of the base plate with Loctite 3106 UV curing glue (CureUV, Delray Beach, FL, USA), cured with 30 s of UV exposure using a Scangrip® UV-PEN (25 mW cm^{-2}, 390–400 nm; SCANGRIP North America Inc., Atlanta, GA, USA). Individual modules (17 mm × 25 mm) were placed in conformal contact with the base plate top surface in alignment with the appropriate base plate channels and holes for bonding at room temperature. All modules had channels 110 μm in height. 1/16" OD PTFE tubing was used to interface the modular device with reservoirs of deionized water and toluene (≥ 95%, Sigma-Aldrich, St, Louis, MO, USA), pumped using an OB1® MK3+ pressure controller (0–2000 ± 0.1 mbar, Elveflow®, Elvesys SAS, Paris, France). Microfluidic T-junction droplet generation using the modular device was imaged using a Pixelink® PL-D725CU camera (Pixelink, Ottawa, Canada) on a Zeiss Axio Observer Z1 microscope (Carl Zeiss AG, Oberkochen, Germany) and images were analyzed using FIJI.[49]

3.3   RESULTS AND DISCUSSION

3.3.1   **sTPE Microfabrication**

Hot Embossing

Fluoroflex exhibits a melting temperature of approximately 210–220 °C. Attempted hot embossing at 200 °C produced a crumbling effect on the polymer pellets, as opposed to pure melting behavior. 220 °C was found to be the minimum temperature at which reliable hot embossing molding could be achieved.

The developed hot embossing protocol was used to create micropatterned sheets of the Fluoroflex polymer within 30 s (**Figure 3.1a**). Half of this time, ~15 s, is spent to heat both the mold and counter-plate of the assembly before pressure is applied through the press. Without this step, the polymer pellets were found to produce less uniform melt distribution, sometimes resulting in air bubbles in the final micropatterned sTPE sheet. The time of the assembly under pressure could be varied depending on the desired thickness of the final sTPE sheet. Spacers could be placed between the two heated plates to control for the final hot-embossed sTPE sheet thickness. A pressing time of 15 s was sufficient for producing sTPE sheets of between 0.5 mm and 1 mm thickness, whereas ~100 μm films could be fabricated by removing spacers and pressing for 30 s. These thin, elastomeric films could feasibly be used for the implementation of on-chip pneumatic "Quake" valves.[57] Hot embossed sTPE sheets can be stored indefinitely for subsequent manipulation or bonding, with no degradation observed throughout the duration of this work. Step-by-step images of the sTPE hot embossing process are shown in **Figure 3.S1**.
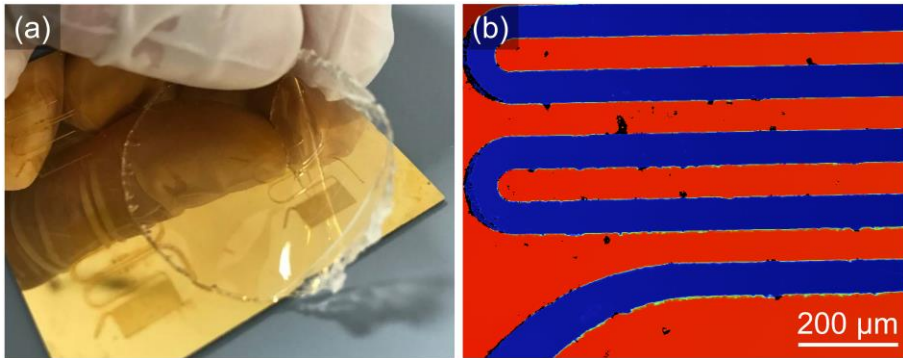
Figure 3.1. (a) Removal of a sheet of Fluoroflex from a nickel-cobalt microfluidic mold after hot embossing for under 30 s to create micro-patterned Fluoroflex sheets, which can be subsequently assembled into microfluidic devices through self-sealing. (b) Profilometer image of serpentine channels (70 μm, 1:1 aspect ratio) patterned into Fluoroflex with nickel-cobalt mold, exhibiting mold-chip fidelity of approximately 3 μm, or less than 5% difference. Dark spots between channels likely indicate the presence of dust particles on the sTPE sheet.

In this work, two types of microfluidic master mold were used for hot embossing micropatterned sTPE: an electroformed nickel-cobalt mold and dry film photoresist-based molds. While the metallic mold is representative of a hot embossing mold for hard thermoplastics, Fluoroflex's elastomeric properties permit the use of less robust molds on glass or silicon wafer substrates. The dry film photoresist molds, consisting of Ordyl® photoresist on glass slides, represent a fast and inexpensive means of microfluidic molding.[58] Fluoroflex's versatility in molding is consistent with that of previously reported sTPEs, and highlights the transferability of such materials; they present a PDMS-like low investment threshold for small-scale implementation, but also possess the scope for large-scale production of thermoplastics.

Self-sealing Bonding Strength

Fluoroflex microfluidic device assembly could be completed manually in a matter of minutes. This is markedly simpler than analogous procedures for glass and hard thermoplastic microfluidic devices, which require diverse and sometimes process-intensive and costly steps for sealing and interfacing.[45] Likewise, other fluoropolymer microfluidic devices reported in literature involve the use of adhesive layers[33,39] or thermal bonding[32,34] for sealing. Even PDMS, which can readily form conformal contact thanks to its elastomeric properties, requires plasma surface activation in order to achieve robust device

sealing. Fluoroflex requires only conformal contact at room temperature for immediate device sealing, or optional baking for 2 hours. The choice of sealing condition between room temperature and baking was found to affect the bonding strength of Fluoroflex.

Pressure delamination tests showed bonded sTPE devices withstanding a maximum testing pressure of 4 bar after baking for 2 h at 185 °C. Room temperature sealing, consisting only of conformal contact between two sTPE layers, demonstrated time-dependent strength. On shorter timescales (i.e., same-day microdevice production), devices sealed at room temperature for 5 min and 3 h before pressure delamination testing showed bonding strengths of 1460 ± 22 mbar and 1799 ± 229 mbar (mean ± standard deviation), respectively. While the bonding strength of room temperature sealing is lower than that achieved by baking, if high pressure capacities are not required, it provides the possibility for near-immediate use of Fluoroflex devices after hot embossing (i.e., rapid prototyping). Room temperature sealing also eliminates the need for an oven, adding to the simplicity and accessibility of microfabrication with Fluoroflex. An additional set of delamination devices bonded at room temperature for 5 min exhibited a bonding strength of 1310 ± 96 mbar, showing little difference between batches of sTPE devices fabricated on different days. In comparison, the strength of PDMS-to-PDMS (irreversible) bonding via air or oxygen plasma surface activation commonly falls between 2 and 3 bar,[59,60] but has been reported in the range of 0.7–4 bar,[61] reflecting its high sensitivity to plasma parameters and environmental conditions. However, reversible sealing of PDMS to PDMS based on conformal contact at room temperature, similar to the sealing done with Fluoroflex, exhibits a bonding strength of approximately 0.4 bar.[59]

Room temperature sealing of Fluoroflex on longer timescales resisted higher pressures, with delamination devices withstanding 2350 ± 285 mbar one day after fabrication and 2850 ± 127 mbar four weeks after fabrication. These long-term investigations, while impractical from a rapid microfabrication point of view, were conducted principally to gain insight into the time-dependent nature of Fluoroflex self-bonding at room temperature. The time dependence of sTPE bonding indicates a behavior similar to that of other sTPE materials. Lachaux et al., for example, described the Flexdym™ sTPE as a "slow adhesive polymer foil" for its intrinsic adhesive and cohesive properties resulting from the re-organization of mobile and covalently branched polymer chains at the interface of two polymer sheets, which is accelerated at elevated temperatures.[40]

Resealing of Fluoroflex after an initial bonding and separation showed decreased bond strength. Delamination devices tested 5 min and 3 h after resealing (at room temperature) exhibited bonding strengths of 990 ± 108 mbar and 1411 ± 273, respectively, both approximately 400 mbar inferior to the bonding strengths of their initial-bond counterparts, i.e., devices tested 5 min and 3 h after their first sealing at room temperature. However, further loss of bonding strength was not found after additional separations and resealings. Devices separated and resealed at room temperature five times before delamination testing (5 min after the last resealing) exhibited a bonding strength of 1030 ± 76 mbar. Moreover, bonding strength could be recovered through baking. Baking for 2 h at 185 °C after separating and resealing five times at room temperature resulted in sTPE devices withstanding the maximum testing pressure of 4 bar. Similarly, devices that were sealed through baking, separated, and baked again also withstood the maximum testing pressure of 4 bar.

Fluoroflex's reversible self-sealing opens new possibilities that are in contrast with the permanent bonding most often utilized with other microfluidic materials, be it PDMS, hard thermoplastics, or glass. Reversible sealing provides a practical advantage of enabling the correction of manual errors or misalignments of multi-layered devices instead of discarding a flawed device. This also gives scope, for example, to separate and clean a device after use before being resealed and re-used, as well as the ability to fabricate modular devices, in which discrete functional device components can simply and quickly be mixed and matched with fast room temperature sealing. Modular microfluidics, leveraging Fluoroflex's self-sealing properties, is discussed further in Section 3.3.6.

The devices made from recycled Fluoroflex pieces showed a bonding strength of 1590 ± 129 mbar, incidentally slightly greater than the bonding strengths of the two sets of analogous devices fabricated with the same sealing conditions, but with raw sTPE pellets. These devices, made from recycled Fluoroflex, demonstrate the potential to reuse not only individual devices through reversible sealing but also the material in its entirety through secondary hot embossing to fabricate new devices. This repurposing could translate to reduced material consumption, and with it, reduced cost for the end-user. A full list of bonding strengths of each of the different sTPE sealing conditions can be found in **Table 3.1**.

Table 3.1. Summary of self-sealing bond strengths of Fluoroflex after variable sealing conditions determined through delamination testing. sTPE delamination devices were sealed at either room temperature (RT) or 185 °C and pressure tested after their first bond or after they had been separated and resealed (re-bond). Finally, one set (n=5) of delamination devices was fabricated using recycled sTPE material that had already been hot-embossed and bonded. Bond strengths are reported as mean ± standard deviation given a maximum testing pressure of 4000 mbar.

Set No.	Sealing Condition		Bond Strength [mbar]
1	First bond, 185 °C	2 h bake at 185 °C, 1 h at RT	4000 ± 0 (max)
2	First bond, RT	5 min at RT	1460 ± 22
3	First bond, RT	5 min at RT (repeated set)	1310 ± 96
4	First bond, RT	3 h at RT	1799 ± 229
5	First bond, RT	1 day at RT	2350 ± 285
6	First bond, RT	4 weeks at RT	2850 ± 127
7	Re-bond, 185 °C	2 h bake at 185 °C, separation, 2 h bake at 185 °C	4000 ± 0 (max)
8	Re-bond, RT	1 day at RT, separation, 5 min at RT	990 ± 108
9	Re-bond, RT	1 day at RT, separation, 3 h at RT	1411 ± 273
10	Re-bond, RT	1 day at RT, 5×(separation, 5 min at RT)	1030 ± 76
11	Re-bond, 185 °C	1 day at RT, 5×(separation, 5 min at RT), 2 h bake at 185 °C	4000 ± 0 (max)
12	Recycled sTPE, RT	Recycled sTPE hot embossing, 5 min at RT	1590 ± 129

It is critical to note that while Fluoroflex can withstand pressures of 4 bar (and likely higher), due to its elastomeric properties and the low thickness (approximately 700–1000 µm) of micropatterned sheets, some channel deformation and bulging occurred at the higher end of testing pressures. Thus, even if sTPE self-sealing withstands higher pressures, a stiffer material, such as glass, would be more suitable for applications requiring pressures above ~3 bar to maintain the integrity of channel geometry.

Molding Resolution

Optical profilometer measurements of micropatterned Fluoroflex sheets showed good molding resolution (**Figure 1.1b**). sTPE sheets preserved the features of the nickel-cobalt mold, reproducing the 70 μm × 70 μm channels to within 3 μm (4.3 %) difference in both channel height and width, likely due to minor shrinkage after thermoforming inherent to thermoplastics.[62]

3.3.2 Solvent Compatibility

Investigating Fluoroflex's compatibility with common organic solvents is a critical step in determining its suitability as a flow chemistry microreactor material. Fluoroflex swelling ratios show significantly less swelling than PDMS across the range of 26 solvents tested (**Table 3.2**).[26] Tetrahydrofuran (THF) (S=1.43), 2-butanone (S=1.44), and acetone (S=1.43) caused the highest degrees of swelling in Fluoroflex. Polar aprotic solvents, including THF, 2-butanone, acetone, 1,2-dimethoxyethane, and n-methylpyrrolidone, generally produced the strongest interactions observed, whereas polar protic solvents, such as alcohols and amines, and non-polar solvents, such as toluene, hexane, and chloroform, produced little to no swelling effect in Fluoroflex.

Table 3.2. Swelling ratios of Fluoroflex and PDMS (where, when D_1 and D_2 are the polymer dimensions before and after solvent swelling, respectively, the swelling ratio, $S=D_2/D_1$) for a selection of common organic solvents of solubility parameters, δ, in [joule$^{1/2}$ cm$^{-3/2}$].[50] Fluoroflex exhibits significantly less swelling than PDMS. PDMS swelling ratios from Lee et al.[26]

Solvent	δ	$S_{Fluoroflex}$	S_{PDMS}
Pentane	14.5	1.00	1.44
Diisopropylamine	14.9	1.00	2.13
Hexane	14.9	1.00	1.35
n-Heptane	15.1	1.01	1.34
Triethylamine	15.3	1.00	1.58
Cyclohexane	16.8	1.00	1.33
1,2-Dimethoxyethane	18.0	1.27	1.32
Xylenes	18.2	1.00	1.41
Toluene	18.2	1.02	1.31
Benzene	18.8	1.00	1.28
Chloroform	18.8	1.01	1.39
Tetrahydrofuran	19.0	1.43	1.38
2-Butanone	19.0	1.44	1.21
Dimethylcarbonate	19.4	1.18	1.03
Chlorobenzene	19.4	1.00	1.22
Dichloromethane	20.3	1.03	1.22
Acetone	20.3	1.43	1.06
1,4-Dioxane	20.5	1.13	1.16
Pyridine	21.7	1.08	1.06
N-Methylpyrrolidone	22.7	1.27	1.03
Acetonitrile	24.3	1.08	1.01
1-Propanol	24.3	1.00	1.09
Dimethylformamide	24.8	1.22	1.02
Nitromethane	25.8	1.03	1.00
Ethanol	26.0	1.00	1.04
Methanol	29.7	1.01	1.02
Water	47.9	1.00	1.00

Lee et al. considered PDMS "highly soluble" and generally incompatible with pure solvents at a swelling ratio threshold of S=1.28. Only three of the 26 solvents tested swelled Fluoroflex to this level, as compared to the 12 solvents that produced this effect in PDMS. With eight solvents still swelling Fluoroflex to a moderate degree (S ≥ 1.10), Fluoroflex's chemical compatibility is inferior to glass, which undoubtedly remains the material of choice when specific and extensive chemical resistances are sought. However, Fluoroflex exhibits greater chemical resistance than that of PDMS and other thermoplastics commonly used in microfluidic devices,[63] allowing a broader range of chemical reactions that could be performed in a polymeric device.

Solubility parameters are often used to estimate the interactions between polymers and solvents and have been vital in evaluating chemical compatibility of materials in place of empirical observation. The first single-component solubility parameter, introduced by Hildebrand and Scott,[64] is an expression of a material's cohesive energy density, whereby solubility (or polymer swelling in a solvent) in a two-phase system is maximized when the two solubility parameters are equal.[27] That is to say in this context, a solvent is more likely to swell or dissolve a polymer if their respective solubility parameters are close or equal to one another.

Fluoroflex's solubility parameter was calculated from the swelling data collected to estimate polymer-solvent interactions of solvents not tested. However, a single-component, Hildebrand solubility parameter model was found to be insufficient in describing the polymer-solvent interactions observed. For example, acetone and dichloromethane both have a Hildebrand solubility parameter of 20.2 joule$^{1/2}$ cm$^{-3/2}$, but acetone is one of the highest swelling solvents (S=1.43) whereas dichloromethane swells Fluoroflex by only a minimal amount (S=1.03). It is clear that a more descriptive model is necessary to describe the observed swelling behavior of Fluoroflex. Charles Hansen's three-component solubility parameter provided greater accuracy in describing solubility interactions, accounting for separate contributions of atomic dispersion forces, permanent dipole-dipole (polar) forces, and hydrogen bonding to the overall cohesive energy density of a material.[50] The Hansen Solubility Parameter (HSP) thus consists of three components, δ_D (dispersion), δ_P (polar) and δ_H (hydrogen bonding), which can be resolved to a total solubility parameter, equivalent to the Hildebrand solubility parameter, δ, through the relationship, $\delta^2 = \delta_D^2 + \delta_P^2 + \delta_H^2$. The three-component HSP can be understood as a point in a three-dimensional solubility space with a solubility radius, R_O. A compound having an HSP that falls within the HSP sphere of another

compound is then expected to produce a solubility interaction, whether it be miscibility (in liquid-liquid cases) or dissolution/swelling (in solid-liquid cases).

Iterative fitting (Data Fit of 1.00) of an HSP resulted in an estimated Fluoroflex HSP of δ=21.2 joule$^{1/2}$ cm$^{-3/2}$, consisting of components δ_D=16.5, δ_P=8.9 and δ_H=9.7 joule$^{1/2}$ cm$^{-3/2}$, with a sphere radius of R_o=7.5 joule$^{1/2}$ cm$^{-3/2}$ (**Figure 3.2**). The HSP fit containing the smallest radius of interaction, R_O, was deemed superior and is presented above. However, it must be noted that given the solvent swelling data set size, room for minor variation in the final HSP exists while still maintaining a Data Fit of 1.00. These nuances in HSP data fitting, further discussed in the supporting information (including **Figure 3.S2**), underscore the inherent difficulties of solubility parameter estimations, particularly in the border regions of solubility spheres[65] and when polymer swelling, as opposed to dissolution, is concerned.[66]
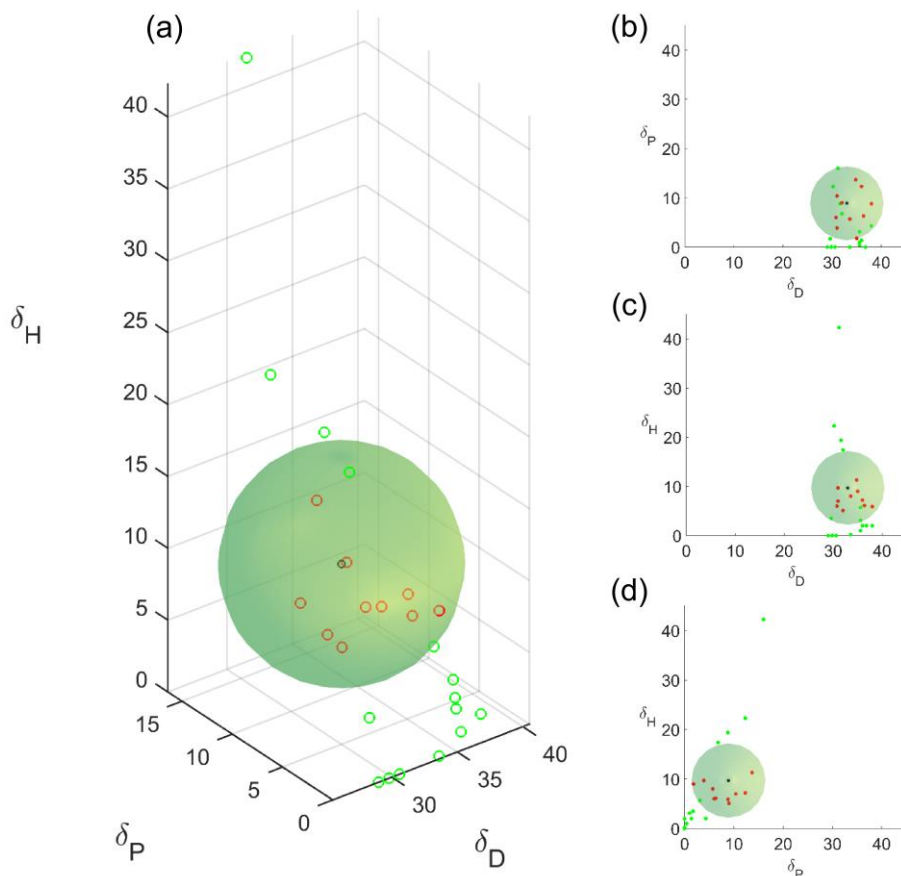
Figure 3.2. Hansen solubility parameter estimation for Fluoroflex based on polymer-solvent swelling data from Table 1: δ_D=16.5, δ_P =8.9 and δ_H =9.7 joule$^{1/2}$ cm$^{-3/2}$, with a sphere radius of R_O=7.5 joule$^{1/2}$ cm$^{-3/2}$. (a) HSP sphere of Fluoroflex with center (black) in a solubility "space," having dispersion, polar and hydrogen bonding dimensions. Red points represent solvents having some swelling effect (S>1.02) on Fluoroflex, while green points represent those producing no or negligible swelling. (b–d) HSP sphere with HSP components shown pair-wise for ease of viewing. Note that a scaling factor of 2 is used for the dispersion component, δ_D, for effective graphical representation of a spherical HSP, as described by Hansen.[50] Graphs in units of [joule$^{1/2}$ cm$^{-3/2}$].

This HSP should thus be used conservatively as a tool by a potential user of Fluoroflex if using a solvent not included in this work, or indeed a solvent mixture that exhibits a certain HSP. Solvent blending, informed by Fluoroflex's HSP, could moreover be a means of mitigating the adverse effects of the few solvents that have high swelling effects on Fluoroflex.

3.3.3 **Optical Properties**

Optical characterization of Fluoroflex was an important step in understanding its suitability for a variety of microfluidic applications, particularly where imaging and irradiation (i.e., photocatalysis on-chip) are necessary.

UV-Vis Spectroscopy

UV-Vis measurements on Fluoroflex sheets showed high optical transparency of the material into the near UV range, with over 50% transmission down to 334 nm (**Figure 3.3a**). This optical transparency is comparable or superior to other thermoplastics used for microfluidics, such as PMMA[67] and PC,[68] and would allow observation and imaging with a range of fluorescent dyes. Both UV irradiation and exposure to acetone (24 h exposure for sTPE swelling, followed by 24 h de-swelling in air) showed little effect on the optical transmission of the sTPE.
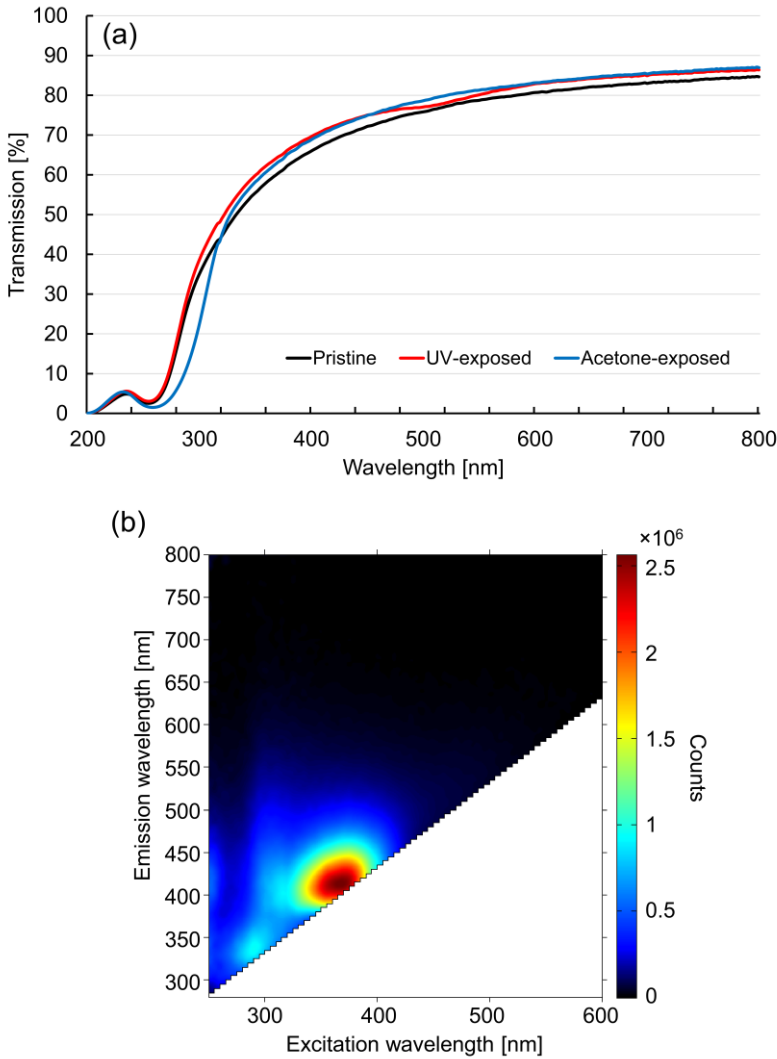
Figure 3.3. (a) UV-Vis spectra of Fluoroflex samples, 1 mm in thickness, exhibiting high optical transmission into the near UV wavelengths. Exposure of sTPE sample to UV light and acetone swelling had a negligible effect on transmission. (b) Fluorescence mapping of Fluoroflex, showing autofluorescence in the UV and violet excitation wavelengths with a peak at 370 nm.

Autofluorescence

Like some other thermoplastics used for microfluidics,[69] Fluoroflex was found to exhibit autofluorescence. Fluorescence mapping revealed peak

autofluorescence at an excitation wavelength of 370 nm (**Figure 3.3b**). This poses limitations of the material for fluorescent imaging, particularly with excitation wavelengths in the violet and UV ranges. Depending on the given application, this needs to be considered when using Fluoroflex microfluidic devices.

Refractive Index

The refractive index of a microfluidic device can be an important property when choosing an optical imaging setup to optimize resolution and clarity.[70,71] Fluoroflex was found to have a refractive index of n=1.36. Its low refractive index compared to glass (n=1.46) and PDMS (n=1.41),[72] in addition to its similarity to the refractive index of water (n = 1.33), could be advantageous in applications involving imaging in aqueous media or with water-immersion objectives.

FTIR Spectroscopy

While solvent swelling and UV (365 nm) exposure had no apparent permanent effect on Fluoroflex samples, these conditions can cause unseen degrading effects on polymers.[73,74] To this end, FTIR measurements were conducted to investigate any structural changes that could occur in Fluoroflex as a result of material swelling and UV exposure. FTIR spectra showed no significant changes across the range of UV and acetone-exposed samples (**Figure 3.S3**), suggesting no material structural alterations occurred as a result of these conditions.

3.3.4   Mechanical & Surface Properties

Tensile Testing

Basic mechanical testing was performed on Fluoroflex to determine general mechanical behavior and quantify the elastomeric properties that can be important in informing material fabrication and deformability. In tensile strength testing (from 0% strain to specimen rupture), the material shows two different regions of deformation (**Figure 3.4a**). The change in behavior takes place between approximately 40% and 70% strain, beyond which the material exhibits lower stiffness. Tensile strength analysis focused on strain levels under 20%, as high levels of strain are not expected during the use of Fluoroflex as a microfluidic device. For this range of deformation, the mechanical behavior of this material is not entirely linear elastic, with decreased stiffness at higher

strain levels, resulting in a mean elastic modulus of 4.75 ± 0.22 MPa and 3.75 ± 0.17 MPa (mean ± standard deviation; n=10) for strains of $\epsilon < 5\%$ and $\epsilon < 20\%$, respectively (**Figure 3.4b**). This tensile stiffness is the same order of magnitude as that of PDMS, which is most often in the range of ~1–3 MPa.[75–77] This relatively low stiffness eases de-molding and is critical for reliably creating conformal contact between sTPE layers for bonding, in contrast with hard thermoplastics, having stiffness in the order of gigapascals.[46] Fluoroflex samples were taken to rupture and exhibited 434 ± 44% elongation at break.
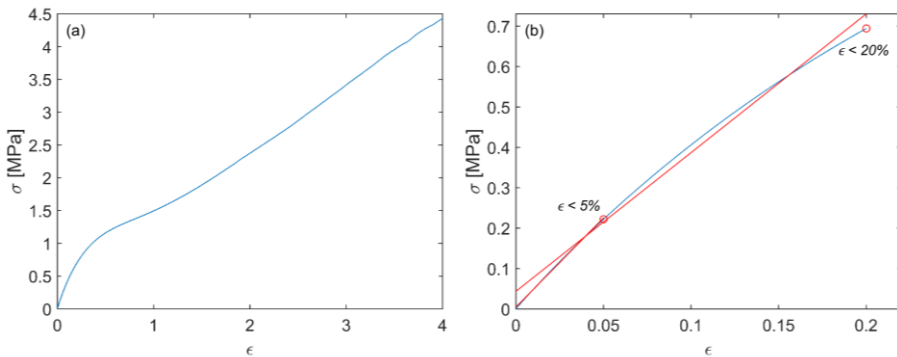
Figure 3.4. (a) The tensile stress-strain curve of a Fluoroflex sample taken to rupture at ~450% strain, showing two distinct regions of stiffness. Higher stiffness was measured in strains up to ~40% before a transition to lower stiffness above ~70% strain. (b) Zoom of the Fluoroflex stress-strain curve for a strain of 0–20%, with linear fits for $\epsilon < 5\%$ and $\epsilon < 20\%$ (red) approximating the mean tensile modulus for these strain ranges.

Surface Wetting

Surface wetting properties can be imperative in anticipating and manipulating precision microfluidic flow control,[78] particularly in multiphase flow.[79–82] Goniometer measurements of water and diiodomethane on Fluoroflex sheets showed hydrophobic surface behavior of Fluoroflex (θ_{Water}=105.0 ± 1.2°, $\theta_{Diiodomethane}$= 64.9 ± 0.7°; n=5) (**Figure 3.S4a–b**). Exposure of samples to acetone prior to contact angle measurements had a negligible effect on the sTPE surface wetting properties (θ_{Water}=105.1 ± 0.8°, $\theta_{Diiodomethane}$= 64.6 ± 1.3°; n=5). The two-component surface energy of Fluoroflex was determined through the Fowkes method [52] to be purely dispersive ($\sigma_{Fluoroflex}$=25.6 mJ m^{-2}). This wetting behavior and low surface energy characteristics are close to those of PDMS.[83] This could permit the use of well-documented PDMS surface wetting

behavior as an analog to inform and evaluate microfluidic flow in Fluoroflex devices.

Surface Roughness

AFM surface roughness evaluations of Fluoroflex revealed that pristine sTPE sheets hot-embossed between silicon wafers (wafer roughness R_{RMS}=1.6 ± 1.0 nm; mean ± standard deviation, n=9 images of one wafer) had a roughness of R_{RMS}=5.7 ± 3.1 nm (n=20 images, two sTPE sheets). Swelling and subsequent de-swelling of Fluoroflex in acetone showed a statistically insignificant effect on surface roughness (R_{RMS}=4.3 ± 2.0 nm; n=19 images, two sTPE sheets; ANOVA: $F_{(1, 37)}$=3.07, p=0.09), with no evidence of surface cracking or degradation after material swelling. It must be noted that sTPE sample microfabrication was not conducted in a cleanroom, thus a slight decrease in sTPE surface roughness after acetone exposure could be the result of the cleaning effects of solvent submersion on surface contaminants. An important contribution in the total roughness comes from isolated defects, such as hills or pits, in the sTPE sheets. In defect-free regions, the roughness can be as low as R_{RMS}=1.6 nm, which can be considered as a lower limit for the surface roughness of Fluoroflex sheets. The surface roughness achievable with Fluoroflex is sufficiently low (<1% relative roughness) as to be considered smooth on a microfluidic scale, having a negligible effect on flow resistance.[84–86] A surface roughness of 5.7 nm in a 50 μm (diameter or width & height) microfluidic channel, for example, represents a relative roughness of ~0.01%. Maintaining low surface roughness in microfluidics also has broader implications in facilitating reliable device bonding[47,87,88] and high optical clarity[89,90] in thermoplastics. Roughness analyses suggest that the limiting factor in achieving good molding reproduction of surface topography with surface roughness below 10 nm would depend on the roughness of the master mold and not on any roughness inherent to the material itself or resulting from the hot embossing process. AFM topography images can be found in **Figure 3.S4c–f**.

3.3.5 **Absorption & Oxygen Permeability**

Small Molecule Absorption

PDMS has been well documented in absorbing a variety of drug and dye compounds, which can have a significant impact on experimental outcomes.[91] In comparison to PDMS, Fluoroflex exhibited minimal residual fluorescence

after rinsing, and no observable absorption into the bulk of the material through the channel walls (**Figure 3.5**), a favorable property for applications as a microreactor.
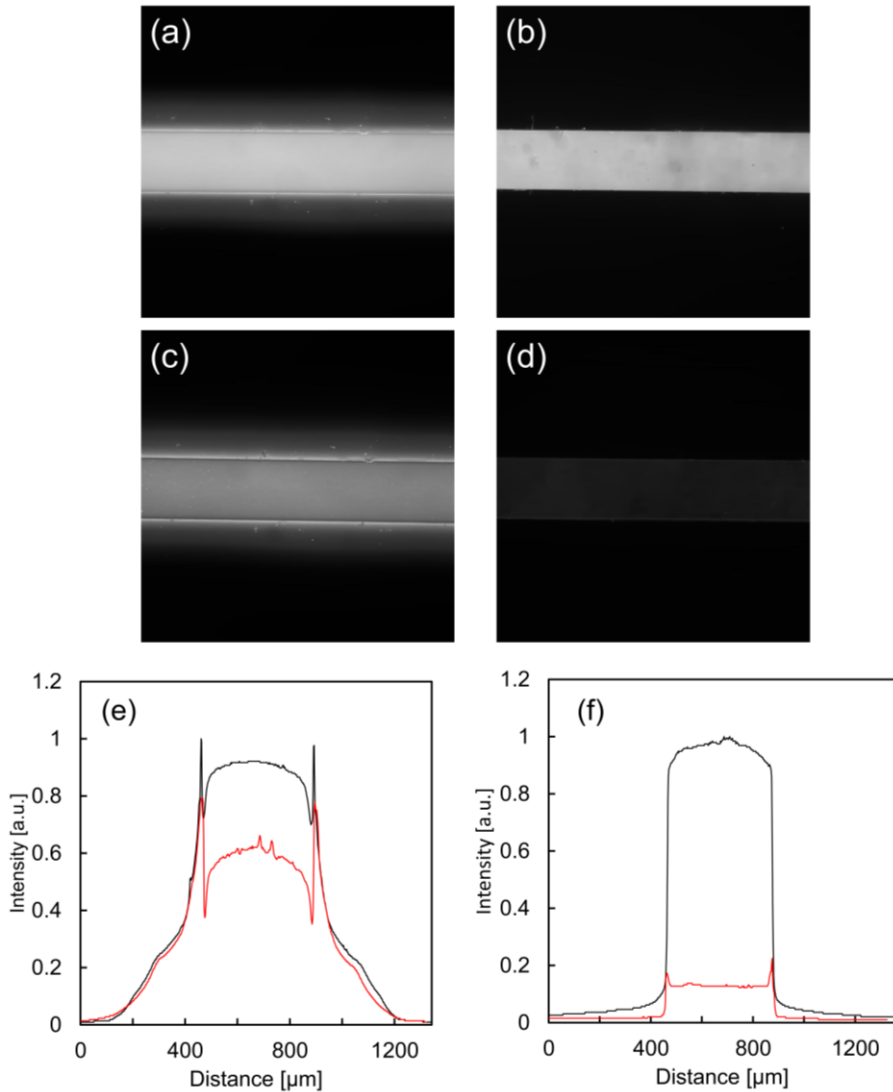
Figure 3.5. Rhodamine B absorption analysis in PDMS and Fluoroflex microchannels measuring 400 μm (width) x 55 μm (height). Fluorescent images of (a) PDMS and (b) Fluoroflex channels containing 100 μM Rhodamine B in water after 24 h incubation. Images (c) and (d) show the same PDMS and Fluoroflex channels, respectively, after rinsing with DI water with corresponding fluorescence intensity line profiles across the

PDMS (e) and Fluoroflex (f) channels, where the black and red lines correspond to the normalized intensity of the channels pre and post rinsing, respectively.

Oxygen Permeability

The presence of oxygen, or lack thereof, can be a critical factor in both biological and chemical experimentation.[92,93] Thus, quantifying the degree to which a given material permits the flux of oxygen from ambient air into a sealed microfluidic channel is of high importance. The oxygen permeability of Fluoroflex was found to be 4.04 ± 0.79 Barrer (mean ± standard deviation) compared to a permeability of 563.5 ± 12.1 Barrer of PDMS. The oxygen permeability of PDMS found experimentally is on the lower end of values reported in literature,[94,95] but still represents an oxygen permeability of more than two orders of magnitude greater than that of Fluoroflex. As compared to PDMS, this provides greater opportunity for the sTPE to be used as a microreactor for oxygen-sensitive chemical reactions or where oxygen concentrations or gradients on-chip must be controlled.

A concise summary of Fluoroflex's key material properties and microfabrication procedure can be found in a material "Specification Sheet" in **Appendix 1**.

3.3.6   **Modular Droplet Generation**

The fast, room temperature self-sealing property of Fluoroflex enables the use of sealed microdevices mere minutes after assembly. At the same time, the reversibility of the bonding allows for the removal, adjustment, and reuse of individual sTPE pieces. By leveraging these characteristics, devices can be easily configured and reconfigured by combining discrete microfluidic components, or modules. To this end, a modular sTPE device for droplet generation was fabricated to demonstrate the simplicity and utility of device modification thanks to fast self-sealing (**Figure 3.S5a–d**).

The modular device initially contained two micropatterned modules: a simple straight channel and a T-junction droplet generator, both bonded at room temperature to the surface of the base plate (**Figure 3.6a**). Water was pumped through the straight channel (250 μm width) to the 100 μm T-junction, where droplets of approximately 90 μm in diameter were formed in a continuous phase of toluene (**Figure 3.6b**). The sTPE exhibited no deformation or leaking caused by the toluene, a solvent that readily swells PDMS. The T-junction

module was then manually removed and a larger T-junction module (250 μm) was put in its place (**Figure 3.6c**). Within minutes, droplets of approximately 140 μm were generated with the new T-junction module without altering any other fluidic connections or pressure control settings (**Figure 3.6d**). Next, the straight channel was replaced with a co-flow Y-channel module, allowing the droplet phase to contain the mixture of two fluids instead of one. To demonstrate this, fluorescent droplets were generated using an aqueous rhodamine B solution (100 mM) from one inlet and pure DI water from the second inlet (**Figure 3.S5e–h**). Other conceivable adjustments would be adding a subsequent module in series, downstream of the droplet generation to increase residence time for droplet viewing, mixing, etc. Extensions of increasingly complex liquid manipulation, with or without droplets, becomes possible by considering a wide variety of modules. The only condition for the modules is that they are designed to fit the dimensions of the base plate fluid connections. Accordingly, the quick self-sealing properties of Fluoroflex would permit true "plug-and-play" operation, effective for rapid prototyping and device optimization – similar to electronic breadboards.

In combination with Fluoroflex's straightforward and transferrable thermoplastic fabrication method, a modular device platform gives scope for the development of the large-scale industrialization of standardized microfluidic devices both in terms of device production and ease of use.[96]
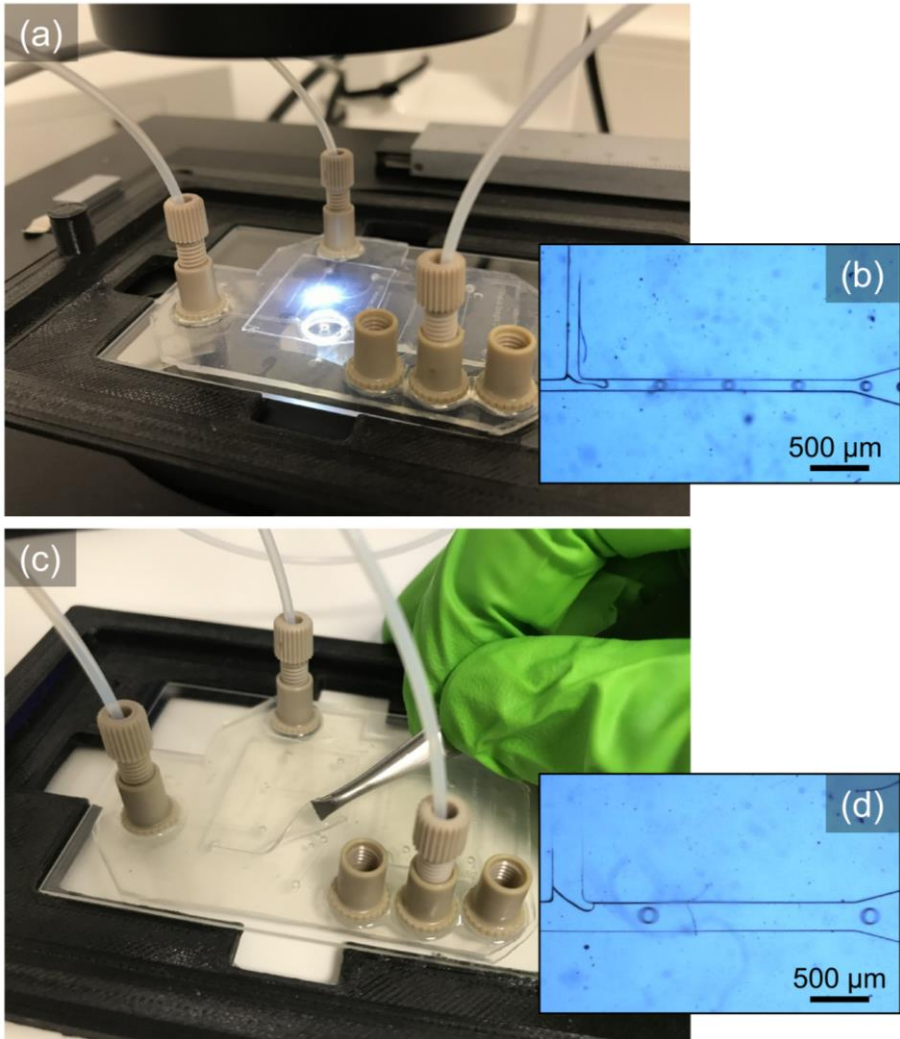
Figure 3.6. Modular microfluidic device based on sTPE room temperature self-sealing. (a) Modular sTPE device consisting of an sTPE base plate and two microfluidic modules (a straight channel, right, and a T-junction droplet generator, left) bonded to the surface of the base plate. Connectors were fixed to the base plate with UV curing glue to allow microfluidic tubing interfacing. Using this first, 100 μm T-junction, water droplets of approximately 90 μm were generated in a continuous phase of toluene (b). The 100 μm T-junction module was then removed with tweezers (c) and replaced with a larger, 250 μm T-junction module, with which droplets of approximately 140 μm were generated (d). Reconfiguration of the device with the second T-junction module was completed in a matter of minutes thanks to the fast and reversible room temperature self-sealing of Fluoroflex.

3.4 CONCLUSIONS

This study introduces a new fluorinated soft thermoplastic elastomer, Fluoroflex. The sTPE can be micropatterned in 30 s with high fidelity by hot embossing using standard microfluidic molds. Fluoroflex exhibits a spontaneous cohesive property upon conformal contact, allowing it to be simply sealed to itself at room temperature or with baking measures in order to assemble closed-channel microfluidic devices. This self-sealing eliminates the need for plasma surface activation, adhesives, or other process-intensive bonding procedures commonly used to seal microdevices. The resulting sTPE self-bonding is reversible and can withstand pressures up to ~2.8 bar with room temperature sealing and at least 4 bar with baking, determined through pressure delamination testing. Its room temperature bonding strength was found to increase with time, but could still achieve a bonding strength of ~1.4 bar after only five minutes. The ease of sTPE device fabrication and material recyclability sharply contrasts with device microfabrication using other common materials and lends heavily to its accessibility and scope for transferability across manufacturing scales.

Fluoroflex's solvent compatibility was determined to exhibit good solvent resistance to a range of common organic solvents. While falling short of the solvent resistance of glass or pure PTFE, it represents a marked improvement over other polymeric materials used for microfluidics, such as PDMS, PC, and PMMA. In addition to more comprehensive solvent resistance, glass would also be more suitable for high-pressure/high-temperature applications.

We also characterized a range of Fluoroflex's material properties pertinent to its use as a microreactor. Namely, it was found to be optically transparent down to the near-UV range, have hydrophobic surface behavior, low surface roughness (~5 nm), oxygen gas permeability two orders of magnitude lower than that of PDMS, and a mean elastic modulus of 3.75 MPa ($\epsilon < 20\%$).

One thing not extensively explored was the potential effects of thermoplastic additives involved in the production of the Fluoroflex raw material. Additives describe a wide range of chemical compounds, such as stabilizers, lubricants, plasticizers, colorants, fillers, flame retardants, and reinforcements, that are often added to plastic materials to improve their performance.[109] Plasticizers, in particular, are commonly used in the production of elastomers, serving to reduce a material's hardness, tensile modulus, glass transition temperature, and melt viscosity, while increasing a material's flexibility, toughness, and

elongation at break.[110] While due to the proprietary nature of Fluoroflex, this cannot be further discussed explicitly, it should be noted that plastic additives can lead to unwanted adverse effects, such as cytotoxicity[111,112] and photodegradation.[74] This should thus be taken into consideration during further material investigations, particularly in the context of potential bio-microfluidics applications.

Finally, droplet generation was conducted in a Fluoroflex device to demonstrate the use of an organic solvent in a precision microfluidic context. The device showcased the fast, reversible self-sealing of the sTPE, allowing for discrete microfluidic components to be interchanged in a "modular" system. Combined with the ease and accessibility of device fabrication, this could allow for rapid prototyping or "plug-and-play" functionality of chemical microreactors.

To our knowledge, this is the first fluorinated thermoplastic that can be rapidly micropatterned and exhibits self-sealing upon conformal contact. We believe it represents a combination of material properties and processing simplicity of broad interest to the microfluidics and flow chemistry communities.

3.5   ACKNOWLEDGEMENTS

3.6 REFERENCES

[1]   D. T. Chiu, A. J. deMello, D. Di Carlo, P. S. Doyle, C. Hansen, R. M. Maceiczyk, R. C. R. Wootton, *Chem* **2017**, *2*, 201.

[2]   A. Manz, N. Graber, H. M. Widmer, *Sensors Actuators B Chem.* **1990**, *1*, 244.

[3]   R. Srinivasan, S. L. Firebaugh, I.-M. Hsing, J. Ryley, M. P. Harold, K. F. Jensen, M. A. Schmidt, in *Proc. Int. Solid State Sensors Actuators Conf. (Transducers '97)*, IEEE, **n.d.**, pp. 163–166.

[4]   W. Ehrfeld, K. Golbig, V. Hessel, H. Löwe, T. Richter, *Ind. Eng. Chem. Res.* **1999**, *38*, 1075.

[5]   M. C. Mitchell, V. Spikmans, A. Manz, A. J. de Mello, *J. Chem. Soc. Perkin Trans. 1* **2001**, 514.

[6]   E. Garcia-Egido, S. Y. F. Wong, B. H. Warrington, *Lab Chip* **2002**, *2*, 31.

[7]   T. Illg, V. Hessel, P. Lçb, J. C. Schouten, *ChemSusChem* **2011**, *4*, 392.

[8]   T. Asai, A. Takata, Y. Ushiogi, Y. Iinuma, A. Nagaki, J. Yoshida, *Chem. Lett.* **2011**, *40*, 393.

[9]   J. Pelleter, F. Renaud, *Org. Process Res. Dev.* **2009**, *13*, 698.

[10]   L. Vaccaro, D. Lanari, A. Marrocchi, G. Strappaveccia, *Green Chem.* **2014**, *16*, 3680.

[11]   K. S. Elvira, X. C. i Solvas, R. C. R. Wootton, A. J. DeMello, *Nat. Chem.* **2013**, *5*, 905.

[12]   N. Convery, N. Gadegaard, *Micro Nano Eng.* **2019**, *2*, 76.

[13]   H. Becker, C. Gärtner, *Electrophoresis* **2000**, *21*, 12.

[14]   S. C. Jacobson, R. Hergenroder, L. B. Koutny, J. M. Ramsey, *Anal. Chem.* **1994**, *66*, 1114.

[15]   D. J. Harrison, K. Fluri, K. Seiler, Z. Fan, C. S. Effenhauser, A. Manz, *Science (80-.)* **1993**, *261*, 895.

[16]   C. Hnatovsky, R. S. Taylor, E. Simova, P. P. Rajeev, D. M. Rayner, V. R. Bhardwaj, P. B. Corkum, *Appl. Phys. A Mater. Sci. Process.* **2006**, *84*, 47.

[17]   N. Burshtein, S. T. Chan, K. Toda-Peters, A. Q. Shen, S. J. Haward, *Curr. Opin. Colloid Interface Sci.* **2019**, *43*, 1.

[18]   T.-L. Chang, Z.-C. Chen, Y.-W. Lee, Y.-H. Li, C.-P. Wang, *Microelectron. Eng.* **2016**, *158*, 95.

[19]   S.-J. Paik, S. Byun, J.-M. Lim, Y. Park, A. Lee, S. Chung, J. Chang, K. Chun, D. "Dan" Cho, *Sensors Actuators A Phys.* **2004**, *114*, 276.

[20]   H. . Wang, R. . Foote, S. . Jacobson, J. . Schneibel, J. . Ramsey, *Sensors Actuators B Chem.* **1997**, *45*, 199.

[21]   J. Liu, J. Shang, J. Tang, Q.-A. Huang, *J. Microelectromechanical Syst.* **2011**, *20*, 909.

[22]   D. J. Harrison, A. Manz, Z. Fan, H. Luedi, H. M. Widmer, *Anal. Chem.* **1992**, *64*, 1926.

[23]   A. Sayah, D. Solignac, T. Cueni, M. A. . Gijs, *Sensors Actuators A Phys.* **2000**, *84*, 103.

[24]   Z. J. Jia, Q. Fang, Z. L. Fang, *Anal. Chem.* **2004**, *76*, 5597.

[25]   P. B. Allen, D. T. Chiu, *Anal. Chem.* **2008**, *80*, 7153.

[26]   J. N. Lee, C. Park, G. M. Whitesides, *Anal. Chem.* **2003**, *75*, 6544.

[27]   J. E. Mark, Ed. , *Physical Properties of Polymers Handbook*, Springer New York, New York, NY, **2007**.

[28]   R. Dangla, F. Gallaire, C. N. Baroud, *Lab Chip* **2010**, *10*, 2972.

[29]   V. Arcella, A. Ghielmi, G. Tommasi, *Ann. N. Y. Acad. Sci.* **2003**, *984*, 226.

[30]   W. R. Dolbier, *J. Fluor. Chem.* **2005**, *126*, 157.

[31]   F. Kotz, P. Risch, D. Helmer, B. Rapp, *Micromachines* **2018**, *9*, 115.

[32]   T. Hizawa, A. Takano, P. Parthiban, P. S. Doyle, E. Iwase, M. Hashimoto, *Biomicrofluidics* **2018**, *12*, 064105.

[33]   S. Begolo, G. Colas, J. L. Viovy, L. Malaquin, *Lab Chip* **2011**, *11*, 508.

[34]   K. Ren, W. Dai, J. Zhou, J. Su, H. Wu, *Proc. Natl. Acad. Sci. U. S. A.* **2011**, *108*, 8162.

[35]   O. Cybulski, S. Jakiela, P. Garstecki, *Lab Chip* **2016**, *16*, 2198.

[36]   J. P. Rolland, R. M. Van Dam, D. A. Schorzman, S. R. Quake, J. M. DeSimone, *J. Am. Chem. Soc.* **2004**, *126*, 2322.

[37]   C. T. Riche, C. Zhang, M. Gupta, N. Malmstadt, *Lab Chip* **2014**, *14*, 1834.

[38]   T. Yang, J. Choo, S. Stavrakis, A. de Mello, *Chem. – A Eur. J.* **2018**, *24*, 12078.

[39]   E. Sano, C. Mori, N. Matsuoka, Y. Ozaki, K. Yagi, A. Wada, K. Tashima, S. Yamasaki, K. Tanabe, K. Yano, Y. Torisawa, *Micromachines* **2019**, *10*, 793.

[40]   J. Lachaux, C. Alcaine, B. Gómez-Escoda, C. M. Perrault, D. O. Duplan, P.-Y. J. Wu, I. Ochoa, L. Fernandez, O. Mercier, D. Coudreuse, E. Roy, *Lab Chip* **2017**, *17*, 2581.

[41]   J. Lachaux, H. Salmon, F. Loisel, N. Arouche, I. Ochoa, L. L. Fernandez, G. Uzan, O. Mercier, T. Veres, E. Roy, *Adv. Mater. Technol.* **2019**, *4*, 1.

[42]   D. J. Case, Y. Liu, I. Z. Kiss, J. R. Angilella, A. E. Motter, *Nature* **2019**, *574*, 647.

[43]   E. Roy, M. Geissler, J. C. Galas, T. Veres, *Microfluid. Nanofluidics* **2011**, *11*, 235.

[44]   E. Roy, J. C. Galas, T. Veres, *Lab Chip* **2011**, *11*, 3193.

[45]   Y. Temiz, R. D. Lovchik, G. V. Kaigala, E. Delamarche, *Microelectron. Eng.* **2015**, *132*, 156.

[46]   E. Roy, A. Pallandre, B. Zribi, M.-C. Horny, F. D. Delapierre, A. Cattoni, J. Gamby, A.-M. Haghiri-Gosnet, in *Adv. Microfluid. - New Appl. Biol. Energy, Mater. Sci.* (Ed.: X.-Y. Yu), InTechOpen, London, UK, **2016**.

[47]   E. Berthier, E. W. K. Young, D. Beebe, *Lab Chip* **2012**, *12*, 1224.

[48]   M. D. Borysiak, K. S. Bielawski, N. J. Sniadecki, C. F. Jenkel, B. D. Vogt, J. D. Posner, *Lab Chip* **2013**, *13*, 2773.

[49]   J. Schindelin, I. Arganda-Carreras, E. Frise, V. Kaynig, M. Longair, T. Pietzsch, S. Preibisch, C. Rueden, S. Saalfeld, B. Schmid, J. Y. Tinevez, D. J. White, V. Hartenstein, K. Eliceiri, P. Tomancak, A. Cardona, *Nat. Methods* **2012**, *9*, 676.

[50]   C. Hansen, *Hansen Solubility Parameters*, CRC Press, **2007**.

[51]   E. C. Harrington, *Ind. Qual. Control* **1965**, *21*, 494.

[52]   F. M. Fowkes, *Ind. Eng. Chem.* **1964**, *56*, 40.

[53]   I. Horcas, R. Fernández, J. M. Gómez-Rodríguez, J. Colchero, J. Gómez-Herrero, A. M. Baro, *Rev. Sci. Instrum.* **2007**, *78*, 013705.

[54]   A. L. Khan, S. Basu, A. Cano-Odena, I. F. J. Vankelecom, *J. Memb. Sci.* **2010**, *354*, 32.

[55]   J. Didden, R. Thür, A. Volodin, I. F. J. Vankelecom, *J. Appl. Polym. Sci.* **2018**, *135*, 1.

[56]   R. Thür, N. Van Velthoven, S. Slootmaekers, J. Didden, R. Verbeke, S. Smolders, M. Dickmann, W. Egger, D. De Vos, I. F. J. Vankelecom, *J. Memb. Sci.* **2019**, *576*, 78.

[57]   M. A. Unger, H. Chou, T. Thorsen, A. Scherer, S. Quake, *Science (80-.).* **2000**, *288*, 113.

[58]   P. Vulto, N. Glade, L. Altomare, J. Bablet, L. Del Tin, G. Medoro, I. Chartier, N. Manaresi, M. Tartagni, R. Guerrieri, *Lab Chip* **2005**, *5*, 158.

[59]   J. C. McDonald, D. C. Duffy, J. R. Anderson, D. T. Chiu, H. Wu, O. J. A. Schueller, G. M. Whitesides, *Electrophoresis* **2000**, *21*, 27.

[60]   M. A. Eddings, M. A. Johnson, B. K. Gale, *J. Micromechanics Microengineering* **2008**, *18*, 067001.

[61]   S. Bhattacharya, A. Datta, J. M. Berg, S. Gangopadhyay, *J. Microelectromechanical Syst.* **2005**, *14*, 590.

[62] R. Novak, C. F. Ng, D. E. Ingber, in *Cell-Based Microarrays. Methods Mol. Biol. Vol 1771* (Eds.: P. Ertl, M. Rothbauer), Humana Press, New York, NY, **2018**, pp. 161–170.

[63] W. A. Woishnis, S. Ebnesajjad, *Chemical Resistance of Thermoplastics*, Elsevier, Oxford, **2012**.

[64] J. H. Hildebrand, R. S. Scott, *The Solubility of Nonelectrolytes. By Joel H. Hildebrand and Robert S. Scott.*, Reinhold Pub. Corp., New York, **1950**.

[65] J. Lara, D. Drolet, C. Hansen, A. Chollot, N. Monta, *Int. J. Curr. Res.* **2017**, *9*, 47860.

[66] M. Vayer, A. Vital, C. Sinturel, *Eur. Polym. J.* **2017**, *93*, 132.

[67] G. A. Diaz-Quijada, R. Peytavi, A. Nantel, E. Roy, M. G. Bergeron, M. M. Dumoulin, T. Veres, *Lab Chip* **2007**, *7*, 856.

[68] D. Ogończyk, J. Węgrzyn, P. Jankowski, B. Dąbrowski, P. Garstecki, *Lab Chip* **2010**, *10*, 1324.

[69] A. Piruska, I. Nikcevic, S. H. Lee, C. Ahn, W. R. Heineman, P. A. Limbach, C. J. Seliskar, *Lab Chip* **2005**, *5*, 1348.

[70] Y. Hanada, T. Ogawa, K. Koike, K. Sugioka, *Lab Chip* **2016**, *16*, 2481.

[71] A. K. Au, W. Lee, A. Folch, *Lab Chip* **2014**, *14*, 1294.

[72] D. N. H. Kim, K. T. Kim, C. Kim, M. A. Teitell, T. A. Zangle, *Microfluid. Nanofluidics* **2018**, *22*, 1.

[73] S. H. Hamid, W. H. Prichard, *Polym. Plast. Technol. Eng.* **1988**, *27*, 303.

[74] E. Yousif, R. Haddad, *Springerplus* **2013**, *2*, 398.

[75] A. Mata, A. J. Fleischman, S. Roy, *Biomed. Microdevices* **2005**, *7*, 281.

[76] S. Deguchi, J. Hotta, S. Yokoyama, T. S. Matsui, *J. Micromechanics Microengineering* **2015**, *25*, 097002.

[77] I. D. Johnston, D. K. McCluskey, C. K. L. Tan, M. C. Tracey, *J. Micromechanics Microengineering* **2014**, *24*, 035017.

[78] H. A. Stone, A. D. Stroock, A. Ajdari, *Annu. Rev. Fluid Mech.* **2004**, *36*, 381.

[79] Q. Kang, D. Zhang, S. Chen, *J. Fluid Mech.* **2005**, *545*, 41.

[80] A. Nabizadeh, M. Adibifard, H. Hassanzadeh, J. Fahimpour, M. Keshavarz Moraveji, *J. Mol. Liq.* **2019**, *273*, 248.

[81] B. Zhao, C. W. MacMinn, R. Juanes, *Proc. Natl. Acad. Sci. U. S. A.* **2016**, *113*, 10251.

[82] M. P. Boruah, A. Sarker, P. R. Randive, S. Pati, S. Chakraborty, *Phys. Fluids* **2018**, *30*, 122106.

[83] M. J. Owen, *Comments Inorg. Chem.* **1988**, *7*, 195.

[84] J. B. Taylor, A. L. Carrano, S. G. Kandlikar, *Int. J. Therm. Sci.* **2006**, *45*, 962.

[85] B. Dai, M. Li, Y. Ma, *Appl. Therm. Eng.* **2014**, *67*, 283.

[86] J. Jia, Q. Song, Z. Liu, B. Wang, *Microsyst. Technol.* **2019**, *25*, 2385.

[87] T. Wang, J. Wu, T. Chen, F. Li, T. Zuo, S. Liu, *Microsyst. Technol.* **2017**, *23*, 1405.

[88] E. Vereshchagina, P. Carmona, E. Andreassen, J. Batalden, M. Plassen, M. M. Mielnik, *Proc. IEEE Int. Conf. Micro Electro Mech. Syst.* **2018**, *2018-Janua*, 1257.

[89] C. Matellan, A. E. Del Río Hernández, *Sci. Rep.* **2018**, *8*, 1.

[90] I. R. G. Ogilvie, V. J. Sieben, C. F. A. Floquet, R. Zmijan, M. C. Mowlem, H. Morgan, *J. Micromechanics Microengineering* **2010**, *20*, 065016.

[91] M. W. Toepke, D. J. Beebe, *Lab Chip* **2006**, *6*, 1484.

[92] M. D. Brennan, M. L. Rexius-Hall, L. J. Elgass, D. T. Eddington, *Lab Chip* **2014**, *14*, 4305.

[93] M. B. Plutschack, B. Pieber, K. Gilmore, P. H. Seeberger, *Chem. Rev.* **2017**, *117*, 11796.

[94] T. C. Merkel, V. I. Bondar, K. Nagai, B. D. Freeman, I. Pinnau, *J. Polym. Sci. Part B Polym. Phys.* **2000**, *38*, 415.

[95] H. X. Rao, F. N. Liu, Z. Y. Zhang, *J. Memb. Sci.* **2007**, *303*, 132.

[96] Y. Q. Fan, H. L. Wang, K. X. Gao, J. J. Liu, D. P. Chai, Y. J. Zhang, *Chinese J. Anal. Chem.* **2018**, *46*, 1863.

[97]   F. Gharagheizi, *J. Appl. Polym. Sci.* **2007**, *103*, 31.

[98]   M. Weng, *J. Appl. Polym. Sci.* **2016**, *133*, 1.

[99]   D. Mathieu, *ACS Omega* **2018**, *3*, 17049.

[100]   E. Stefanis, C. Panayiotou, *Int. J. Thermophys.* **2008**, *29*, 568.

[101]   K. Adamska, A. Voelkel, *Int. J. Pharm.* **2005**, *304*, 11.

[102]   O. Segarceanu, M. Leca, *Prog. Org. Coatings* **1997**, *31*, 307.

[103]   E. Stefanis, C. Panayiotou, *Int. J. Pharm.* **2012**, *426*, 29.

[104]   M. J. Louwerse, A. Maldonado, S. Rousseau, C. Moreau-Masselon, B. Roux, G. Rothenberg, *ChemPhysChem* **2017**, *18*, 2999.

[105]   R. Inglev, G. Woyessa, O. Bang, J. Janting, *J. Light. Technol.* **2019**, *37*, 4776.

[106]   M. Huth, C.-W. Chen, J. Köhling, V. Wagner, *Appl. Clay Sci.* **2018**, *161*, 412.

[107]   K. V. Kurada, M. Dutta, A. Jana, S. De, *J. Appl. Polym. Sci.* **2020**, *137*, 1.

[108]   C. Bordes, V. Fréville, E. Ruffin, P. Marote, J. Y. Gauvrit, S. Briançon, P. Lantéri, *Int. J. Pharm.* **2010**, *383*, 236.

[109]   J. N. Hahladakis, C. A. Velis, R. Weber, E. Iacovidou, P. Purnell, J. Hazard. Mater. 2018, 344, 179.

[110]   J. K. Fink, A Concise Introduction to Additives for Thermoplastic Polymers, John Wiley & Sons, Inc., Hoboken, NJ, USA, 2009.

[111]   H. Xu, D. Dinsdale, B. Nemery, P. H. M. Hoet, Toxicol. Sci. 2003, 72, 92.

[112]   L. Zimmermann, G. Dierkes, T. A. Ternes, C. Völker, M. Wagner, Environ. Sci. Technol. 2019, 53, 11467.

SUPPORTING INFORMATION TO CHAPTER 3

3.7 SUPPORTING INFORMATION
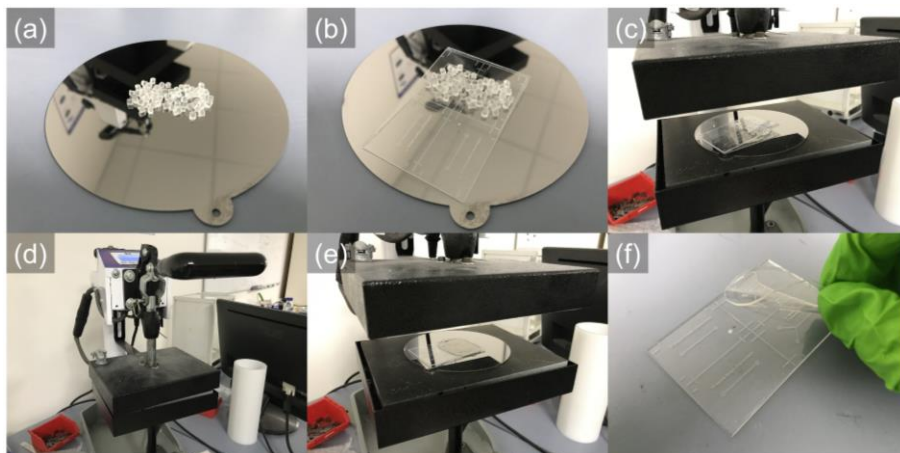
Figure 3.Sl. Fluoroflex hot embossing. (a) Raw sTPE pellets are placed on a flat, smooth surface used as a counter-plate for hot embossing (nickel-cobalt plate shown). (b) A microfluidic master mold (Ordyl® dry film photoresist on glass) is placed atop the pellets. Note that only half of the mold is being used in this instance. (c) The assembly is placed on a manual heat press with both plates heated to 220 °C. (d) The upper plate is brought into contact with the assembly and left for 15 s while the assembly is allowed to heat before pressure is manually applied for 15 s to thermoform the melted pellets. (e) After the upper plate is lifted, the hot embossing assembly is removed from the press and separated from the counter-plate using tweezers and isopropanol to ease the separation. (f) Finally, the micropatterned sTPE sheet can be removed from the mold for subsequent manipulation.

HSP Fitting: Initial iterative fitting (Data Fit > 0.96) of an HSP resulted in an estimated Fluoroflex HSP of δ=21.2 joule$^{1/2}$ cm$^{-3/2}$, consisting of components δ_D=16.5, δ_P=10.9, and δ_H=7.6 joule$^{1/2}$ cm$^{-3/2}$, with a sphere radius of R_O=8.4 joule$^{1/2}$ cm$^{-3/2}$ (Figure S2). A 100% fit was not achieved, with 1,4-dioxane falling outside of the HSP sphere boundaries while swelling Fluoroflex a modest amount (S=1.13). This irregularity likely highlights a limitation of HSP fitting relating to the molecular volume of solvents. Hansen recognized that the molecular volume of compounds can affect solubility interactions, whereby solvents with relatively low molecular volumes can produce swelling effects at greater solubility parameter distances than expected. He described the complexity of integrating a molecular volume factor into the solubility parameters, which are based on thermodynamic properties, because effects from the molecular volume originate from kinetic phenomena, i.e., diffusion and other free volume considerations.[1] Ostensibly, the molecular volume of solvents is partially accounted for in the dispersion solubility parameter component, δ_D, making it problematic to explicitly incorporate into Hansen's solubility model. That being said, a solvent's molecular volume can be a useful fourth parameter to consider in order to help describe polymer swelling anomalies. While 1,4-dioxane is not among the smallest of solvents tested (85.7 cm^3 mol^{-1}), smaller solvents such as acetonitrile and nitromethane (52.9 cm^3 mol^{-1} and 54.3 cm^3 mol^{-1}, respectively) exhibited a minor swelling effect on Fluoroflex and may evidence the impact of molecular volume on HSP fitting. The inclusion of these two highly polar solvents results in HSP sphere fitting away from non-polar 1,4-dioxane, resulting in its outlier status. However, small-volume acetonitrile and nitromethane, which swell Fluoroflex to a lesser degree than 1,4-dioxane, are more probable outliers in the Hansen solubility model. Taking this into consideration, HSP fitting was repeated with the exclusion of acetonitrile and nitromethane from the dataset and a Data Fit of 1.00 was obtained, as presented in the main text.
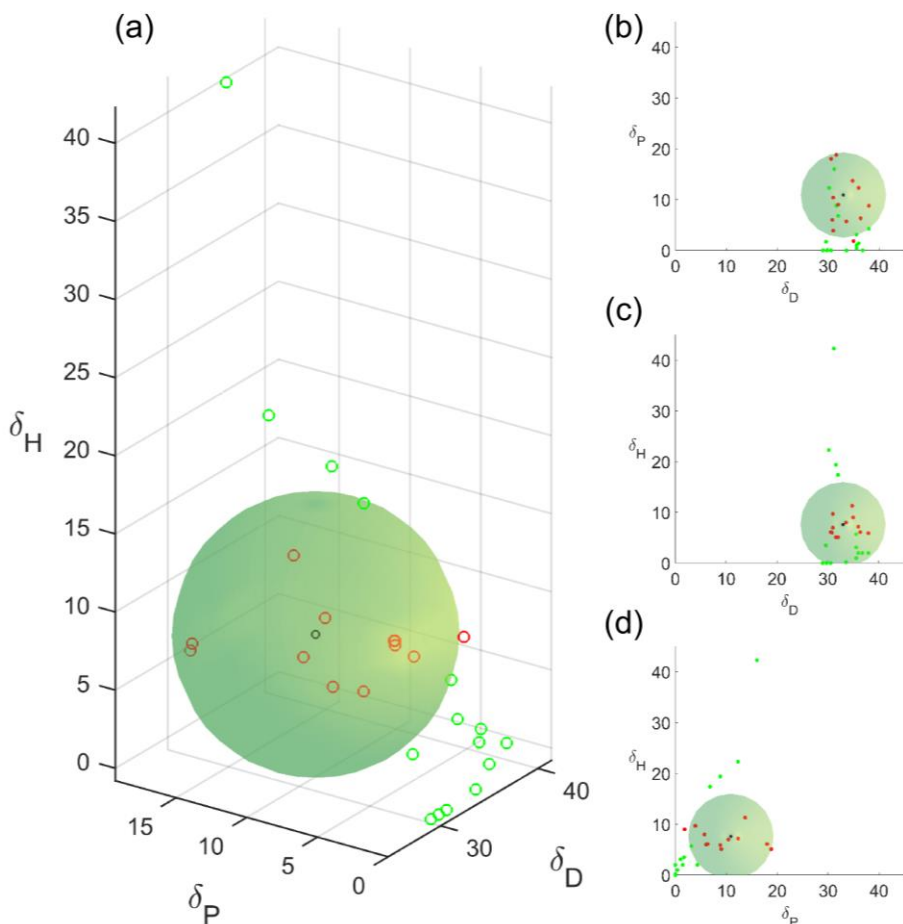
Figure 3.S2. Hansen solubility parameter estimation for Fluoroflex based on polymer-solvent swelling data from Table 1, including acetonitrile and nitromethane: δ_D=16.5, δ_P =10.9, and δ_H =7.6 joule$^{1/2}$ cm$^{-3/2}$, with a sphere radius of R_o=8.4 joule$^{1/2}$ cm$^{-3/2}$. (a) HSP sphere of Fluoroflex with center (black) in a solubility "space," having dispersion, polar and hydrogen bonding dimensions. Red points represent solvents having some swelling effect (S>1.02) on Fluoroflex, while green points represent those producing no or negligible swelling. (b–d) HSP sphere with HSP components shown pair-wise for ease of viewing. Note a scaling factor of 2 is used for the dispersion component, δ_D, for effective graphical representation of a spherical HSP, as described by Hansen.[1]

Efforts to improve the HSP system have been made, including improved data fitting methods,[2,3] theoretical HSP estimations based on group contributions,[4,5] alternative experimental methods of HSP determination[6,7] and the introduction of a 4th parameter by splitting the hydrogen bonding

component into donor and acceptor contributions, each with proposed adjustments to the HSP system.[8,9] The fitting method proposed by Gharagheizi[2] was investigated for possible improvement of swelling data fitting with the inclusion of acetonitrile and nitromethane. While this method has been shown to improve certain HSP fits by utilizing the Nelder-Mead algorithm for optimization, it produced no improved fit in the case of Fluoroflex's HSP given our swelling data set. In the case of excluding acetonitrile and nitromethane, a Data Fit of 1.00 was already achieved. Other, more integral, modifications of the HSP components have undoubtedly been proven effective in increasing the HSP's descriptiveness in certain cases, particularly for the solubility of small molecules,[9] but the HSP system in its standard form, consisting of three components and a radius of interaction, remains widely accepted for polymer solubility investigations,[10–13] with existing datasets of solvent and material HSPs gathered over the years. Additional exploration into other HSP variations was outside the scope of this work.

Hansen further discusses room for variation on his standard, sphere-based fitting method. The inclusion of a scaling factor of "2" for the dispersion parameter during solubility plotting was developed from experimental data and found to correctly and conveniently represent solubility data as a sphere that encompasses thermodynamically favorable solubility interactions.[1] This implies that, fundamentally, the interaction sphere that describes the three different intermolecular interactions is, more accurately, an ellipsoid. While it was found that using a scaling factor of "2" was a good approximation for most material interactions studied, Hansen did not exclude the possibility that using different multipliers for the respective axes in the three-dimensional solubility space could lead to better fits for complex mixtures or materials.[1] Due to the good data fit achieved with the Fluoroflex solvent swelling data using Hansen's standard, spherical method, investigation into alternative scaling factors for ellipsoidal solubility spaces was not investigated.
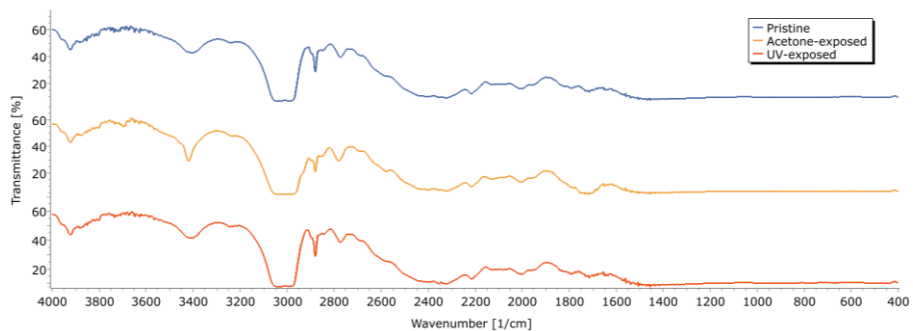
Figure 3.S3. FTIR spectra (transmission) of hot embossed Fluoroflex sheets. Samples exposed to acetone (a solvent that swells Fluoroflex to a high degree) for 24 hours or UV light (365 nm) for 8 hours showed no significant shift in FITR spectra as compared to pristine sTPE samples.
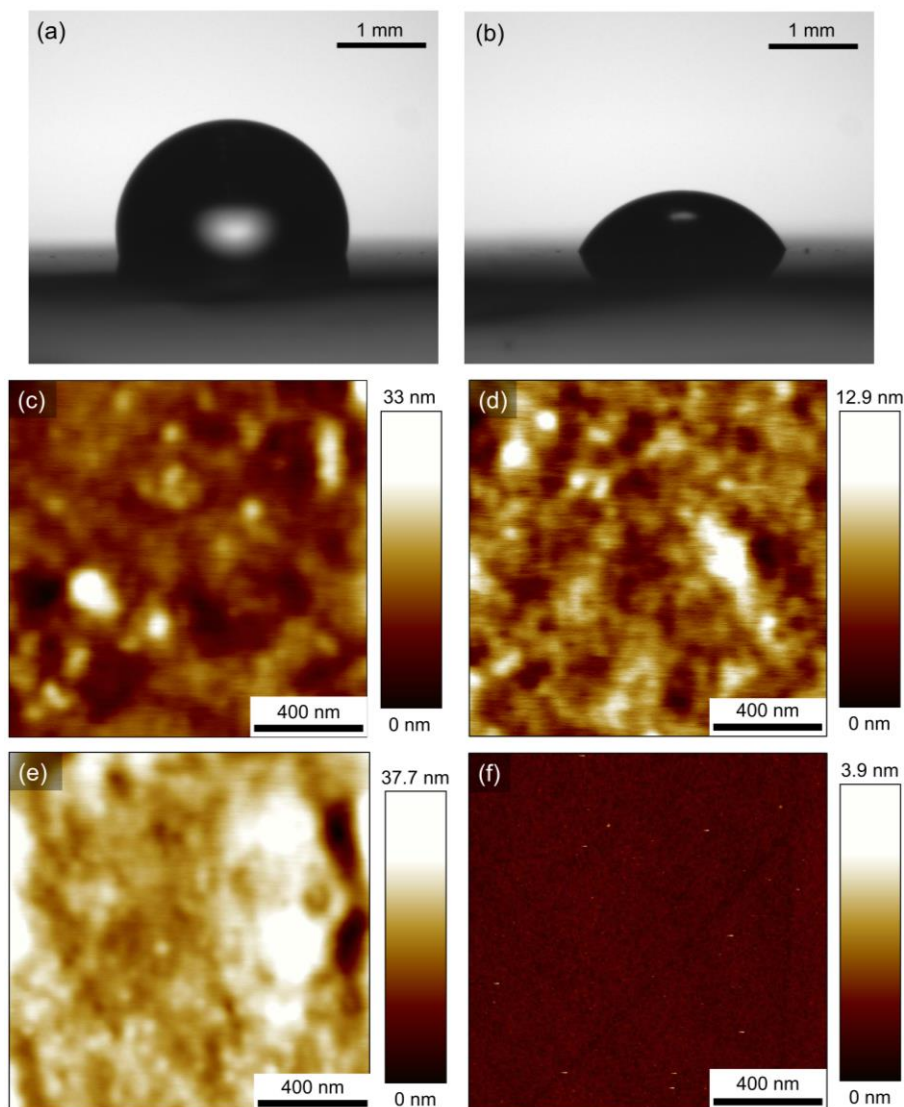
Figure 3.S4. Fluoroflex surface characteristics. Static contact angle (pendant drop method) of (a) water (105.0°) and (b) diiodomethane (64.9°) on a Fluoroflex sheet, exhibiting hydrophobic surface behavior. (c–f) 2 μm × 2 μm AFM surface topography images. (c) Shows a pristine Fluoroflex sheet having surface roughness of R_{RMS}=3.5 nm. (d) Shows a pristine Fluoroflex sheet demonstrating surface roughness of R_{RMS}=1.6 nm, found to be the lower limit of measured sTPE surface roughness. (e) Shows an acetone-exposed sTPE sample of surface roughness R_{RMS}=4.4 nm. (f) Shows a silicon wafer used for hot embossing of Fluoroflex samples of roughness R_{RMS}=0.2 nm. This represents an optimal silicon wafer roughness, however, the average roughness of the silicon wafer samples was found to be R_{RMS}=1.6 ± 1.0 nm (mean ± standard deviation), likely reflecting contaminants that resulted from a non-clean room microfabrication process.
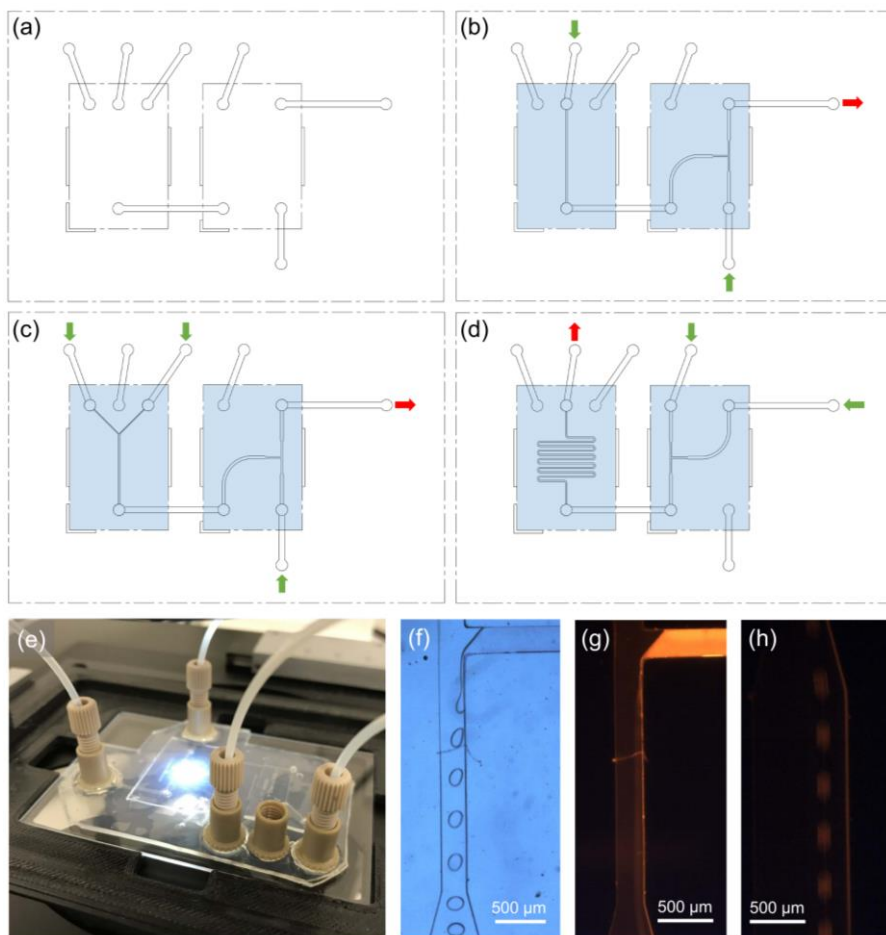
Figure 3.S5. (a) Schematic of the modular Fluoroflex device baseplate that contains seven discrete channels to make connections between the microfluidic inlets, outlets, and modules. The two dashed rectangles in the center indicate the surface area on which two modules can be placed. The larger, outer dashed rectangle represents the size of a 75 mm × 50 mm glass, which serves as a rigid support for the modular device. (b) The schematic is shown with the inclusion of a straight channel module (left) and a T-junction droplet generator module (right) in blue. Green and red arrows indicate the modular device inlets and outlet, respectively. (c) A co-flow Y-channel replaces the straight channel in order to generate droplets with a mixture of two liquids. (d) While data in this configuration is not shown, the device could be reconfigured with a serpentine channel downstream from the droplet generator for increased droplet residence, mixing or observation time. (e) A modular device in the configuration shown in (c) to generate droplets containing a mixture of rhodamine B in water solution with pure DI water. Droplet generation images under brightfield (f) and fluorescent (g, h) observation. Note that partial mixing of the rhodamine B solution and pure water had occurred by the time the fluid stream reached the T-junction.

References

[1]   C. Hansen, *Hansen Solubility Parameters*, CRC Press, **2007**.

[2]   F. Gharagheizi, *J. Appl. Polym. Sci.* **2007**, *103*, 31.

[3]   M. Weng, *J. Appl. Polym. Sci.* **2016**, *133*, 1.

[4]   D. Mathieu, *ACS Omega* **2018**, *3*, 17049.

[5]   E. Stefanis, C. Panayiotou, *Int. J. Thermophys.* **2008**, *29*, 568.

[6]   K. Adamska, A. Voelkel, *Int. J. Pharm.* **2005**, *304*, 11.

[7]   O. Segarceanu, M. Leca, *Prog. Org. Coatings* **1997**, *31*, 307.

[8]   E. Stefanis, C. Panayiotou, *Int. J. Pharm.* **2012**, *426*, 29.

[9]   M. J. Louwerse, A. Maldonado, S. Rousseau, C. Moreau-Masselon, B. Roux, G. Rothenberg, *ChemPhysChem* **2017**, *18*, 2999.

[10]   R. Inglev, G. Woyessa, O. Bang, J. Janting, *J. Light. Technol.* **2019**, *37*, 4776.

[11]   M. Huth, C.-W. Chen, J. Köhling, V. Wagner, *Appl. Clay Sci.* **2018**, *161*, 412.

[12]   K. V. Kurada, M. Dutta, A. Jana, S. De, *J. Appl. Polym. Sci.* **2020**, *137*, 1.

[13]   C. Bordes, V. Fréville, E. Ruffin, P. Marote, J. Y. Gauvrit, S. Briançon, P. Lantéri, *Int. J. Pharm.* **2010**, *383*, 236.

Design of a Thermoplastic Fluoroelastomer Microfluidic Packed Bed Photoreactor

Abstract

This chapter presents the design and proof-of-concept demonstration of a packed bed photoreactor using the Fluoroflex sTPE material and PDMS microbeads as polymer supports for photoactive molecules. PDMS microbeads are synthesized using microfluidic flow focusing, then injected into a Fluoroflex microchannel containing a micropillar array to trap the microbeads. An on-chip functionalization procedure is used to coat the microbeads with an amine-functional siliceous layer, allowing the subsequent surface attachment of organic molecules. This is demonstrated with the attachment of fluorescein to the microbeads. PDMS microbeads are also functionalized (in batch) with a photocatalytic molecule. These microbeads were then used for a photo-activated debromination reaction, giving scope for implementing bead-supported photocatalysts inside a Fluoroflex microdevice for heterogeneous flow photocatalysis.

CHAPTER 4 – DESIGN OF A THERMOPLASTIC FLUOROELASTOMER MICROFLUIDIC PACKED BED PHOTOREACTOR

4.1 INTRODUCTION

The use of microfluidics in chemistry, also known as continuous flow chemistry, has provided the modern chemist with an alternative toolset to perform research – microreaction technology. As opposed to the conventional round-bottom flask, performing chemical reactions in microfluidic devices is advantageous for several reasons, including fast mixing, efficient heat and mass transfer, and small reagent volumes.[1] These characteristics, largely thanks to the small surface-area-to-volume ratios at the micro-scale, can allow for reactions with higher speed, selectivity, and safety when using microfluidic flow chemistry techniques.[2] Two areas where flow chemistry has proven to be particularly valuable have been heterogeneous catalysis and photochemistry.[3,4] Heterogeneous catalysis benefits from micro-scale operations, where large surface-area-to-volume ratios maximize the interaction between solid catalysts and liquid reagents, for example.[5] Catalysts can be immobilized on microfluidic channel walls, or better yet, on microparticles filling a microchannel for even greater surface area; this latter concept forms the basis of packed bed reactors.[4] A typical packed bed reactor, however operates on the macro-scale; this poses limitations for their use in for photochemical reactions, which rely on light to provide the reaction-triggering energy. Small characteristic dimensions of microchannels (< 1000 μm) promote efficient and homogeneous irradiation of the reaction mixture, even with strongly light absorbing and scattering conditions, that simply cannot be reproduced in batch/macro systems that have far greater light path lengths and/or use non-transparent reaction vessels.[6]

Chapter 3 presents material characterization and microfluidic evaluation of the soft thermoplastic fluoroelastomer material called Fluoroflex. It was shown to exhibit high resistance to organic solvents and be easily thermoformable for the rapid fabrication of microfluidic devices, suggesting its utility as a flow chemistry microreactor. Moreover, its optical transparency allows the possibility of a range of photochemistry reactions.

This chapter presents the design and proof-of-concept demonstration of a microfluidic packed bed photoreactor system using a Fluoroflex microdevice filled with polydimethylsiloxane (PDMS) microbeads to act as solid catalyst supports. Microbead fabrication and functionalization is described and followed by a preliminary evaluation of a photo-redox reaction using functionalized microbeads as heterogeneous catalysts. In addition to capitalizing on Fluoroflex's favorable material properties, the system concept leverages the facile fabrication techniques of both Fluoroflex and PDMS to give scope for rapid prototyping of customizable microfluidic packed bed photoreactors.

4.2   MATERIALS AND METHODS

4.2.1   Droplet Generator Device

Flow-focusing PDMS devices were used for droplet generation. Micropatterned PDMS slabs (SYLGARD™ 184, Dow Inc., Midland, MI, USA) were fabricated using standard soft lithography techniques[7] with a master mold consisting of Ordyl® dry film photoresist (55 µm thickness, ElgaEurope s.r.l., Milan, Italy) on a 75 mm × 50 mm glass slide (Corning Inc., Corning, NY, USA). The devices were sealed to a 76 mm × 26 mm glass slide (Thermo Fisher Scientific, Waltham, MA, USA) after surface treatment in a plasma cleaner (PDC-002, 200 mTorr, 30W, 2 min, Harrick Plasma, Ithaca, NY, USA). Channel dimensions at the flow-focusing junction were 55 µm × 100 µm (height × width). The droplet generator device is shown in **Figure 4.1**.
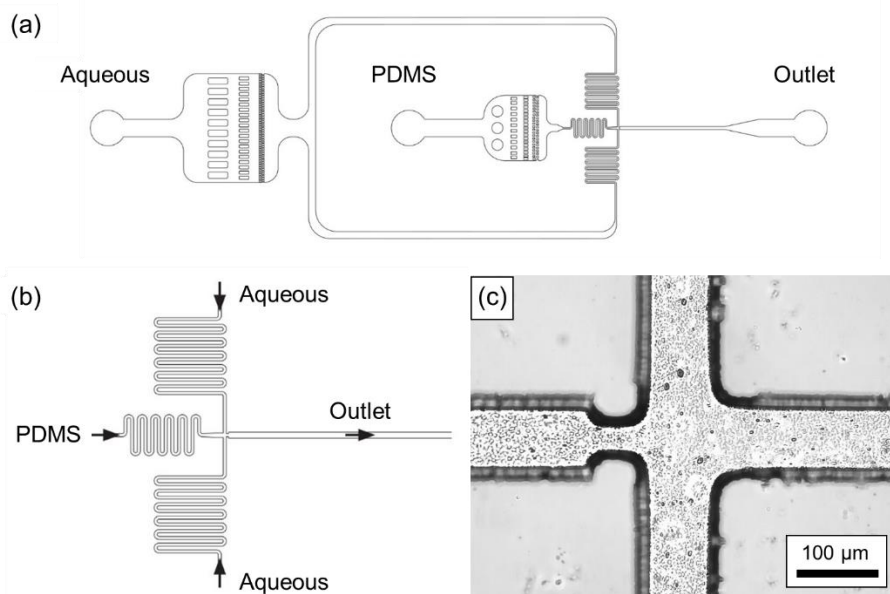
Figure 4.1. Microfluidic flow-focusing droplet generation device. (a) Schematic showing the inlets for the continuous water phase and the droplet PDMS-toluene phase and the outlet, downstream from the flow-focusing junction, shown in detail in (b). (c) Microscope image of the flow-focusing junction.

4.2.2 PDMS Bead Synthesis

Bead generation followed the protocol described previously.[8] Droplet generator devices were treated with a laboratory corona treater (BD-20AC, Electro-Technic Products, Chicago, IL, USA) after which, a surfactant solution of 0.5% (w/v) sodium dodecyl sulfate (Sigma Aldrich, Saint Louis, MO, USA) in distilled water was injected into all channels of the devices to maintain surface hydrophilicity before bead generation. An OB1® MK3+ pressure controller (0–2000 ± 0.1 mbar, Elveflow®, Elvesys SAS, Paris, France) was used to pump the surfactant solution as a continuous phase through the side channels at the flow-focusing junction and a 1:1 mixture of toluene and 10:1 PDMS base-crosslinker solution (SYLGARD™ 184, Dow Inc., Midland, MI, USA) as the droplet-forming phase through the central channel. Droplets were collected and left for 24 h at room temperature for PDMS curing to form solid micro beads. Microbeads were subsequently imaged using a Zeiss Axio Observer Z1 microscope (Carl

Zeiss AG, Oberkochen, Germany), and image analysis was conducted using FIJI software.[9]

4.2.3 sTPE Device Fabrication

A Fluoroflex microfluidic device was fabricated using the rapid hot embossing method described in Chapter 3. An Ordyl® on glass mold was used, containing a microbead reactor design consisting of a 110 μm × 2 mm × 24 mm (height × width × length) channel with an array of 60 μm pillars with 30 μm spacing at the outlet end of the channel. Raw Fluoroflex sTPE pellets were placed between a polished metallic plate (Eden Tech SAS, Paris, France) and the Ordyl® mold and pressed using a manual heat press (DC8, Geo Knight & Co Inc., Brockton, MA, USA) at 220 °C for approximately 30 s. After cooling for 1 min, the mold assembly was disassembled using tweezers and isopropanol to facilitate the separation between the mold and the hot-embossed sTPE sheet. A secondary sTPE sheet was hot embossed, using a plain glass slide instead of a mold, resulting in a flat, featureless sTPE sheet. Holes were then punched in the micropatterned sTPE sheet at the inlet and outlet locations using a steel hole punch before placing it in conformal contact with the featureless sTPE sheet. The assembly was then baked in an oven for 2 h at 185 °C (DKN612C, Yamoto Scientific Co. Ltd., Tokyo, Japan) to achieve robust self-bonding between the two layers.

4.2.4 Functional Molecule Preparation

The functionalization of the PDMS microbeads was conducted with fluorescein and a perixanthenoxanthene derivative (PXX). For fluorescein preparation, just prior to use for PDMS functionalization, a 1 mM solution of fluorescein sodium salt (Sigma Aldrich) in water was prepared and mixed with an equal volume of 100 mM solution of Woodward's Reagent K (Sigma Aldrich) to produce reactive carboxylic acid sites on the fluorescein molecules for subsequent coupling to the microbeads.

The synthesis of the PXX derivate started with synthesizing the asymmetric binol by reaction with the commercially available 2-bromo-6-naphthol and the previously synthesized 6-xylene-2-naphthol. A previously reported ring-closing reaction,[10] followed by Suzuki coupling with the suitable boronic acid,

provided the PXX-phenyl methyl ester derivative. After hydrolysis, it was reacted with oxalyl chloride to form the PXX acyl chloride derivative that was later used for microbead functionalization.

4.2.5 Bead Packing and Functionalization

The PDMS micro bead suspension in surfactant solution was injected into the bead reactor channel using a syringe, with the beads becoming trapped by the pillar array near the outlet of the channel. DI water was then injected to wash the surfactant from the beads before beginning the PDMS surface modification protocol described by Beal et al. A 1:2 (v/v) solution of (3-aminopropyl)triethoxysilane (APTES, 99%, Sigma Aldrich) in ethanol was injected into the channel and left to incubate for 5 min at room temperature.[11] The APTES solution was removed from the channel by syringe, and an aqueous ammonium hydroxide solution (28% NH_3 in H_2O, Sigma Aldrich) was injected and left to incubate in the channel for 3 min for base catalysis to occur. The ammonium hydroxide solution was removed, and the channel was left overnight to dry before further functionalization.

PDMS microbeads were then functionalized in the microchannel with fluorescein. The channel was rinsed for 5 min with water using a syringe. The fluorescein solution was then injected into the channel and left to incubate at room temperature for 10 min to allow amide bonding between the PDMS-fixed APTES and the activated fluorescein. The channel was then flushed thoroughly with DI water to remove the fluorescein solution. The microchannel was imaged with a fluorescent microscope (Zeiss Axio Observer Z1, Carl Zeiss AG). The on-chip functionalization workflow is illustrated in **Figure 4.2**.
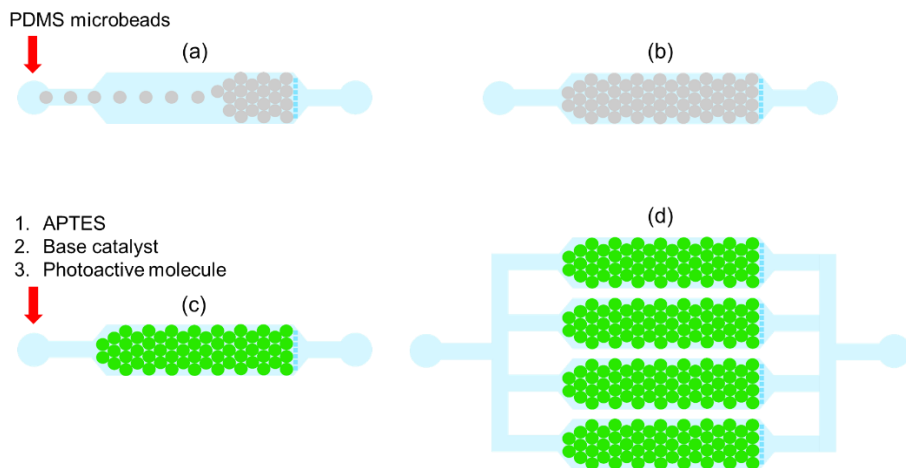
Figure 4.2. On-chip microbead functionalization workflow. (a) PDMS microbeads are injected into the microchannel, containing a pillar array at its output, until the microchannel is packed with microbeads (b). (c) Microbead functionalization is performed with the injection of an APTES solution. After incubation for the diffusion of APTES into the surface of the PDMS microbeads, a base catalyst is introduced for hydrolysis to occur, forming an amine-functional surface layer on the microbeads. A photoactive molecule can then be coupled to this surface layer with the formation of an amide bond. This work demonstrates this process using fluorescein as the photoactive molecule. (d) Shows the concept of channel parallelization, in which multiple microbead-filled channels can be positioned in parallel for the potential to scale up synthesis volumes.

The functionalization of PDMS microbeads with PXX was conducted in batch (outside of a microfluidic device). The microbeads were loaded inside a solid phase peptide synthesis syringe, whereupon alternating cycles of air bubbling and vacuum, the same steps were followed as for the microbead functionalization inside the Fluoroflex device, but using the PXX solution instead of the Fluorescein solution (i.e., APTES solution, base catalysis, PXX solution). PXX-functionalized microbead imaging was performed with a Zeiss LSM880 Airyscan Fast confocal microscope (Carl Zeiss AG). Fluorescence spectra of PXX-functionalized microbeads were measured on an Agilent Cary Eclipse fluorescence spectrophotometer (Agilent Technologies, Santa Clara, CA, USA).

4.2.6 **Debromination Photoreaction**

The PXX-activated photoreaction studied was the debromination of 4'-bromoacetophenone in acetonitrile (ACN), using N,N'-diisopropylethylenediamine (DIPEA) as electron donor under nitrogen gas. Irradiation was provided by an array of blue LEDs (460 nm, 14 W). The reaction was conducted with either PXX in solution, as reported by Scuitto et al.,[12] or with PXX-functionalized PDMS microbeads in suspension. The latter was performed with 35 mg of microbeads with an approximate chromophore loading of 0.1–0.3 mM g^{-1}. Nuclear magnetic resonance (NMR) spectra of the reaction output were recorded on a Bruker Fourier 300 MHz spectrometer at room temperature (Bruker, Billerica, MA, USA).

4.3 RESULTS AND DISCUSSION

4.3.1 **PDMS Microbead Synthesis**

PDMS droplets were formed at the flow-focusing junction, a common microfluidic geometry for producing microdroplets,[13] using a PDMS-toluene mixture. This mixture reduced the droplet phase viscosity sufficiently to ensure that flow could readily be achieved (**Figure 4.3a**). After PDMS droplet formation and collection, the liquid PDMS-toluene mixture cured overnight to form solid beads measuring approximately 100–150 μm in diameter, in addition to small "satellite" beads of approximately 20 μm diameter and smaller (**Figure 4.3a–b**). PDMS beads were not monodisperse – optimization of droplet generation parameters and the flow focusing device design would be necessary to achieve monodisperse beads,[14] but this was outside the scope of this work. The surfactant in the aqueous phase prevented the coalescence of PDMS droplets following droplet generation. PDMS was chosen as a material as it is common in many microfluidics labs and has shown that its surface can be readily functionalized with a number of materials.[11,15–18] In particular, PDMS's interaction with APTES allows for facile surface modification and subsequent coupling with other molecules in a lab setting.

Microbeads in other polymeric materials, as well as glass, are commercially available, and have indeed been functionalized for use in microchannels.[18–21] However, in-house fabrication of microbeads give scope for varying the size of the PDMS microbeads with relative ease, by adjusting fluid parameters and flow

focusing geometries.[22] Regulation of the microbead size allows for precise control over the functional surface area present in a microreactor. While smaller microbeads result in an increased surface area, they also produce an increased microfluidic resistance, and consequent back pressure, by effectively reducing the void space for fluid flow in a microchannel.[23] In extreme cases, this can cause microchannel clogging. This is an important factor to take into consideration in the design of a packed bed reactor, and can be subject to optimization with user control over the microbead size.[24]
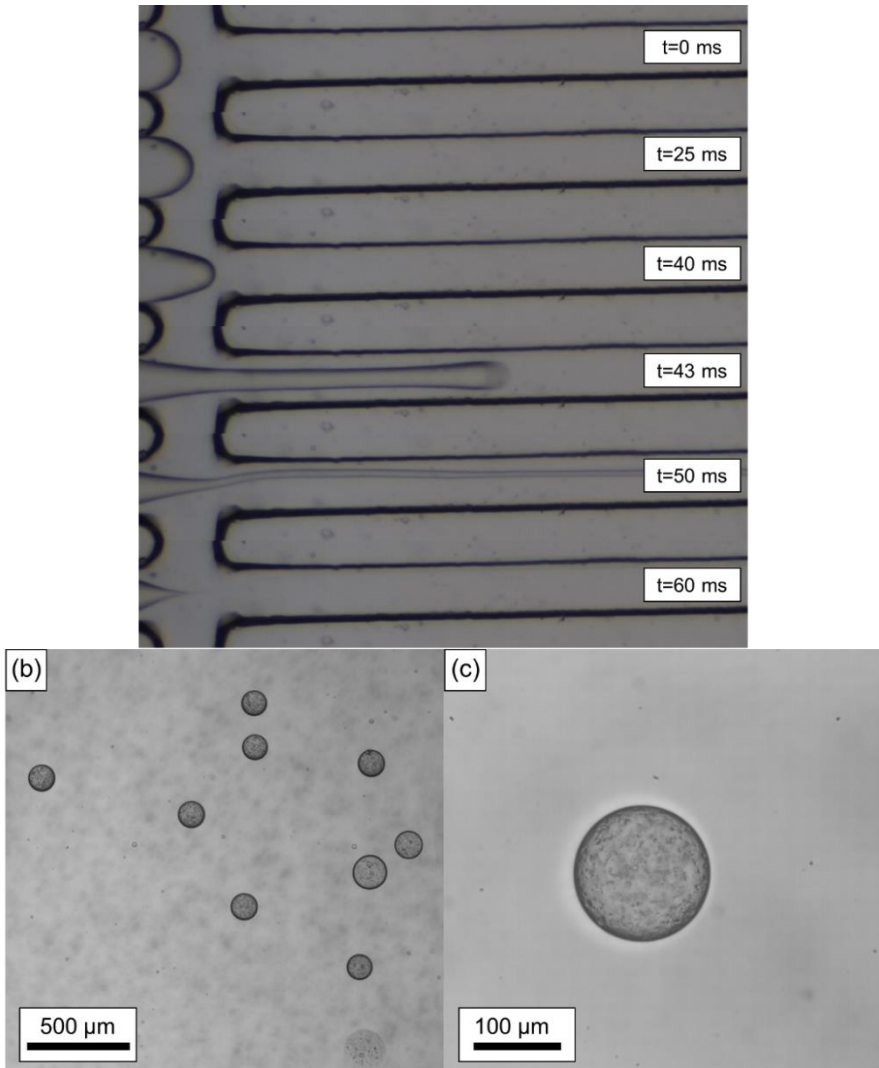
Figure 4.3. PDMS microbead synthesis. (a) Zoom of the microfluidic flow focusing junction during droplet generation, representing PDMS droplet generation of

approximately 15 Hz. (b–c) Microscope images of the PDMS beads after polymer curing where beads of approximately 100–150 μm diameter can be seen, along with smaller "satellite" beads (< 20 μm).

4.3.2 Microchannel Filling and Functionalization

PDMS beads could be injected into the pillar-array device with ease using a syringe, creating a packed structure (**Figure 4.4a–c**). Following injection of PDMS microbeads into the device, all PDMS surface functionalization steps were sequentially conducted in the device. This resulted in a streamlined process as compared to microbead functionalization in batch, that is, outside of a microfluidic device. Inside the device, the pillar array acted as a filter for the beads, allowing successive steps (i.e., bead washing, APTES incubation, base-catalyzed hydrolysis and fluorescent molecule attachment) to be performed without the need for the alternating filtration steps for bead-solution separation and subsequent handling for microchannel insertion. Furthermore, performing a heterogeneous catalytic reaction inside of a microreactor like this eliminates the need for a subsequent step to separate the microbeads/particles from the final reaction solution, as would be necessary for such a reaction in batch conditions.
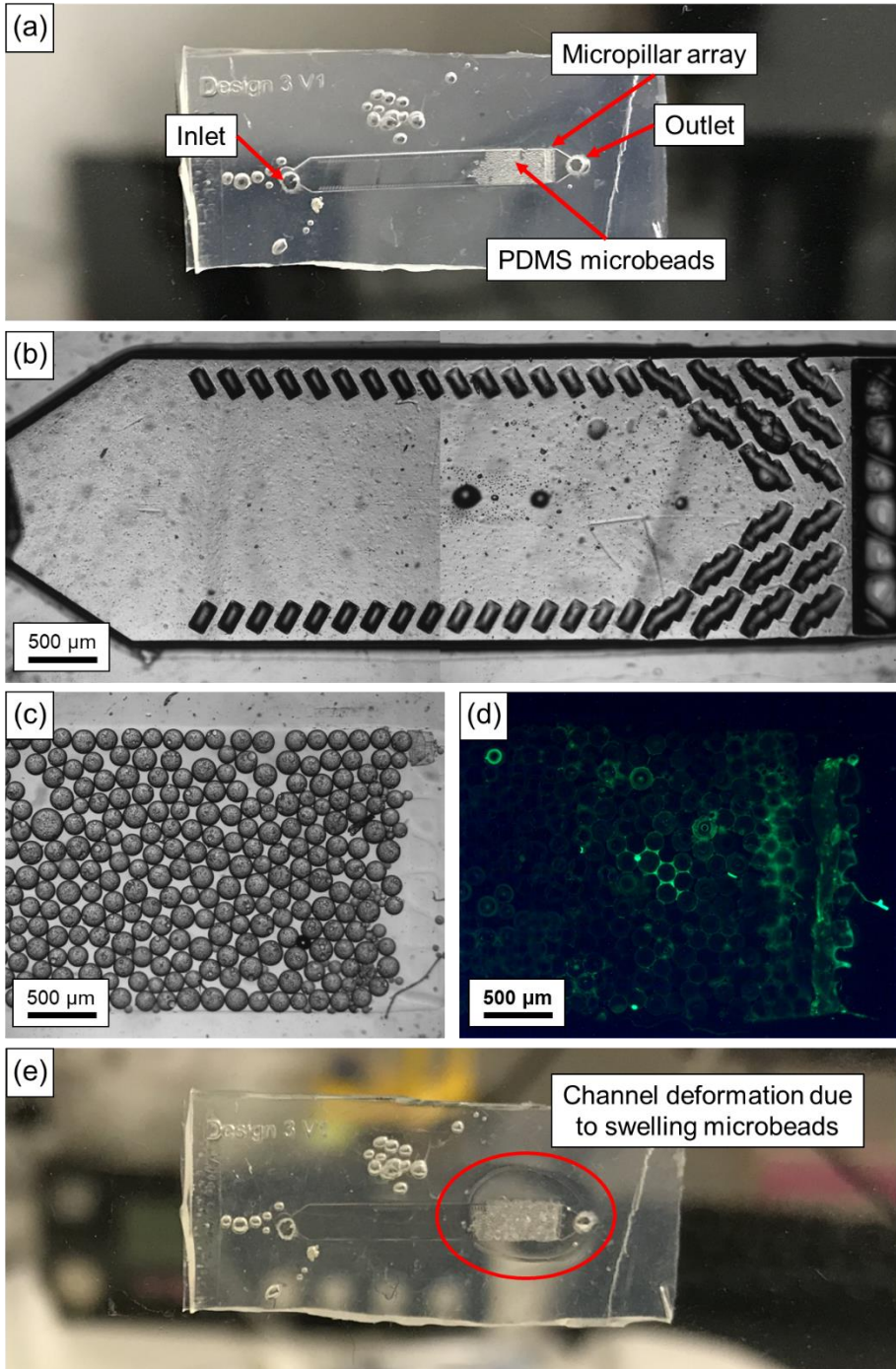
Figure 4.4. Functionalized bead microchannel. (a) Photo of the Fluoroflex microchannel partially filled with PDMS microbeads. (b) Microscope image of the Fluoroflex

microchannel with an array of pillars, primarily located at the outlet (right side) of the channel. (c) PDMS microbeads were injected into the channel, blocked from exiting by the pillar array at the end of the channel. (d) Fluorescence on and around the PDMS microbeads after on-chip functionalization with APTES, followed by fluorescein (475 nm excitation wavelength). (e) Photo of the Fluoroflex device during PDMS microbead swelling due to toluene exposure. Elastic material deformation can be observed at the right-hand side of the channel. However, no microchannel delamination occurred.

Beal et al. reported the facile surface functionalization of PDMS with APTES to achieve hydrophilic surface layers inside of microchannels.[11] PDMS's tendency to swell in organic solvents[25] can be exploited for the uptake of alkoxysilanes, such as tetraethoxysilane (TEOS) and APTES, at the material surface before the deposition of a siliceous layer via aqueous catalysis. This surface modification can be achieved in under 10 min, notably faster and easier than comparable methods of APTES surface deposition on glass.[26,27] In the case of the deposition of amine-ended APTES, functionality via the reactive amine groups is incorporated into the surface of the PDMS, permitting subsequent attachment of a number of organic molecules through amide bonding.[28–33] The versatility of the APTES surface coating is demonstrated by attachment of both fluorescein, and separately, PXX to the PDMS beads, as illustrated in **Figure 4.5**. This ease and versatility is an important factor when considering the limited methods for incorporating heterogeneous catalysts in microreactors.[34,35]

Figure 4.5. Scheme of the APTES surface modification of PDMS with base catalysis, as described by Beal et al.[11] Diffusion of APTES precursor into the bulk of the PDMS is followed by a hydrolysis reaction that forms a siliceous layer at the interface of the PDMS surface and the aqueous base solution. Critically, amine end-groups of APTES can be present at the surface, allowing subsequent attachment of various organic molecules, such as PXX (bottom left) and fluorescein (bottom right).

While the attachment of fluorescein to the PDMS microbeads did not serve any subsequent catalytic purpose, it allowed a qualitative evaluation of the effectiveness of the APTES microbead coating. The microbeads exhibited fluorescence after extensive flushing of the channel with water, suggesting the coupling of fluorescein to the APTES-coated beads through amide bonding (**Figure 4.4d**). This is similar to the coupling mechanism of the carboxyl groups of eosin to the amine groups of APTES, described by Kizilel et al.[28]

PDMS's susceptibility to organic solvents is utilized to facilitate its interaction with APTES, raising the question: can functionalized PDMS microbeads be used for reactions involving organic solvents? To evaluate this, toluene was injected into the fluorescein-functionalized bead channel and allowed to incubate for 30 min. Toluene is a solvent that readily swells PDMS, so is generally avoided

for use in PDMS microchannels.[25] Indeed, the PDMS microbeads exhibited swelling within seconds. However, due to Fluoroflex's resistance to toluene and other non-polar organic solvents, no device swelling or delamination occurred, as would likely be the case in a PDMS device. Moreover, the elastomeric properties of Fluoroflex permit the volumetric change of the PDMS without de-bonding of the device – the microchannel exhibited minor stretching to accommodate for the swelling microbeads (**Figure 4.4e**). After the removal of toluene from the microchannel, PDMS microbeads quickly reassumed their original size while maintaining their fluorescence.

In comparison to microfluidic packed bed photoreactors in literature, the Fluoroflex-PDMS system offers a few benefits. Most other reactors operate on larger scales,[36–39] using capillaries or columns that require larger and more power-intensive light sources. Fernández-Catalá et al. demonstrated a microchip-format packed bed photoreactor with a commercially available microreactor having significantly reduced footprint and flow channel dimensions.[40] This enabled photo-oxidation reactions with low residence time and low light energy input to be implemented. A comparable Fluoroflex microreactor platform, in addition to a small footprint and light path distances, would give users a high degree of customization at a lower cost. This is in contrast with the expensive glass-based reactor used by Fernández-Catalá et al., and can be attributed to Fluoroflex's accessible and transferrable hot embossing fabrication process and the lower material costs of thermoplastics.[41–43] Microchannel designs could thus be easily modified for reactor prototyping, while still giving scope for scale-up and parallelization. Moreover, the amine functionality of the PDMS-APTES microbeads allows for the attachment of a variety of molecules, adding to the customizability of this platform.

4.3.3 **PXX-Functionalized Microbead Characterization**

Perixanthenoxanthene is an organic dye with numerous derivatives that can be synthesized to possess tunable photoredox properties, as demonstrated by Sciutto et al. through dehalogenation reactions of organic halides.[12] Due to its proven utility for photoreactions, it was chosen to evaluate a Fluoroflex platform for heterogeneous photocatalysis.

PDMS microbeads were also functionalized in batch but using PXX instead of fluorescein. The batch funcationalization procedure was not as streamlined as

the on-chip functionalization, requiring filtration between each step to separate the microbead from the solutions used using peptide synthesis syringes. However, handling of the microbeads in batch facilitated subsequent fluorescent characterization. Confocal microscopy images of PXX beads showed homogeneous fluorescence of the microbeads after the PXX functionalization procedure (**Figure 4.6a–c**). Furthermore, fluorescence spectrophotometer measurements of functionalized beads exhibited emission spectra matching that of PXX in solution (**Figure 4.6d**), demonstrating conservation of PXX's photoactive properties after microbead coupling. In contrast, the removal of the APTES step in the functionalization process resulted in microbeads exhibiting no fluorescence. These results confirm the presence of PXX on the microbeads, strongly suggesting coupling of the PXX molecule to an APTES surface layer.
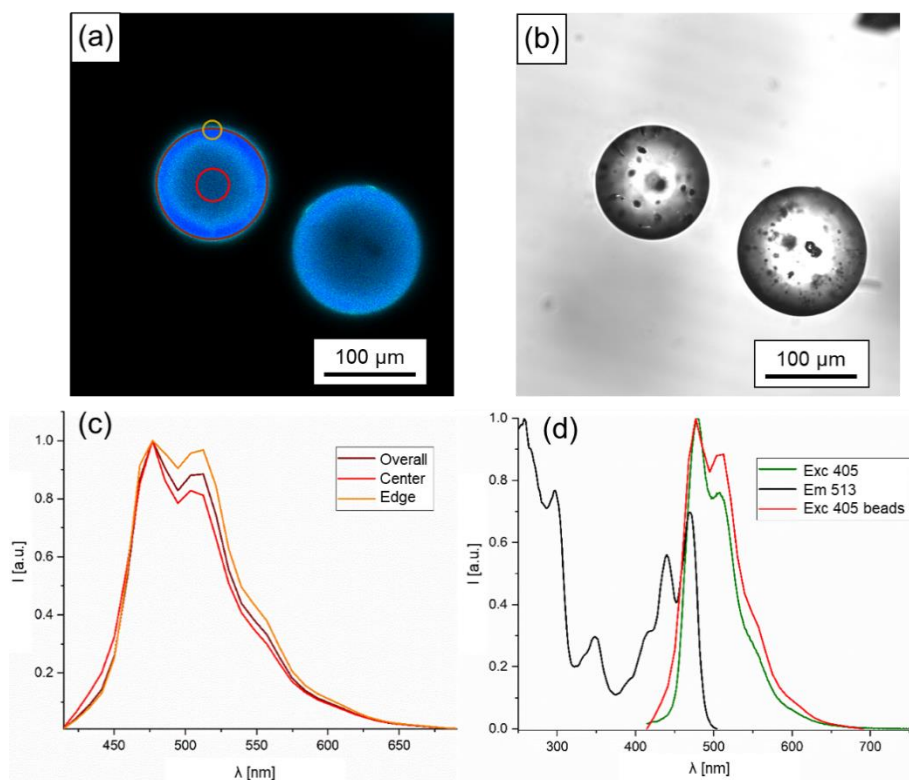
Figure 4.6. PXX-functionalized microbead characterization. Confocal microscopy images in (a) fluorescence (λ_{exc}=405 nm) and (b) transmission modes. (c) Fluorescence emission spectra exhibited by different parts of a microbead, showing consistent fluorescence profiles. (d) Fluorescence spectrophotometer measurements showing

emission (λ_{exc}=405 nm, green) and excitation spectra (λ_{em}=513 nm, black) of PXX in aerated CH_2Cl_2 solution at room temperature. The functionalized PDMS microbeads exhibit a matching emission spectrum (λ_{exc}=405 nm, red) to that of PXX, showing successful attachment of the chromophore to the microbeads.

Additionally, batch debromination reactions were conducted with PXX in solution and PXX on microbeads to evaluate the feasibility of performing reactions with bead-immobilized PXX. Using PXX-functionalized microbeads in suspension, 60% product conversion was achieved after 48 h (**Figure 4.7**), matching the result found when using PXX in solution. This further demonstrates the preservation of PXX's photoactive properties after coupling to the PDMS microbeads, whereby photocatalysis remain achievable using the APTES-microbead system.
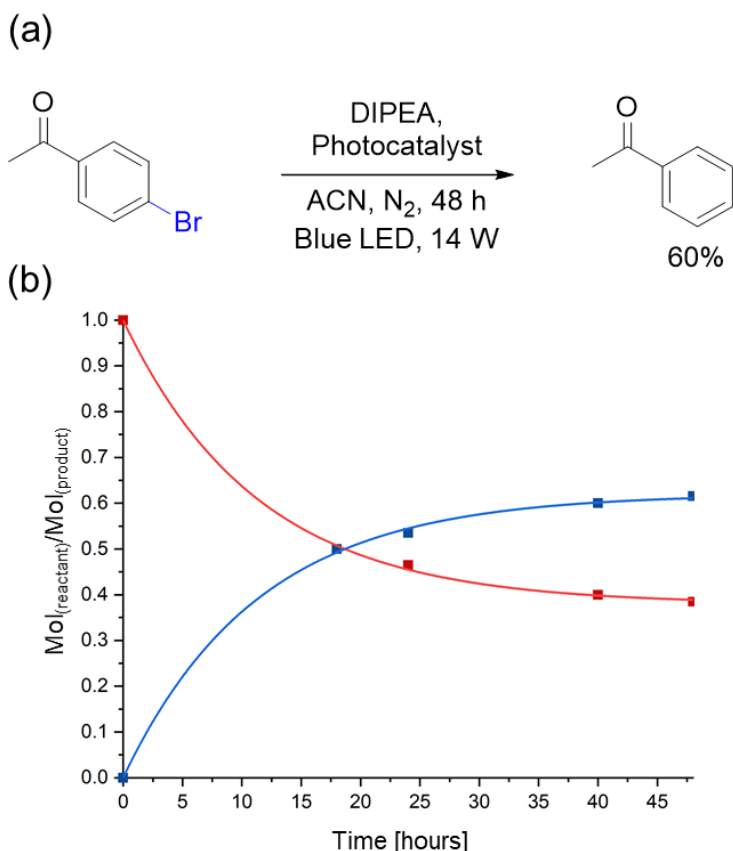
Figure 4.7. Microbead-supported photoreaction. (a) Reaction scheme of 4'-bromoacetophenone debromination using PXX-functionalized microbeads in

suspension. (b) Product conversion over time, measured by ^{1}H NMR (reactant in red, product in blue).

This gives scope for implementing PXX-functionalized microbeads in a packed bed photoreactor, such as the Fluoroflex platform described above, to take advantage of operating on the microfluidic scale. Advantages would notably include more efficient irradiation, thanks to small microchannel dimensions, and the immobilization of the beads by on-chip micropillar arrays. This could allow for faster and more streamlined reactions using less photocatalyst. For example, the reaction solution could be recycled through a microfluidic bead reactor until reaction completion. Critically, in this proposed workflow, the photocatalyst would remain inside the channel, avoiding an ensuing separation step during work up.

4.4   CONCLUSIONS AND OUTLOOK

This chapter describes the design and proof-of-concept evaluation of a microfluidic device based on the Fluoroflex material for use as packed bed photoreactor. PDMS microbeads were synthesized and functionalized with fluorescein inside the Fluoroflex microchannel. The effectiveness of the APTES microbead coating was then verified with fluorescence microscopy, offering a streamlined method of attaching photoactive molecules to polymer supports via APTES coupling. Microbeads were also functionalized with a PXX derivative and subsequently used for the debromination of 4'-bromoacetophenone in batch. As a photocatalyst, bead-immobilized PXX performed similarly to PXX in solution, both resulting in a conversion of approximately 60%. This preliminary reaction demonstrates the potential to use PDMS-APTES as a support for photocatalytic species and offers clear next steps toward the realization of a Fluoroflex microfluidic packed bed photoreactor.

Future work would investigate the implementation of PXX-functionalized beads inside of a Fluoroflex microchannel. This entails employing the on-chip functionalization method that was demonstrated with fluorescein, followed by conducting the debromination reaction in a continuous flow manner. The reaction could be adjusted using several microfluidic parameters, including flow rate, channel length, and microbead size. Using a fixed reactor geometry (such as the one described above), a range of bead sizes approximately 20–120 μm would be investigated, representing the typical size range of heterogeneous

catalyst supports used in packed bed microreactors.[44] Initial experiments would utilize the largest microbeads and low reagent flow rates (e.g., 1–10 μL min^{-1}), a precautionary approach to avoid high back pressures inside the device, which could lead to channel deformation or delamination, before being better informed by preliminary trials. If a flow rate-based flow control system, such as a syringe pump, is being used, it would be imperative to include a pressure sensor upstream of the device to monitor device pressure during flow experiments.

We would expect product conversion rates to increase (toward a maximum of 60% conversion, in the case of the debromination reaction discussed) by using low flow rates, long channels, and small microbeads – these parameters would serve to increase the reaction residence time as well as the effective catalytic surface area. Low flow rates, however, entail low throughput, and long channels with small microbeads can produce prohibitively high back pressures. The optimization challenge would therefore be to use the highest flow rate possible while maintaining maximum product conversion with a pumping pressure within the limits of the microfluidic device.

Looking further, parallelization of flow reactions for higher throughput synthesis could be envisioned. As opposed to further increasing the channel length to increase reaction residence time, channel parallelization can serve to minimized internal microfluidic resistances, while scaling up the number of functional microbeads and volume throughput. Parallel channels could feasibly be micropatterned on a single device (such as shown in **Figure 4.2d**), maintaining a small footprint and minimizing peripheral equipment.

One key advantage of the packed bead reactor concept is the immobilization of the catalytic molecule, avoiding the need for separation during work up, and in theory reducing the amount of catalyst that is needed. It also implies the continuous and repeated use of the catalytic molecules for reactions. Therefore, it would be necessary to perform further investigation into any potential leaching of the chromophore from the microbeads as well as its capacity for prolonged use, which would become a determining factor of a microreactor's longevity.

Fluoroflex and PDMS are materials that facilitate rapid prototyping, and would allow the variation of these microfluidic parameters with relative ease and low cost; hot embossing with inexpensive master molds would allow fast and straightforward modification of Fluoroflex microchannel designs, and tuning of

microfluidic flow focusing would allow for user defined control of PDMS microbead size. Moreover, by using Fluoroflex, a thermoplastic, fabrication scale-up can easily be envisioned, permitting a smooth transfer from research-based demonstration to large-scale implementation. It should be noted that an eventual scale-up of device production will likely entail a change from PDMS microbeads to commercially available polymer or glass microbeads, whose surfaces can also undergo functionalization.

4.5 REFERENCES

[1] T. Schwalbe, V. Autze, G. Wille, *Chim. Int. J. Chem.* **2002**, *56*, 636.

[2] F. M. Akwi, P. Watts, *Chem. Commun.* **2018**, *54*, 13894.

[3] T. Van Gerven, G. Mul, J. Moulijn, A. Stankiewicz, *Chem. Eng. Process. Process Intensif.* **2007**, *46*, 781.

[4] R. Munirathinam, J. Huskens, W. Verboom, *Adv. Synth. Catal.* **2015**, *357*, 1093.

[5] X. Liu, B. Ünal, K. F. Jensen, *Catal. Sci. Technol.* **2012**, *2*, 2134.

[6] M. Oelgemoeller, *Chem. Eng. Technol.* **2012**, *35*, 1144.

[7] D. C. Duffy, J. C. McDonald, O. J. A. Schueller, G. M. Whitesides, *Anal. Chem.* **1998**, *70*, 4974.

[8] S. C. Lesher-Pérez, G.-A. Kim, C. Kuo, B. M. Leung, S. Mong, T. Kojima, C. Moraes, M. D. Thouless, G. D. Luker, S. Takayama, *Biomater. Sci.* **2017**, *5*, 2106.

[9] J. Schindelin, I. Arganda-Carreras, E. Frise, V. Kaynig, M. Longair, T. Pietzsch, S. Preibisch, C. Rueden, S. Saalfeld, B. Schmid, J. Y. Tinevez, D. J. White, V. Hartenstein, K. Eliceiri, P. Tomancak, A. Cardona, *Nat. Methods* **2012**, *9*, 676.

[10] T. Kamei, M. Uryu, T. Shimada, *Org. Lett.* **2017**, *19*, 2714.

[11] J. H. L. Beal, A. Bubendorfer, T. Kemmitt, I. Hoek, W. Mike Arnold, *Biomicrofluidics* **2012**, *6*, 1.

[12] A. Sciutto, A. Fermi, A. Folli, T. Battisti, J. M. Beames, D. M. Murphy, D. Bonifazi, *Chem. - A Eur. J.* **2018**, *24*, 4382.

[13] S. Xu, Z. Nie, M. Seo, P. Lewis, E. Kumacheva, H. A. Stone, P. Garstecki, D. B. Weibel, I. Gitlin, G. M. Whitesides, *Angew. Chemie - Int. Ed.* **2005**, *44*, 724.

[14] A. Lashkaripour, C. Rodriguez, L. Ortiz, D. Densmore, *Lab Chip* **2019**, *19*, 1041.

[15] A. R. Abate, D. Lee, T. Do, C. Holtze, D. A. Weitz, *Lab Chip* **2008**, *8*, 516.

[16] J. Zhang, Y. Chen, M. A. Brook, *Langmuir* **2013**, *29*, 12432.

[17] L. Yu, C. M. Li, Y. Liu, J. Gao, W. Wang, Y. Gan, *Lab Chip* **2009**, *9*, 1243.

[18] X. Guan, H. Zhang, Y. Bi, L. Zhang, D. Hao, *Biomed. Microdevices* **2010**, *12*, 683.

[19] D. N. Kim, Y. Lee, W. G. Koh, *Sensors Actuators, B Chem.* **2009**, *137*, 305.

[20] J. A. Thompson, X. Du, J. M. Grogan, M. G. Schrlau, H. H. Bau, *J. Micromechanics Microengineering* **2010**, *20*, 115017.

[21] J. He, X. Mu, Z. Guo, H. Hao, C. Zhang, Z. Zhao, Q. Wang, *Eur. J. Clin. Microbiol. Infect. Dis.* **2014**, *33*, 2223.

[22] W. Lee, L. M. Walker, S. L. Anna, *Phys. Fluids* **2009**, *21*, 032103.

[23] M. B. Plutschack, B. Pieber, K. Gilmore, P. H. Seeberger, *Chem. Rev.* **2017**, *117*, 11796.

[24] K. G. Allen, T. W. von Backström, D. G. Kröger, *Powder Technol.* **2013**, *246*, 590.

[25] J. N. Lee, C. Park, G. M. Whitesides, *Anal. Chem.* **2003**, *75*, 6544.

[26]   P. Mela, S. Onclin, M. H. Goedbloed, S. Levi, M. F. García-Parajó, N. F. Van Hulst, B. J. Ravoo, D. N. Reinhoudt, A. Van Den Berg, *Lab Chip* **2005**, *5*, 163.

[27]   M. Qin, S. Hou, L. K. Wang, X. Z. Feng, R. Wang, Y. L. Yang, C. Wang, L. Yu, B. Shao, M. Q. Qiao, *Colloids Surfaces B Biointerfaces* **2007**, *60*, 243.

[28]   S. Kızılel, V. H. Pérez-Luna, F. Teymour, *Langmuir* **2004**, *20*, 8652.

[29]   E. A. Smith, W. Chen, *Langmuir* **2008**, *24*, 12405.

[30]   A. B. Sieval, R. Linke, G. Heij, G. Meijer, H. Zuilhof, E. J. R. Sudhölter, *Langmuir* **2001**, *17*, 7554.

[31]   Y. Y. Lua, M. V. Lee, W. J. J. Fillmore, R. Matheson, A. Sathyapalan, M. C. Asplund, S. A. Fleming, M. R. Linford, *Angew. Chemie - Int. Ed.* **2003**, *42*, 4046.

[32]   A. G. Frutos, J. M. Brockman, R. M. Corn, *Langmuir* **2000**, *16*, 2192.

[33]   J. Ma, F. Strieth-Kalthoff, T. Dalton, M. Freitag, J. L. Schwarz, K. Bergander, C. Daniliuc, F. Glorius, *Chem* **2019**, *5*, 2854.

[34]   B. Bin Xu, Y. L. Zhang, S. Wei, H. Ding, H. B. Sun, *ChemCatChem* **2013**, *5*, 2091.

[35]   L. A. Truter, V. Ordomsky, J. C. Schouten, T. A. Nijhuis, *Appl. Catal. A Gen.* **2016**, *515*, 72.

[36]   M. Borges, D. García, T. Hernández, J. Ruiz-Morales, P. Esparza, *Catalysts* **2015**, *5*, 77.

[37]   S. Sarkar, S. Chakraborty, C. Bhattacharjee, *Ecotoxicol. Environ. Saf.* **2015**, *121*, 263.

[38]   I. M. Arabatzis, N. Spyrellis, Z. Loizos, P. Falaras, *J. Mater. Process. Technol.* **2005**, *161*, 224.

[39]   K. Ö. Hamaloğlu, E. Sağ, A. Tuncel, *J. Photochem. Photobiol. A Chem.* **2017**, *332*, 60.

[40]   J. Fernández-Catalá, G. Garrigós-Pastor, Berenguer-Murcia, D. Cazorla-Amorós, *J. Environ. Chem. Eng.* **2019**, *7*, 103408.

[41]   E. Roy, A. Pallandre, B. Zribi, M.-C. Horny, F. D. Delapierre, A. Cattoni, J. Gamby, A.-M. Haghiri-Gosnet, in *Adv. Microfluid. - New Appl. Biol. Energy, Mater. Sci.* (Ed.: X.-Y. Yu), InTechOpen, London, UK, **2016**.

[42]   J. Lachaux, C. Alcaine, B. Gómez-Escoda, C. M. Perrault, D. O. Duplan, P.-Y. J. Wu, I. Ochoa, L. Fernandez, O. Mercier, D. Coudreuse, E. Roy, *Lab Chip* **2017**, *17*, 2581.

[43]   C.-W. Tsao, *Micromachines* **2016**, *7*, 225.

[44]   M. Solsona, J. C. Vollenbroek, C. B. M. Tregouet, A. E. Nieuwelink, W. Olthuis, A. Van Den Berg, B. M. Weckhuysen, M. Odijk, *Lab Chip* **2019**, *19*, 3575.

CHAPTER 5

Market Study: Fluoroflex & Flow Chemistry Microreactors

Abstract

This market study evaluates the Fluoroflex material as a microreactor for the flow chemistry research market. It is intended to provide industrial contextualization to the material characterization and scientific evaluation of Fluoroflex presented in Chapter 3. An analysis of current flow chemistry microreactor technologies is presented, summarizing the advantages, disadvantages, and market presence of each one compared to Fluoroflex. Flow chemist researcher interviews were conducted as a source of primary information to evaluate the limitations and needs in flow chemistry research settings; a notable finding is that tubing-based microreactors are preferred to currently available microchip reactors. Finally, an evaluation of the flow chemistry research market size is provided, utilizing Google Scholar publication results to quantify the growth of microfluidic flow chemistry in several research areas, with an average growth rate of 27% over the past five years. An estimation of the market value for Fluoroflex microreactors is subsequently made, ranging from 6,000–66,000 EUR per year.

CHAPTER 5 – MARKET STUDY: FLUOROFLEX & FLOW CHEMISTRY MICROREACTORS

5.1 INTRODUCTION

Since its emergence in the 1990s, microfluidics has offered the potential for improved biological and chemical research by utilizing intrinsic advantages of working at the microscale, including high surface-area-to-volume ratios, rapid mass and heat transfer, analytical integration, and precision fluid manipulation.[1] The progression and spread of microfluidic techniques, however, has tended more toward the biological sciences and less toward chemical analysis and synthesis, also known as microfluidic flow chemistry, for which microdevices were originally conceived.[2,3] Several reasons have been discussed as bottlenecks in the continued development of microfluidics for chemistry,[4–6] and one potential difficulty may be found in the materials available for microreactor fabrication. There is a lack of microreactor materials that both fulfill the material property needs of flow chemistry and can be readily obtained at a modest price. Chapter 3 of this dissertation presents a new material, called Fluoroflex, which offers a potentially attractive alternative to current materials for microreactor fabrication. The Fluoroflex material was characterized, and proof-of-concept microreactor devices for flow chemistry were demonstrated.

A PhD in industry, in addition to promoting entrepreneurial training and development as a part of the PhD studies, aims to pursue scientific research that has direct market relevance. Market research plays a critical role in bridging the gap between initial scientific demonstration and further product research & development.[7,8] The resource investment required to progress from a technological proof-of-concept to a marketable – ideally profitable – product necessitates careful consideration and understanding of the target market. This entails gathering insights on the market size, growth, needs, and accessibility, the competitor technology landscape, and customer needs, values, and behavior. These are all important factors that can provide the rationale necessary in deciding if a product investment should or should not be made. In addition, this discovery and insight gathering process can identify key stakeholders and pathways to accessing the market.

The scientific evaluation and characterization of Fluoroflex in Chapter 3 demonstrated its utility as a material for solvent-resistant microfluidic devices. To this end, this chapter consists of a market study analyzing the market implications of Fluoroflex as a material for microfluidic devices for flow chemistry, a field of research in which solvent-resistant devices are essential. Data gathered in this market study complements the scientific evaluation of the Fluoroflex material to define its strengths, needs, and benefits as a potential microreactor product. These insights can be leveraged for a well-designed new product development cycle that will address the needs of potential customers/end-users.

5.1.1 Research and Objectives and Questions

The research objective of this study is to provide market contextualization of the scientific research conducted in this dissertation on the novel soft thermoplastic fluoroelastomer (Fluoroflex) for use as microreactor devices for flow chemistry. This market contextualization encompasses a quantitative investigation of the flow chemistry research market size and trends, an analysis of the competitive landscape for chemical microreactor technology, and interview-based primary research to evaluate market needs, and specifically, interest in the Fluoroflex material.

The core hypothesis of this market study is:

Flow chemistry is a growing field of research, but the lack of affordable and accessible microreactor materials is limiting its development. Therefore, there is a flow chemistry market need for a material with which low-cost microreactor devices can easily be fabricated.

To validate this hypothesis, the following research questions will be investigated:

1. What microfluidic flow chemistry reactor solutions currently exist on the market?

2. What are the main limitations in microfluidic flow chemistry setups, or what improvements are desired?

3. Do flow chemists perceive value in a solvent resistant polymer material for microreactors?

4. What is the size of the microfluidic flow chemistry market?

5.2 Research Methodology

5.2.1 Competitive Landscape Review

A review was conducted of competitors in the field of flow chemistry microreactor technology. This included an overview of typical microreactor systems along with the most common materials used to make them, including the Fluoroflex sTPE material. An analysis of strengths and weaknesses was conducted for each of the material classes with respect to key features, such as performance, cost, ease of use, and technology maturity. These material summaries were informed through peer-reviewed journal articles concerning microreactor technology. Examples of commercially available microreactors in each class of materials, along with their typical price-ranges, are also provided. These were informed through content on manufacturer and distributor websites.

5.2.2 Researcher Surveys

Primary data was collected through interviews and questionnaires of researchers. The primary target group consisted of researchers actively working with microfluidic flow chemistry techniques (Group 1), with the aim of understanding why flow chemists use flow methods, what their microfluidic setups consist of and what their opinion on a solvent resistant polymer material for microdevices (Fluoroflex) is. In addition, a secondary target group considered was conventional chemists (Group 2), i.e., researchers using more classic batch methods and not continuous flow microfluidic methods. While less central to this study, the aim of Group 2 data collection was to understand why conventional chemists do not use microfluidic flow methods for their chemistry research, and in particular, if the reasoning was linked to a perceived shortcoming or lack of satisfactory microreactor technology.

Interview and questionnaire participants were primarily corresponding authors (principal investigators and career researchers) of peer-reviewed scientific journal articles in a range of chemistry journals, such as the *Journal of Flow Chemistry*, the *Journal of Organic Chemistry, Analytical Chemistry, Organic Letters*, and the *Journal of Photochemistry and Photobiology A: Chemistry*. Potential participants were contacted by email proposing participation in the market study. Potential participants were selected regardless of age, gender, or geographic location.

Interviews via videoconference calls were used for Group 1 data collection, whereas written questionnaires via email were used for Group 2 data collection due to the more limited set of questions and data collection aims involved. Interview questions and questionnaires can be found in **Appendix 2**. Questions were formulated to minimize response bias by avoiding formulations that were leading, negative, or were based on assumptions, such as prior knowledge or experience with microfluidics.

Assumptions: It was assumed that of the selection of researchers contacted through the range of scientific journals, while limited in sample size, was representative of the broader flow chemistry and chemistry fields of research. It was also assumed that any participation bias was negligible, that is to say, researchers that agreed to participate in the study (i.e., the sample) did not systematically differ from those that chose not to participate.

5.2.3   Market Sizing

The flow chemistry research market size was quantified using scientific publications as a metric, specifically, using the Google Scholar search engine. With every Google Scholar search, the number of search results is displayed, each one, in principle, corresponding to a scholarly publication, including journal and conference papers, theses, dissertations, abstracts, technical reports, and pre-prints from a wide range of journals, university repositories, and professional societies. By using keywords and search tools, namely the designation of the publication date, the size of specific fields of research over time can be estimated based on the occurrence of publications within a particular date range.

Keywords were divided into two sets: (1) keywords describing common, broad themes in chemistry research in which flow chemistry methods are applied, and

(2) keywords denoting relevance to microfluidics (i.e., microfluidic flow chemistry in this context). The keywords used were:

Keywords set (1): Flow chemistry, chemical synthesis, organic synthesis, photochemistry, green chemistry, drug discovery.

Keywords set (2): microfluidics, microreactor, droplets.

A keyword from set (1) could be combined with the keywords from set (2) in order to quantify the microfluidic flow chemistry relevance within the broad chemistry theme. **Table 5.1** illustrates how these keyword combinations were used with Google Scholar in this study. Keywords were used in this manner to quantify publications in different categories of chemistry research, as well as their microfluidics relevance over the last five years (between 2015 and 2019, inclusive).

Table 5.1. Example of Google Scholar keyword combinations for determining microfluidic flow chemistry relevance within broad chemistry themes. "Chemical synthesis" and "flow chemistry" are both (set 1) keywords describing broad themes in chemistry research, whereas "microfluidics," "microreactor," and "droplets" are (set 2) keywords describing microfluidics-based research. Thus, combining a set (1) keyword with the set (2) keywords gives us the microfluidics flow chemistry-relevant publications within the broader chemistry theme. For example, "Chemical synthesis" had 24300 results from 2019, of which, 3100 were relevant to microfluidic flow chemistry (13%). "Flow chemistry" on the other hand is a much smaller theme than "Chemical synthesis," with only 1370 results from 2019, but with much higher microfluidic relevance in the field (47%). It must be noted that flow chemistry does not necessarily imply microfluidic flow chemistry. Flow chemistry techniques can be used at meso and macro scales, but the focus of this work is on microfluidic flow chemistry. Quotation marks and "OR" are both Google Scholar search operators. Quotation marks force an exact-match search, and the "OR" operator returns results for all search terms involved, individually or together. The search term <"Chemical synthesis" microfluidics OR microreactor OR droplets>, therefore, returns results that have an exact match for the term "Chemical synthesis" but are also related to the terms microfluidics, microreactor, or droplets, including any combination of the three.

Google Scholar Search Term	Number of Results (2019)	Microfluidic Flow Chemistry Relevance
"Chemical synthesis"	24300	
"Chemical synthesis" microfluidics OR microreactor OR droplets	3100	3100/24300 = **13%**
"Flow chemistry"	1370	
"Flow chemistry" microfluidics OR microreactor OR droplets	650	650/1370 = **47%**

Market value sizing was conducted for each of the chemistry research themes investigated. The total addressable market (TAM; meaning the size of the largest possible market) figures and growth estimates were obtained from marketing analyst firm reports. The serviceable available market (SAM; meaning the part of the market that fits the product being offered, i.e., flow chemistry researchers), of the Fluoroflex material was found by estimating the number of potential customers as a function of the Google Scholar publication results in each chemistry field that were relevant to microfluidics. The serviceable obtainable market (SOM; meaning the proportion of the SAM that could realistically be captured, factoring in competition) was estimated by

multiplying the SAM by a hypothetical market penetration rate achievable with Fluoroflex as a material for chemical microreactors.

Assumptions: It was assumed that Google Scholar search results provided a representative indication of the flow chemistry research market size and trends. It must be noted that while the keyword selection search operators were used to limit the inclusion of irrelevant results in the Google Scholar searches, keyword searches undoubtedly retrieve results that are unrelated to the intended search. It was assumed that irrelevant results would represent a small minority of overall search results. Thus, market evaluation through Google Scholar accurately depicts the quantity and trends of chemistry-related publications with some margin of error.

Market value sizing estimates (i.e., SAM and SOM) were obtained based on the following assumptions: (i) a chemistry lab group generating a microfluidics-relevant publication is a potential customer. (ii) the average chemistry PI generates three publications per year (based on scientific publishing data from Italy[9]), and a single PI represents one possible customer. (iii) The average market penetration rate for a new product, like Fluoroflex, is 3%.[10] (iv) An expected upfront cost for hot embossing equipment is from 2000–3000 EUR (dominated by the cost of a heat press), and the estimated yearly consumable cost of the raw material is 500 EUR. Averaging the equipment cost over 5 years would yield an approximate annual cost of 1000 EUR.

5.3   RESULTS AND DISCUSSION

5.3.1   Technology Landscape Analysis

Microreactor Introduction

Arguably the most important instrument in any flow chemistry toolset is the microreactor. Where the conventional chemist has a round-bottom flask, the flow chemist has a microreactor. By performing chemistry at the micro-scale, microreactors take advantage of high surface-area-to-volume ratios and rapid mass and heat transfer. Further, microreactors enable reactions with greater speed, selectivity, and safety, typically with a reduced footprint when compared to their batch counterparts (this can vary depending on the surrounding control and analytical equipment used for microreaction setups[11]). The major

components of a typical microreactor consist of fluid reagent delivery, micromixer, microreactor, reaction quenching mechanism, and product recovery, as shown in **Figure 5.1**. Flow chemistry setups reported in literature can also contain supplemental components such as sensors (i.e., pressure, flow rate, or temperature), pressure regulators, and in-line chemical analytical equipment (i.e., mass spectrometry, nuclear magnetic resonance spectroscopy). However, this work focuses solely on the microreactor vessel itself. While a wide variety of microreactor formats exist, no single option has been shown to be the best for all situations. The microreactor material must also be considered, each with its distinct advantages and drawbacks from numerous perspectives, including material properties, cost, and ease of fabrication. These aspects make for a diverse field of microreactor technology, in which the Fluoroflex microdevice, a focus of this PhD, is a potential newcomer. This section aims to provide a brief review of the microreactor competitive technology landscape, summarizing the advantages and disadvantages of each one, as well as prominent commercially available versions and their prices, when this information is available. A broad range of aspects is considered in the summaries of microreactor material advantages and disadvantages, such as microreactor performance, cost, availability, ease of use, and technological/product maturity. Note that this is not a comprehensive review of microfluidic materials and fabrication methods – a number of reviews to this end can be found in literature.[12,13]
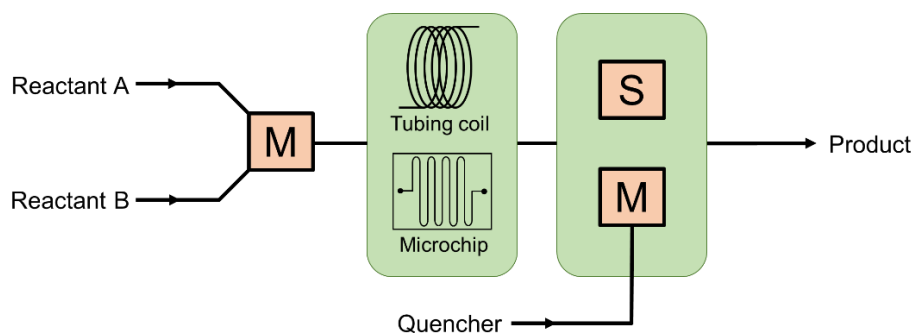
Figure 5.1. Schematic of the typical microreactor components (M=micromixer and S=separator), consisting of fluid delivery into a micromixer, followed by reaction in a microreactor vessel and subsequent mixing with a reaction quencher and/or product separation. The two primary formats of microreaction technology used are tubing coils and microchips, that is, microfabricated devices consisting of a network of channels. Packed bed reactors, commonly used for performing heterogeneous catalysis and other reactions with solid reagents,[14] will not be discussed in the scope of this study.

Microcapillary/Tubing Reactors

One of the broad categories of microreactors is capillary or tubing-based reactors. These consist of simple tubing, often shaped into a coil, in which reagents can flow for a reaction to occur. By varying the fluid flow rate, tubing inner diameter, and tubing length, the user can define the reaction residence time inside of the tubing reactor. Various, standardized connectors exist for interfacing the tubing with a fluid pumping system at its inlet and fluid collection at its outlet. Note that all other microreactors summarized in this section are microchip format reactors. Tubing coils can be immersed in liquid baths for temperature control during a reaction.

Advantages

Simplicity: Compared to microchips, tubing provides a microreactor solution with low complexity and straightforward fluid flow principles based on a few parameters. Little expertise in microfabrication or microfluidic principles is needed. Furthermore, connectors for tubing and microcapillaries are standardized and widely available. **Availability & low cost**: compared to microchip reactors, tubing can be purchased at modest prices and widespread availability, making them highly expendable and replaceable should reactor damage, fouling, or blockage occur. **Multiple materials**: tubing can readily be found in several different materials. The most commonly used for chemical microreactors are fluoropolymers, such as perfluoroalkoxy (PFA) and fluorinated ethylene propylene (FEP), and stainless steel (SS), providing versatility to flow chemistry setups. **Material properties**: depending on the material chosen, tubing reactors can possess high chemical resistance (fluoropolymers and SS), good optical properties (fluoropolymers), and high-pressure capacity and thermal conductivity (SS). **Scale-up**: due to the constant geometry and widespread availability of tubing of different sizes, working with tubing reactors allows scaling up reactions for higher throughput with relative ease.

Disadvantages

Limited performance: while the simple, invariable geometry of tubing reactors can be viewed as one of its strengths, it can also be a limitation; compared to microchips, limited control over precision flow patterns and heat transfer can be achieved with tubing reactors. **Slow mixing**: tubing reactors are

usually used with simple T-junction mixing units, which are far less efficient than dedicated micromixer channels that can exist on microchips and can have a negative effect on reaction outcomes.[15] **Large footprint**: in comparison to microchips, tubing reactors simply take up more space. Smaller-scale microchips, possessing more efficient heat transfer properties, requires less auxiliary heat exchange equipment.[16] **Limited process monitoring**: due to their physical size and shape, tubing reactors do not facilitate many online process monitoring techniques, such as FTIR and surface-enhanced Raman spectroscopy, which can be integrated directly with microchip reactors.[17,18]

On the Market

Fluoropolymer tubing is widely available from large manufacturers, such as Idex (USA) and Saint-Gobain (France), at amenable prices. For example, 15 m of FEP or PFA tubing can be purchased for approximately 100–150 USD. A similar quantity of SS tubing can be found for approximately 215 USD (Idex). Prices reported here are indicative of low quantity purchases. As with most scientific consumable products, prices are expected to reduce when purchasing in higher quantities. Tubing coil microreactors typically consist of several hundred centimeters to several meters of tubing.[19]

Glass Microreactors

When it comes to microchips, glass is one of the most commonly used materials in flow chemistry research. Glass devices consist of a network of microchannels, most often achieved using wet etching methods, but other techniques, such as dry etching and micro sandblasting are also used.[20,21]

Advantages

Chemical resistance: glass possesses excellent chemical inertness, allowing it to be used with a wide range of solvents and chemical compounds. **Optical transparency**: the high optical transparency of glass enables process monitoring inside the microchannels and can allow for photochemistry to be performed. **High T/P**: glass chips can withstand operation at high pressure and temperatures, which can be advantageous for chemical processes.[22] **Product maturity**: a number of companies offer off-the-shelf glass microreactors with dedicated connectors and compatibility with supporting equipment in complete flow chemistry setups (i.e., for temperature control, reagent injection, product extraction).

Disadvantages

Cost: In comparison to other microreactor types, glass reactors are expensive due to the material cost as well as the fabrication procedures used. This is discussed in more detail in the paragraph below, with examples of glass microreactors on the market. **Fragility**: being a brittle material, glass reactors must be handled with care to avoid breakage, especially when considering the high cost of replacement reactors. **Intensive fabrication**: methods of glass microfabrication require expensive equipment and potentially hazardous chemicals, making in-house fabrication of glass microreactors inaccessible to labs without sufficient expertise or means.

On the Market

Commercially available glass microreactors are produced by numerous companies, such as Syrris (UK), Little Things Factory (Germany), Ehrfeld Mikrotechnik (Germany), Chemtrix (The Netherlands), Vapourtec (UK), Corning (USA), Dolomite Microfluidics (UK), Micronit (The Netherlands) and Microfluidic ChipShop (Germany). These microreactors often cost 1000–2000 USD in addition to specialized connectors that must be purchased for fluidic interfacing, which can cost 1500–3000 USD. These represent the average price range of glass reactors – the Lonza FlowPlate® from Ehrfeld Mikrotechnik, for example, is priced at approximately 22,000 USD, not including the process plate (17,000 USD) required for running reactions (note that prices can vary and that discounts for academic research labs are often negotiated). Companies such as Microfluidic ChipShop and Micronit, on the other hand, offer the lowest cost glass microreactors at 170 USD (per chip) and 165 USD (per pack of three chips), respectively. However, these microreactors still require the use of handling platforms of 1500 USD and more, and the devices themselves are fabricated using micro-sandblasting, which, in comparison to glass devices fabricated through wet and dry etching techniques, produce flow channels with reduced resolution and optical clarity due to the high channel surface roughness.

Metal, Silicon, and Ceramic Microreactors

While less common in current flow chemistry research, microreactors can be fabricated in several other materials, including metals, ceramic (most often silicon carbide), and silicon. Metal reactors can be fabricated using various techniques, such as electroforming, conventional machining, and laser ablation.[23] Silicon microreactors can be manufactured using etching

techniques similar to those used for glass, and are often bonded to glass for device sealing [21]. Silicon carbide, a relatively new material in the field of microfluidics, has been microfabricated using laser micromachining techniques.[24,25]

Advantages

Chemical resistance: while exact chemical resistance varies between these materials, they possess good chemical resistance, similar to that of glass. **High T/P**: they can also handle a wide range of pressure and temperature conditions, facilitating process intensification. **Thermal conductivity**: these materials possess high thermal conductivity, which allows for more efficient and homogeneous heating, especially in comparison to glass, which has relatively low thermal conductivity.[12,22]

Disadvantages

Opacity: metals, silicon and ceramics are not optically transparent, preventing photochemistry reactions and channel observation. **Intensive fabrication**: compared to polymeric materials, devices in metal, silicon, and ceramics entail more intensive fabrication processes, limiting the possibility for in-house fabrication and increasing costs. **Cost**: material and fabrication costs result in high costs for microreactors with these materials. **Fragility**: With the exclusion of metals, ceramic and silicon are fragile materials, like glass, posing practical issues to their handling and the potential need for replacement. **Intensive fabrication**: like for glass, micromachining techniques of these materials entail expensive equipment and require microfabrication expertise, making in-house fabrication mostly inaccessible. **Lack of off-the-shelf options**: while microreactors using these materials have been commonly reported in literature, few microreactors can be purchased as off-the-shelf products. Instead, custom devices via fabrication labs are the norm, where the flow chemists themselves must handle the design of the microreactor.

On the Market

Custom silicon chips are fabricated by several MEMS/microfabrication foundries, such as Micronit (The Netherlands), Micralyne (Canada), and C2MI (Canada). However, it is uncommon for them to deal in small quantities of devices, with single microchips incurring high costs. A single silicon-glass microchip from Micronit costs approximately 15,000 – 20,000 EUR. Silicon

carbide has been commercialized by companies such as Mersen (France) and ESK (Germany).

Polydimethylsiloxane

The most common material used for microfluidics, albeit primarily for biological applications, polydimethylsiloxane (PDMS) is an elastomeric material that can be micropatterned using the now-common replica molding technique called soft lithography technique, in which a liquid base polymer and crosslinker mixture is poured atop a master mold to achieve PDMS microchannels.[26]

Advantages

Facile fabrication: using soft lithography, PDMS devices can be made with relatively little sophisticated equipment and microfabrication expertise (compared to the above materials). Thanks to this accessibility, custom PDMS devices are most commonly made in-house. **Low cost**: the price of raw PDMS material and the surrounding fabrication equipment meant that PDMS devices can be realized at low cost, making them easily expendable/replaceable. **Optical transparency**: the high optical transparency of PDMS facilitates microchannel observation and potential photochemistry applications. Flexibility: due to the elastic nature of PDMS, on-chip pneumatic valves, and micropump integration can be achieved.[27]

Disadvantages

Poor chemical resistance: PDMS is notoriously affected by a large range of organic solvents. High degrees of material swelling, and eventual device destruction, can occur, rendering PDMS largely inutile for many organic chemistry applications.[28] **Low-pressure operation**: the pressure capacity of a typical PDMS device rarely exceeds 3 bar.[29] Furthermore, its elastomeric properties entail channel deformation at low to moderate pressures. **Low throughput**: The soft lithography technique excels at small scale production, such as in a research lab setting, however, it is not well suited for large scale device production. This presents a complication for the potential wider adoption and transfer of PDMS microfluidic systems to industry.

On the Market

As mentioned above, the use of PDMS devices in microfluidic research is dominated by in-house production of custom chips with raw PDMS material. A 1.1 kg kit of a common PDMS formulation (SYLGARD 184) can be purchased for approximately 200 USD, which, depending on device dimensions is sufficient to fabricate 50+ devices. While less common, PDMS devices can also be purchased as off-the-shelf products (e.g., ~100 USD per chip from Darwin Microfluidics or Mesobiotech) or customized to the user's specifications (e.g., 1200 USD for five custom chips from FivePhoto Biochemicals).

Thermosets (NOA & OSTE)

While less widespread than other materials reported herein, microreactors made from thermoset resins have shown utility for flow chemistry. Particularly promising are thiol-ene-based materials,[30] such as Nordland Optical Adhesive (NOA)[31] and, more recently, off-stoichiometry thiol-ene (OSTE) polymers.[32] They both come in liquid form and can be UV-cured atop a microfluidic mold in a similar manner to the replica molding of PDMS.

Advantages

Chemical resistance: Thiol-ene thermoset polymers exhibit high chemical resistance compared to other polymeric materials, allowing its use for synthetic chemistry applications. **Optical transparency**: NOA also exhibits high optical transparency, for effective observation and photochemistry applications. **Facile fabrication**: NOA device fabrication uses micropatterned PDMS slabs as master molds for replica molding,[33] taking advantage of PDMS's flexibility and simple fabrication. This results in a relatively accessible fabrication procedure, with low thresholds of cost and required expertise. Alternatively, OSTE polymers undergo an initial UV cure, after which they possess elastomeric properties, allowing the use of rigid microfluidic master molds that are common in soft lithography PDMS fabrication. A second, heat curing step for dry bonding renders the final OSTE rigid, permitting increased pressure operation as well as the straightforward integration of both stiff and flexible components in a single device. **Low/medium price**: while the price of raw OSTE is approximately two times that of PDMS, and NOA is almost ten times, the fabrication procedure helps keep overall costs down in comparison to devices in glass, silicon, metal, and ceramic. **Transferable fabrication**: while NOA device fabrication relies on micropatterned PDMS molds, making it rather low throughput and unsuited to large-scale production, this is not the case for

OSTE polymers. It has been shown compatible with reaction injection molding,[34] giving scope for the fabrication of larger device quantities.

Disadvantages

Cost: while the overall cost of device fabrication may be inferior to those of glass microreactors, the raw material is more expensive than other polymeric materials, such as PDMS and thermoplastics. **No off-the-shelf microreactors**: Although an OSTE formulations have been commercialized (under the name Ostemer®) specifically for microfluidic applications, there are no pre-made thiol-ene microreactors on the market, meaning flow chemists must fabricate their own if they want to use this material.

On the Market

NOA can be purchased in small quantities – 1 oz. bottles (~30 g) – for approximately 50 USD. Ostemer® 322 Crystal Clear, made specifically for microfluidics and MEMs applications can be purchased for between 460 USD (250 g bottle) and 1800 USD (2 kg bottle).

Hard Thermoplastics

Hard thermoplastic materials, such as polycarbonate (PC), poly(methyl methacrylate) (PMMA), polystyrene (PS), and cyclic olefin copolymer (COC) are rigid, melt-processable materials which can be molded at elevated temperatures through methods such as hot embossing and injection molding. Hard thermoplastics can alternatively be machined or 3D printed.

Advantages

Cost: the raw material cost of thermoplastics is low, not only when compared to glass, silicon, metals, and ceramics, but other polymeric materials like PDMS and NOA as well. **Mass fabrication**: industrial processing techniques, such as injection and molding, can be used to mass-produce thermoplastic microchips. In combination with the low material costs, this can permit the fabrication of very inexpensive devices that are easily expendable/replaceable.[35] **Off-the-shelf availability**: following from the low cost, mass fabrication of thermoplastic devices, pre-made, off-the-shelf microchips can readily be found. **Optical transparency**: hard thermoplastics generally possess good optical transparency, though some autofluorescence can be exhibited.[36]

Disadvantages

Poor chemical resistance: Hard thermoplastics generally possess poor to moderate chemical resistance, like PDMS. The exception to this is hard fluoropolymers, like polytetrafluoroethylene (PTFE). PTFE microchips have been demonstrated, but with greater processing difficulty than conventional thermoplastics – some examples of hard fluoropolymer devices and their fabrication difficulties are discussed in Chapter 3 of this dissertation. **Small scale fabrication**: while hard thermoplastics excel at cheap mass production of microchips, fabrication on smaller scales presents complications. Master molds must be able to handle the high temperatures and pressures required for hard thermoplastic molding and subsequently withstand de-molding from a rigid surface.[37] This results in mold costs that can be prohibitive to research lab scales when a relatively small amount of devices are needed, rendering in-house fabrication largely inaccessible.

On the Market

Off-the-shelf hard thermoplastic microchips in a wide variety of designs can be purchase from Microfluidic ChipShop for approximately 50 USD per chip. uFluidix (Canada) alternatively offers custom hard thermoplastic microchips for prices that decrease progressively from 120 USD for a single chip to 15 USD per chip if 10,000 are ordered.

Soft Thermoplastic Fluoroelastomer (Fluoroflex)

Soft thermoplastic elastomer (sTPE) materials are thermoplastic materials (similar to PC, PMMA, etc.), but that possess low stiffness and elastomeric properties (similar to PDMS). Similar to other thermoplastics, sTPE microchips can be fabricated using thermoforming methods like hot embossing and injection molding. Fluoroflex, the focus of this market study, is a fluoropolymer sTPE from which microchip reactors can be fabricated. Its key material properties and fabrication procedure are discussed in detail in Chapter 3 of this dissertation.

Advantages

Good chemical compatibility: while less chemically inert than glass and silicon, Fluoroflex possesses good chemical resistance to a wide range of organic solvents, representing improved solvent compatibility as compared to most other polymeric materials. **Optical transparency**: Fluoroflex has good optical

transparency down to the near-UV range, making microchannel observation and photochemistry a possibility. **Self-sealing**: thanks to its intrinsically adhesive properties, Fluoroflex can form a bond with itself, streamlining device fabrication by eliminating the need for adhesives or surface treatment for bonding. **Transferable fabrication**: sTPE materials share the high-throughput, mass fabrication techniques of hard thermoplastics. However, due to their low stiffness, molding can be achieved with lower pressures and temperatures, and subsequent de-molding is facilitated.[38] This allows for the use of low-cost microfluidic master molds and less equipment for microfabrication, making small-scale in-house fabrication highly accessible, while also giving scope for scale-up to industrial manufacturing levels. **Low cost**: while Fluoroflex is a new material that has not yet been commercialized, due to its thermoplastic nature and facile fabrication methodology, it is expected that devices should be relatively low cost, similar to that of hard thermoplastic devices, allowing for expendable/replaceable microreactors.

Disadvantages

Low-pressure operation: being a flexible material, high pressures deform channels and cause microchip bulging. Without supplementary rigid supporting materials, this limits the use of Fluoroflex devices to low pressures (<3 bar). **Low technology maturity**: being a new material that is not yet on the market, Fluoroflex microreactors lacks the product maturity that exists with glass and hard thermoplastic devices, including integration with peripheral equipment, bespoke connector solutions, and vital user feedback. **Autofluorescence**: Fluoroflex, like some other thermoplastics, exhibits some autofluorescence, potentially limiting its use in applications where fluorescence detection is required.

On the Market

Fluoroflex is not currently on the market. Seeing as the material has been developed by Eden Tech, a French company that has commercialized other sTPE materials, such as Flexdym™, the commercialization of Fluoroflex could be expected.

Table 5.2 provides a summary of the respective advantages and disadvantages of each microreactor type discussed above.

Table 5.2. Summary table of the advantages and disadvantages of common flow chemistry microreactor types, in addition to those of Fluoroflex.

Microreactor Type	Advantages	Disadvantages
Microcapillary/Tubing	Simplicity Availability & low cost Material options Scale-up	Limited performance Slow mixing Large footprint
Glass	Chemical resistance Optical transparency Hight T/P Product maturity	High cost Fragility Intensive fabrication
Metal, Silicon, Ceramic	Chemical resistance High T/P Thermal conductivity	High cost Opacity Intensive fabrication Fragility Limited off-the-shelf options
PDMS	Facile fabrication Low cost Optical transparency	Poor chemical resistance Low-pressure operation Low-throughput fabrication
Thermosets (OSTE, NOA)	Chemical resistance Optical transparency Facile fabrication Transferable fabrication Low/medium price	Cost (vs. other polymers) No off-the-shelf microreactors
Hard Thermoplastic	Low cost Mass fabrication Off-the-shelf availability Optical transparency	Poor chemical resistance Small scale fabrication
sTPE (Fluoroflex)	Chemical resistance Optical transparency Self-sealing Transferable fabrication Low cost (estimated)	Low-pressure operation Low technology maturity Autofluorescence

5.3.2 Researcher Surveys

A review of chemistry literature can reveal what types of microreactor devices are used, and with what frequency, but the reasoning behind a researcher's selection of a particular microreactor is rarely discussed. In addition to the rationale used to decide what type of microreactor should be used for a research project, researcher opinions on microreactor technology based on perceived drawbacks and limitations are also often absent from research articles. Researcher surveys aimed to fill these gaps in information that could play a

critical role in informing the development and marketing of a new tool for researchers.

11 researchers belonging to group 1 (flow chemists) were interviewed, and 5 researchers belonging to group 2 (conventional chemists) responded to written questionnaires. In total, 70 researchers were contacted. Considering the small sample size used, this data is intended to be a preliminary evaluation of the flow chemistry research market to give insight and guidance for a future, more targeted and broad, evaluation. Flow chemistry researcher survey findings are discussed in relation to key themes that emerged as commonalities among researcher responses and were found to be pertinent to the research questions of this study. These key flow chemistry themes are followed by a summary of conventional chemist interview responses at the end of this section.

Tubing Reactors vs. Microchips

When it comes to selecting a microreactor for flow chemistry, researchers have a choice of different materials and reactor formats (i.e., tubing coils vs. microfluidic chips), as discussed in detail in Section 5.3.1. Consideration of which type(s) of microreactor researchers choose, and why, must be taken in order to better understand the microreactor technology landscape and how Fluoroflex may fit into it. While various materials can be used to make microreactors, the two broadest categories in microreaction technology are tubing-based reactors and microchip reactors. It can be seen in literature that tubing reactors are the most common type of microreaction technology currently in use.[19] Indeed, eight out of eleven flow chemistry researchers interviewed used tubing reactors as the primary tool in their microfluidic setups. However, most also possessed microchips (made predominantly out of glass) but used them to a much lesser degree than their tubing reactors. When asked about the reasoning behind this choice, the universal answer was cost. As described above, a 15 m section of fluoropolymer tubing (i.e., FEP, PFA) can be purchased for approximately 100-150 USD, whereas most commercial glass reactor platforms typically cost 2000 USD and often times more.

While researchers expressed general satisfaction in their use of tubing-based reactors, they recognized the possible added value in using microchips – these benefits include more efficient mixing, a more compact reactor footprint, and the ability to perform more complex flow manipulations. However, in most cases, the drawbacks of higher cost and complexity of microchip systems overshadowed any potential benefits that they would bring. This was evidenced

by numerous interviewed researchers explaining that their labs only use their microchips for specific reactions that could not be suitably performed in tubing reactors.

The problem of cost is compounded if reactors must be replaced. A common problem cited in researcher interviews was microreactor clogging. This can readily occur when working with a heterogeneous catalyst or solid precipitates that form during a reaction due to the micro-scale of tubing and microchip channels. Solving and troubleshooting clogging issues can require a degree of microfluidic engineering experience, which may not be available in pure chemistry labs. If clogging is possible, researchers generally preferred to work with tubing, which due to its low cost, could be easily disposed of without much concern, as opposed to attempting to unblock expensive glass microchips. Furthermore, glass is a fragile material, and breaking glass microchips is another source of concern. A few interviewees expressed apprehension about working with glass devices due to this, particularly when students or inexperienced lab members were involved.

It should also be noted that among interviewees using microchips, very few fabricated their devices in-house, with the majority instead opting for ready-made commercially available devices. This highlights that microfabrication and flow chemistry are two distinct sets of expertise that do not necessarily overlap. Thus, it is unsurprising that researchers choose off-the-shelf microreactor options instead of investing the time and resources to develop the microfabrication expertise necessary to create devices themselves, especially when considering the process-intensive fabrication procedures of glass devices in particular. This low accessibility to microfabrication capabilities, in addition to cost, represents a limitation in current flow chemistry research.

Simple Flow Control

Investigating the entire microfluidic systems implemented by flow chemistry researchers was done to understand their workflow and better identify their needs and values in microfluidic technology. To this end, researchers' flow control systems, integrally linked to microreactor technology, were explored to identify value points that could accompany those of the microfluidic flow reactors themselves.

All interviewees used syringe pumps as their primary or sole method of flow control, expressing satisfaction with pump performance for their applications. Syringe pumps were chosen for several reasons: (1) amenable cost, (2)

widespread availability, (3) simplicity in implementing fluid flow, and (4) medium to high pumping pressure capabilities. Following syringe pumps in popularity were high-performance liquid chromatography (HPLC) pumps, which were occasionally used for applications requiring higher pressures and/or flow rates.

This presents a contrast with another large category of flow control in microfluidics – pressure controllers, which have more widespread use in microfluidic applications for biology. Commercial microfluidic pressure controllers can often be characterized by a high performance, stable pressure outputs, relatively low pressure capacities, and relatively high cost. Pressure controllers allow the fast switching of pumping pressures with high precision and minimal fluctuations. Syringe pumps, on the other hand, exhibit relatively slow flow switching by ramping between any two given set flow rates. They also produce flow pulsations, related to the syringe pump step motor distance, that are accentuated at low flow rates.[39] Unlike syringe pumps, however, pressure controllers are tailored to manipulating low pressures. For example, common pressure controllers, such as the OB1 Mk3+ from Elveflow®, the MFCS™-EZ from Fluigent, the Mitos P-Pump from Dolomite Microfluidics do not exceed 10 bar capacity. They moreover come with higher price tags. These characteristics of common pressure controllers reflect the fact that they are tailored for biological research applications, in which relatively low pressures, low flow rates, and high precision/fast flow switching are desired,[40] and merit the increased cost. In flow chemistry applications, complex flow control is rarely needed – simple pumping of reagents at a constant flow rate often suffices.

Altogether, the lower cost and higher pressure capacity of syringe pumps make them the typical choice for flow chemists, with no notable complaints from interviewees. Flow control therefore should not be considered a current limitation in flow chemistry.

Material Selection & Fluoroflex

Following a choice between tubing-based reactors and microchip reactors, flow chemists must choose a microreactor material. The common rationale for selecting a material is its chemical compatibility, temperature and pressure capacity, and optical transparency, particularly in photochemistry applications. As mentioned above, the near-universal material choices among interviewees were fluoropolymers (FEP or PFA) for tubing reactors and glass for microchips. While reactor material choice was highly reaction specific, interviewees did not

consider the material selection to be a main focal point of their work. Their focus, understandably, remained on the chemistry, and as long as a material is compatible with the conditions of a given reaction, it would be considered for use.

In regards to Fluoroflex as a material option of microreactors, interviewees expressed openness and interest. In accordance with the opinions described above, as long as a material meets the requirements of a chemical reaction, it would be considered. Furthermore, interviewees were attracted to the idea of microchip-format reactors at low cost, seen as a significant barrier to greater use of microchip reactors were the costs associated with the currently available glass devices. A low-cost polymer device would position microchips closer to tubing reactors, as expendable, disposable devices.

While interviewees expressed interest in Fluoroflex, a few mitigating factors must be taken into account. Firstly, for Fluoroflex to indeed be adopted by flow chemists, its material properties should fulfill all the constraints of the reactions it is intended for. While Fluoroflex possesses good chemical compatibility, operation under high pressures would be a likely point of concern. As discussed in Chapter 3, Fluoroflex can withstand pressures of at least 4 bar. However, due to its elastomeric properties and thin device dimensions, device deformation occurs at pressures above approximately 3 bar. Further investigation into its high-pressure bonding performance as well as further technological development to account for device deformation (i.e., rigid supports to restrict polymer bulging) should be considered. Fluoroflex must otherwise be reserved for reactions at low pressures. Secondly, even if interviewees expressed interest in a solvent-resistant polymer like Fluoroflex, this does not necessarily mean they would use it to replace their current microreactor technologies if it became available. As discussed above, researchers conveyed general satisfaction with their tubing-based reactors, and it is unclear if the advantages of moving to a microchip system are great enough to motivate the transition.

The Conventional Chemist Take on Flow Chemistry

The primary aim of including a small number of conventional chemist interviews in this study was to identify any current shortcomings or inadequacies in microfluidic technology for flow chemistry (i.e., microreactors or and flow control equipment) were recognized as barriers to a transition from batch to flow chemistry. More specifically, could Fluoroflex directly address a shortcoming in microreaction technology that would drive an increased

interest in flow chemistry among conventional chemists? To this end, Group 2 interviewees were asked if they had ever considered using microfluidics and about the reasons behind their response. Most researchers had never considered using microfluidic flow chemistry methods, citing unfamiliarity with the field and the added complexity to their research that it would bring. One interviewee had considered using microfluidics for the potential advantages it could provide his research, but stopped short of searching for the cost of the equipment necessary to implement it, seeing it as more of a technical issue that diverged from the fundamental chemistry principles in which he research interests lie. No one aspect of microfluidic flow chemistry technology can likely be identified as the source of general disinterest toward flow chemistry techniques. Instead, the ensemble of technical differences between batch and flow chemistry, in conjunction with a broad unfamiliarity with the field, is more likely the bottleneck. Thus, while the increasing popularity of flow chemistry and a greater push for flow chemistry teaching at an undergraduate level[41,42] over time may change opinions on the matter, Fluoroflex, and any improvements it could bring to microreaction technology, is unlikely to directly affect the conventional chemist.

5.3.3 Market Size

Publication Quantification

The Set (1) keywords used for Google Scholar searches – Flow chemistry, chemical synthesis, organic synthesis, photochemistry, green chemistry, and drug discovery – were aimed at describing common general themes in chemistry research in which flow chemistry is highly applicable and often advantageous.[4] While there is without a doubt overlap between the respective chemistry themes, the selection gives a broad view across the range of research subjects that comprise the flow chemistry research market. Google Scholar results for each keyword, along with the proportion that is microfluidics relevant, were mapped across the last five full years, and summarized graphically in **Figure 5.2**.
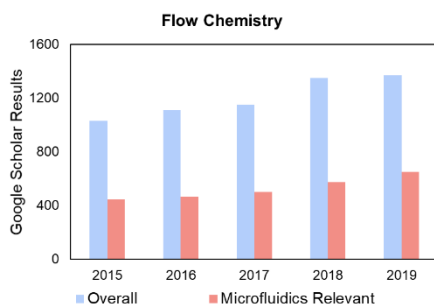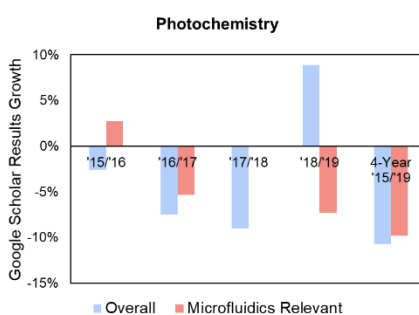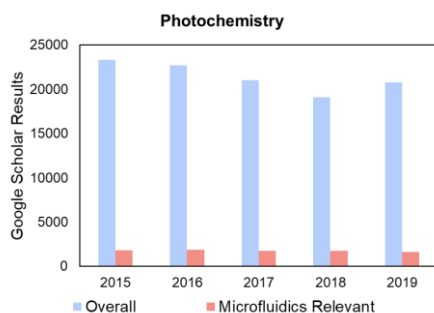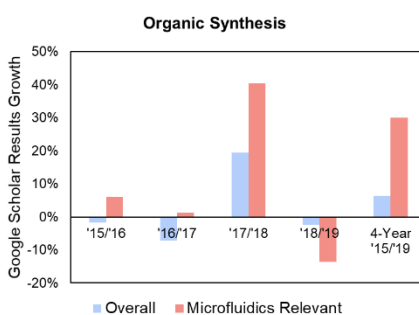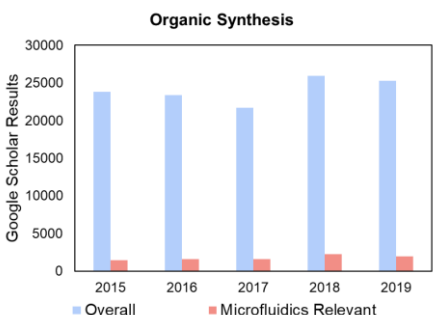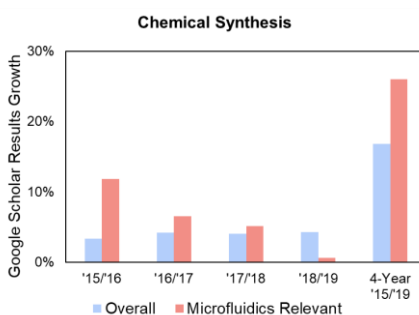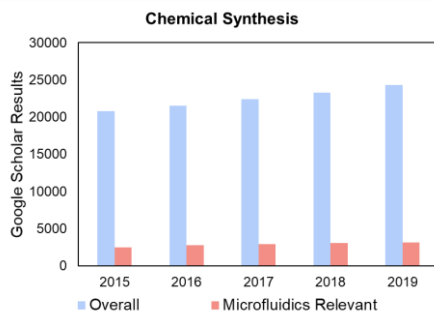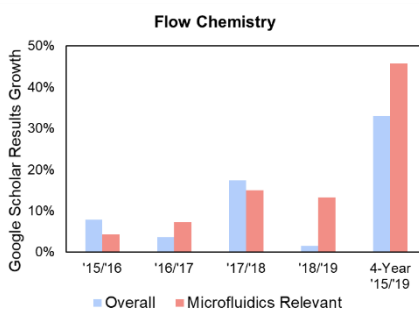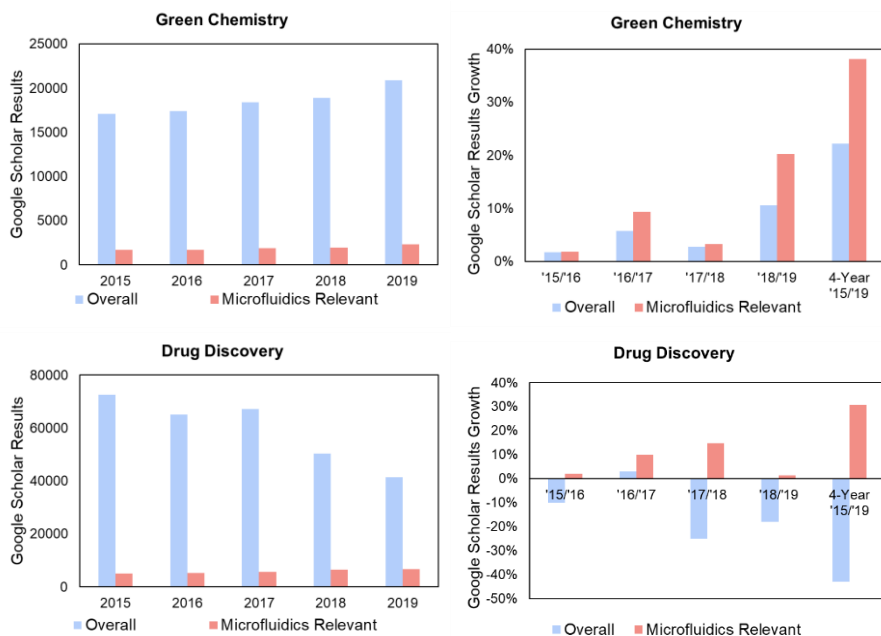
Figure 5.2. Google Scholar keyword search results. Graphs in the left hand column show the number of overall search results for each set (1) keyword (blue) alongside the number of microfluidics-relevant results (red; % of overall publications) within the chemistry theme by year. Microfluidics-relevant results were found using the combination of a set (1) keyword with the microfluidics-relevant keywords of set (2), as described in Section 5.2.3. The proportion of results that are microfluidics-relevant is shown in yellow. Graphs in the right hand column show year-on-year (YoY) growth of both overall and microfluidics-relevant publication results for each chemistry theme.

The size of each chemistry theme based on Google Scholar publication results varied widely, with flow chemistry consisting of 6010 results published in the past five years and drug discovery consisting of 296,700 in the past five years. Flow chemistry, however, shows the highest growth at 33% in the past five years, whereas drug discovery publications have decreased by 43% over the past five years. This small absolute size but high growth rate reflects the relative novelty of flow chemistry techniques in research compared to conventional batch chemistry research. Likewise, photochemistry has shown an 11% decrease in the number of publications over the past five years, while chemical synthesis, organic synthesis, and green chemistry have shown moderate growth of 17%, 6%, and 22%, respectively.

Microfluidics-relevant publications represent modest proportions in each of these fields, ranging from 8% to 16% of overall publications in 2019. This is with the understandable exception of flow chemistry publications, of which nearly half were microfluidics-relevant in 2019. Within each of the growing fields, the microfluidics-relevant publications are becoming an increasingly significant proportion of the total publications, with even higher four-year growth rates of 46% (compared to 33% overall) for flow chemistry, 26% (compared to 17% overall) for chemical synthesis, 30% (compared to 6% overall) for organic synthesis, and 38% (compared to 22% overall) for green chemistry. Even within the field of drug discovery, which has decreased in size over the past five years, microfluidics-relevant publications have increased in number. And in photochemistry, microfluidics-relevant publications decreased at a smaller rate than overall publications

These figures highlight that while microfluidics has achieved only modest adoption and market penetration across much of the range of chemistry themes investigated, it is rapidly growing in popularity and use in chemistry research, having an average four-year growth rate of 27% across the chemistry themes evaluated.

Market Value Estimation

Google Scholar publication search results were subsequently used to estimate the value of the flow chemistry research market. By assuming that an average chemistry research PI publishes three articles per year and that a PI represents one possible customer, we can estimate the total number of potential customers of Fluoroflex with the number of microfluidic flow chemistry-relevant publications in any given year. For example, in 2019, there were 1370 "flow chemistry" publications, of which 457 were microfluidics-relevant (47% relevance rate). Assuming three publications per year, this is the equivalent of approximately 215 PIs in microfluidic flow chemistry, each of which is a potential customer (i.e., serviceable customers). Jensen approximates the average market penetration for a new product is between 2 and 6%.[10] Thus, assuming a market penetration rate of 3% for Fluoroflex, the 215 serviceable customers translate to 6 serviceable obtainable customers.

The National Science Board reported a 3.8% overall increase in scientific publication output over the ten years between 2008 and 2018,[43] possibly reflecting an increasing publishing rate per individual researcher over time. While this increase could serve to inflate the estimated number of potential

customers, it was deemed low enough to be neglected for the five-year period investigated in this study.

With an assumed price of 1000 EUR per year for Fluoroflex, the resulting SAM and SOM are 215,000 EUR and 6,000 EUR, respectively. Similar results for each of the chemistry fields investigated are summarized in **Table 5.3**. This price estimate is based on a business model of selling raw Fluoroflex material and hot embossing equipment to enable flow chemistry labs to autonomously fabricate microreactors. This is similar to the business model of Eden Tech, the French company that commercialized the sTPE material Flexdym™, which sells raw polymer sheets and vacuum heat presses for hot embossing. It is also analogous to the product value chain of PDMS, in which raw material is commonly sold for in-house device fabrication. Accordingly, this business model was chosen for an initial evaluation of the Fluoroflex material as a product.

Table 5.3. Summary of market size estimations for each of the six chemistry themes investigated. Publication data is from Google Scholar search results for 2019 publications. Key assumptions used in the market value calculations are italicized. TAM values for the global flow chemistry, chemical synthesis, organic synthesis, photochemistry, green chemistry, and drug discovery markets were obtained from market analysis firm reports from Grand View Research (flow chemistry, photochemistry), Industry Research (chemical synthesis, organic synthesis), P&S Intelligence (green chemistry) and BBC Research (drug discovery).

Field/Keyword	Flow Chemistry	Chemical Synthesis	Organic Synthesis	Photo chemistry	Green Chemistry	Drug Discovery
Year	2019	2019	2019	2019	2019	2019
Publications	1370	24,300	25,300	20,800	20,900	41,400
Publications per lab	*3*	*3*	*3*	*3*	*3*	*3*
Total potential customers	457	8100	8433	6933	6967	13800
Microfluidics relevance	47%	13%	8%	8%	11%	16%
Potential µfluidic flow chemistry customers	215	1053	675	555	766	2208
Market penetration rate	*3%*	*3%*	*3%*	*3%*	*3%*	*3%*
Potential Fluoroflex customers	6	32	20	17	23	66
Price of Fluoroflex per year	*1,000 €*	*1,000 €*	*1,000 €*	*1,000 €*	*1,000 €*	*1,000 €*
Total Addressable Market (TAM)	US$ 1.2B (2018)	US$ 7B (2020)	US$ 7B (2020)	US$ 1.7B (2016)	US$ 20B (2020)	US$ 35.2B (2016)
Serviceable Market (SAM)	215,000 €	1,053,000 €	675,000 €	555,000 €	766,000 €	2,208,000 €
Serviceable Obtainable Market (SOM)	6,000 €	32,000 €	20,000 €	17,000 €	23,000 €	66,000 €

SOM values across the six chemistry themes investigated range from 6,000 EUR to 66,000 EUR per year, corresponding to between 6 and 66 serviceable obtainable customers in the fields of "flow chemistry" and "drug discovery," respectively. It must be noted that the market size is reported as a yearly figure, as the Fluoroflex material can be viewed as a consumable product (analogous to the tubing used in tubing microreactors). While this range of SOM values is rather low, the growth of the market (27% on average, as discussed above) and the potential for greater market penetration with greater technological maturity and product development should also be considered.

These market size estimates depend highly on the critical assumptions made, notably the market penetration and a price point of a new Fluoroflex product. Being a new product with no clear analogous products (i.e., commercialized polymer for chemical microreactors) for comparison, there is no highly relevant market performance data that can be used as a guide for the Fluoroflex market estimations. In a market with existing similar products, such as commercialized glass microreactors, or microfluidic tubing, typical product price and market penetration can more reliably be estimated. As such, conservative assumptions of 3% market penetration and a price of 1000 EUR were made. 1000 EUR includes the price of the amount of Fluoroflex material sufficient for one year (500 EUR) along with the approximate cost of hot embossing equipment (i.e., a manual heat press similar to the one described in Chapters 3 and 4; 2500 EUR) averaged over a period of five years.

This approach is assuming the sale of raw material for researchers to fabricate microchips in-house. However, an alternative business approach could be taken by selling prefabricated off-the-shelf microreactors, like German company Microfluidic ChipShop, which offers a range of off-the-shelf microdevices in plastic and glass. This latter approach could provide for increased revenue, as individual microdevices would be sold at a higher price point than the raw material. It could moreover prove to be a more strategic and marketable approach to selling a Fluoroflex product. In researcher interviews, flow chemists preferred simplicity in microreaction technology, frequently having no microfabrication expertise and using only tubing reactors. The sale of raw material would require flow chemistry labs to develop some level of microfabrication expertise, an unfamiliar area that could prove to be a barrier in initial adoption and willingness-to-buy. It is thus unlikely that flow chemists would readily adopt this material if it required in-house device fabrication. An offering of off-the-shelf Fluoroflex devices instead of the raw material with microfabrication equipment is thus a more rational approach to the sale of Fluoroflex for flow chemistry. The sale of raw material could be a more viable approach if microfluidic device foundries, like Microfluidic ChipShop, which have high levels of microfabrication capacity and expertise, were targeted. With this approach, the end-user base (flow chemist researchers) remains the same but differs from the customer base (microfluidic chip manufacturers).

While Flexdym™ is also an sTPE, it differs from Fluoroflex in its target market – microfluidic biologists. Microfluidic biology has long gone hand in hand with in-house device design and microfabrication,[44] based largely on the soft lithography techniques developed by the Whitesides group in the late 90s.[26]

Furthermore, in cell biology applications, high variability and complexity in chip design and function are often desired – microfluidic organ-on-chip platforms are good examples of highly complex and multi-layered devices at the cutting edge of biological microfluidics.[45,46] This contrasts with microfluidic flow chemistry, in which fluid manipulations are comparatively simple (often consisting of mixing, reaction, and quenching steps). As a result, flow chemists most often use tubing reactors and standardized microchips with which high levels of customization and variability are unnecessary.[19] Indeed, both approaches to the sale of Fluoroflex – raw material and read-made devices – could be implemented simultaneously, however further speculation on business and marketing approaches is outside the scope of this study.

Market size estimates reported herein directly consider the flow chemistry academic research market and not industrial flow chemistry activities. This market study's focus on academic customers, as opposed to industrial customers, was based on the fact that microfluidic techniques are still dominated by academic research.[1,47] In addition, research labs have traditionally represented early-adopters or generators of new technologies, and could therefore represent agents of technological change and pathways to accessing industrial markets.[48] Indeed, there are expectations that greater transfer of microfluidic flow chemistry to industry will occur as technological demonstrations reach higher levels of maturity in academia.[4] Furthermore, targeting academic labs, in which teaching is conducted and scientific experience is acquired, could serve to expand the end-user base by familiarizing a greater number of chemists to microfluidic techniques with microchip devices. This could prove particularly true by providing inexpensive and expendable microchips, in contrast to the expensive and fragile glass microchips that are currently the norm, which researchers in interviews expressed hesitation to using when students or inexperienced lab members are involved.

The TAM figures reported reflect the total market size, including industry, showing that while the SOM figures – below 100,000 EUR – are small, there is much room for growth in the market at large, not to mention the high rate of growth exhibited by the microfluidic flow chemistry market itself.

5.4   CONCLUSIONS AND OUTLOOK

This market study on flow chemistry microreactors is intended to provide a market contextualization in support of the material characterization and microfluidic device development work conducted on the Fluoroflex material, covering a competitive landscape analysis, researcher interviews, and market size and value estimations for a Fluoroflex microreactor product.

The flow chemistry microreactor competitive landscape is highly varied but dominated by tubing reactors and glass microchip reactors. From a material standpoint, Fluoroflex presents a competitive combination of accessible microchip reactor technology and low cost, making it a direct competitor with glass microchip reactor products currently available on the market. The primary limitation in the utility of Fluoroflex as a flow chemistry microreactor is the pressure capacity. Flow chemistry research reported in literature is often performed at pressures of 10 bar and greater for process intensification. This was also supported through researcher interviews, in which flow chemists cited a medium to high pressure capacity of their microreactors as an important characteristic. While the maximum bonding strength of Fluoroflex was not evaluated (a maximum testing pressure of 4 bar was used), the bulging and deformation of the flexible material pose issues even if pressures of greater than 4 bar can be reached. Further technological innovation could be envisioned, such as simple compression between two rigid plates of plastic or glass, to reduce the Fluoroflex microreactor deformation under elevated pressures, but innovation to this end has yet to be realized. As a result, Fluoroflex devices must be used at low pressures only, mitigating its advantages over alternative reactor materials for the time being.

Based on researcher interviews, a limitation that exists in current flow chemistry setups is the cost of microchip-style reactors. According to interviewees, glass reactors are sparingly used due to their high cost. Most interviewees also expressed interest in the idea of low-cost polymer microchips, as long as its material properties fulfilled the criteria of their reactions, citing benefits that microchips can enable, such as fast mixing, a small footprint, and multi-step reactions. That being said, many reactions do not necessitate microchips, with tubing reactors being sufficient. This raises the question: while the cost of glass microreactors can be prohibitive, how significant is the need for microchips to replace tubing reactors? While most recognized the benefits of using microchip reactors over tubing reactors, of those currently using tubing reactors, none had major problems or difficulties with them in

their research. Thus, it is unclear if the benefits of a low-cost microchip platform, while clear, would be sufficient prompt to change from tubing-based systems. Looking forward, the further evaluation and quantification of the market need for microchips of tubing reactors should be investigated in more depth. Moreover, to better investigate the potential pain points of tubing microreactor technology, greater inclusion of graduate students and post-docs should be included in research interviews. While PIs, the focus of the interviews in this study, represent the researchers with concrete buying power, they tend to have less hands-on involvement with lab work, and consequently may have less insight into the difficulties faced when manipulating microreactors.

Following from this uncertainty, conservative estimates (3%) for the market penetration of a Fluoroflex microreactor were used, resulting in modest market value estimations of 6000–66,000 EUR, depending on the market segment. Taking into account that flow chemistry is a rapidly growing market, with an average four-year growth rate of 27%, these valuations could prove to be much higher. While Fluoroflex is still in the early stages of what could be a product development cycle, two possible market strategies could be envisioned: sale of off-the-shelf microreactors or direct sale of the raw material with the equipment necessary for hot embossing fabrication. It would be most sensible to primarily offer off-the-shelf devices when targeting flow chemists. While the fabrication of sTPE devices is relatively facile, it would still require flow chemists to invest in some amount of microfabrication expertise and optimization, which can seem daunting and would likely limit adoption. The next steps would involve a determination of which types and designs of off-the-shelf microchips would be most desired by flow chemists.

This also raises the possibility of an oversight in the initial conception of this market study in targeting flow chemists as the most likely customer base for the early adoption of Fluoroflex microfluidic technology. A broader, more preliminary, customer discovery stage should have been evaluated. It may be found, for example, that microfluidicists (i.e., microfluidics researchers/engineers) are a more suitable customer base for early adoption due to their greater experience in microchip fabrication and a greater focus on microfluidic technology development than flow chemists. As an analogy, microfluidic devices in PDMS were first adopted by microfluidicists and only later by biologists for more fundamental research once technological capabilities were further demonstrated.[49] Future investigation should thus evaluate microfluidicists, as well as alternative groups, as primary customer base targets.

In conclusion, Fluoroflex presents potential as a microreactor material for flow chemistry, primarily due to the envisioned low cost of such microreactors in comparison to existing technologies. For targeting flow chemists, a business model of selling off-the-shelf devices should be adopted. In parallel, further technological development could increase Fluoroflex's competitive advantage over other microreactor technologies, notably address medium/high-pressure operation as well as integration with surrounding flow chemistry equipment, including a robust method of interfacing devices with fluid injection equipment. However, while the microfluidic flow chemistry market is growing rapidly, the market need for low-cost microchips to replace tubing microreactors remains imprecise and must be investigated further. Following from flow chemist researcher interviews, it is possible that flow chemists are not the most suitable group to target for initial adoption of the Fluoroflex material – other groups, notably microfluidicists, may be more appropriate, and should be included in a broader customer discovery process.

5.5 REFERENCES

[1]   N. Convery, N. Gadegaard, *Micro Nano Eng.* **2019**, *2*, 76.

[2]   D. T. Chiu, A. J. deMello, D. Di Carlo, P. S. Doyle, C. Hansen, R. M. Maceiczyk, R. C. R. Wootton, *Chem* **2017**, *2*, 201.

[3]   A. Manz, N. Graber, H. M. Widmer, *Sensors Actuators B Chem.* **1990**, *1*, 244.

[4]   K. S. Elvira, X. C. i Solvas, R. C. R. Wootton, A. J. DeMello, *Nat. Chem.* **2013**, *5*, 905.

[5]   Y. Liu, X. Jiang, *Lab Chip* **2017**, *17*, 3960.

[6]   F. M. Akwi, P. Watts, *Chem. Commun.* **2018**, *54*, 13894.

[7]   R. E. Davis, *J. Prod. Innov. Manag.* **1993**, *10*, 309.

[8]   V. Krishnan, K. T. Ulrich, *Manage. Sci.* **2001**, *47*, 1.

[9]   C. A. D'Angelo, G. Abramo, *Proc. ISSI 2015 Istanbul 15th Int. Soc. Sci. Inf. Conf.* **2015**, 909.

[10]   M. Jensen, *The Everything Business Planning Book: How to Plan for Success in a New or Growing Business*, Adams Media, **2001**.

[11]   T. Schwalbe, V. Autze, G. Wille, *Chim. Int. J. Chem.* **2002**, *56*, 636.

[12]   K. F. Jensen, B. J. Reizman, S. G. Newman, *Lab Chip* **2014**, *14*, 3206.

[13]   P. L. Suryawanshi, S. P. Gumfekar, B. A. Bhanvase, S. H. Sonawane, M. S. Pimplapure, *Chem. Eng. Sci.* **2018**, *189*, 431.

[14]   R. Munirathinam, J. Huskens, W. Verboom, *Adv. Synth. Catal.* **2015**, *357*, 1093.

[15]   S. Watanabe, S. Ohsaki, A. Fukuta, T. Hanafusa, K. Takada, H. Tanaka, T. Maki, K. Mae, M. T. Miyahara, *Adv. Powder Technol.* **2017**, *28*, 3104.

[16]   M. R. Ozdemir, A. Koşar, O. Demir, C. Öžzenel, O. Bahçivan, in *ASME 2010 10th Bienn. Conf. Eng. Syst. Des. Anal. Vol. 5*, ASMEDC, **2010**, pp. 703–710.

[17]   I. J. Jahn, O. Žukovskaja, X.-S. Zheng, K. Weber, T. W. Bocklitz, D. Cialla-May, J. Popp, *Analyst* **2017**, *142*, 1022.

[18]   A. Perro, G. Lebourdon, S. Henry, S. Lecomte, L. Servant, S. Marre, *React. Chem. Eng.* **2016**, *1*, 577.

[19]   M. B. Plutschack, B. Pieber, K. Gilmore, P. H. Seeberger, *Chem. Rev.* **2017**, *117*, 11796.

[20]   N. Van Toan, M. Toda, T. Ono, *Micromachines* **2016**, *7*, 51.
[21]   C. Iliescu, H. Taylor, M. Avram, J. Miao, S. Franssila, *Biomicrofluidics* **2012**, *6*, 1.
[22]   S. Marre, Y. Roig, C. Aymonier, *J. Supercrit. Fluids* **2012**, *66*, 251.
[23]   O. de la Iglesia, V. Sebastián, R. Mallada, G. Nikolaidis, G. Coronas, G. Kolb, R. Zapf, V. Hessel, J. Santamaría, *Catal. Today* **2007**, *125*, 2.
[24]   S. G. Newman, L. Gu, C. Lesniak, G. Victor, F. Meschke, L. Abahmane, K. F. Jensen, *Green Chem.* **2014**, *16*, 176.
[25]   Y. Huang, X. Wu, H. Liu, H. Jiang, *J. Micromechanics Microengineering* **2017**, *27*, 065005.
[26]   D. C. Duffy, J. C. McDonald, O. J. A. Schueller, G. M. Whitesides, *Anal. Chem.* **1998**, *70*, 4974.
[27]   M. A. Unger, H. Chou, T. Thorsen, A. Scherer, S. Quake, *Science (80-.).* **2000**, *288*, 113.
[28]   J. N. Lee, C. Park, G. M. Whitesides, *Anal. Chem.* **2003**, *75*, 6544.
[29]   S. Bhattacharya, A. Datta, J. M. Berg, S. Gangopadhyay, *J. Microelectromechanical Syst.* **2005**, *14*, 590.
[30]   D. Sticker, R. Geczy, U. O. Häfeli, J. P. Kutter, ACS Appl. Mater. Interfaces 2020, 12, 10080.
[31]   D. Bartolo, G. Degré, P. Nghe, V. Studer, *Lab Chip* **2008**, *8*, 274.
[32]   C. F. Carlborg, T. Haraldsson, K. Öberg, M. Malkoch, W. Van Der Wijngaart, Lab Chip 2011, 11, 3136.
[33]   P. Wägli, A. Homsy, N. F. De Rooij, *Procedia Eng.* **2010**, *5*, 460.
[34]   N. Sandström, R. Z. Shafagh, A. Vastesson, C. F. Carlborg, W. van der Wijngaart, T. Haraldsson, J. Micromechanics Microengineering 2015, 25, 075002.
[35]   T. D. Boone, Z. H. Fan, H. H. Hooper, A. J. Ricco, H. Tan, S. J. Williams, *Anal. Chem.* **2002**, *74*, 78 A.
[36]   A. Piruska, I. Nikcevic, S. H. Lee, C. Ahn, W. R. Heineman, P. A. Limbach, C. J. Seliskar, *Lab Chip* **2005**, *5*, 1348.
[37]   E. Roy, A. Pallandre, B. Zribi, M.-C. Horny, F. D. Delapierre, A. Cattoni, J. Gamby, A.-M. Haghiri-Gosnet, in *Adv. Microfluid. - New Appl. Biol. Energy, Mater. Sci.* (Ed.: X.-Y. Yu), InTechOpen, London, UK, **2016**.
[38]   M. D. Borysiak, K. S. Bielawski, N. J. Sniadecki, C. F. Jenkel, B. D. Vogt, J. D. Posner, *Lab Chip* **2013**, *13*, 2773.
[39]   Z. Li, S. Y. Mak, A. Sauret, H. C. Shum, *Lab Chip* **2014**, *14*, 744.
[40]   C. K. Byun, K. Abi-Samra, Y.-K. Cho, S. Takayama, *Electrophoresis* **2014**, *35*, 245.
[41]   K. P. L. Kuijpers, W. M. A. Weggemans, C. J. A. Verwijlen, T. Noël, *J. Flow Chem.* **2020**.
[42]   V. Kairouz, S. K. Collins, *J. Chem. Educ.* **2018**, *95*, 1069.
[43]   National Science Board, *Publications Output: U.S. Trends and International Comparisons*, **2019**.
[44]   J. El-Ali, P. K. Sorger, K. F. Jensen, *Nature* **2006**, *442*, 403.
[45]   S. N. Bhatia, D. E. Ingber, *Nat. Biotechnol.* **2014**, *32*, 760.
[46]   M. L. Coluccio, G. Perozziello, N. Malara, E. Parrotta, P. Zhang, F. Gentile, T. Limongi, P. M. Raj, G. Cuda, P. Candeloro, E. Di Fabrizio, *Microelectron. Eng.* **2019**, *208*, 14.
[47]   Yole Développement, *Status of the Microfluidics Industry 2019*, **2019**.
[48]   F. Meyer-Krahmer, U. Schmoch, *Res. Policy* **1998**, *27*, 835.
[49]   E. Berthier, E. W. K. Young, D. Beebe, *Lab Chip* **2012**, *12*, 1224.

CHAPTER 6

Conclusions and Outlook

CHAPTER 6 – CONCLUSIONS AND OUTLOOK

6.1 GENERAL CONCLUSIONS

This dissertation focuses on soft thermoplastic elastomer materials to fabricate microfluidic devices for both cell culture and flow chemistry applications. It aims to characterize sTPE material properties and use them to develop microfluidic tools that can address the drawbacks of currently used materials.

Chapter 1 provides a brief introduction to microfluidic technology and its applications in biological and chemical sciences. The evolution and proliferation of microfluidic techniques have been limited by current materials used to make microfluidic devices, whether it be deficiencies in their material properties, fabrication practicalities, or cost. Deficiencies are especially apparent in the most ubiquitous microfluidic material currently in use, polydimethylsiloxane (PDMS). The advantages and disadvantages of the most common microfluidic device materials are summarized, including glass, silicon, PDMS, and hard plastics. In addition, soft thermoplastic elastomers (sTPE), a comparatively new class of materials, are introduced. sTPEs possess material properties and fabrication methodologies that make them an attractive alternative for microfluidic device manufacturing. In particular, sTPE materials provide for accessible device fabrication, with the flexibility to transfer across different fabrication scales. That is to say, devices can not only be made in small quantities (i.e., academic research), at low cost and with little expertise, but feasibly in large amounts as well (i.e., industrial implementation), thanks to thermoplastic mass production techniques, such as injection molding and roll-to-roll hot embossing. Specifically, the two materials investigated in this dissertation are Flexdym™, a commercially available sTPE with demonstrated utility for biological applications, and Fluoroflex, a novel fluoropolymer sTPE that has shown promise for microfluidic flow chemistry applications.

In **Chapter 2**, a composite thermoplastic device for membrane-based cell culture is presented. The device replicates the "barrier model" microfluidic geometry, consisting of two microfluidic flow chambers separated by a thin, porous membrane. Microfluidic barrier model devices have been used for recreating *in vivo* conditions on-chip by simulating tissue-tissue interfaces and even organ functional units (i.e., organ-on-chip technology), showing high value for pharmaceutical development and pathogenesis investigation. The

composite device consists of two micropatterned Flexdym™ layers separated by a commercially available porous polycarbonate membrane. The composite device fabrication procedure consists of a 2-minute hot embossing cycle, the formation of conformal contact between the layers, and the subsequent self-sealing with a baking step. The whole process can be completed in under 2.5 hours, using minimal equipment and expertise. This contrasts with barrier model devices in literature, most commonly made from PDMS. In particular, PDMS requires a relatively long curing time (between 2 and 48 hours) and plasma surface activation to achieve bonding. Moreover, thin, porous PDMS membranes are difficult and time-consuming to fabricate, with low throughput. These fabrication aspects give PDMS barrier model devices low transferability, with little scope for scaling up manufacturing volumes. These represent bottlenecks that have hindered the more general adoption of microfluidic techniques among biologists and broader industrial players. Flexdym™ addresses these bottlenecks by leveraging rapid hot embossing for thermoplastic microchannel formation and its intrinsically adhesive property, allowing spontaneous bonding with itself and other thermoplastics without the need for surface activation or additional adhesives. The combination of these advantages of Flexdym™ with an off-the-shelf membrane proven for use in cell culture results in a fully thermoplastic microfluidic platform with faster, more streamlined fabrication, while, critically, possessing scope for scale-up.

A key part of this chapter was evaluating the bonding strength that could be achieved between the Flexdym™ layers and the polycarbonate membrane. Specifically, the pressure capacity that a Flexdym™-polycarbonate bond can withstand was assessed as a critical parameter in future microfluidic chip development. A system of automated delamination testing was designed, device burst pressure testing in a reproducible and high-throughput manner. Delamination testing showed that at bonding distances of 200 µm and greater, the Flexdym™-polycarbonate bond could withstand over 0.5 bar. At a bonding distance of 1 mm, representative of typical microfluidic channels without small microfeatures, devices reliably withstood a maximum testing pressure of approximately 1.9 bar. This bonding strength is sufficient for most biological applications. Flow tests demonstrated that the flow rates and shear stresses that could be generated within the device pressure limits were suitably high for cell culture. Finally, a validation of the composite platform's utility for membrane-based cell culture was performed through cell trials. Human dermal fibroblasts cultured on the polycarbonate membrane inside devices showed good adhesion and proliferation for seven days.

Chapter 3 introduced a novel sTPE material, Fluoroflex, whose fluoropolymer material composition suggests an enhanced chemical resistance compared to other polymers used for microfluidics, namely PDMS. To this end, this chapter focused on extensive material characterization and microfabrication development of Fluoroflex with the intended use for flow chemistry applications. The principal subject of material characterization was chemical resistance. Fluoroflex exhibited good chemical resistance during polymer swelling tests, when exposed to a range of common organic solvents, such as toluene, hexane, chloroform, and dichloromethane. In comparison, PDMS displays high degrees of swelling with many of these solvents, rendering it unusable for many organic chemistry applications. Based on the polymer swelling data collected, an estimation of the Hansen Solubility Parameter of Fluoroflex was made. This parameter can be used to predict Fluoroflex-solvent interactions with solvents that were not included in swelling experiments. Fluoroflex additionally possesses high optical transparency, low surface roughness, and low oxygen permeability, important properties for its use as a microreactor. Other material properties, such as its mechanical stiffness and surface wetting, were characterized and could inform the handling and microfluidic operation of Fluoroflex devices.

A microfabrication protocol was developed, whereby raw Fluoroflex pellets undergo a 30-second hot embossing cycle to yield micropatterned polymer sheets. Like Flexdym™, inexpensive and easily-made master molds can be used for Fluoroflex hot embossing, setting these sTPE materials apart from hard thermoplastics, which require robust, and expensive master molds for device manufacturing. Fluoroflex sheets can subsequently be placed in conformal contact to achieve self-bonding. With an additional 2-hour baking step, the Fluoroflex self-bond could withstand maximum testing pressures of 4 bar during delamination testing. Room temperature sealing, with no baking step, was also possible, with Fluoroflex devices withstanding approximately 1.4 bar pressures after only 5 minutes of conformal contact. This rapid room temperature bonding proved to be reversible and it allowed for the near-immediate use of Fluoroflex devices after hot embossing, contributing to the simplicity and transferability of the fabrication process. The fast, and reversible, room-temperature seal-sealing was leveraged to create a modular microfluidic platform using Fluoroflex. Discrete microfluidic modules (e.g., Y-channel, T-junction, serpentine channel, etc.) could be interchangeably bonded to a manifold baseplate and used for flow experiments within minutes. Droplet generation (water in toluene) was shown using T-junctions of two different

sizes, demonstrating the modular, "plug-and-play" operation enabled by Fluoroflex's self-sealing properties, all while using an organic solvent.

Chapter 4 builds on the Fluoroflex material characterization and microfluidic demonstration of Chapter 3 by presenting the design and preliminary evaluation of a Fluoroflex microfluidic packed bed photoreactor system. PDMS microbeads were synthesized to act as solid photocatalyst supports, approximately 100–150 μm in diameter. PDMS microbeads were packed into a Fluoroflex microchannel containing an array of micropillars, then subjected to a surface functionalization procedure. 3-aminopropyltriethoxysilane (APTES), an aminosilane, was used to form base-functionalized PDMS microbeads. Critically, the APTES surface layer possessed amine functionality, allowing the immobilization of organic molecules, such as photocatalysts, to the PDMS-APTES microbeads inside the Fluoroflex microchannel. This concept was demonstrated by coupling fluorescein to the on-chip microbeads, which were visualized with fluorescence microscopy to evaluate the effectiveness of the APTES microbead coating. Performing the functionalization entirely on-chip allowed for a streamlined process of achieving micro-scale polymer supports for photoactive molecules – an analogous functionalization process carried out in batch requires filtration between each step to separate the microbeads from the reagent solutions.

Separately, PDMS beads were functionalized in batch with APTES, followed by a derivative of the photoactive perixanthenoxanthene (PXX) molecule instead of fluorescein. PXX derivatives are organic molecules that have been shown to possess photo-redox properties. Accordingly, PXX-catalyzed debromination reactions were conducted in batch using either PXX in solution or PXX-functionalized microbeads in suspension as heterogeneous catalyst supports. The reactions resulted in identical reagent/product conversions, demonstrating the conservation of PXX's photocatalytic properties after attachment to APTES on PDMS microbeads. This demonstration offers clear next steps in implementing PXX, or other photocatalysts, in the Fluoroflex/PDMS microbead packed bed photoreactor system.

Chapter 5 consisted of a flow chemistry microreactor market evaluation. This was done in support of the material characterization and microfluidic evaluation of the Fluoroflex material presented in Chapters 3 and 4, in which its utility as a flow chemistry microreactor was demonstrated. This study aimed to investigate the flow chemistry microreactor market to evaluate the market placement of a Fluoroflex microreactor product, giving an industrial context to

the academic research conducted during this PhD study. To this end, a competitor analysis was presented, summarizing the advantages and disadvantages of materials currently used for microreactor fabrication, as well as their associated commercially available products. Fluoroflex's combination of material properties and low estimated cost offer an attractive alternative to current microreactor solutions.

Interviews of flow chemistry researchers were conducted to identify user-defined limitations in current microreactor technology and openness to new material alternatives. It was found that the majority of interviewees used microcapillary (i.e., tubing) microreactors, citing their simplicity and cost-effectiveness in comparison to glass microchip reactors, the next most commonly used microreactor format. Despite the theoretical advantages of using microchips over tubing-based reactors and interviewee openness to new materials, the heavy inclination toward tubing reactors calls into question the market need for microchip reactors, as few concrete issues with tubing reactors were raised. This is a critical point when considering developing a new microchip reactor product (i.e., Fluoroflex) and should be investigated further. Interviewees also reported a near-ubiquitous use of pre-made, off-the-shelf microreactors. This reflects little to no microfabrication expertise present in typical chemistry labs, in sharp contrast with microfluidics labs, which overwhelmingly fabricate devices in-house and focus on biological applications. Consequently, the best marketing strategy to target flow chemists would be the sale of off-the-shelf Fluoroflex devices.

Lastly, a flow chemistry market size estimation was made using publications as a metric (using the Google Scholar search engine), showing an average four-year growth rate of 27% in publications across the flow chemistry themes investigated. Publication data was translated to potential customers of a Fluoroflex microreactor product (i.e., academic researchers). The market value was estimated to be between 6,000–66,000 EUR per year, depending on the flow chemistry market segment.

6.2 OUTLOOK

This PhD has consisted primarily of microfluidic platform development and proof-of-concept demonstrations using novel sTPE materials. The work presented provides a broad scope for future work and logical next steps toward the utilization of sTPE devices in biological and flow chemistry applications, representing a transition from the microfluidics development focus of this dissertation to actual research implementation.

Flexdym™ Cell Culture Platform

Building off of the cell culture validation of the Flexdym™-polycarbonate barrier model device, the next steps would be the development of more complex cell culture models toward an organ-on-chip study. The operation and performance of the device could be directly compared to cutting-edge PDMS barrier model platforms in literature. During these comparisons, particular attention should be paid to the relatively low small molecule absorption of Flexdym™. This should be leveraged to demonstrate not only matching, but improved barrier model performance compared to PDMS in the domain of *in vitro* drug testing. An additional comparison between the fabrication times of the composite barrier model platform and an analogous PDMS device would allow for better quantification of the fabrication advantages of the thermoplastic system. The comparative durations could be evaluated for the fabrication of both a single device and multiple devices to demonstrate the improved manufacturing scalability of sTPE materials over PDMS.

From a microfluidic device engineering standpoint, attempts to fabricate thin porous sTPE membranes, something that has yet to be reported, could allow for a barrier model device to be made entirely from sTPE, and prove valuable for cell culture applications. In contrast to the relatively stiff polycarbonate membrane, using an sTPE membrane could notably enable the mechanical stretching of cell substrates to mimic specific human tissues that undergo periodic stretching in the body (e.g., lung, gut tissue).[1] The recently reported FlexdymSC formulation, which can be spin-coated to form thin sTPE membranes, would be a good candidate for this objective.[2] Throughout further development, critical consideration must always be given to the balance between device performance and facile fabrication methodologies; the latter was one of the benefits of using the off-the-shelf polycarbonate membrane.

Fluoroflex Chemically Compatible Microreactors

Following the demonstration of Fluoroflex's suitability as a flow chemistry microreactor based on its material properties, the next step would be to perform microfluidic flow chemistry inside of a Fluoroflex device. While no specific application or reaction is envisioned, it should ideally take advantage of the modularity that Fluoroflex's rapid and reversible self-sealing enables. This modularity allows high throughput testing of different microfluidic configurations that could facilitate process and reaction optimization. Moreover, because typical chemists have little expertise in microfluidic device design and fabrication, providing a set of "plug-and-play" modules could ease the transition between batch chemistry and microfluidic techniques. In this same vein, further technological development of Fluoroflex as a microfluidic platform is needed to make it more broadly and easily usable. This includes the development of a connector solution to replace the commercial connectors that were reported in Chapter 3, which required an adhesive to be fixed to the Fluoroflex device – this undermines the benefit gained by Fluoroflex's robust, and adhesive-free, self-sealing. Due to the low thickness of Fluoroflex substrates, some form of connectors is needed. sTPE connectors should be developed to permit a device made entirely out of Fluoroflex. The material's elasticity could be used to directly accept the insertion of microfluidic tubing, similar to how PDMS device ports deform around tubing without the need for a supplementary connector. Alternatively, thicker sheets of Fluoroflex (> 2.5 mm) could be used to eliminate the need for connectors.

A second point of technological development would be to address the deformation of Fluoroflex under pressures above ~3 bar, a limitation that could hinder its broader use in synthetic flow chemistry. Using thicker sTPE sheets could improve this, or perhaps a system of rigid plates (of plastic, glass, or metal) to provide a compressive force on the device and limit channel bulging. Additionally, while it is not discussed in this dissertation, Fluoroflex microdevices should not necessarily be limited to use in a flow chemistry context. Investigation of its biocompatibility could lead to its utility for biological applications, taking advantage of low absorption properties compared to PDMS. Furthermore, reversible room temperature bonding could prove useful for interchangeably manipulating cells in and out of a microchannel environment without harming the cells with adhesives or elevated temperatures for device sealing. Accompanying investigation into the surface modification of Fluoroflex would inform its suitability for the attachment of cells and biomolecules. Surface modification could also have

implications for chemistry applications, such as heterogeneous catalysis using Fluoroflex as a polymer support.

To add to Fluoroflex's reconfigurability through reversible bonding, the bulk material itself can be recycled. Microfluidic devices, dominated by PDMS, are generally single-use. This reality of material waste is somewhat in opposition to the notions of greater sustainability through reduced reagent consumption in microfluidics. Conscious use and reuse, when possible, of a polymer like Fluoroflex could lead to less waste generated in microfluidics and more sustainable research practices.

Functional Microbead Photoreactor

Among the potential applications of Fluoroflex for synthetic flow chemistry is the packed bed photoreactor concept presented in Chapter 4. The preliminary work presents clear next steps for experimentation discussed extensively in the conclusion section of the chapter. In brief, these would consist principally of the implementation of PXX-functionalized microbeads, thus far used only in batch, inside of a Fluoroflex microchannel to perform the photoactivated debromination reaction in flow. The reaction performance and duration could be compared to results from batch trials, and could be optimized by varying reactor parameters, including the microbead size, channel dimensions, and reagent flow rate. The implementation of parallel packed bed channels could limit the microfluidic resistance (and consequent back pressures) of the system, while increasing throughput. This would aim at achieving a volume and product throughput that is comparable to or higher than that of batch methods while consuming less catalyst and energy in the process.

Fluoroflex Market Evaluation

Following the work presented in Chapter 5, a more extensive exploration of the potential Fluoroflex market should take a broader approach. More fundamental customer discovery should be conducted, considering not only flow chemists as the most likely end-user. Microfluidics researchers, for example, may be more likely to be early adopters of Fluoroflex technology. Alternatively, targeting industrial customers, namely microfluidic foundries, which have extensive experience in material handling and microfluidic device development, could represent a promising path for Fluoroflex's first commercial steps. In a flow chemistry context, the attractiveness of microchip reactors as opposed to microcapillary reactors must be investigated further through additional (or more extensive) flow chemist interviews, as these

findings could make or break Fluoroflex's value as a microchip reactor product. A greater number of graduate students and postdocs should be targeted for interviews to better understand the technical end-users' needs and pain points when working with current microreaction technology.

The wide-ranging data collected on the Fluoroflex material, both scientific and market-oriented, has produced important insight into how this material could most effectively be used. Accordingly, a few recommendations may be given for its future development as a material for microfluidics. The points of further technical development concerning a robust interfacing/connector system and a feasible manner of working at elevated pressures are critical, especially the former. A common theme from flow chemistry researcher interviews was that working with microfluidics is complicated, and that convoluted, non-standardized connector solutions only compound this complexity. This attitude likely extends beyond chemists to biologists and other potential beneficiaries of microfluidic techniques who are not principally "microfluidicists." Consequently, developing a material system – from fabrication to end-use – with simplicity and practicality in mind will be key in attracting new users. Moreover, academic literature and reports of the sTPE being used will play a significant role in building credible visibility of the material's capabilities and encouraging potential new users to invest the time and resources to work with a new material system. Therefore, the challenge comes in identifying and targeting the researchers most willing and likely to generate these formative demonstrations.

Following the findings of the market study (Chapter 5), it is likely that targeting flow chemists is not the optimal path toward these initial market breakthroughs. An analogy can perhaps be found in the market positioning of the Ostemer® material. While it presents a highly promising solution for flow chemistry microreaction technology due to its solvent resistance and versatile fabrication procedure, publications involving its use are predominately focused on biological applications and this is mirrored in how it is marketed. This reflects the current dominance of biology-focused applications in microfluidics research, whereby the microfluidicists who represent a group likely to generate new microfluidic material demonstrations will most commonly do so in a biological context. Consequently, Fluoroflex's suitability for such applications (i.e., its biocompatibility, surface modification, etc.) should be investigated in order to effectively target microfluidicist research groups that will produce foundational validations in academic literature, even if the material eventually proves to be more apt for flow chemistry applications.

In his article titled, "Engineers are from PDMS-land, Biologists are from Polystyrenia," Berthier perfectly describes the disconnect between microfluidics engineers, who develop new microfluidic devices, and biologists, who use them.[3] Their differing approaches to research and limited communication have led to a "culture clash" over material selection for microfluidic device fabrication. The former prefers PDMS for its simple fabrication and the latter prefers polystyrene for its superior properties and familiarity. This insight can also be extended to microfluidics' intersection with chemistry, where the complicated and expensive microdevices currently available attract relatively few chemists to work with flow methods. These unfortunate divides between inventors and users can justly be blamed for hindered progress in microfluidics over the last 30 years. sTPE materials, while far from a magic bullet to solve all the challenges that the field of microfluidics faces, can make a step toward bridging these gaps. With continued development and microfluidic demonstration, these materials can aid in the advancement of science and technology by fulfilling the engineer's fabrication requirements and the researcher's performance needs. In what is a highly interdisciplinary field, communication and awareness of the needs of others is paramount. In whichever direction sTPEs, or any other materials, are further developed for microfluidic devices, it should be done so in close collaboration with those that will be using them.

6.3 REFERENCES

[1]   S. N. Bhatia, D. E. Ingber, *Nat. Biotechnol.* **2014**, *32*, 760.
[2]   J. Lachaux, H. Salmon, F. Loisel, N. Arouche, I. Ochoa, L. L. Fernandez, G. Uzan, O. Mercier, T. Veres, E. Roy, *Adv. Mater. Technol.* **2019**, *4*, 1.
[3]   E. Berthier, E. W. K. Young, D. Beebe, *Lab Chip* **2012**, *12*, 1224.

APPENDICES

APPENDIX 1 – FLUOROFLEX SPECIFICATION SHEET

Fluoroflex Soft Thermoplastic Fluoroelastomer Specification Sheet

Overview

Name	Fluoroflex
Description	A fluoroelastic terpolymer Poly(TFE-ter-E-ter HFP) material which is melt-processable (thermoplastic), transparent, and features enhanced self-sealing properties (TFE=tetrafluoroethylene, E=ethylene, HFP=hexafluoropropylene).
Recommended applications	• Flow chemistry microreactors • Microfluidic rapid prototyping • Modular microfluidics
Storage	Room temperature (pellet or sheet form).
Handling	With gloves, to preserve polymer surface cleanliness.

Process Compatibility

Micro-structuring	Thermoplastic melt-processing (e.g., hot embossing).
Post processing	Reversible self-bonding after conformal contact, without adhesives or surface treatment.
Mold compatibility	Soft-lithography molds (e.g., SU-8/silicon, dry-film photoresist/glass), metallic molds.

Material Properties

Melt temperature	200 °C
Self-bonding pressure capacity	• RT bonding, 5 min: 1.4 bar • RT bonding, 3 hr: 1.8 bar • 185 °C baking, 2 hr: 4 bar
Refractive index	1.36
Optical transmittance	> 50% transmittance from 335 nm to 800 nm
Autofluorescence	Some autofluorescence, with peak excitation at 370 nm
Young's modulus	3.75 MPa (< 20% strain)
Elongation at break	~435%
Solvent resistance	Non-polar solvents (e.g., toluene, chloroform, hexane), alcohols, amines. Susceptible to some polar aprotic solvents (e.g., acetone, 2-butanone, tetrahydrofuran).
Hansen Solubility Parameter	δ=21.2, δ_D=16.5, δ_P=8.9, δ_H=9.7, R_O=7.5 [joule$^{1/2}$ cm$^{-3/2}$]
Oxygen gas permeability	4.04 Barrer
Surface energy	σ=25.6 mJ m^{-2}, purely dispersive (hydrophobic surface behavior)
Surface roughness	< 10 nm on hot embossed polymer sheets

Fluoroflex Micro Hot Embossing
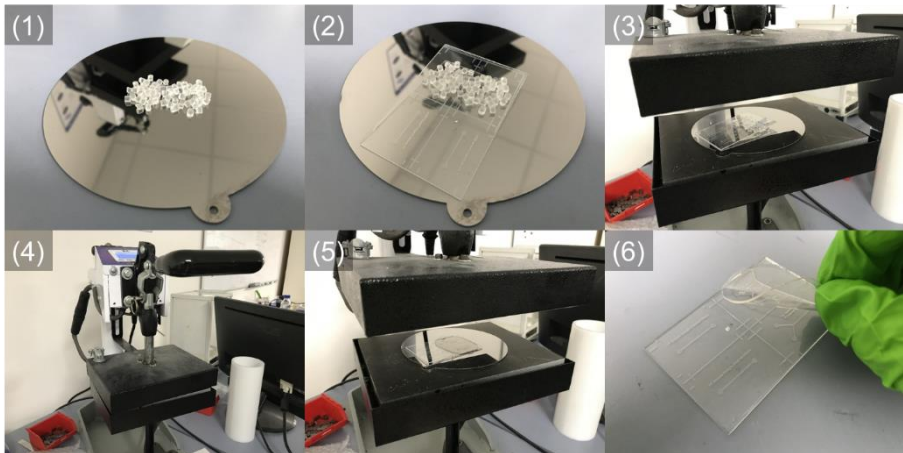
(1) Place raw Fluoroflex pellets on rigid, smooth counter plate. Note that Fluoroflex material can be recycled, meaning that raw pellets can be replaced with Fluoroflex sheets or scraps that have already undergone one or more hot embossing cycles.

(2) Place the microfluidic master mold atop the Fluoroflex pellets, with the microstructured side facing the pellets.

(3) Place the counter plate-Fluoroflex-mold assembly in the heat press hot embosser, heated to 220 °C. Spacers may be placed around the assembly to control for final Fluoroflex sheet thickness.

(4) Bring the two heated plates into contact with the assembly and let stand for 15 s under not supplementary pressure to heat the assembly before pressure is applied. Apply pressure for approximately 30 s, or until desired Fluoroflex sheet thickness is achieved.

(5) Open heat press and remove the assembly. Let cool for approximately 1 min before attempting disassembly. Using tweezers, remove the master mold and micropatterned Fluoroflex sheet from the counter plate. Isopropanol can ease the separation process.

(6) Peel off the micropatterned Fluoroflex sheet from the master mold. It can be subsequently bonded to other Fluoroflex sheets through the formation of conformal contact.

Fluoroflex Self-bonding
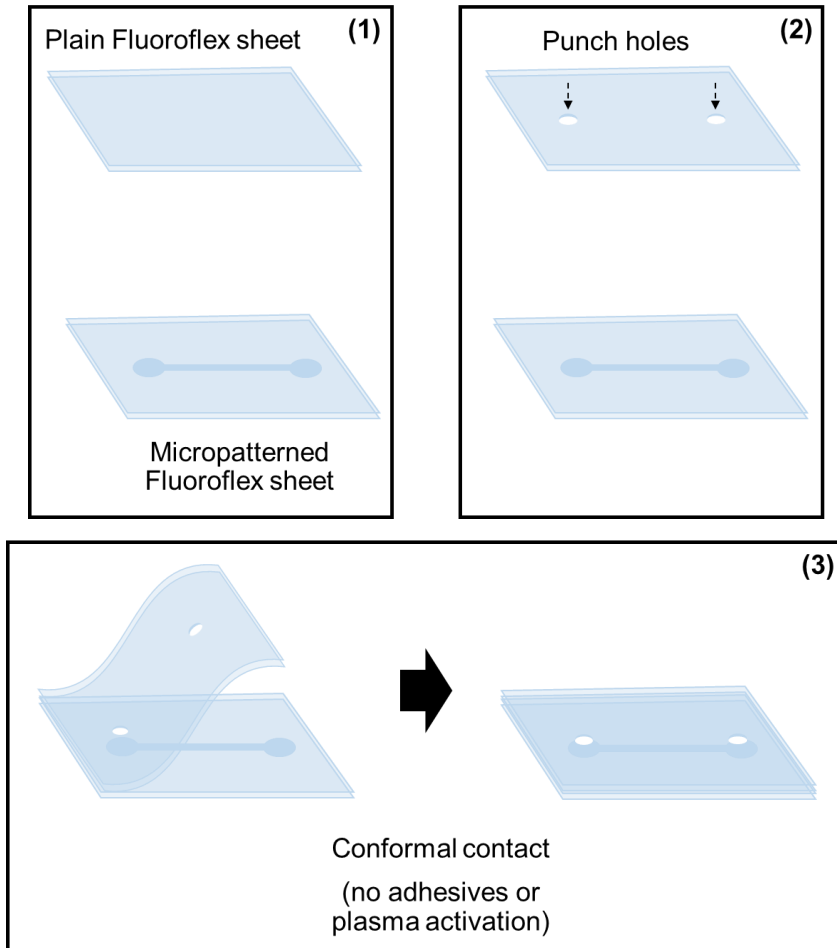
Fluoroflex can be reversibly bonded to itself upon the formation of conformal contact.

(1) To assemble a microfluidic device with Fluoroflex self-bonding, a micropatterned polymer sheet and a plain polymer sheet are needed (more complex multi-layer devices are also possible).

(2) Punch holes in one of the sheets at the appropriate port locations for microfluidic interfacing.

(3) Place the two sheets in conformal contact, applying even pressure to ensure good contact is made. Self-bonding occurs at room temperature, allowing near-immediate device use, but can be enhanced with baking at 185 °C for 2 hr.

APPENDIX 2 – MARKET STUDY RESEARCHER INTERVIEW QUESTIONNAIRES

Market Study Researcher Interview Questionnaires

Segmentation questions

1. Can you tell me briefly about your research?

2. Do you use microfluidics in your research?

Questions Group 1: Flow Chemists

1. Why do you use microfluidics in your research? How long have you/your lab been using microfluidics?

2. What are the most important parameters you take into consideration when designing your microfluidic setup?

3. Could you describe the microfluidic setup that you use? (Flow control, devices/reactor, peripheral equipment for sensing/analysis, etc.)

4. How did you decide on the type of flow control that you use?

5. What is the most difficult part about the flow control in your experiments?

6. Can you tell me more about the microreactors that you use?

7. How did you decide on this type of microreactor? (tubing/chip/other vessel)

8. How did you decide on the material that the microreactor would be made out of? Have you ever tried using different materials?

9. Do you have any complaints about the microreactors you use? (Anything from their cost, performance, lifetime, compatibility etc.)

10. What are your thoughts on solvent resistant plastics as a material for microreactors?

Admin Questions Group 1

1. Where did you buy your equipment from?

2. Could you give us a ballpark of the budget you had for your microfluidic set-up?

Closing Questions Group 1

1. If you had a magic wand, what would you change about your project?

2. If you could go back in time, what do you wish you had known when you started working with microfluidics?

3. Is there anything that we didn't cover that you would like to add?

Questions Group 2: Conventional Chemists

1. Can you tell me briefly about your research?

2. What do you know about microfluidics for chemistry, also called flow chemistry? And/or microfluidics in general?

3. Have you ever considered using microfluidic techniques as a tool in your research?

4. If yes to Q3:

    a. Why? (Why would it be beneficial?/How would it enable you?)

    b. How far did you investigate into using microfluidics?

    c. Why did you stop pursuing using microfluidics?

5. If no to Q3:

    a. Why? (Why is it not worth investigating?)

CURRICULUM VITAE

PERSONALIA

Name:	Alexander H. McMillan
Address:	67 Rue d'Avron, 75020 Paris, France
Mobile phone:	+33 6 19 69 35 74
E-mail:	alexanderhmcmillan@msn.com
Date of Birth:	May 12, 1995
Place of Birth:	St. Louis, Missouri, USA

EDUCATION AND WORK EXPERIENCE

2017 – 2020   PhD candidate Bioscience Engineering (Marie Curie ITN)
KU Leuven // Elvesys Microfluidics Innovation Center
Leuven, Belgium // Paris, France

2012 – 2017   MEng Mechanical & Electrical Engineering
University of Edinburgh
Edinburgh, UK

2017 – 2018   Business Division Manager
Darwin Microfluidics
Paris, France

LANGUAGES

English – native   French – proficient

VOLUNTEERING ACTIVITIES

2013 – 2017   President (2015–2016), organizing committee member
Edinburgh University Mountaineering Club
University of Edinburgh Sports Union
Edinburgh, UK

PUBLICATION LIST

[1]   **A. H. McMillan**, J. Mora-Macías, J. Teyssandier, R. Thür, E. Roy, I. Ochoa, S. De Feyter, I. F. J. Vankelecom, M. B. J. Roeffaers, Sasha Cai Lesher-Pérez
Self-sealing Thermoplastic Fluoroelastomer Enables Rapid Fabrication of Modular Microreactors
Accepted for publication by *Nano Select*, **2021**; doi:10.1002/nano.202000241

[2]   **A. H. McMillan**, E. K. Thomée, A. Dellaquila, H. Nassman, T. Segura, S. C. Lesher-Pérez
Rapid Fabrication of Membrane-Integrated Thermoplastic Elastomer Microfluidic Devices
Micromachines, **2020**, 11, 731

[3]   A. Dellaquila, E. K. Thomée, **A. H. McMillan**, S. C. Lesher-Pérez
Lung-on-a-chip Platforms for Modeling Disease Pathogenesis
In *Organ-on-a-Chip,* Academic Press: Cambridge, MA, USA, **2020**, pp. 133–180

CONFERENCE PARTICIPATION

[4]   **A. H. McMillan**, E. Roy, M. B. J. Roeffaers, S. C. Lesher-Pérez
Poster presentation: Novel Thermoplastic Fluoroelastomer for Rapid Fabrication of Chemically Compatible Microdevices.
45th International Conference on Micro & Nano Engineering,
Rhodes, Greece, **September 2019**

[5]   **A. H. McMillan**, E. K. Thomée, A. Dellaquila, S. C. Lesher-Pérez
Poster presentation: Fabrication and Characterization of Flexdym-Polycarbonate Devices: Implementing New Materials for Organ-on-chip Technologies.
23rd International Conference on Miniaturized Systems for Chemistry and Life Sciences (μTAS 2019)
Basel, Switzerland, **October 2019**

[6]   **A. H. McMillan**, E. Roy, M. B. J. Roeffaers, S. C. Lesher-Pérez
Poster presentation: Novel Thermoplastic Fluoroelastomer for Rapid Fabrication of Chemically Compatible Microdevices.
Microfluidics 2019: from laboratory tools to process development,
Rueil-Malmaison, France, **November 2019**